3 1761 11552785 5

Digitized by the Internet Archive
in 2022 with funding from
University of Toronto

https://archive.org/details/31761115527855

CA1
EP 321
-79R15

Pacific Marine Science Report 79-15

LIBRARY
FEB 5 1981
University of Toronto

TIDAL ANALYSIS BASED ON HIGH AND LOW WATER OBSERVATIONS

by

M.G.G. Foreman

and

R.F. Henry

INSTITUTE OF OCEAN SCIENCES, PATRICIA BAY
Sidney, B.C.

For additional copies or further information please write to:

Department of Fisheries and Oceans
Institute of Ocean Sciences
P.O. Box 6000
Sidney, B.C. CANADA
V8L 4B2

CA1
EP321
-79R15

Pacific Marine Science Report 79-15

TIDAL ANALYSIS BASED ON HIGH AND LOW WATER OBSERVATIONS

by

M.G.G. Foreman and R.F. Henry

Institute of Ocean Sciences, Patricia Bay

Sidney, B.C.

1979

TABLE OF CONTENTS

Page

Abstract iii

Acknowledgments iv

PART I : GENERAL DESCRIPTION

1. INTRODUCTION 1

2. METHOD OF ANALYSIS 2

2.1 Choice of Constituents 2

2.2 Least Squares Fitting of Sinusoidal Constituents to High and Low Water Data 2

3. NUMERICAL TESTS 3

3.1 Harmonic Analyses 4

3.2 High-Low Analyses 6

3.2.1 High-Low sequence with gaps 7

3.2.2 High-Low analysis with timing errors 7

3.3 Conclusions 8

PART II : DETAILS OF PROCEDURES

4. LEAST SQUARES FIT WITH MODIFIED GRAM-SCHMIDT ALGORITHM 9

5. MODIFICATIONS TO RESULTS OF LEAST SQUARES ANALYSIS 13

5.1 Nodal Modulation 13

5.2 Astronomical Argument Corrections 14

5.3 Inference 15

TABLE OF CONTENTS (Cont.)

PART III : COMPUTER PROGRAM FOR HIGH-LOW ANALYSIS

Page

6. GENERAL DESCRIPTION OF PROGRAM 19

6.1 Routines Required 19
6.2 Data Input 19
6.3 Output 23
6.4 Program Conversion, Storage and Dimension Guidelines 24

7. APPENDICES:

1. Results of 12-month hourly height harmonic analysis 26
2. List of possible constituents (and their frequencies) in the high-low computer program analysis 28
3. Data input on file reference number 8 for the computer program 30
4. Sample data input on file reference number 9 for the computer program 36
5. Sample data input on file reference number 5 for the computer program 37
6. Computer program output corresponding to the input of Appendices 3, 4 and 5. 38

8. REFERENCES 39

LIST OF TABLES

1. Computed Amplitudes and Phases of Principal Constituents 5

2. Test Analyses With and Without Inference 17

Abstract

Part I of this report describes a method for tidal analysis based on high and low water observations and also discusses the results of various test runs. Part II gives detailed information on certain aspects of the calculations and Part III is a user's manual for the relevant computer program.

Wherever possible, terminology, computations and computer input and output formats are in accord with two earlier reports (Foreman, 1977, 1978) dealing with equally spaced tidal height and current data.

Users who wish to receive updates of the computer programs should send their names, addresses and type of computer used for implementation to the authors.

ACKNOWLEDGEMENTS

The writers wish to thank the staff of Tides and Current Section, Institute of Ocean Sciences, Patricia Bay for their cooperation and assistance and Mrs. S. Osborne, Miss B. Peirson and Mrs. S. McKenzie for typing this report.

1. INTRODUCTION.

It is customary nowadays, in tidal heights analysis, to use hourly values of surface elevation obtained either from a digital tide gauge or by sampling a continuous record of water level. However, there is a mass of historical tidal data in the form of times and magnitudes of successive high and low water levels, and even today there are situations in which it is convenient to record tidal elevations in this form. The fact that the time intervals between successive tidal extrema vary considerably means that most standard computer programs (e.g. Foreman, 1977) used for tidal (harmonic) analysis of conventional hourly-sampled data are not applicable. Yet these are generally based on least squares fitting of tidal frequency constituents to the data and there is no reason, in principle, why irregularly-spaced data cannot be analysed in the same way. In such an approach to analysis of high and low water levels which, for convenience, we term "high-low analysis", there is an upper limit to the tidal constituent frequencies which can be included. Basic sampling theory shows that constituents which are sampled fewer than two times per cycle become irretrievably confused with lower frequency constituents - a type of error known as "aliasing". Knowing the times and magnitudes of low and high waters should be somewhat better than simply having two elevation samples per tidal cycle, since the time derivative of surface elevation is zero at extrema. Assuming that, on average, four extrema occur per (lunar) day, it may be possible, using all the information implicit in the extremal amplitudes and times, to resolve constituents with periods as low as six hours. A conservative position is taken in the test cases described later in §3, where no attempt is made to determine constituents above semi-diurnal frequency. It is shown, however, that failure to use the derivative information leads to less accurate estimation of semi-diurnal constituents - a result probably attributable to aliasing of terdiurnal and quarter-diurnal constituents. This effect will be more noticeable in locations where higher-frequency constituents are relatively large, for instance, in shallow water.

Although high and low water observations have been taken over many months at a few locations, a record length of one month was taken in the numerical tests as being more typical. Consequently, low-frequency constituents (e.g. fortnightly, monthly) were omitted from the analysis, since they often show considerable variation from month to month due to meteorological effects; there is no theoretical obstacle to their inclusion, however.

Visual observations of tidal extrema often cover daylight hours only, in which case either one or two observations per day are missing and, at some sites, no observations at all were made on Sundays. These defects affect the accuracy of high-low analysis, and use of longer records is the obvious countermeasure. The missing data points cause no practical difficulty in least squares fitting procedures originally set up for unevenly spaced data.

A most important consideration in analyses based on high and low water data is the reliability of the observed times. Ideally, observations of water level should be made from some time before the extreme value until some time

afterward, and then plotted so that the peak value and its time of occurrence can be estimated accurately. But, even so, short period waves introduce error into all the observations and it is reasonable to expect a minimum random error in times of high and low water of the order of a few minutes; the effect of such random timing errors is discussed later. If the correct observation procedure, outlined above, is not followed, the times of extrema made by most observers tend to be several minutes late. Consistent errors of this type affect the phases of constituents by a calculable amount, since the period of each constituent is known, and corrections are possible if some estimate of the timing error can be made.

Previous work on tidal analysis of high and low water observations ranges from the traditional sequential methods discussed by Schureman, 1958, which yield only moderately accurate estimates of the principal constituents, to least squares analysis (e.g. Zetler, Schuldt, Whipple and Hicks, 1965) essentially similar to that used here. The purpose of the present report is to combine an efficient least squares algorithm with the full suite of nodal modulation, astronomical argument correction and full inference calculations, while maintaining maximum compatibility of terminology and format with other tidal analysis programs currently in use at the Institute of Ocean Sciences.

2. METHOD OF ANALYSIS.

2.1 Choice of Constituents.

The magnitude of tidal constituents usually does not vary rapidly with latitude or longitude and, if no prior information is available from the site in question, it is fairly safe to assume that the same constituents will dominate the tidal behaviour at the new location as at other known stations in the same geographical area. In the numerical tests below, selection of first magnitude constituents was simple, since conventional harmonic analysis results for the test site were already available. The diurnals O_1 and K_1 and semi-diurnals N_2, M_2 and S_2 were, clearly, most significant; in certain tests, the diurnal P_1 and semi-diurnal K_2 were also included, being inferred from K_1 and S_2, respectively (see §5.3). Constituents outside the diurnal to semi-diurnal frequency range were excluded for reasons discussed in §1. A constant term, Z_o, was included as a matter of course, since surface elevations are seldom measured directly relative to mean water level. It may be noted that, with a record length of one month, the system of equations to be solved is substantially over-determined and there is no difficulty in adding minor constituents if desired.

2.2 Least Squares Fitting of Sinusoidal Constituents to High and Low Water Data.

Assuming that a sequence of high and low water observations, y_i, and the corresponding times, t_i, $i = 1,...N$, at which they occurred are given, we wish to find a function

$$y(t) = A_o + \sum_{j=1}^{M} A_j \cos 2\pi(\sigma_j t - \phi_j), \qquad (1)$$

in which the constituent frequencies σ_j and the number of constituents M are specified beforehand, but the amplitudes A_j and phases ϕ_j remain to be chosen so that the values $y(t_i)$ of the fitting function at the sampling instants t_i agree as well as possible with the contemporaneous observed elevations y_i, that is,

$$y_i - \left[A_o + \sum_{j=1}^{M} A_j \cos 2\pi(\sigma_j t_i - \phi_j)\right] = \varepsilon_i \simeq 0, \; i = 1,\ldots N \tag{2}$$

Further, at the observation times t_i, the time derivative $y'(t)$ of the fitting function should be approximately zero, that is

$$y'(t_i) = -\sum_{j=1}^{M} 2\pi\sigma_j A_j \sin 2\pi(\sigma_j t_i - \phi_j) = \delta_i \simeq 0 \tag{3}$$

The fitting errors ε_i, δ_i, cannot be reduced exactly to zero when the number of arbitrary constants (2M + 1) in the expression for $y(t)$ is less than 2N, the number of equations (2) and (3) to be satisfied. A commonly adopted compromise in such over-determined problems is to minimize the sum of the squares of errors at the observation times, which means, in the present case, choosing the A_j and ϕ_j so as to minimize the error function

$$E = \sum_{i=1}^{N}\left\{\left[y_i - y(t_i)\right]^2 + \left[wy'(t_i)\right]^2\right\} = \sum_{i=1}^{n}\left\{\varepsilon_i^{\,2} + w^2\delta_i^{\,2}\right\} \tag{4}$$

that is, to find a "least squares fit" to the available data. The inclusion of an arbitrary positive weighting coefficient w in (4) permits control of the emphasis to be placed on satisfying the zero derivative condition compared to that placed on having $y(t)$ fit the observed elevations accurately. For instance, w = 1.0 indicates that equal emphasis is given to both conditions, whereas w = 0 means that the requirement that $y'(t)$ should be approximately zero at each t_i is simply ignored.

Details of the algorithm used for numerical minimization of E in (4) are given in §4.

3. NUMERICAL TESTS.

To test the effectiveness and accuracy of high-low analysis by least squares fit, some numerical experiments were carried out on surface level

observations collected in 1974 at Prince Rupert, B. C., a fairly typical West Coast port with relatively deep approaches, where the tide is predominantly semi-diurnal with significant diurnal contributions. In order to have some basis for judging the high-low analysis, four conventional harmonic analyses of hourly heights were carried out first.

3.1 Harmonic Analyses.

Analysis 1.

A full 12-month hourly height harmonic analysis (Foreman, 1977) for 1974 is listed in Appendix 1. The constant component plus the major diurnal and semi-diurnal constituents from this 68-constituent analysis form the first row of Table 1. That there is little non-tidal contribution to water level variation at Prince Rupert is evident from the fact that the residual elevation, after removal of tidal constituents found in Analysis 1, had an r.m.s. value of 0.13 m, which is approximately 2% of the tidal range.

Since seasonal variation at Prince Rupert is very slight and one-month analyses were the principal topic of interest, all subsequent tests were confined to a single arbitrarily-selected month - January, 1974.

Analysis 2.

Hourly heights for January, 1974 were analysed for the suite of 36 constituents which can be resolved from a 31-day record using a Rayleigh (resolution) criterion value of 0.97 (Foreman, 1977, p.16). Constituents P_1, ρ_1, ν_2 and K_2, which can only be obtained by inference in a one-month analysis (see §5.3), were omitted.

Analysis 3.

Though otherwise similar to Analysis 2 above, this case used 40 constituents, P_1, ρ_1, ν_2 and K_2 being inferred from K_1, Q_1, N_2 and S_2, using inference constants calculated from the one-year Analysis 1.

Comparison of Analyses 1, 2 and 3 shows clearly how much more accurately the constituents K_1, N_2 and S_2 can be estimated from monthly records when inference is used. Of course, in this example, the inference constants are optimum, since they were calculated from a longer record at the same site; in practice, inference constants may have to be estimated from data at a neighbouring site, which can result in a less marked improvement.

Since tidal constituent frequencies are not harmonics of a single fundamental frequency, the results obtained by least squares fit analysis depend on the number of constituents included. The effect on the major constituents of omitting many of the minor constituents can be seen on comparing the 40-constituent Analysis 3 with the following :

TABLE 1: Computed Amplitudes and Phases of Principal Constituents

ANALYSIS NO.	ANALYSIS DETAILS	NO. OF CONSTI-TUENTS[1]	Z_0	O_1		P_1		K_1		N_2		V_2		M_2		S_2		K_2	
			AMP.	AMP.	PH.	AMP.	PH.	AMP.	PH.	AMP.	PH.	AMP.	PH.	AMP.	PH.	AMP.	PH.	AMP.	PH.
H.A. 1	12 month. (Jan-Dec 74)	68	3.8714	0.3125	132.5	0.1606	135.8	0.5144	139.5	0.3952	14.9	0.0766	16.5	1.9564	35.8	0.6446	59.3	0.1738	50.7
H.A. 2	31 day (Jan 74) No inference	36	3.8972	0.3154	132.8	-	-	0.6489	152.7	0.4699	12.4	-	-	1.9358	35.5	0.6644	72.9	-	-
H.A. 3	31 day. With inference	40	3.8972	0.3154	132.8	0.1700	137.2	0.5444	140.9	0.3972	14.8	0.0770	16.4	1.9358	35.5	0.6791	58.1	0.1831	49.5
H.A. 4	31 day. With inference	9	3.8971	0.3168	131.4	0.1681	137.5	0.5386	141.1	0.4035	15.2	0.0782	16.8	1.9321	35.3	0.6739	57.4	0.1817	48.8
H-L. 5	31 day. w=1. No inference	6	3.8873	0.3133	130.4	-	-	0.6405	152.7	0.4176	12.2	-	-	1.9497	35.8	0.6877	71.6	-	-
H-L. 6	31 day. w=1. With inference	9	3.8873	0.3133	130.4	0.1677	137.3	0.5374	140.9	0.3532	14.6	0.0685	16.2	1.9497	35.8	0.7028	56.8	0.1895	48.1
H-L. 7	31 day. w=0. With inference	9	3.8868	0.3095	131.8	0.1664	139.1	0.5330	142.8	0.3037	19.2	0.0589	20.9	1.9725	39.1	0.7062	59.9	0.1904	51.3
H-L. 8	31 day with gaps. With inference.w=1.	9	3.8531	0.3146	130.2	0.1665	142.9	0.5332	146.5	0.3470	15.0	0.0673	16.6	1.9572	35.6	0.6793	56.8	0.1831	48.2
H-L. 9	31 day. Timing errors With inference.w=1.	9	3.8874	0.3183	130.0	0.1684	137.6	0.5393	141.3	0.3580	15.2	0.0694	16.9	1.9533	35.8	0.6981	56.6	0.1882	48.0
H-L.10	31 day. Timing errors With inference.w=0.	9	3.8876	0.3127	131.9	0.1656	139.4	0.5305	143.1	0.3058	20.1	0.0593	21.8	1.9828	39.4	0.7048	59.7	0.1900	51.1

Amplitudes in metres; phases in degrees

[1]Including mean (constant term)

Analysis 4.

This test is a monthly harmonic analysis identical to Analysis 3 but for the fact that only five major, plus three inferred constituents and a constant term are included in the least square fit. These are the constituents included in most of the high-low analyses, described below.

3.2 High-Low Analyses.

The heights and times of high and low waters used in the following tests were taken from a strip-chart record. The times are estimated to lie within 3 minutes of actual high or low water; heights are correct to within ±1.5 cm (0.05 ft). As explained in §2.2, the relative importance accorded to the fact that the time derivative of elevation is zero at high and low water is reflected in the magnitude of the weighting coefficient in the least-square-fit procedure.

Analysis 5.

This is a least square fit of five major constituents to 119 consecutive high and low waters (times and magnitudes) at Prince Rupert in January, 1974. No inference of P_1, ν_2 and K_2 was carried out. The zero derivative information was accorded the same significance as the elevation readings, i.e. the weighting coefficient, w, was taken as unity.

Comparing Analysis 5 with 2, it is clear that high-low analysis is capable of determining constant, diurnal and semi-diurnal constituents with very satisfactory accuracy. That inference is a useful additional feature in high-low analysis is verified in the following test :

Analysis 6.

This high-low analysis of the data already examined in Analysis 5 employs the same five major constituents, but also infers P_1,ν_2 and K_2, using the same inference constants as in Analyses 3 and 4.

Comparing these results with Analysis 5, and referring also to the constituents found in the one-year Analysis 1, one finds the same degree of improvement in constituents K_1, N_2 and S_2 as when inference was introduced into the harmonic analysis (Analysis 3 versus Analysis 2). It can be concluded that inference is worthwhile in high-low analysis whenever reasonably reliable inference constants are available.

Analysis 7.

This test is identical to Analysis 6, except that the zero derivative information is not used (zero weighting coefficient). Inference was applied as in the foregoing test.

The results of Analysis 7 obviously differ from Analysis 3 rather more than Analysis 6 does; in other words, omission of derivative information impairs high-low analysis somewhat. Nevertheless, Analysis 7 is close enough to Analysis 3 to be considered quite satisfactory. This is an important conclusion, since Analysis 7 is probably representative of the results which can be expected from irregularly-spaced sets of elevation observations which are not necessarily extrema. In fact, the computer program used for high-low analyses can be used unchanged for any arbitrarily-chosen set of observations, provided the derivative weighting coefficient, w, is zero.

3.2.1 High-Low Sequences with Gaps.

High and low waters which occurred during hours of darkness are often missing from records taken visually. In some cases, no readings were made on Sundays. In order to find out the effects of such gaps on the accuracy of high-low analyses, the data already used in Analyses 5 through 7 were modified by deleting observations made between 9 p.m. and 5 a.m. (local time) on weekdays and Saturdays, and all day Sunday. This reduced the total number of observations for January, 1974 from 119 to 73.

Analysis 8.

The reduced set of observations described above was subjected to high-low analysis for 5 major and 3 inferred constituents, with unit weighting for the derivative information.

The results in Table 1 agree slightly less well with Analysis 3 than the various earlier analyses based on 119 observations but, nevertheless, are remarkably close.

3.2.2 High-Low Analysis with Timing Errors.

In order to simulate the effects of errors in timing when high and low water are estimated purely by eye, the genuine data already used in Analyses 5 to 8 were altered by adding randomly-generated timing errors, uniformly distributed in the range -15 to +15 minutes, to the individual observation times. The magnitudes of the observed high and low waters were not altered.

Analysis 9.

A high-low analysis of the data with simulated timing errors, as described above, was carried out using inference and with a weighting coefficient of 1.0 for the zero derivative condition.

Analysis 10.

The preceding analysis was repeated with a weighting coefficient of zero, i.e. the fact that the observed elevations were known to be maxima or minima was ignored.

The results of Analyses 9 and 10 show that the former gives estimates closer to the true tidal content of the data as defined by Analyses 3 and 4.

3.3 CONCLUSIONS.

It is clear from the numerical tests in §3 that "high-low analysis", consisting of a least-squares fit of major diurnal and semi-diurnal tidal constituents to high and low water levels can yield very satisfactory estimates of amplitudes and phases of the constituents involved, at least for records about one month in length. It is expected that minor constituents of semi-diurnal and lower frequencies can be resolved where longer records are available. However, higher frequency constituents are best considered as noise, since even taking the derivative information into account, the upper limit placed by sampling theory on the resolvable frequencies is somewhere between semi-diurnal and quarter-diurnal.

The tests analyses indicate that

(i) it is always best to use rather than to ignore the information that the observations of elevation are also extrema,

(ii) the estimates of some major constituents are improved by "inferring" certain subsidiary constituents,

(iii) a lack of night-time observations and occasional missing days impair high-low analysis only slightly, and

(iv) high-low analysis is fairly insensitive to errors of several minutes in the observed times of high or low water.

PART II. DETAILS OF PROCEDURES.

4. Least Squares Fit with Modified Gram-Schmidt Algorithm.

The original system of overdetermined equations which gives rise to the least squares fit problem is

$$\left.\begin{aligned} y(t_i) - y_i = A_o + \sum_{j=1}^{M} A_j \cos 2\pi(\sigma_j t_i - \phi_j) - y_i &= 0 \\ y'(t_i) = -\sum_{j=1}^{M} 2\pi\sigma_j A_j \sin 2\pi(\sigma_j t_i - \phi_j) &= 0 \end{aligned}\right\} i = 1,\ldots N \qquad (5)$$

in the notation of §2. It is convenient to change variables to $C_o = A_o$, $C_j = A_j \cos 2\pi\phi_j$, $S_j = A_j \sin 2\pi\phi_j$, $j = 1,\ldots M$, since the above equations then become

$$\begin{aligned} C_o + \sum_{j=1}^{M} (C_j \cos 2\pi\sigma_j t_i + S_j \sin 2\pi\sigma_j t_i) &= y_i \\ \sum_{j=1}^{M} 2\pi\sigma_j (C_j \sin 2\pi\sigma_j t_i - S_j \cos 2\pi\sigma_j t_i) &= 0 \end{aligned} \qquad (6)$$

which are linear in the new unknowns C_o, C_j, S_j. The A_j and ϕ_j can be recovered later from the C_j, S_j by means of the formulas

$$\begin{aligned} A_j &= (C_j^2 + S_j^2)^{\frac{1}{2}} \\ 2\pi\phi_j &= \tan^{-1} \frac{S_j}{C_j} \end{aligned} \qquad (7)$$

We now review the reasons for prefering the Modified Gram-Schmidt least squares fit algorithm to that used in the harmonic analysis of hourly heights (Foreman, 1977). Given an overdetermined system of equations written in the matrix form $Ax = b$, a common approach to the linear least squares fit problem is to form and solve the normal equations $A^TAx = A^Tb$. These are not overdetermined, but are frequently ill-conditioned, making the solutions very sensitive to roundoff errors, etc. In order to preserve accuracy, it is preferable to compute the least squares solution directly from the original overdetermined equations by orthogonalization procedures, such as Householder triangularization, singular value decomposition or the Modified Gram-Schmidt method. For instance, solution by normal equations requires double precision arithmetic to give the same accuracy as Householder's method achieves in single precision (Barrodale et al., 1978).

Nevertheless, when the number of equations N is much larger than the number of parameters M, the normal equations approach has its advantages. Not only do the formation and solution of these equations require about half as many operations as an orthogonalization technique, but if these equations can be formed directly from the data rather than from the overdetermined system, then only M(M+1)/2 storage locations, as opposed to at least NM, are required. This is, in fact, why the normal equations were used in the harmonic tidal heights analysis of hourly observations (Foreman, 1977). There, the normal equations are formed directly and efficiently (the use of trigonometric identities avoids rounding errors usually encountered with cumulative sums) and aggravation of the problem's already ill-conditioned nature is avoided. The storage savings can be significant - for instance, in a one-year analysis, where the approximate values for N and M are 8760 and 137, respectively. In fact, on some installations, there may not be sufficient storage for an overdetermined array of these dimensions.

Since the numbers of observations and constituents will generally be smaller when high-low analysis is used, storage considerations will be less important. Also, the identities used to form the normal equations in the regularly sampled case no longer apply. Orthogonalization methods are, therefore, preferable and the Modified Gram-Schmidt algorithm (Barrodale et al., 1974) was selected, since it is competitive in all respects with the Householder method and was already available on the Institute of Ocean Sciences' computer.

Orthogonalization methods obtain the least squares solution to the matrix equation $Ax = b$ by forming an equivalent system of equations which is easier to solve. In particular, the classical Gram-Schmidt technique does this by calculating an orthogonal set[+] of vectors $\{q_1,\ldots q_{n+1}\}$ such that for $k = 1,\ldots n+1$, the set $\{q_1,..q_k\}$ spans the same k-dimensional subspace as the given set of linearly independent vectors $\{a_1,..a_k\}$, where the set $\{a_1,..a_{n+1}\}$ are the columns of the augmented matrix $A{:}b$ arising from the overdetermined system $Ax = b$. The set of mathematical formulas which calculate the q_j vectors iteratively are as follows:

$$q_1 = a_1 \tag{8}$$

$$q_j = a_j - \sum_{i=1}^{j-1} r_{ij} q_i \qquad j = 2,..n \tag{9}$$

where

$$r_{ij} = \frac{a_j^T q_i}{q_i^T q_i} \tag{10}$$

+ the set of vectors $\{q_1,\ldots q_n\}$ is said to be orthogonal if $q_i^T q_j = 0$ for all $i \neq j$. If, in addition, $q_i^T q_i = 1$, the set is orthonormal.

In order to convert these equations to matrix notation, let A be the matrix with columns a_j, Q be the matrix with columns q_j and R be the upper triangular matrix with unit diagonal elements and super-diagonal elements given by (10). Then equations (8) through (10) can be written as A = QR.

The Modified Gram-Schmidt method is a variation of the classical technique which makes use of the fact that the value of the inner product $a_j^T q_i$ in equation (10) will not change if a_j is replaced by any vector of the form

$$a_j^{(i)} = a_j - \sum_{k=1}^{i-1} \alpha_k q_k \tag{11}$$

where the α_k are a set of arbitrary numbers. In particular, if one chooses the numbers α_k so as to minimize the norm of the vector $a_j^{(i)}$, it can be shown that replacing a_j by $a_j^{(i)}$ in the classical Gram-Schmidt orthogonalization produces a method that is more stable numerically. This algorithm, which has become known as Modified Gram-Schmidt (MGS), is described by the following equations (Lawson and Hanson, 1974) :

$$a_j^{(i)} = a_j \quad j = 1,..n \tag{12}$$

$$q_i = a_i^{(i)} \tag{13}$$

$$d_i^2 = q_i^T q_i \tag{14}$$

$$r_{ij} = \frac{a_j^{(i)T} q_i}{d_i^2} \tag{15}$$

$$a_j^{(i+1)} = a_j^{(i)} - r_{ij} q_i \tag{16}$$

Equations (15) and (16) are for $j = i+1,...n$; equations (13) through (16) are for $i = 1,...n$.

In order to use the Modified Gram-Schmidt orthogonalization to minimize the sum of the squares of the residuals (i.e. $\| Ax - b \|^2$) for the over-determined system Ax = b, first form the augmented m x (n + 1) matrix A' = [A:b]. A' is then orthogonalized to obtain

$$A' = Q'R' \tag{17}$$

where the column vectors given by (13) constitute the m x (n + 1) matrix Q', and R' is an upper triangular matrix with unit diagonal elements and super-diagonal elements given by (15). Defining D' to be the (n + 1) x (n + 1)

diagonal matrix with elements specified by (14), a new m x m orthogonal+ matrix Q_o is introduced such that

$$Q_o \begin{bmatrix} D' \\ 0 \end{bmatrix} = Q', \text{ where 0 has dimension } (m-n+1) \times (n+1)$$

This means that the first n+1 columns of Q_o will be q_i/d_i^2 for i = 1,..n+1 and the remaining m-n+1 need only complete the orthonormal set. Partitioning R' and D' into $\begin{bmatrix} R & c \\ 0 & 1 \end{bmatrix}$ and $\begin{bmatrix} D & 0 \\ 0 & d_{n+1} \end{bmatrix}$ respectively,

where both D and R are n x n, we can then write

$$A' = Q_o \begin{bmatrix} D' \\ 0 \end{bmatrix} R' = Q_o \begin{bmatrix} DR & Dc \\ 0 & d_{n+1} \\ 0 & 0 \end{bmatrix} .$$

Making use of the property that $\| B^T x \| = \| x \|$ for any orthogonal matrix B, it then follows that

$$\| Ax - b \|^2 = \| Q_o^T (Ax - b) \|^2$$

$$= \| D(Rx-c) \|^2 + d_{n+1}^2 .$$

Therefore, the minimum value of $\|Ax - b\|^2$ is d_{n+1}^2 and is attained by the vector x_o which satisfied Rx = c.

A later version of MGS (Barrodale et al., 1974) is more efficient, in that the matrix equation Rx = c is solved as part of the orthogonalization process. Specifically, A' is now defined as the larger partitioned matrix $A' = \begin{bmatrix} A & b \\ I & 0 \end{bmatrix}$, where I is the n x n identity matrix and 0 is the n x 1 vector of zeros. Applying MGS to A' results in the following matrix of orthogonal columns $\begin{bmatrix} Q & r \\ R^{-1} & -R^{-1}c \end{bmatrix}$ where [Q r] is the Q' of equation (17) and R,c are the same as in the partition of R'.

Thus, the least squares solution $x_o = R^{-1}c$ can be easily removed from this matrix.

+ An orthogonal matrix Q satisfies the condition $Q^T = Q^{-1}$. As a result, its columns form an orthonormal set.

Moreover, since

$$A' = \begin{bmatrix} A & b \\ I & 0 \end{bmatrix} = \begin{bmatrix} Q & r \\ R^{-1} & -R^{-1}c \end{bmatrix} \begin{bmatrix} R & c \\ 0 & 1 \end{bmatrix} = \begin{bmatrix} QR & Qc+r \\ I & 0 \end{bmatrix}$$

it follows that $Q = AR^{-1}$, $b = AR^{-1}c+r$ and hence $r = b - Ax_o$ is the vector of residuals corresponding to the least squares solution of the over-determined system.

5. MODIFICATIONS TO RESULTS OF LEAST SQUARES ANALYSIS.

5.1 Nodal Modulation.

The tidal potential contains many more sinusoidal constituents than are commonly sought in tidal analysis. Due to the small frequency differences between many of these (and the great length of record required for their separation) and the relatively small expected amplitude of some, it is not feasible to analyse for all of them. The standard approach is to lump together constituents which have the same first three Doodson numbers (see Godin, 1972) and to assume that each such cluster can be replaced by a single sinusoid having the same frequency as the major constituent (in terms of tidal potential amplitude) in the cluster. This major contributor lends its name to the cluster and lesser constituents are termed its satellites. An amplitude and phase is then calculated from the data for each apparent major constituent (in fact, for the replacement sinusoid representing each cluster). However, since these values represent the cumulative effect of all constituents in the cluster and the latter all differ slightly in frequency, the amplitude and phase of the replacement sinusoid vary slowly in time and do not provide a basis for predicting the contribution of the cluster to the tidal signal at a subsequent time. To avoid this difficulty, the time-invariant amplitude and phase of the major constituent in each cluster are calculated from those of the replacement sinusoid. This adjustment procedure is known as "nodal modulation". To predict the contribution of the cluster at a later time, the major constituent is first calculated and then the nodal modulation corrections to its amplitude and phase are applied in the reverse sense to obtain the contribution of the cluster as a whole.

In this report, the replacement sinusoid for the jth cluster is first written as

$$A_j \cos 2\pi[\sigma_j t_1 - \phi_j] \tag{18}$$

where A_j and ϕ_j are termed the raw amplitude and raw local phase. Time t_1 is measured from the mid-point of the record being analysed. A customary notation for (18) is

$$f_j(t)\, a_j \cos 2\pi [\sigma_j t_1 - \theta_j + u_j(t)], \tag{19}$$

which expresses the relation between the cluster contribution in terms of the amplitude, a_j, and phase, θ_j, of its major constituent. The nodal modulation terms of $f_j(t)$ and $u_j(t)$ vary slowly with time and, for records up to one year in length, very little error is introduced by assuming them to be constant and equal to their value at $t_1 = 0$, the midpoint of the record. Further details of the nodal modulation calculations and the evaluation of $f_j(t)$ and $u_j(t)$ are given in Foreman (1977, p. 42).

5.2 Astronomical Argument Corrections.

The astronomical argument correction arises from the need to express all constituent phase lags with respect to a universal time and space origin. Instead of regarding each tidal constituent as the result of a particular component in the tidal potential, an artificial causal agent can be attributed to each constituent in the form of a fictitious star which travels around the equator with angular speed equal to that of its corresponding constituent. Making use of this conceptual aid, the astronomical argument of a given tidal constituent can be viewed as the angular position (longitude) of its fictitious star. For historical reasons, all such arguments or longitudes are expressed relative to the Greenwich meridian and can, consequently, be expressed as functions of time only. The replacement sinusoid (19) is often written as

$$f_j(t)\, a_j \cos 2\pi[\, V_j(t) + u_j(t) - g_j] \qquad (20)$$

where $V_j(t)$ is the longitude of the fictitious star relative to Greenwich and the new time variable t has an absolute datum such as some calendrical landmark. g_j is termed the 'Greenwich phase lag' of the jth constituent.

Ignoring the minute effects of long-term changes in the astronomical variables (see Foreman, 1977, p. 15).

$$V_j(t) = \sigma_j t + V_{oj}$$

where V_{oj} is a phase correction due to the change of time datum. If t_c is the midpoint of the record on the new time scale, t, then $t = t_1 + t_c$ and

$$\begin{aligned} A_j \cos 2\pi[\sigma_j t_1 - \phi_j] &= A_j \cos 2\pi[\sigma_j t - \sigma_j t_c - \phi_j] \\ &= A_j \cos 2\pi[\, V_j(t) - V_{oj} - \sigma_j t_c - \phi_j] \\ &= A_j \cos 2\pi[\, V_j(t) - V_j(t_c) - \phi_j] \end{aligned}$$

Comparing this with (20), we see that the Greenwich phase lag is, in fact

$$g_j = \phi_j + V_j(t_c) + u_j(t_c)$$

5.3 Inference.

Inference is the term used in tidal analysis to describe the extraction of certain important constituents excluded at the least squares fit stage on the grounds of insufficient record length but deduced afterwards from included constituents to which they bear a known amplitude and phase relationship. When accurate inference constants (amplitude ratio and phase difference) are available, inference not only yields amplitudes and phases for the inferred constituents, but also significantly reduces periodic variations in the estimated amplitudes and phases of the reference constituents. The computational steps involved in inference are given in detail in Foreman (1977). That material will not be repeated here, but should be read in the light of the following comments.

The question of when constituents should be included directly in the least squares analysis, and when they should be inferred is not easily answered. The Rayleigh criterion, which is used to select constituents in the harmonic analysis of hourly tidal heights (see Foreman, 1977, p.16), is incomplete in its presumption that a record of length T is required to distinguish constituents with a frequency separation of T^{-1}. In fact, it conflicts with the algebraic viewpoint whereby, for any four independent observations, one can obtain four equations and solve for four unknowns (2 amplitudes and 2 phases), regardless of the frequency separation. The missing consideration in both of these viewpoints is that sea-level observations contain, in addition to discrete tidal signals, contributions from a continuous noise spectrum of geophysical origin and from random errors in recording the observations. Taking these effects into account, Munk and Hasselmann (1964) showed that meaningful information can be gained about the frequencies σ_1 and σ_2 provided that

$$|\sigma_2 - \sigma_1| > \frac{T^{-1}}{(\text{signal/noise level})^{\frac{1}{2}}} .$$

It is interesting that essentially the same result can be derived by considering the sensitivity of solutions of a linear system to the condition number of its coefficient matrix. The following account is based on the detailed discussion in Ortega (1972). If $K(A) = \|A\|\|A^{-1}\|$, is the condition number+ of matrix A and $x, \hat{x}$ are such that $Ax = b$ and $A\hat{x} = b + \delta b$, then

$$\frac{\|x - \hat{x}\|}{\|x\|} \leq K(A) \frac{\|\delta b\|}{\|b\|} \qquad (21)$$

+ The conventional condition number K(A) defined here differs from the normalized condition number C(A) calculated during the solution of the normal equations in hourly heights analysis (Foreman, 1977, p.38). Whereas K(A) is unity for a diagonal matrix and assumes higher values for more ill-conditioned matrices, C(A) lies between 0 and 1; 0 corresponds to a singular matrix and 1 to a diagonal matrix.

In order to apply this result to the present problem, assume that $Ax = b$ are the normal equations in matrix form arising from a least squares fit for the amplitudes and phases of several tidal constituents. In particular, assume that the right-hand sides b and $b + \delta b$ are respectively calculated from observations without and with background noise; that is, b assumes observations from a signal that is comprised purely of tidal components whereas $b + \delta b$ assume the same signal plus noise. The effect of seeking amplitudes and phases corresponding to frequencies σ_1 and σ_2 that are relatively close, i.e. $|\sigma_2 - \sigma_1| < T^{-1}$, is to make the appropriate rows in A more linearly dependent (see Foreman, 1977, p.33, regarding the structure of A), and so increase K(A). Hence, in the presence of substantial background noise, one can expect a significant difference between the calculated set of parameters $\hat{x}$ and their "true" values, x. Assuming that accurate inference parameters are available, inference in such a case would yield better results, because solving for the parameters of only one frequency, σ_1 or σ_2, would remove the linearly dependent rows and reduce K(A). On the other hand, if the noise level is very small, the effect of a large condition number resulting from two close frequencies would be counteracted and a reasonably accurate set of parameters $\hat{x}$ could be expected without inference.

Table 2 gives the results of tests designed to demonstrate these points. Two 15-day records of hourly tidal heights were simulated, one using only the constituents Z_o, O_1, K_1, M_2 and S_2, and the other with these same constituents plus random background noise. Specifically, the tidal signal varied over the range [2.77, 47.23], while the uniformly distributed random noise added the range [-2.5, 2.5]. Three sets of six consecutive 60-hour harmonic analyses were executed; the first searching directly for all constituents; the second searching for only Z_o, K_1, and M_2; and the third one extending the second by inferring O_1 and S_2 from K_1 and M_2 respectively (inference parameters were calculated from a 15-day analysis which sought all constituents). In order to compare performances, means and standard deviations were calculated for each amplitude and phase over the six analyses in each series.

Results from the analyses of the tidal record with no background noise (Tests 1 to 4, Table 2) demonstrate a clear advantage to seeking all constituents directly in the least squares fit. The small non-zero standard deviations are attributable wholly to the fact that the data was rounded to four digits, making $\|\sigma b\|$ slightly larger than zero. The standard deviations for the runs with inference (Test 4) are not zero because of simplifying assumptions in the inference method itself.

However, when random noise with range [-2.5, 2.5] is also present in the tidal record (Tests 5 to 8), the standard deviations for the inference runs (Test 8) are consistently less than those obtained by the direct inclusion of all constituents in the least squares fit. This is a consequence of a reduction in K(A) from 120.1 for Test 6 to 2.884 for Test 7.+

+ The L_∞ norm was used in equation (21).

TABLE 2: Test Analyses With and Without Inference

			TEST NO.	Z_0	O_1		K_1		M_2		S_2	
				AMP.	AMP.	PHASE	AMP.	PHASE	AMP.	PHASE	AMP.	PHASE
Time Series Record Comprised of Tidal Signals Only	15 Day Analysis		1	25.000	3.6927	297.5	5.2474	179.1	9.0649	220.3	4.2249	69.9
	Direct Inclusion of all Constituents	Mean	2	25.000	3.6921	297.5	5.2473	179.1	9.0640	220.3	4.2254	69.9
		Standard Deviation		0.000	0.0053	0.0	0.0021	0.1	0.0033	0.0	0.0022	0.0
	Direct Inclusion of only Z_0, K_1, M_2	Mean	3	25.043	-	-	6.1607	179.4	9.5420	220.4	-	-
		Standard Deviation		0.056	-	-	2.5702	32.0	3.0983	19.6	-	-
	Direct Inclusion of Z_0, K_1, M_2, Inference of O_1, S_2	Mean	4	25.043	3.7212	298.7	5.2879	180.3	9.0395	220.3	4.2130	69.8
		Standard Deviation		0.056	0.1167	2.5	0.1658	2.5	0.1267	0.5	0.0590	0.5
Time Series Record Comprised of Tidal Signals and Uniform [-2.5,2.5] Random Noise	15 Day Analysis		5	24.998	3.6464	296.5	5.3706	178.4	9.0095	220.5	4.3133	70.9
	Direct Inclusion of all Constituents	Mean	6	24.982	3.6099	292.4	5.4752	178.6	9.5465	222.1	5.1590	75.5
		Standard Deviation		0.171	0.7488	5.0	0.6763	7.0	1.2292	4.8	0.9437	9.7
	Direct Inclusion of only Z_0, K_1, M_2	Mean	7	25.025	-	-	6.1948	178.3	9.4681	220.2	-	-
		Standard Deviation		0.150	-	-	2.6406	29.2	3.2069	19.5	-	-
	Direct Inclusion of Z_0, K_1, M_2 Inference of O_1, S_2	Mean	8	25.025	3.6014	297.2	5.3043	179.1	8.9170	220.1	4.2690	70.5
		Standard Deviation		0.150	0.2047	3.8	0.3016	3.8	0.2915	1.8	0.1395	1.8

Amplitudes in metres; phases in degrees

(Corresponding values for C(A), the normalized condition numbers routinely included in the harmonic analysis program output, were 0.9697 and 0.0069.) The average value of $\|\delta b\|/\|b\|$ for the six runs of Test 6 was 0.0531 while, for Test 7, it was 0.0479. Consequently, applying equation (21), we anticipate a maximum change in C_j and S_j (§4) of 638% in the direct inclusion case and 13.8% when inference is used (assuming accurate inference constants are available).

However, for most tidal analyses, equation (21) cannot be applied, since $\|\delta b\|/\|b\|$ is unknown. Munk and Hasselmann (1964) derive a more useful formula for estimating the amplitude variances of close constituents in the presence of noise. Specifically, if the underlying noise spectrum is $S(\sigma)$ and the two neighbouring constituents have frequencies σ_1 and σ_2, then the estimated variance of either amplitude is $3\, S(\sigma)\pi^{-2}\, |\sigma_2 - \sigma_1|^{-2} T^{-3}$. Applying this result to the previous test data yields expected standard deviations of 0.576 and 0.622 in the O_1/K_1 and M_2/S_2 amplitude ratios, respectively. Although these values are much closer to those in Table 2 than the upper bound estimate derived from equation (21), it should be noted that they are all underestimates.

For actual sea-level observations, Munk and Bullard (1963) estimate the geophysical noise level (due mainly to atmospheric excitation) at tidal frequencies to be $S(\sigma) = 1$ cm^2/(cycle per day). Applying this value to a 30-day harmonic analysis in which both P_1 and K_1 are sought directly (these constituents require 183 days to differ by one cycle) yields an expected standard deviation of 0.613 cm in either amplitude. However, a sequence of twelve-monthly analyses at Prince Rupert, in which both P_1 and K_1 (and three other constituent pairs that also require approximately six months to differ by one cycle) was sought directly, produced standard deviation estimates of 17.2 and 18.4 cm, respectively, for the amplitudes. Thus, in this case, $S(\sigma) = 1$ cm^2/(cycle per day) is a gross underestimate. It is worth noting that, with accurate inference parameters, the two amplitude standard deviations, after inference, reduce to 0.54 and 1.72 cm, respectively. (In each case, this is 3.3% of the amplitude.)

PART III. COMPUTER PROGRAM FOR HIGH-LOW ANALYSIS.

6. GENERAL DESCRIPTION OF PROGRAM.

This program analyses irregularly-sampled tidal heights observations over a specified period of time. Although these observations are normally taken at high and low water, the program can also be used when the observations are not extreme values. Amplitudes and Greenwich phase lags are calculated for all requested constituents by a least squares fit method (§4), coupled with nodal modulation (§5.1). If the record length is such that certain important constituents cannot be resolved satisfactorily by including them directly in the least squares fit, provision is made for inference of their amplitudes and phases (§5.3).

6.1 Routines Required.

(1) MAIN ..... reads input data, controls all output and calls other routines.

(2) MGS ..... does a least squares fit (with the Modified Gram-Schmidt Algorithm) to find coefficients of the sine and cosine terms corresponding to each of the specified constituent frequencies.

(3) VUF ..... reads required information and calculates the nodal and astronomical argument corrections for all constituents.

(4) INFER ..... reads required information and calculates the amplitude and phase of requested inferred constituents, as well as adjusting the amplitude and phase of the constituents used for inference.

(5) CDAY ..... returns the consecutive day number from a specific origin for any given date in the range 1901 to 1999, and vice versa.

Routines VUF, INFER and CDAY are identical to those of the same name in the tidal heights analysis program used for hourly observations (Foreman, 1977).

6.2 Data Input.

Three files or devices are used for input. File reference number 8 contains the tidal constituent information that is necessary for the nodal and astronomical argument calculations; file inference number 9 contains the observed tidal heights and their times; and file reference number 5 contains analysis type and tidal station information. A listing of file reference number 8, along with sample input corresponding to file reference numbers 9 and 5, are given in Appendices 3, 4 and 5, respectively.

I. File reference number 8 is a subset of the similarly-numbered file in Foreman (1977 §1.3). For most analyses, its contents should not require changing (see 6.4 for the circumstances under which this file might be changed). It contains the following three types of data, and is read in through entry point OPNVUF of subroutine VUF.

(i) Two cards specifying values for the astronomical arguments SO, HO, PO, ENPO, PPO, DS, DH, DP, DNP, DPP in the format (5F13.10).

SO - mean longitude of the moon (cycles) at the reference time origin.

HO - mean longitude of the sun (cycles) at the reference time origin.

PO - mean longitude of the lunar perigee (cycles) at the reference time origin.

ENPO - negative of the mean longitude of the ascending node (cycles) at the reference time origin.

PPO - mean longitude of the solar perigee (perihelion) at the reference time origin.

DS, DH, DP, DNP, DPP are their respective rates of change over a 365-day period at the reference time origin.

(ii) At least one card for all the main tidal constituents specifying their Doodson numbers and phase shift, along with as many cards as are necessary for the satellite constituents. The first card for each such constituent is in the format (6X, A5, 1X, 6I3, F5.2, I4) and contains the following information :

KON	= constituent name;
II,JJ,KK,LL,MM,NN	= the six Doodson numbers for KON;
SEMI	= the phase correction for KON;
NJ	= the number of satellite constituents.

A blank card terminates this data type.

If NJ > 0, information on the satellite constituents follows, three satellites per card, in the format (11X,3(3I3,F4.2,F7.4,IX,I1,1X)). For each satellite the values read are :

LDEL,MDEL, NDEL	= the last three Doodson numbers of the main constituent subtracted from the last three Doodson numbers of the satellite constituent;
PH	= the phase correction of the satellite constituent relative to the phase of the main constituent;
EE	= the amplitude ratio of the satellite tidal potential to that of the main constituent.

IR = 1 if the amplitude ratio has to be multiplied by the latitude correction factor for diurnal constituents,

= 2 if the amplitude ratio has to be multiplied by the latitude correction factor for semi-diurnal constituents,

= otherwise if no correction is required to the amplitude ratio.

(iii) One card specifying each of the shallow water constituents and the main constituents from which they are derived. The format is (6X,A5,I1,2X,4(F5.2,A5,5X)) and the respective values read are:

KON = the name of the shallow water constituent;

NJ = the number of main constituents from which it is derived;

COEF,KONCO = combination number and name of these main constituents.

The end of these shallow water constituents is denoted by a blank card.

II. File reference number 9 contains only one type of data, the observed tidal heights and times. For convenience, the input format was chosen to be the same as the daily high-low output produced by the tidal heights *prediction* program (Foreman, 1977, p.54). Specifically, each record has the format (2X,I5,2I3,I2,6(I3,I2,F5.1)) and contains the following information:

ISTN = tidal station number;

ID,IM,IY = day, month, and year of subsequent observations;

ITH,ITM,HT = times (in hours and minutes), and height, of up to six observations for the specified date. If there are less than six observations for a day, they are padded to that number with the values 99,99 and 99.9 for the times and heights, respectively. If there are more than six observations on a given day, as many records are included as necessary, each with the same repeated date.

Missing days and/or missing observations (highs,lows) are permissible.

However, it is necessary that the records be ordered according to date.

III. File reference number 5 contains five types of data.

(i) One record for the variables MF,IDERV,WT in the format (2I5,F5.2).

MF = the number of constituents, including the constant term, Z_o, to be included in the least squares fit.

IDERV = 1 if all observations are extreme values and it is desired to use the derivative conditions in the least squares fit,

= 0 otherwise.

WT = the weight to be applied to the derivative condition when IDERV = 1. A recommended value is WT = 1.0.

(ii) One record for each of the MF constituents to be included in the fit. Each record contains the variables NAME and FREQ in the format (A5,2X,F13.10). NAME is the constituent name, which should be left-justified in the alphanumeric field, while FREQ is its frequency measured in cycles per hour. In order that there be sufficient information available to calculate the astronomical argument and nodal corrections, all these constituents must be included in the list given in Appendix 2. The order in which the constituents are input is also the order in which the results are output. The constant term Z_o must be first.

(iii) One record in the format (6(3X,I2)) containing the following information on the time period of the analysis:

ID1,IM1,IY1 - day, month, year of the beginning of the analysis period;

ID2,IM2,IY2 - day, month, year of the end of the analysis period.

(iv) One record in the format (I5,5A4,1X,A4,4I5) containing the following tidal station information:

JSTN = tidal station number;

(NSTN(I),I=1,5)= tidal station name;

ITZ = time zone in which the observations were recorded;

LATD,LATM = station latitude in degrees and minutes;

LOND,LONM = station longitude in degrees and minutes.

(v) One record for each possible inference pair. The format is (2(4X,A5,E16.10),2F10.3) and the respective values read (through entry point OPNINF of subroutine INFER) are:

KONAN and SIGAN = the name and frequency of the analysed constituent to be used for the inference;

KONIN and SIGIN = the name and frequency of the inferred constituent;

R = amplitude ratio of KONIN to KONAN;

ZETA = the Greenwich phase lag of the inferred constituent subtracted from the Greenwich phase lag of the analysed constituent.

These are terminated by one blank record.

As before, constituent names should be left-justified in the alphanumeric field, frequencies are measured in cycles per hour, and all constituents must belong to the list in Appendix 2.

6.3 Output.

At present, only line printer (file reference number 6) output is produced by the high-low analysis program. The first page simply echoes the requested constituents to be included in the fit, the analysis period and tidal station information, and the heights and times of the observed heights. The second page notes whether or not the derivative conditions were used for all observations and, if so, the value of the requested weight. It also gives the following direct results from the least squares fit: Z_o amplitude and coefficients of the cosine and sine terms of all other constituents; the largest residual value in the overdetermined system of the equations and the residual sum of squares; the standard deviation of the right-hand sides of the overdetermined system and the root mean square residual error. The third and final page gives the raw amplitudes and raw local phases followed by the nodally-corrected amplitudes and Greenwich phases for all constituents. If there has been inference, these values are repeated with correction, and the new residual root mean square value is specified.

In the event that a least squares solution cannot be found because a dependent column is encountered during the orthoganalization procedure, a message to this effect along with the suggested corrective procedure is printed. If the column dependency is borderline, a slight increase in the value of the variable TOLER may be sufficient to obtain the solution. However, it is generally better to remove from the least squares analysis, the constituent (or its nearest neighbour, depending on which one has the smaller expected amplitude) corresponding to this tidal coefficient parameter. That is, if column 2n-1 or 2n is dependent, then remove constituent n or its nearest neighbour. If inference parameters are available, the amplitude and phase for this constituent can still be obtained indirectly through inference.

The final page of output produced by the sample data input found in Appendices 3, 4 and 5 is listed in Appendix 6.

6.4 Program Conversion, Storage and Dimension Guidelines.

The high-low analysis program was tested on the UNIVAC 1106 computer installation at the Institute of Ocean Sciences, Patricia Bay. Although the program was written in basic ASCII FORTRAN, some changes may be required before it can be used on other installations. These may include:

(i) replacing all calls to routine INPROD in subroutine MGS when the FORTRAN compiler does not permit a single column of a two-dimensional array to be passed to a one-dimensional array through a subroutine call. Such changes will not be necessary when FORTRAN compilers store two-dimensional arrays by columns (and this is the standard FORTRAN convention). However, if this condition is not met, the INPROD calls are located in lines 102, 122, 135, 156 and 173 of subroutine MGS and the replacement code is specified in the comment statements preceding these CALL statements.

(ii) deleting some or all REAL*8 declaration statements. These are used either to permit alphanumeric strings longer than 4 characters (which is the ASCII FORTRAN single precision word-length) to be used (e.g. constituent names are read in A5 format), or to gain computational precision in the average, standard deviation, and vector inner product calculations. CDC installations may not require double precision variables for the latter of these cases because their single precision accuracy is about 1.5 times that for IBM and UNIVAC (= 8.1 digits), and do not require them for the former because their single precision word-length of six characters is longer than the maximum alphanumeric string size of 5 required by this program.

(iii) altering the variable list structure for the ENTRY statements OPNINF and OPNVUF, and references to them.

(iv) changing some, or all of the file reference (or device) numbers from their present values, in order to conform with local machine restrictions.

(v) altering the input tolerance, variable TOLER, for the Modified Gram-Schmidt routine. If the inner product of an orthogonalized column with itself is less than TOLER, the column is considered to be dependent. Typically, TOLER is chosen to be less than 10**(-D) where D represents the number of decimal digits of accuracy available. However, if the overdetermined matrix is poorly scaled, it may be necessary to either choose a much larger value or remove the corresponding constituent from the analysis. On the UNIVAC, a conservative value of 10**(-7) was chosen for TOLER.

The program, in its present form,requires approximately 3000 and 73000 UNIVAC words for the storage of its instructions and arrays, respectively.

A large part of this is for the array Q which stores the overdetermined system of linear equations and is presently dimensioned to handle approximately 800 observations with the derivative condition and 20 constituents. If the analysis is much smaller than this and memory requirements are restrictive on a particular installation, or there is a need to economize, the program size can be cut significantly by reducing the size of this array and resetting variables NMAXP1 and NMAXPM appropriately.

In the event that changes are required to the program, restrictions on the minimum dimension of all arrays and minimal values of special parameters are as follows:

Let

MC be the total number of constituents, including Z_o and any inferred constituents;

NOBS be the number of tidal height observations;

NR be the number of input records of observed tidal heights.

MPAR be 2*MC - 1.

NEQ be NOBS*2 if all the observations are extremes and the derivative condition is to be included for each, and NOBS otherwise.

Then, in the main program, parameters MXNDAY, NMAXP1 and NMAXPM should be at least NR, MPAR + 1, and NEQ + MPAR respectively; arrays FREQ, NAME, AMP, PH, AMPC, and PHG should have minimum dimension MC; arrays X and Y should have minimum dimension NOBS; arrays ITH, ITM, and HT should have minimum dimension 6; array P should have minimum dimension MPAR; and array Q should have the exact dimension of NMAXPM by NMAXP1. In subroutine MGS, arrays Q and X have variable dimensions, and should be the same as Q and P in the main program.

The dimensions of any array in subroutine VUF need only be changed if a new constituent is to be added to the list in Appendix 2. In such an event, the contents of the data file associated with file reference number 8 must also be augmented in order to permit calculation of astronomical argument and nodal corrections for this constituent. In order to understand the structure of this file and the resultant calculations, consult Foreman (1977). Restrictions on the minimal array dimensions can be found there, also, as well as in the comment statements of the subroutine itself.

In subroutine INFER, array KON is passed in the argument list from the main program and so need only be dimensioned 2; and arrays KONAN, SIGAN, KONIN, SIGIN, R and ZETA can presently accommodate a maximum of 9 inferred constituents.

In subroutine CDAY, arrays NDP and NDM should have dimension 12.

Appendix 1

Results of 12-month Hourly Height Harmonic Analysis at Prince Rupert

ANALYSIS OF HOURLY TIDAL HEIGHTS STN 9354 1H 1/ 1/74 TO 24H 31/12/74
NO.OBS.= 8760 NO.PTS.ANAL.= 8760 MIDPT=12H 2/ 7/74 SEPARATION = .97

NO	NAME	FREQUENCY	STN	M-Y/ M-Y	A	G	AL	GL
1	Z0	.00000000	9354	174/1274	3.8714	.00	3.8714	.00
2	SA	.00011407	9354	174/1274	.0914	16.54	.0914	198.90
3	SSA	.00022816	9354	174/1274	.0382	123.29	.0382	282.99
4	MSM	.00130978	9354	174/1274	.0407	168.78	.0407	349.98
5	MM	.00151215	9354	174/1274	.0315	117.93	.0315	350.31
6	MSF	.00282193	9354	174/1274	.0186	138.21	.0186	191.79
7	MF	.00305009	9354	174/1274	.0262	115.87	.0262	329.15
8	ALP1	.03439657	9354	174/1274	.0032	160.44	.0033	202.92
9	2Q1	.03570635	9354	174/1274	.0084	133.10	.0086	358.08
10	SIG1	.03590872	9354	174/1274	.0105	123.66	.0105	37.34
11	Q1	.03721850	9354	174/1274	.0539	126.49	.0541	222.52
12	RHO1	.03742087	9354	174/1274	.0124	148.42	.0125	291.94
13	O1	.03873065	9354	174/1274	.3125	132.46	.3069	99.73
14	TAU1	.03895881	9354	174/1274	.0030	229.33	.0030	171.87
15	BET1	.04004044	9354	174/1274	.0029	117.40	.0028	88.26
16	NO1	.04026859	9354	174/1274	.0262	154.12	.0267	226.77
17	CHI1	.04047097	9354	174/1274	.0028	93.30	.0028	247.84
18	P11	.04143851	9354	174/1274	.0062	132.25	.0062	319.60
19	P1	.04155259	9354	174/1274	.1606	135.83	.1609	145.25
20	S1	.04166667	9354	174/1274	.0239	116.03	.0166	273.30
21	K1	.04178075	9354	174/1274	.5144	139.48	.5096	120.39
22	PSI1	.04189482	9354	174/1274	.0075	175.39	.0074	346.53
23	PHI1	.04200891	9354	174/1274	.0090	105.80	.0090	255.21
24	THE1	.04309053	9354	174/1274	.0048	177.12	.0048	334.56
25	J1	.04329290	9354	174/1274	.0274	150.35	.0289	355.64
26	SO1	.04460268	9354	174/1274	.0064	185.40	.0063	218.25
27	OO1	.04483084	9354	174/1274	.0157	162.82	.0150	313.97
28	UPS1	.04634299	9354	174/1274	.0015	193.89	.0014	227.14
29	OQ2	.07597494	9354	174/1274	.0030	338.98	.0036	312.64
30	EPS2	.07617732	9354	174/1274	.0097	12.04	.0104	33.79
31	2N2	.07748710	9354	174/1274	.0437	350.01	.0484	194.66

32	MU2	.07768947	9354	174/1274	.0400	8.25	.0410	259.91
33	N2	.07899925	9354	174/1274	.3952	14.90	.3982	86.61
34	NU2	.07920162	9354	174/1274	.0766	16.53	.0774	139.60
35	H1	.08039733	9354	174/1274	.0119	33.41	.0125	335.32
36	M2	.08051140	9354	174/1274	1.9564	35.79	1.9730	340.04
37	H2	.08062547	9354	174/1274	.0213	351.04	.0214	118.61
38	MKS2	.08073956	9354	174/1274	.0052	263.28	.0050	349.19
39	LDA2	.08182118	9354	174/1274	.0134	25.99	.0136	331.13
40	L2	.08202355	9354	174/1274	.0507	40.61	.0514	23.76
41	T2	.08321926	9354	174/1274	.0367	47.98	.0367	225.62
42	S2	.08333333	9354	174/1274	.6446	59.26	.6444	59.38
43	R2	.08344741	9354	174/1274	.0051	210.45	.0063	208.38
44	K2	.08356149	9354	174/1274	.1738	50.65	.1658	192.44
45	MSN2	.08484549	9354	174/1274	.0069	178.48	.0070	51.13
46	ETA2	.08507364	9354	174/1274	.0088	67.09	.0096	67.00
47	MO3	.11924206	9354	174/1274	.0065	50.14	.0064	321.65
48	M3	.12076710	9354	174/1274	.0208	344.58	.0210	81.09
49	SO3	.12206399	9354	174/1274	.0017	199.42	.0017	166.81
50	MK3	.12229215	9354	174/1274	.0036	11.20	.0036	296.36
51	SK3	.12511408	9354	174/1274	.0176	139.35	.0174	120.38
52	MN4	.15951065	9354	174/1274	.0031	221.55	.0031	237.51
53	M4	.16102280	9354	174/1274	.0060	248.95	.0061	137.45
54	SN4	.16233258	9354	174/1274	.0012	263.18	.0012	335.02
55	MS4	.16384473	9354	174/1274	.0023	267.35	.0024	211.71
56	MK4	.16407289	9354	174/1274	.0018	209.96	.0018	295.99
57	S4	.16666667	9354	174/1274	.0020	249.54	.0020	249.78
58	SK4	.16689483	9354	174/1274	.0019	246.62	.0018	28.52
59	2MK5	.20280355	9354	174/1274	.0043	231.69	.0043	101.10
60	2SK5	.20844741	9354	174/1274	.0004	180.85	.0004	162.00
61	2MN6	.24002205	9354	174/1274	.0019	151.41	.0020	111.62
62	M6	.24153420	9354	174/1274	.0031	173.43	.0032	6.17
63	2MS6	.24435613	9354	174/1274	.0027	199.67	.0027	88.28
64	2MK6	.24458429	9354	174/1274	.0012	183.55	.0011	213.83
65	2SM6	.24717807	9354	174/1274	.0004	172.66	.0004	117.15
66	MSK6	.24740623	9354	174/1274	.0004	210.72	.0004	296.87
67	3MK7	.28331495	9354	174/1274	.0018	294.16	.0018	107.82
68	M8	.32204560	9354	174/1274	.0028	224.80	.0029	1.79

Appendix 2

List of Possible Constituents (And Their Frequencies) In the High-Low Computer Program Analysis

Z0	0.0
SSA	0.0002281591
MM	0.0015121518
MF	0.0030500918
2Q1	0.0357063507
Q1	0.0372185026
O1	0.0387306544
BET1	0.0400404353
CHI1	0.0404709654
P1	0.0415525871
K1	0.0417807462
PHI1	0.0420089053
J1	0.0432928981
S01	0.0446026789
UPS1	0.0463429898
2NS2	0.0746651643
ST1	0.0748933234
EPS2	0.0761773161
ST3	0.0772331498
2N2	0.0774870970
SNK2	0.0787710897
NU2	0.0792016198
OP2	0.0802832416
H1	0.0803973266
H2	0.0806254748
ST5	0.0809677189
LDA2	0.0818211815
2SK2	0.0831051742
S2	0.0833333333
K2	0.0835614924
ETA2	0.0850736443
2SM2	0.0861552660
SKM2	0.0863834251
NO3	0.1177299033
SA	0.0001140741
MSM	0.0013097808
MSF	0.0028219327
ALP1	0.0343965699
SIG1	0.0359087218
RHO1	0.0374208736
TAU1	0.0389588136
NO1	0.0402685944
PI1	0.0414385130
S1	0.0416666721
PSI1	0.0418948203
THE1	0.0430905270
2PO1	0.0443745198
OO1	0.0448308380
ST36	0.0733553835
ST37	0.0748675353
OQ2	0.0759749451
ST2	0.0764054753
O2	0.0774613089
MU2	0.0776894680
N2	0.0789992488
ST4	0.0794555670
GAM2	0.0803090296
M2	0.0805114007
MKS2	0.0807395598
ST6	0.0815930224
L2	0.0820235525
T2	0.0832192592
R2	0.0834474074
MSN2	0.0848454852
ST7	0.0853018034
ST38	0.0863576370
2SN2	0.0876674179
MO3	0.1192420551

M3	0.1207671010
SO3	0.1220639878
SP3	0.1248859204
ST8	0.1566887168
3MS4	0.1582008687
MN4	0.1595106495
ST40	0.1607946422
ST10	0.1612509604
KN4	0.1625607413
MK4	0.1640728931
S4	0.1666666667
MNO5	0.1982413039
3MP5	0.1999816149
2MP5	0.2025753884
MSK5	0.2056254802
2SK5	0.2084474129
2NM6	0.2385098983
2MN6	0.2400220501
ST41	0.2413060429
MSN6	0.2428439828
ST42	0.2441279756
2MK6	0.2445842938
2SM6	0.2471780673
S6	0.2500000000
ST15	0.2802906445
ST16	0.2830867891
ST17	0.2861368809
3MN8	0.3205334508
M8	0.3220456027
ST21	0.3235835426
3MK8	0.3250956944
ST23	0.3276894680
ST25	0.3608020452
4MK9	0.3638263489
ST28	0.4010448515
ST29	0.4038667841
ST31	0.4069168759
ST33	0.4471596822
ST34	0.4858903367
NK3	0.1207799950
MK3	0.1222921469
SK3	0.1251140796
N4	0.1579984976
ST39	0.1592824904
ST9	0.1597388086
M4	0.1610228013
SN4	0.1623325821
MS4	0.1638447340
SL4	0.1653568858
SK4	0.1668948258
2MO5	0.1997534558
MNK5	0.2012913957
2MK5	0.2028035475
3KM5	0.2058536393
ST11	0.2372259056
ST12	0.2387380574
ST13	0.2402502093
M6	0.2415342020
MKN6	0.2430721419
2MS6	0.2443561347
NSK6	0.2458940746
MSK6	0.2474062264
ST14	0.2787527046
M7	0.2817899023
3MK7	0.2833149482
ST18	0.3190212990
ST19	0.3207616099
ST20	0.3233553835
3MS8	0.3248675353
ST22	0.3264054753
ST24	0.3279176271
ST26	0.3623141970
ST27	0.3666482815
M10	0.4025570033
ST30	0.4053789360
ST32	0.4082008687
M12	0.4830684040
ST35	0.4874282766

Appendix 3

Data Input on File Reference Number 8 For the Computer Program

```
  .7428797055   .7771900329   .5187051308   .3631582592   .7847990160  000GMT 1/1/76
13.3594019864   .9993368945   .1129517942   .0536893056   .0000477414  INCR./365DAYS
      Z0       0  0  0  0  0  0 0.0     0
      SA       0  0  1  0  0 -1 0.0     0
      SSA      0  0  2  0  0  0 0.0     0
      MSM      0  1 -2  1  0  0  .00     0
      MM       0  1  0 -1  0  0 0.0     0
      MSF      0  2 -2  0  0  0 0.0     0
      MF       0  2  0  0  0  0 0.0     0
      ALP1     1 -4  2  1  0  0 -.25    2
      ALP1    -1  0  0 .75 0.0360R1     0 -1  0 .00 0.1906
      2Q1      1 -3  0  2  0  0-0.25    5
      2Q1     -2 -2  0 .50 0.0063      -1 -1  0 .75 0.0241R1  -1  0  0 .75 0.0607R1
      2Q1      0 -2  0 .50 0.0063       0 -1  0 .0  0.1885
      SIG1     1 -3  2  0  0  0-0.25    4
      SIG1    -1  0  0 .75 0.0095R1     0 -2  0 .50 0.0061      0 -1  0 .0  0.1884
      SIG1     2  0  0 .50 0.0087
      Q1       1 -2  0  1  0  0-0.25   10
      Q1      -2 -3  0 .50 0.0007      -2 -2  0 .50 0.0039     -1 -2  0 .75 0.0010R1
      Q1      -1 -1  0 .75 0.0115R1    -1  0  0 .75 0.0292R1    0 -2  0 .50 0.0057
      Q1      -1  0  1 .0  0.0008       0 -1  0 .0  0.1884      1  0  0 .75 0.0018R1
      Q1       2  0  0 .50 0.0028
      RHO1     1 -2  2 -1  0  0-0.25    5
      RHO1     0 -2  0 .50 0.0058       0 -1  0 .0  0.1882      1  0  0 .75 0.0131R1
      RHO1     2  0  0 .50 0.0576       2  1  0 .0  0.0175
      O1       1 -1  0  0  0  0-0.25    8
      O1      -1  0  0 .25 0.0003R1     0 -2  0 .50 0.0058      0 -1  0 .0  0.1885
      O1       1 -1  0 .25 0.0004R1     1  0  0 .75 0.0029R1    1  1  0 .25 0.0004R1
      O1       2  0  0 .50 0.0064       2  1  0 .50 0.0010
      TAU1     1 -1  2  0  0  0-0.75    5
      TAU1    -2  0  0 .0  0.0446      -1  0  0 .25 0.0426R1    0 -1  0 .50 0.0284
      TAU1     0  1  0 .50 0.2170       0  2  0 .50 0.0142
      BET1     1  0 -2  1  0  0 -.75    1
```

```
BET1    0 -1  0 .00 0.2266
NO1      1  0  0  1  0  0-0.75   9
NO1    -2 -2  0 .50 0.0057    -2 -1  0 .0  0.0665    -2  0  0 .0  0.3596
NO1    -1 -1  0 .75 0.0331R1  -1  0  0 .25 0.2227R1  -1  1  0 .75 0.0290R1
NO1     0 -1  0 .50 0.0290     0  1  0 .0  0.2004     0  2  0 .50 0.0054
CHI1     1  0  2 -1  0  0-0.75   2
CHI1    0 -1  0 .50 0.0282     0  1  0 .0  0.2187
PI1      1  1 -3  0  0  1-0.25   1
PI1     0 -1  0 .50 0.0078
P1       1  1 -2  0  0  0-0.25   6
P1      0 -2  0 .0  0.0008     0 -1  0 .50 0.0112     0  0  2 .50 0.0004
P1      1  0  0 .75 0.0004R1   2  0  0 .50 0.0015     2  1  0 .50 0.0003
S1       1  1 -1  0  0  1-0.75   2
S1      0  0 -2 .0  0.3534     0  1  0 .50 0.0264
K1       1  1  0  0  0  0-0.75  10
K1     -2 -1  0 .0  0.0002    -1 -1  0 .75 0.0001R1 -1  0  0 .25 0.0007R1
K1     -1  1  0 .75 0.0001R1   0 -2  0 .0  0.0001     0 -1  0 .50 0.0198
K1      0  1  0 .0  0.1356     0  2  0 .50 0.0029     1  0  0 .25 0.0002R1
K1      1  1  0 .25 0.0001R1
PSI1     1  1  1  0  0 -1-0.75   1
PSI1    0  1  0 .0  0.0190
PHI1     1  1  2  0  0  0-0.75   5
PHI1   -2  0  0 .0  0.0344    -2  1  0 .0  0.0106     0  0 -2 .0  0.0132
PHI1    0  1  0 .50 0.0384     0  2  0 .50 0.0185
THE1     1  2 -2  1  0  0 -.75   4
THE1   -2 -1  0 .00  .0300    -1  0  0 .25 0.0141R1   0 -1  0 .50  .0317
THE1    0  1  0 .00  .1993
J1       1  2  0 -1  0  0-0.75  10
J1      0 -1  0 .50 0.0294     0  1  0 .0  0.1980     0  2  0 .50 0.0047
J1      1 -1  0 .75 0.0027R1   1  0  0 .25 0.0816R1   1  1  0 .25 0.0331R1
J1      1  2  0 .25 0.0027R1   2  0  0 .50 0.0152     2  1  0 .50 0.0098
J1      2  2  0 .50 0.0057
001      1  3  0  0  0  0-0.75   8
001    -2 -1  0 .50 0.0037    -2  0  0 .0  0.1496    -2  1  0 .0  0.0296
001    -1  0  0 .25 0.0240R1  -1  1  0 .25 0.0099R1   0  1  0 .0  0.6398
001     0  2  0 .0  0.1342     0  3  0 .0  0.0086
UPS1     1  4  0 -1  0  0 -.75   5
UPS1   -2  0  0 .00 0.0611     0  1  0 .00 0.6399     0  2  0 .00 0.1318
UPS1    1  0  0 .25 0.0289R1   1  1  0 .25 0.0257R1
OQ2      2 -3  0  3  0  0 0.0    2
```

```
OQ2    -1  0  0 .25 0.1042R2    0 -1  0 .50 0.0386
EPS2     2 -3  2  1  0  0 0.0     3
EPS2   -1 -1  0 .25 0.0075R2  -1  0  0 .25 0.0402R2    0 -1  0 .50 0.0373
2N2      2 -2  0  2  0  0 0.0     4
2N2    -2 -2  0 .50 0.0061     -1 -1  0 .25 0.0117R2  -1  0  0 .25 0.0678R2
2N2     0 -1  0 .50 0.0374
MU2      2 -2  2  0  0  0 0.0     3
MU2    -1 -1  0 .25 0.0018R2  -1  0  0 .25 0.0104R2    0 -1  0 .50 0.0375
N2       2 -1  0  1  0  0 0.0     4
N2     -2 -2  0 .50 0.0039     -1  0  1 .00 0.0008     0 -2  0 .00 0.0005
N2      0 -1  0 .50 0.0373
NU2      2 -1  2 -1  0  0 0.0     4
NU2     0 -1  0 .50 0.0373      1  0  0 .75 0.0042R2   2  0  0 .0  0.0042
NU2     2  1  0 .50 0.0036
GAM2     2  0 -2  2  0  0 -.50    3
GAM2   -2 -2  0 .00 0.1429     -1  0  0 .25 0.0293R2   0 -1  0 .50 0.0330
H1       2  0 -1  0  0  1-0.50    2
H1      0 -1  0 .50 0.0224      1  0 -1 .50 0.0447
M2       2  0  0  0  0  0 0.0     9
M2     -1 -1  0 .75 0.0001R2  -1  0  0 .75 0.0004R2   0 -2  0 .0  0.0005
M2      0 -1  0 .50 0.0373      1 -1  0 .25 0.0001R2   1  0  0 .75 0.0009R2
M2      1  1  0 .75 0.0002R2   2  0  0 .0  0.0006     2  1  0 .0  0.0002
H2       2  0  1  0  0 -1 0.0     1
H2      0 -1  0 .50 0.0217
LDA2     2  1 -2  1  0  0-0.50    1
LDA2    0 -1  0 .50 0.0448
L2       2  1  0 -1  0  0-0.50    5
L2      0 -1  0 .50 0.0366      2 -1  0 .00 0.0047     2  0  0 .50 0.2505
L2      2  1  0 .50 0.1102      2  2  0 .50 0.0156
T2       2  2 -3  0  0  1 0.0     0
S2       2  2 -2  0  0  0 0.0     3
S2      0 -1  0 .0  0.0022      1  0  0 .75 0.0001R2   2  0  0 .0  0.0001
R2       2  2 -1  0  0 -1-0.50    2
R2      0  0  2 .50 0.2535      0  1  2 .0  0.0141
K2       2  2  0  0  0  0 0.0     5
K2     -1  0  0 .75 0.0024R2  -1  1  0 .75 0.0004R2   0 -1  0 .50 0.0128
K2      0  1  0 .0  0.2980      0  2  0 .0  0.0324
ETA2     2  3  0 -1  0  0 0.0     7
ETA2    0 -1  0 .50 0.0187      0  1  0 .0  0.4355     0  2  0 .0  0.0467
ETA2    1  0  0 .75 0.0747R2   1  1  0 .75 0.0482R2   1  2  0 .75 0.0093R2
```

```
ETA2    2  0  0 .50 0.0078
M3       3  0  0  0  0  0 -.50   1
M3      0 -1  0 .50  .0564

2P01 2   2.0 P1        -1.0 O1
S01  2   1.0 S2        -1.0 O1
ST36 3   2.0 M2         1.0 N2       -2.0 S2
2NS2 2   2.0 N2        -1.0 S2
ST37 2   3.0 M2        -2.0 S2
ST1  3   2.0 N2         1.0 K2       -2.0 S2
ST2  4   1.0 M2         1.0 N2        1.0 K2       -2.0 S2
ST3  3   2.0 M2         1.0 S2       -2.0 K2
O2   1   2.0 O1
ST4  3   2.0 K2         1.0 N2       -2.0 S2
SNK2 3   1.0 S2         1.0 N2       -1.0 K2
OP2  2   1.0 O1         1.0 P1
MKS2 3   1.0 M2         1.0 K2       -1.0 S2
ST5  3   1.0 M2         2.0 K2       -2.0 S2
ST6  4   2.0 S2         1.0 N2       -1.0 M2      -1.0 K2
2SK2 2   2.0 S2        -1.0 K2
MSN2 3   1.0 M2         1.0 S2       -1.0 N2
ST7  4   2.0 K2         1.0 M2       -1.0 S2      -1.0 N2
2SM2 2   2.0 S2        -1.0 M2
ST38 3   2.0 M2         1.0 S2       -2.0 N2
SKM2 3   1.0 S2         1.0 K2       -1.0 M2
2SN2 2   2.0 S2        -1.0 N2
NO3  2   1.0 N2         1.0 O1
MO3  2   1.0 M2         1.0 O1
NK3  2   1.0 N2         1.0 K1
SO3  2   1.0 S2         1.0 O1
MK3  2   1.0 M2         1.0 K1
SP3  2   1.0 S2         1.0 P1
SK3  2   1.0 S2         1.0 K1
ST8  3   2.0 M2         1.0 N2       -1.0 S2
N4   1   2.0 N2
3MS4 2   3.0 M2        -1.0 S2
ST39 4   1.0 M2         1.0 S2        1.0 N2       -1.0 K2
MN4  2   1.0 M2         1.0 N2
ST40 3   2.0 M2         1.0 S2       -1.0 K2
ST9  4   1.0 M2         1.0 N2        1.0 K2       -1.0 S2
```

M4	1	2.0	M2						
ST10	3	2.0	M2	1.0	K2	-1.0	S2		
SN4	2	1.0	S2	1.0	N2				
KN4	2	1.0	K2	1.0	N2				
MS4	2	1.0	M2	1.0	S2				
MK4	2	1.0	M2	1.0	K2				
SL4	2	1.0	S2	1.0	L2				
S4	1	2.0	S2						
SK4	2	1.0	S2	1.0	K2				
MNO5	3	1.0	M2	1.0	N2	1.0	O1		
2MO5	2	2.0	M2	1.0	O1				
3MP5	2	3.0	M2	-1.0	P1				
MNK5	3	1.0	M2	1.0	N2	1.0	K1		
2MP5	2	2.0	M2	1.0	P1				
2MK5	2	2.0	M2	1.0	K1				
MSK5	3	1.0	M2	1.0	S2	1.0	K1		
3KM5	3	1.0	K2	1.0	K1	1.0	M2		
2SK5	2	2.0	S2	1.0	K1				
ST11	3	3.0	N2	1.0	K2	-1.0	S2		
2NM6	2	2.0	N2	1.0	M2				
ST12	4	2.0	N2	1.0	M2	1.0	K2	-1.0	S2
ST41	3	3.0	M2	1.0	S2	-1.0	K2		
2MN6	2	2.0	M2	1.0	N2				
ST13	4	2.0	M2	1.0	N2	1.0	K2	-1.0	S2
M6	1	3.0	M2						
MSN6	3	1.0	M2	1.0	S2	1.0	N2		
MKN6	3	1.0	M2	1.0	K2	1.0	N2		
2MS6	2	2.0	M2	1.0	S2				
2MK6	2	2.0	M2	1.0	K2				
NSK6	3	1.0	N2	1.0	S2	1.0	K2		
2SM6	2	2.0	S2	1.0	M2				
MSK6	3	1.0	M2	1.0	S2	1.0	K2		
ST42	3	2.0	M2	2.0	S2	-1.0	K2		
S6	1	3.0	S2						
ST14	3	2.0	M2	1.0	N2	1.0	O1		
ST15	3	2.0	N2	1.0	M2	1.0	K1		
M7	1	3.5	M2						
ST16	3	2.0	M2	1.0	S2	1.0	O1		
3MK7	2	3.0	M2	1.0	K1				
ST17	4	1.0	M2	1.0	S2	1.0	K2	1.0	O1

ST18	2	2.0 M2	2.0 N2		
3MN8	2	3.0 M2	1.0 N2		
ST19	4	3.0 M2	1.0 N2	1.0 K2	-1.0 S2
M8	1	4.0 M2			
ST20	3	2.0 M2	1.0 S2	1.0 N2	
ST21	3	2.0 M2	1.0 N2	1.0 K2	
3MS8	2	3.0 M2	1.0 S2		
3MK8	2	3.0 M2	1.0 K2		
ST22	4	1.0 M2	1.0 S2	1.0 N2	1.0 K2
ST23	2	2.0 M2	2.0 S2		
ST24	3	2.0 M2	1.0 S2	1.0 K2	
ST25	3	2.0 M2	2.0 N2	1.0 K1	
ST26	3	3.0 M2	1.0 N2	1.0 K1	
4MK9	2	4.0 M2	1.0 K1		
ST27	3	3.0 M2	1.0 S2	1.0 K1	
ST28	2	4.0 M2	1.0 N2		
M10	1	5.0 M2			
ST29	3	3.0 M2	1.0 N2	1.0 S2	
ST30	2	4.0 M2	1.0 S2		
ST31	4	2.0 M2	1.0 N2	1.0 S2	1.0 K2
ST32	2	3.0 M2	2.0 S2		
ST33	3	4.0 M2	1.0 S2	1.0 K1	
M12	1	6.0 M2			
ST34	2	5.0 M2	1.0 S2		
ST35	4	3.0 M2	1.0 N2	1.0 K2	1.0 S2

Appendix 4

Sample Data Input on File Reference Number 9 For the Computer Program: Prince Rupert
High and Low Water Observations for January 1974

```
9354  1  174  619534.8 1252220.7 1830457.9 9999 99.9 9999 99.9 9999 99.9
9354  2  174  019211.1  720532.8 1359191.0 1944426.8 9999 99.9 9999 99.9
9354  3  174  132244.9  818549.5 15 7176.8 2123447.0 9999 99.9 9999 99.9
9354  4  174  248269.2  919580.8 1613140.0 2244482.7 9999 99.9 9999 99.9
9354  5  174  357264.9 1015616.5 1710 93.2 2335518.5 9999 99.9 9999 99.9
9354  6  174  5 1249.0 1111657.0 18 3 44.9 9999 99.9 9999 99.9 9999 99.9
9354  7  174  029557.3  557216.9 12 6680.3 1851  9.3 9999 99.9 9999 99.9
9354  8  174  118595.9  651191.2 1256704.2 1941-17.1 9999 99.9 9999 99.9
9354  9  174  2 4624.1  742159.7 1349712.3 2023-21.8 9999 99.9 9999 99.9
9354 10  174  246648.7  833138.5 1440696.4 21 8 -8.8 9999 99.9 9999 99.9
9354 11  174  328662.5  918143.1 1531677.9 2148 54.6 9999 99.9 9999 99.9
9354 12  174  411685.2 1012167.8 1617646.3 2226105.7 9999 99.9 9999 99.9
9354 13  174  453674.4 1112190.1 17 8585.6 2312153.0 9999 99.9 9999 99.9
9354 14  174  542645.0 12 3220.9 18 5551.1 2357236.9 9999 99.9 9999 99.9
9354 15  174  631638.4 1314243.7 19 9516.4 9999 99.9 9999 99.9 9999 99.9
9354 16  174  054288.8  736603.1 1438251.2 2036492.7 9999 99.9 9999 99.9
9354 17  174  210329.7  850601.6 1554235.8 2225514.0 9999 99.9 9999 99.9
9354 18  174  337366.4  947648.7 17 7229.8 2313539.2 9999 99.9 9999 99.9
9354 19  174  438335.0 1038603.6 1744171.2 9999 99.9 9999 99.9 9999 99.9
9354 20  174  0 8533.3  527292.7 1130615.4 1816144.2 9999 99.9 9999 99.9
9354 21  174  049565.8  612280.1 12 7623.3 1855108.8 9999 99.9 9999 99.9
9354 22  174  124574.9  651264.4 1240637.9 1929 94.2 9999 99.9 9999 99.9
9354 23  174  150577.7  724236.4 1320644.0 1956 90.8 9999 99.9 9999 99.9
9354 24  174  214597.6  754219.7 1353650.4 2021101.4 9999 99.9 9999 99.9
9354 25  174  243605.3  832207.1 1424627.7 2051 99.4 9999 99.9 9999 99.9
9354 26  174  315602.8  9 2193.0 15 2614.0 2115118.8 9999 99.9 9999 99.9
9354 27  174  339616.5  943197.8 1538585.6 2150146.2 9999 99.9 9999 99.9
9354 28  174  4 8611.4 1015202.3 1621556.8 2219178.4 9999 99.9 9999 99.9
9354 29  174  445606.6 11 7206.7 17 0519.0 2255207.8 9999 99.9 9999 99.9
9354 30  174  526579.2 12 4203.9 1759484.0 2337256.4 9999 99.9 9999 99.9
9354 31  174  627598.4 1311236.4 19 7478.2 9999 99.9 9999 99.9 9999 99.9
```

Appendix 5

Sample Data Input on File Reference Number 5 For the Computer Program: A High-Low Analysis of the Observations in Appendix 4 which includes the Constituents Z_o, Mm, Msf, O_1, K_1, N_2, M_2, and S_2; infers P_1, ν_2 and K_2; and uses the Zero Derivative Information with Weighting Coefficient equal to 1.0.

```
    8     1 1.0
Z0        0.000
MM        0.0015121518
MSF       0.0028219327
O1        0.0387306544
K1        0.0417807462
N2        0.0789992488
M2        0.0805114007
S2        0.0833333333
   01    01    74    31    01    74
 9354PRINCE RUPERT BC      PST     54    19  130    20
    K1         0.0417807462    P1         0.0415525871    0.3122    3.65
    S2         0.0833333333    K2         0.0835614924    0.2696    8.61
    N2         0.0789992488    NU2        0.0792016198    0.1938   -1.63
```

Appendix 6

Final Page of Computer Program Output Corresponding to the Input of Appendices 3, 4 and 5.

HARMONIC TIDAL ANALYSIS RESULTS:
RAW AMPLITUDES AND RAW LOCAL PHASES ARE FOLLOWED BY NODALLY CORRECTED AMPLITUDES AND GREENWICH PHASES

Z0	.000000000	388.728	.00	388.728	.00
MM	.001512152	22.970	23.09	22.970	128.86
MSF	.002821933	7.844	-8.81	7.844	185.90
O1	.038730654	31.793	-178.81	31.330	130.42
K1	.041780746	64.604	-61.71	64.050	152.74
N2	.078999249	41.696	-49.64	41.763	12.17
M2	.080511400	195.485	-131.73	194.971	35.75
S2	.083333333	68.772	71.70	68.771	71.58

THE SAME RESULTS WITH INFERENCE

Z0	.000000000	388.728	.00	388.728	.00
MM	.001512152	22.970	23.09	22.970	128.86
MSF	.002821933	7.844	-8.81	7.844	185.90
O1	.038730654	31.793	-178.81	31.330	130.42
P1	.041552586	16.791	-17.88	16.777	137.29
K1	.041780746	54.201	-73.51	53.737	140.94
N2	.078999248	35.263	-47.25	35.319	14.56
NU2	.079201619	6.883	297.55	6.845	16.19
M2	.080511400	195.485	-131.73	194.971	35.75
S2	.083333332	70.285	56.87	70.284	56.75
K2	.083561491	18.892	159.07	18.949	48.14

AND THE ROOT MEAN SQUARE RESIDUAL ERROR AFTER INFERENCE IS .100923+002

8. REFERENCES

Barrodale, I. and G.F. Stuart , 1974. A Fortran Program for Linear Least Squares Problems of Variable Degree. Proceedings of the Fourth Manitoba Conference on Numerical Mathematics. pp. 191-204.

Barrodale, I. and R.E. Erikson , 1978. Algorithms for Least-Squares Linear Prediction and Maximum Entropy Spectral Analysis. Mathematics Department Report DM-142-IR, University of Victoria. 49 pp.

Foreman, M.G.G., 1977. Manual for Tidal Heights Analysis and Prediction. Pacific Marine Science Report 77-10, Institute of Ocean Sciences, Patricia Bay, Victoria, B.C. 97 pp.

Foreman, M.G.G., 1978. Manual for Tidal Currents Analysis and Prediction. Pacific Marine Science Report 78-6, Institute of Ocean Sciences, Patricia Bay, Victoria, B.C. 70 pp.

Godin, G., 1972. The Analysis of Tides. University of Toronto Press, Toronto. 264 pp.

Lawson, C.L. and R.J. Hanson , 1974. Solving Least Squares Problems. Prentice-Hall Inc., Englewood Cliffs, New Jersey. 340 pp.

Munk, W.H. and E.C. Bullard , 1963. Patching the Long-Wave Spectrum Across the Tides. Journal of Geophysical Research, 68(12), pp. 3627-3634.

Munk, W.H. and K. Hasselmann , 1964. Super-resolution of Tides. Studies on Oceanography (Hidaka volume), Tokyo. pp. 339-344.

Ortega, J.M., 1972. Numerical Analysis - A Second Course. Academic Press, New York. 193 pp.

Schureman, P., 1958. Manual of Harmonic Analysis and Prediction of Tides, U.S. Department of Commerce Special Publication No. 98. Government Printing Office, Washington. 317 pp.

Zetler, B.D., M.D. Schuldt , R.W. Whipple , and S.D. Hicks , 1965. Harmonic Analysis of Tides from Data Randomly Spaced in Time. Journal of Geophysical Research, 70(12), pp. 2805-2811.

CA1
EP 321
-79R16

Pacific Marine Science Report 79-16

Publications

OCEANOGRAPHIC OBSERVATIONS IN ROBESON CHANNEL, N.W.T. 1971

by

R.H. Herlinveaux

INSTITUTE OF OCEAN SCIENCES, PATRICIA BAY
Sidney, B.C.

For further copies or additional information please write to:

Department of Fisheries and Oceans
Institute of Ocean Sciences
P.O. Box 6000
Sidney, B.C. CANADA
V8L 4B2

Pacific Marine Science Report 79-16

CA1
EP321
-79R16

OCEANOGRAPHIC OBSERVATIONS IN ROBESON CHANNEL, N.W.T. 1971

by

R.H. Herlinveaux

Institute of Ocean Sciences, Patricia Bay
Sidney, B.C.

1979

Abstract

Oceanographic observations were taken through the ice in Robeson Channel during April and May 1971. These observations were water bottle samples for temperature and salinity, current meter profiles to depth of 70 metres and continuous current meter observations under the ice from each side of the channel.

During the spring months of April and May 1971, oceanographic observations were made through the ice in Robeson Channel at locations situated between Ellesmere Island and Greenland (Figure 1). These observations were part of a cooperative program carried out by Defence Research Establishment Pacific of the Department of National Defence and Marine Sciences Directorate of the Department of Environment (now Ocean and Aquatic Sciences, Department of Fisheries and Oceans).

PROGRAM:

First, a main-camp tent was set up on the ice in mid-channel of Robeson Channel opposite Wrangel Bay (Figure 2). A hole was then blasted in the 1 metre thick sea ice and a work tent, complete with a gas-fired heater, was erected over the hole (Figures 2 and 3). A light bulb, powered by the main camp electric generator (when operative) was inserted into the ice hole to prevent it from re-freezing, however, daily chiselling was also required to loosen newly formed ice so it could be flushed out of the hole.

At the main camp, three oceanographic casts and several bathythermograph lowerings and plankton hauls were made through this hole. A continuous recording current meter was suspended on a wire on one side of the hole but was later found to have malfunctioned. A time-series of vertical current velocity profiles below the ice was taken with only some success due to malfunctions of the current meter's direction sensing unit. With the use of a helicopter, continuous recording current meters were transported to two additional locations on both sides of Robeson Channel and installed at 5 metres' depth below the ice (Figure 4). These were in operation for 15 days. Two oceanographic casts were also made at these two current-meter sites.

Equipment Used

Recording Current Meters. A Braincon current meter with a photographic film recorder was used with a modified collapsible tail (Figure 4). This tail folded in against the body so that the assembly could be lowered down a 9" hole. A candy "life-saver" held the tail into the body of the meter and after approximately 20 minutes the "candy" dissolved and released the tail to its operating position under the ice. When the current meter was retrieved, the tail assembly was forced to fold downwards as the meter was pulled up the hole.

Current Profilers. A Hydro Products Savonius rotor current meter was used to obtain a number of vertical current profiles. Some trouble was experienced with the direction sensing unit which depends on a spring-loaded contact on a toroid resistor. Also, the Savonius rotor jammed on several occasions due to a build-up of ice crystals on its reed switch. For longer periods of observation a Rustrak recorder was used during the silent hours and when no one was up.

Hole Stoppers. "Weiner"-shaped rubber bladders (Figure 4) were inflated in the ice holes on both sides of the channel to prevent the holes

from freezing in. The bladders leaked slowly from their valve stems causing the bags to soften, resulting in partially refrozen holes.

Water Sampling Bottles. Fjarlie water bottles were used to collect water samples because of their ability to pass easily through a 9" diameter hole. The bottles were housed in a heated, insulated, 6-bottle carrying case for use from the helicopter.

Sample Bottles. Samples were drawn into 5-ounce citrate bottles.

Bathythermographs. A bathythermograph, operable to a depth of 270 metres, was used and functioned well provided that the unit was warm prior to inserting it into cold water.

Oceanographic winch. A winch, designed and built at the DREP workshop, was used for raising and lowering oceanographic instruments. This winch (Figure 3) worked well when driven by a 3/4 horsepower electric drill motor run off the main a.c. power generator. The unique design of the winch and block assembly, which stood above the hole, permitted one man to operate it from inside the tent. When the winch was used away from the main camp and transported by the helicopter, a Stihl power-saw motor was used to provide power.

OCEANOGRAPHIC OBSERVATIONS

Each of the five oceanographic casts, three at the main camp and one on each side of Robeson Channel, sampled temperatures and salinities vs depth. The samples were obtained using reversing water bottles and thermometers. After the reversing bottles were retrieved and when the auxiliary thermometer had reached equilibrium, the reversing thermometers were read and recorded. The samples for salinity determination were drawn into 5-oz citrate bottles and stored for later analysis at the Pacific Environment Institute using an inductive salinometer.

Figures 5 to 9 inclusive are plots of salinity (S), temperature (T) and sigma-T (G) vs depth in metres. Locations are shown in inset in Figure 1. STN-ROB1, STN-ROB2 and STN-ROB3 were at the main camp in the middle of Robeson Channel, STN-ROB4 was on the Greenland side, and STN-ROB5 was on the Ellesmere Island side. (The data from which these plots in Figures 5 to 9 inclusive were obtained is listed in Appendix I.) Figure 10 compares cross-channel salinities and temperatures in the spring of 1971 (upper two diagrams) with data collected in the same section in the summer of 1971 (Herlinveaux and Sadler, 1973) (lower two diagrams). Figure 11 shows temperature vs salinity (TS) plots for all five oceanographic casts taken during the spring of 1971.

The bathythermograms are presented in Appendix II and are hand-drawn reproductions of the slides.

Currents

Current meter records, each of 15 days' duration and taken from a depth of 5 m at each side of Robeson channel (Figure 1), were digitized and processed on a computer. (The raw data print-out for the two positions is

listed in Appendix III.) Frequency distributions of direction and speed are shown in Figure 12 for the east side of the channel and Figure 13 for the west side. Polar coordinate histogram plots of direction and direction frequency are shown in Figures 14 and 15. Vector trajectory plots of water movements on either side of the channel are plotted in Figures 16 and 17. Figure 18 shows time-series plots of speed and direction at both locations.

The current velocities obtained at the mid-channel camp at various depths down to 100 metres are presented, in part, in Figure 19. There were occasions when current meter directions were erratic and therefore unreliable. The currents shown in Figure 19 were selected to give the reader an idea of the variation with depth observed. The rest of the data remain on file.

When not being used for profiling, the current meter at the camp was fitted with a two-channel Rustrak recorder and suspended at various depths. These data are not presented but are on file at the Institute of Ocean Sciences, Patricia Bay.

INTERPRETATION

The oceanographic data shown in Figures 5 to 9 inclusive show a 50 metre thick upper layer above a halocline and thermocline extending down to 200 metres. Below 200 metres, there is a gradual increase in salinity and temperature. Minor temperature inversions occur in the upper 30 metres probably caused by cloud-like water layers moving in the channel. Most of the variation in the water column occurs at and below sill-depth of 130 metres, which limits the exchange of deeper-water into the Nares Strait system. A comparison of Figures 5, 6 and 7 will give some idea of the variation to be expected over a period of 13 days.

The cross-section distributions of temperature and salinity observed in the spring and summer of 1971 (Figure 10) show that isotherms and isohalines tend to slope upwards to Ellesmere Island in the upper 100 metres and downward below 200 metres. In the upper layer, temperatures from spring to summer increased by about 0.7°C at the surface and by about 0.2°C at 50 metres. At mid-depth, very little change is seen and, at the bottom, the temperature decreased by 0.1°C. In summer salinities decreased at the surface possibly due to runoff, ice melt or both. In both spring and summer, the salinities were least along the Greenland side, probably associated with runoff from Greenland drainage. This suggests there is a component of flow to the north or at least a more sluggish southerly flow both in spring and summer. The slopes of the isotherms and isohalines further suggest that there are differences in the channel flow normal to its cross section - likely more vigorous in the down-channel direction on its westerly side.

Figure 11 is a TS plot derived from the five oceanographic casts. The plots are arc-shaped with the centre of the curve at about 34.00‰, which corresponds to the lower end of the halocline. This TS suggests there are only two water masses involved in this area - warm bottom water from the Atlantic, via Baffin Bay, and surface Arctic Ocean water moving south from the Lincoln Sea.

Figures 14 and 15 are polar plots of all the current directions and speeds recorded from the west side and east side of Robeson Channel respectively. These figures show the number of observations in each 10° segment of direction and are an alternate way of presenting the data shown in Figures 12 and 13.

To illustrate the net movements in Robeson Channel, vector trajectory plots are shown in Figures 16 and 17. Comparison of the two figures shows that, for the 14 days, the net movement down-channel was 17 km on the east side and 50 km on the west side. The down-channel residual currents are three times greater on the west side than the east side at 5 m depths - an expected result of the Coriolis effect acting on an otherwise uniform cross-channel flow.

Figure 18 illustrates the tidal influence on water movements. It is evident that there is a marked semi-diurnal fluctuation in current direction and amplitude, more so during the spring tides but tending to be diurnal during neap tides.

The water movements in Robeson Channel have a strong tidal component - more in evidence during spring tides than during neap tides. Strong southerly trending residual currents are evident in Robeson Channel which, at times, exceed the magnitude of tidal currents. Therefore the best time to work in Robeson Channel on the bottom or on the foreshore would be during the neap tides.

Figure 19 shows the current directions and speeds from the surface to 80 metres, measured in mid-channel. There were many profiles obtained, but the direction unit malfunctioned at times although the speed unit did work. Figure 19 shows that the currents generally increased with depth down to 80 metres. The swiftest currents observed were 50 cm/s at a depth of 75 metres, while movement immediately under the sea ice was 15 cm/s.

It is recommended, before any further physical oceanography is planned for Robeson Channel, that the data in this report should be analyzed in concert with that reported by Chow, 1975 and Sadler, 1976.

REFERENCES

Chow, R.A. 1975 Near-surface current in Robeson Channel. Defence Research Establishment Ottawa Rept. No. 709, 63 pp.

Herlinveaux, R.H. and H.E. Sadler. 1973. Oceanographic features of Nares Strait in August 1971. Marine Sciences Directorate, Pacific Region, Victoria, B.C. 104 pp. PMSR unpublished.

Sadler, H.E. 1976. The flow of water and heat through Nares Strait. Defence Research Establishment Ottawa Rept. No. 736, 184 pp.

LIST OF FIGURES

Figure 1 Location of Robeson Channel south of Lincoln Sea and the positions of oceanographic observations.

Figure 2 Ice camp layout mid channel Robeson Channel with living quarters and electronics tent on left and oceanographic tent on right.

Figure 3 Inside view of oceanographic tent with specially designed winch.

Figure 4 Current meter being retrieved from ice hole with rubber tube hole stopper lying on ice.

Figure 5 Temperature, salinity and sigma-T distribution at mid-channel Robeson Channel.

Figure 6 Temperature, salinity and sigma-T distribution at mid-channel Robeson Channel.

Figure 7 Temperature, salinity and sigma-T distribution at mid-channel Robeson Channel.

Figure 8 Temperature, salinity and sigma-T distribution at the east side of Robeson Channel.

Figure 9 Temperature, salinity and sigma-T distribution at the west side of Robeson Channel.

Figure 10 Cross channel distribution of temperature and salinity taken during the spring and summer 1971.

Figure 11 TS plots of all data collected during the spring 1971 operations.

Figure 12 Frequency distribution of all the direction and rate observation taken on the east side of the channel during spring 1971.

Figure 13 Frequency distribution of all the direction and rate observations taken on the west side of the channel during spring 1971.

Figure 14 Number of observations in each 10° segment of direction on the west side of channel.

Figure 15 Number of observations in each 10° segment of direction on the east side of channel.

Figure 16 Vector trajectory plot of all the observations taken on the east side of channel.

Figure 17 Vector trajectory plot of all the observations on the west side of the channel.

Figure 18 Speed and direction plots for the two sets of data collected on the east and west side of Robeson Channel.

Figure 19 Examples of three speed and direction plots with depth observed through the ice at the mid-channel camps.

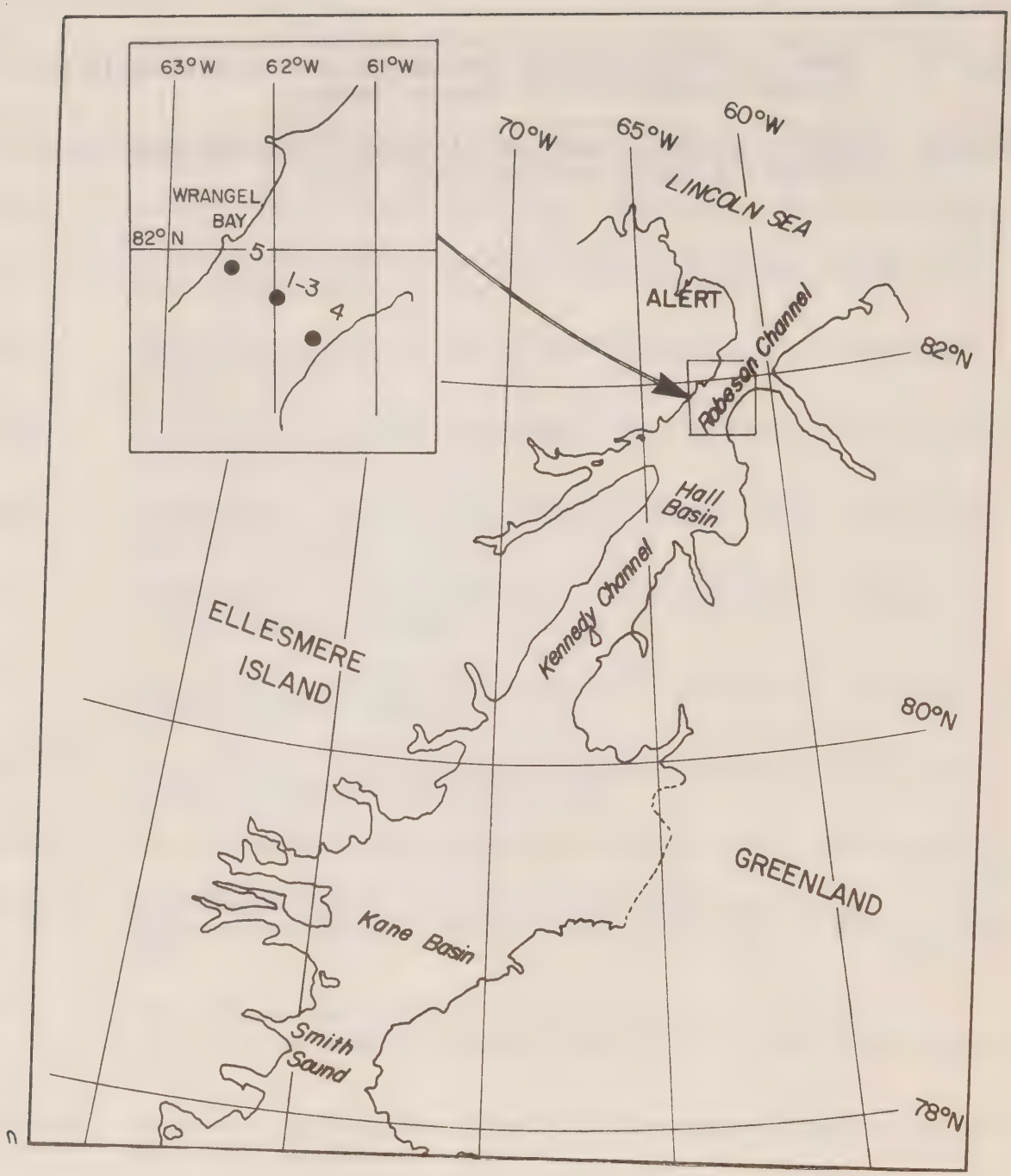

Figure 1 Location of Robeson Channel south of Lincoln Sea and the positions of oceanographic observations.

Figure 2 Ice Camp layout mid channel Robeson Channel with living quarters and electronics tent on left and oceanographic tent on right.

Figure 3 Inside view of oceanographic tent with specially designed winch.

Figure 4 Current meter being retrieved from ice hole with rubber tube hole stopper laying on ice.

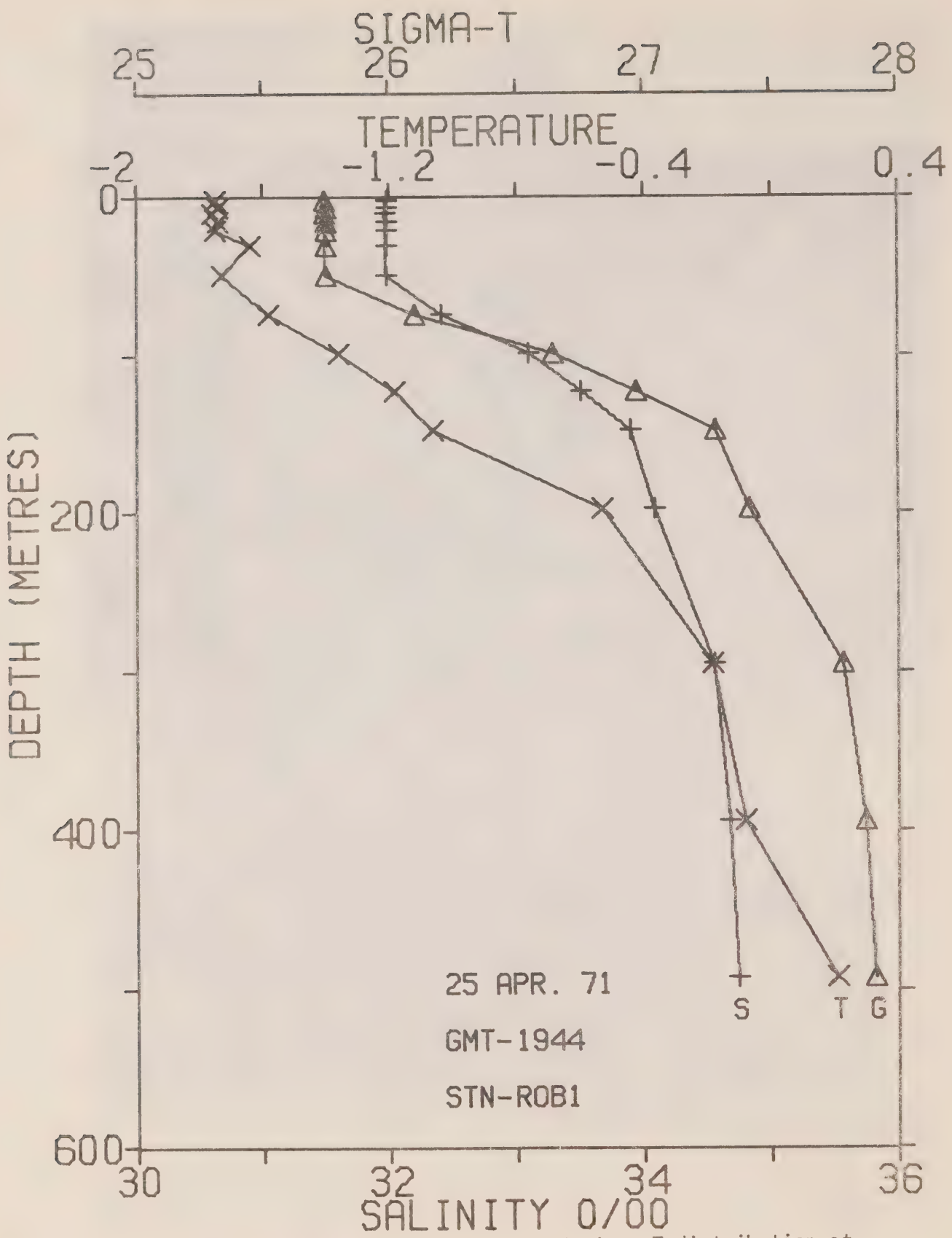

Figure 5 Temperature, salinity and sigma-T distribution at mid-channel Robeson Channel.

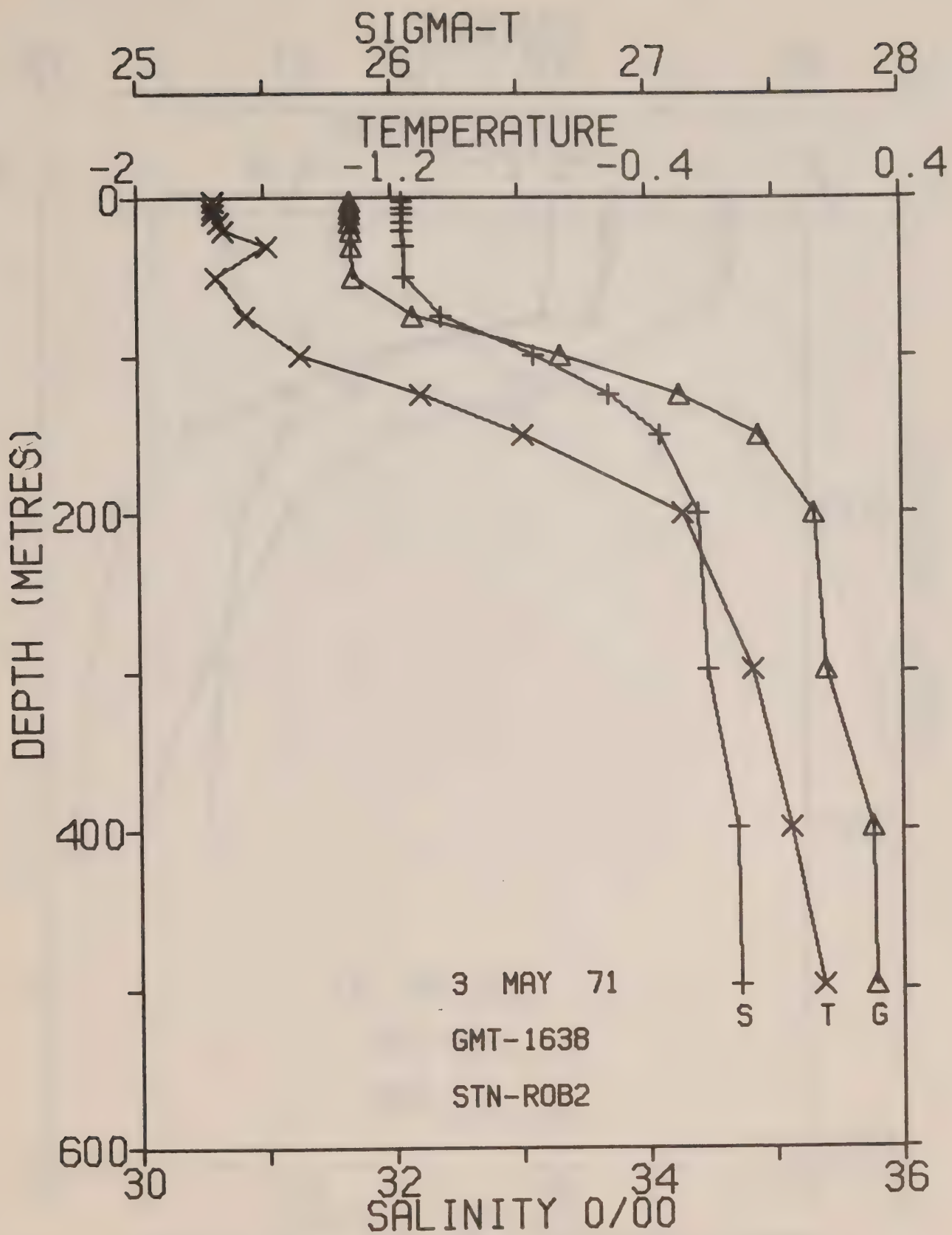

Figure 6 Temperature, salinity and sigma-T distribution at mid-channel Robeson Channel.

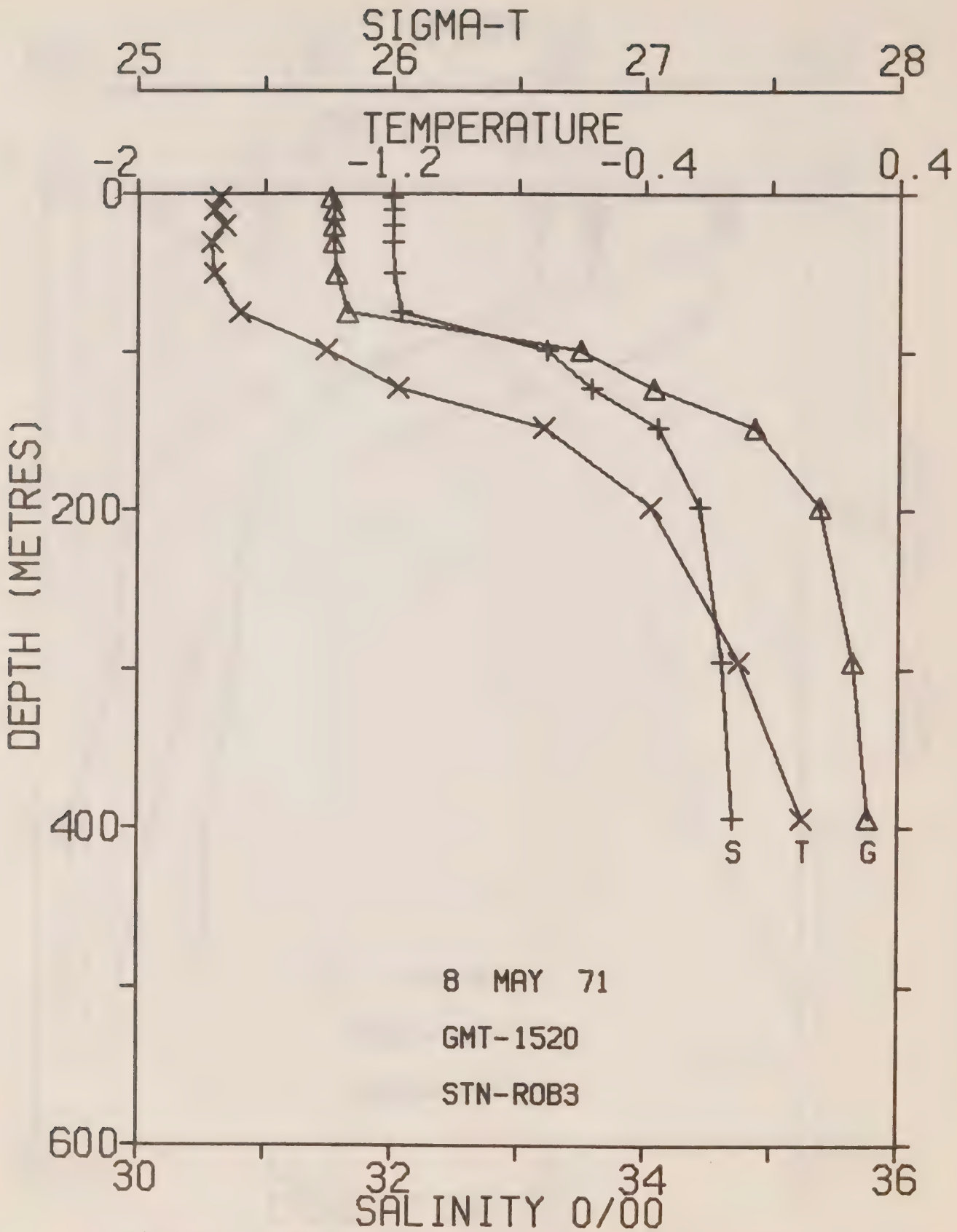

Figure 7 Temperature, salinity and sigma-T distribution at mid-channel Robeson Channel

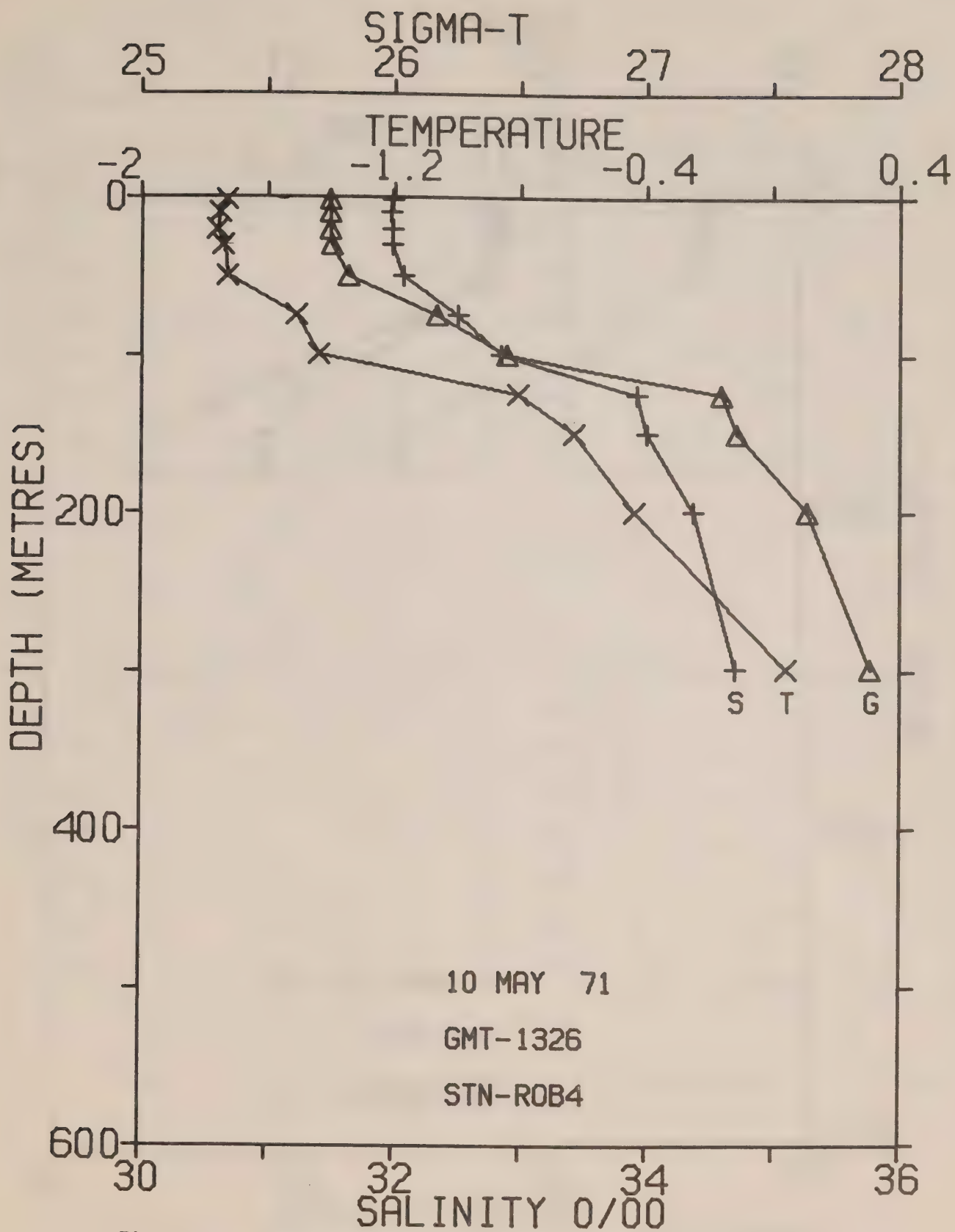

Figure 8 Temperature, salinity and sigma-T distribution at the east side of Robeson Channel.

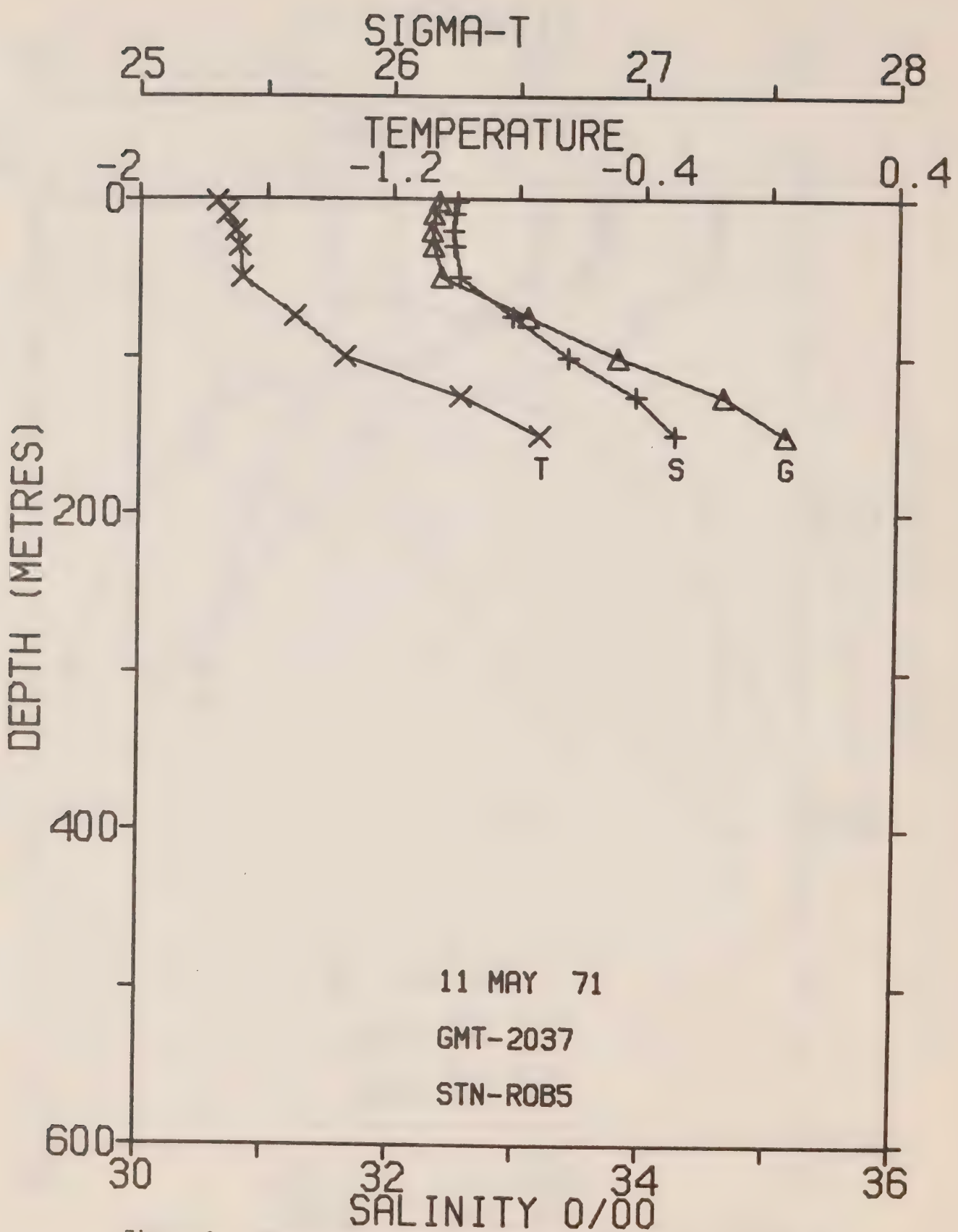

Figure 9 Temperature, salinity and sigma-T distribution at the west side of Robeson Channel.

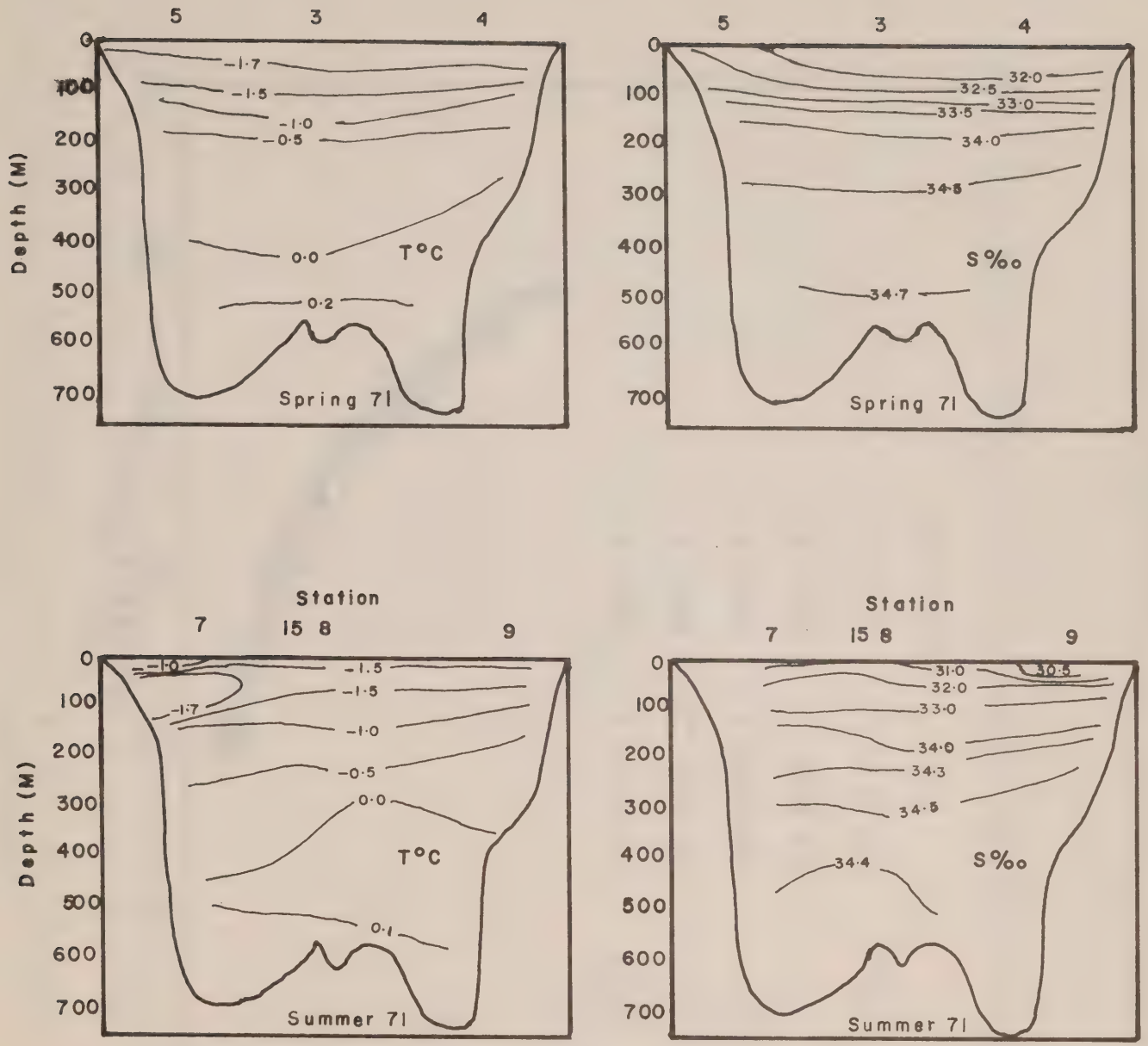

Figure 10 Cross channel distribution of temperature and salinity taken during the spring and summer 1971.

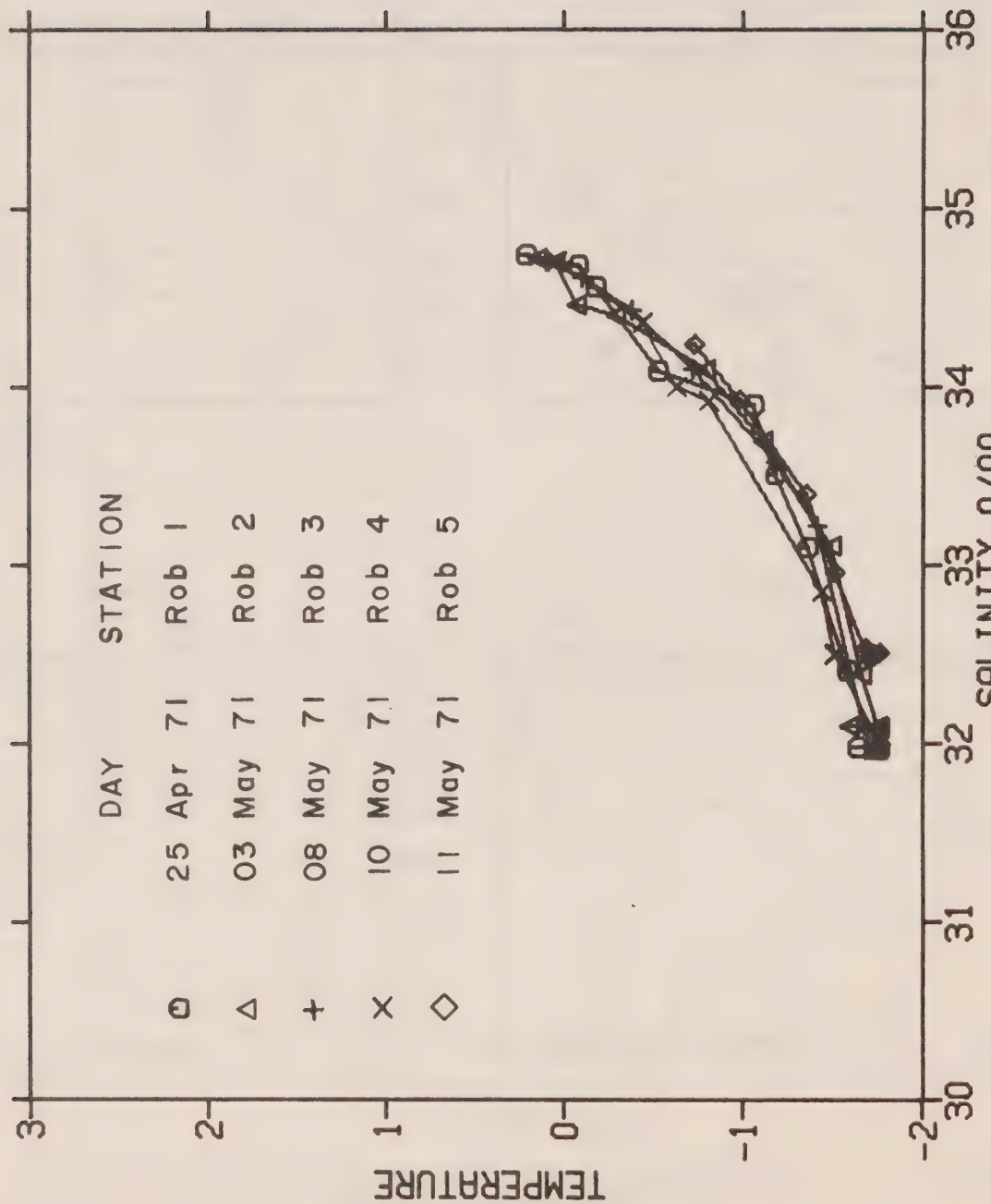

Figure 11 TS plots of all data collected during the spring 1971 operations.

FREQUENCY DISTRIBUTION OF DIRECTION AND RATE

STN 002 DEPTH 005 ROBESON EAST 81 51.5 N 61 43.0 W LENGTH OF RECORD= 14 DAYS

START OF RECORD 30 MN 15 HR 26 DY 04 MO 71 YR RATE OF OBSER.= 3 PER HOUR

CMS/SEC

DIR	001 TO 004	005 TO 009	010 TO 014	015 TO 019	020 TO 024	025 TO 029	030 TO 034	035 TO 039	040 TO 044	045 TO 049	050 TO 054	055 TO 059	060 TO 064	065 TO 069	070 TO 074	075 TO 079	080 TO 084	085 TO 089	090 TO 094	095 TO 099	100 TO 104	105 TO 109	110 TO 114	115 TO 119	120 TO 124	
0- 9	003	018	006	002																						29
10- 19	004	012	007																							23
20- 29	002	009	006	001																						18
30- 39	002	011	002	003	001																					19
40- 49	002	007	009	002																						20
50- 59	002	019	004	003	003																					31
60- 69	003	013	006	007	004																					33
70- 79	003	005	009	005	005																					27
80- 89	001	003	004	005	006		001																			20
90- 99	004	012	005	003	001	002	001																			28
100-109	003	002	004	005	002																					16
110-119	001	006	003	004	002																					16
120-129	003	011	004	001	001																					20
130-139	003	011																								14
140-149	001	012	002																							15
150-159	004	009	002	003																						18
160-169	001	012	006	005	002																					26
170-179	001	012	013	009	005																					40
180-189	002	015	012	006	002	001																				38
190-199	005	020	006	009	002	002																				44
200-209	001	007	010	007	006	005																				36
210-219		017	017	015	012	005																				66
220-229	002	019	010	013	011																					55
230-239	006	013	008	005	001																					33
240-249	002	007	004	004	001																					18
250-259	001	009	002	010	002																					24
260-269	001	006	003	001																						11
270-279	002	004	007	002																						15
280-289	005	009	005	005																						24
290-299	004	007	007	006	003																					27
300-309	006	017	015	007	001	002																				48
310-319	002	016	009	014	001																					42
320-329	002	022	014	006																						44
330-339	003	012	011	002																						28
340-349	001	021	007	004	001																					34
350-359	003	019	011																							33
	424		174		17		0		0		0		0		0		0		0		0		0		0	1033
	91		250		75		2		0		0		0		0		0		0		0		0			

NUMBER OF ZERO RATES 0

Figure 12 Frequency distribution of all the direction and rate observations taken on the east side of the channel during spring 1971.

FREQUENCY DISTRIBUTION OF DIRECTION AND RATE

STN 003 DEPTH 004 ROBESON WEST 81 59.0 N 62 20.0 W LENGTH OF RECORD= 14 DAYS

START OF RECORD 00 MN 16 HR 26 DY 04 MO 71 YR RATE OF OBSER.= 3 PER HOUR

CMS/SEC

DIR	001 TO 004	005 TO 009	010 TO 014	015 TO 019	020 TO 024	025 TO 029	030 TO 034	035 TO 039	040 TO 044	045 TO 049	050 TO 054	055 TO 059	060 TO 064	065 TO 069	070 TO 074	075 TO 079	080 TO 084	085 TO 089	090 TO 094	095 TO 099	100 TO 104	105 TO 109	110 TO 114	115 TO 119	120 TO 124	
0- 9	006	009	008	008																						31
10- 19	004	009	007	007	001																					28
20- 29	003	013	003	003																						22
30- 39	006	010	002																							18
40- 49	004	005																								9
50- 59	009	002																								11
60- 69	006	005																								11
70- 79	002	008																								10
80- 89	006	003																								9
90- 99	004	001																								5
100-109	002	002	001																							5
110-119	005	005	001																							11
120-129	001	002	001																							4
130-139		002	004	001																						7
140-149	004	014	005																							23
150-159	003	009	011																							23
160-169	001	019	014	003																						37
170-179	008	027	017	013																						65
180-189	004	026	022	014	009																					75
190-199	006	048	020	013	009	004																				100
200-209	009	036	050	028	011	002																				136
210-219	007	022	029	012	006	001																				77
220-229	005	019	020	016																						60
230-239	004	018	020	008																						50
240-249	006	017	011	003																						37
250-259	003	008	007	002																						20
260-269	005	011	007																							23
270-279	002	007	001	001																						11
280-289	002	011	004																							17
290-299	001	007	001																							9
300-309		004																								4
310-319	004	009																								13
320-329	003	008	002																							13
330-339	008	003	002																							13
340-349	002	005	001																							8
350-359	006	009	010	002																						27
		413		134		7		0		0		0		0		0		0		0		0		0		1022
	151		281		36		0		0		0		0		0		0		0		0		0		0	

NUMBER OF ZERO RATES 0

Figure 13 Frequency distribution of all the direction and rate observations taken on the west side of the channel during spring 1971.

002000 3015260471 R0B1

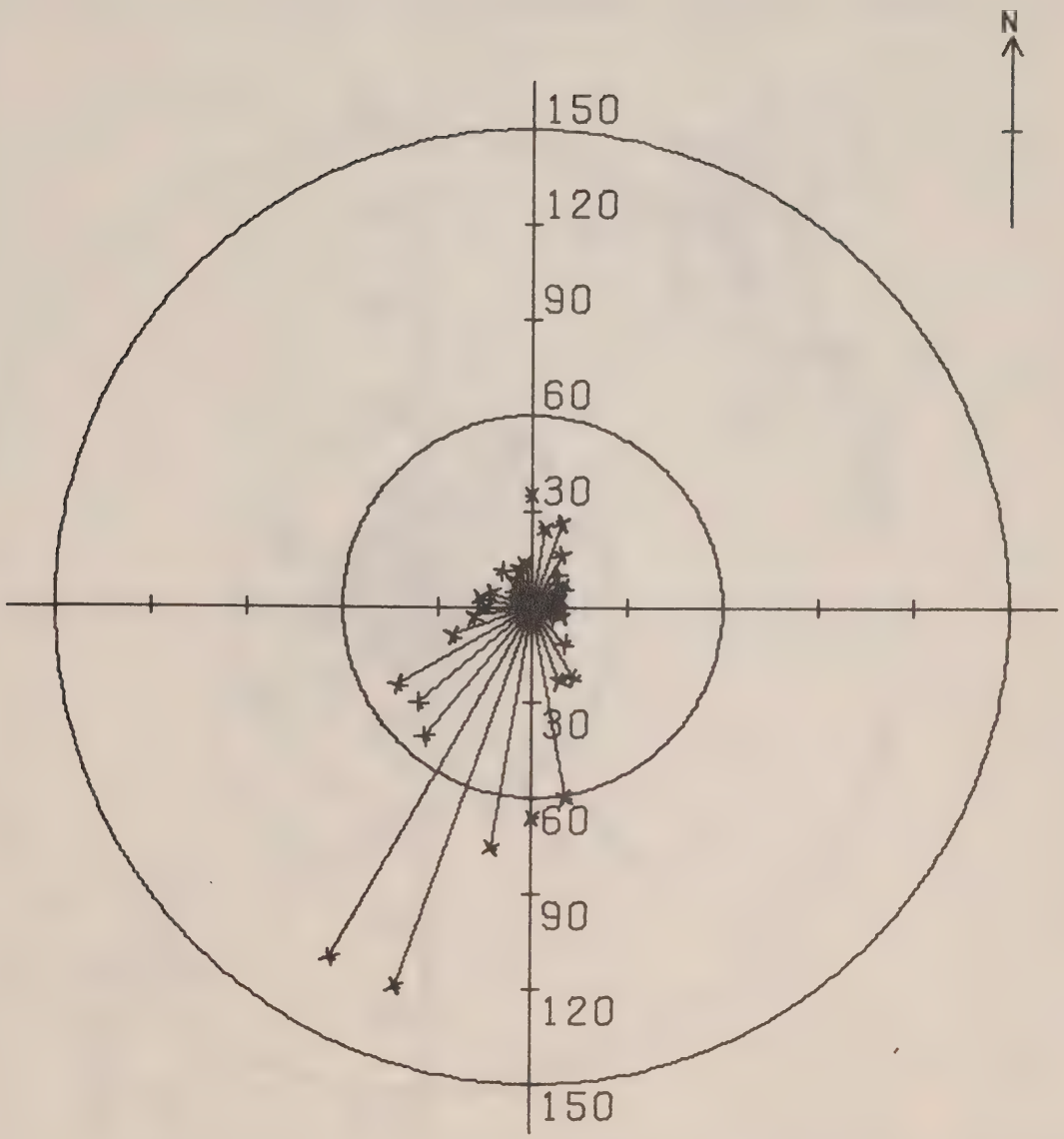

Figure 14 Number of observations in each 10° segment of direction on the west side of channel.

003000 0016260471 ROB2

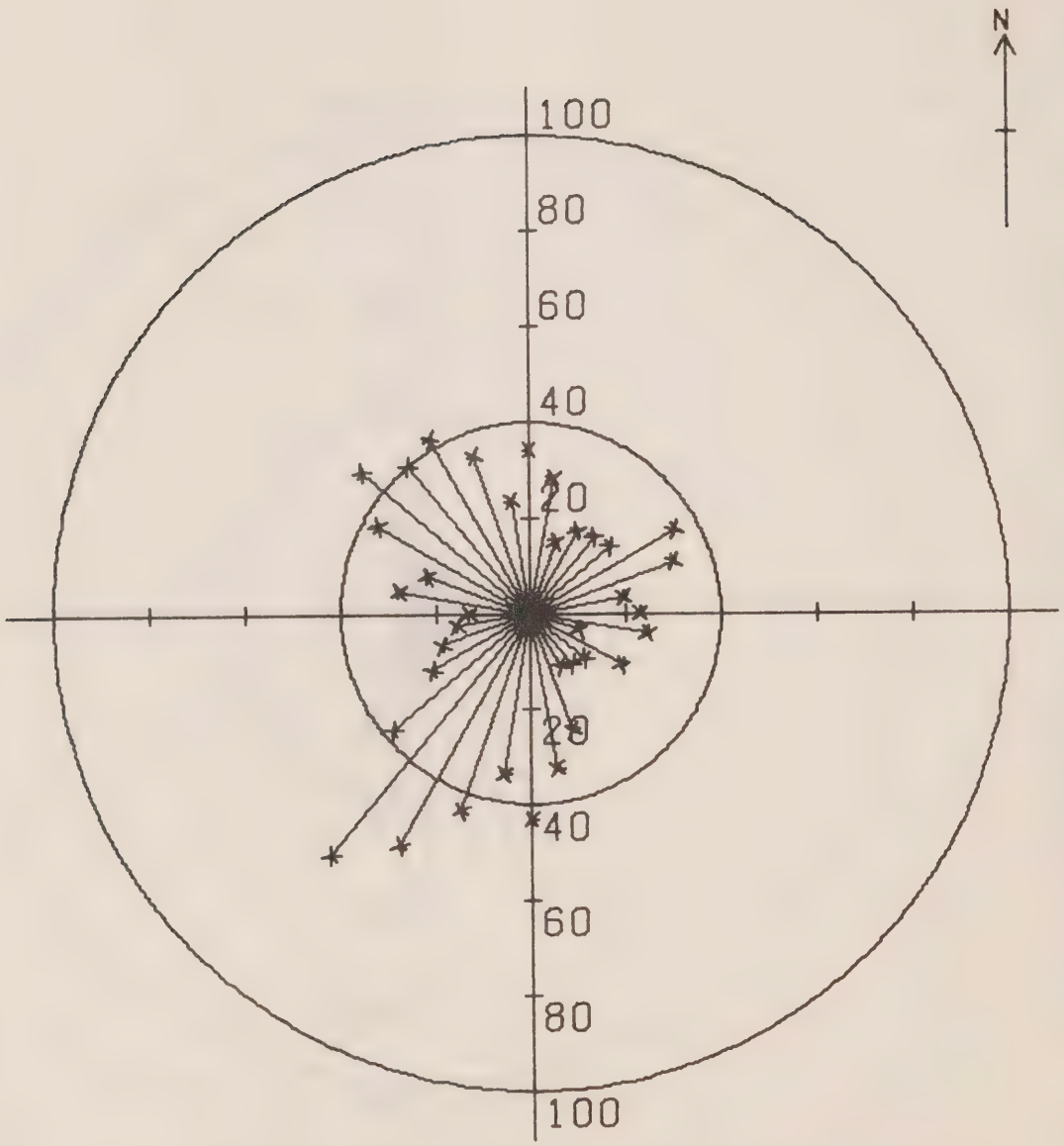

Figure 15 Number of observations in each 10° segment of direction on the east side of channel.

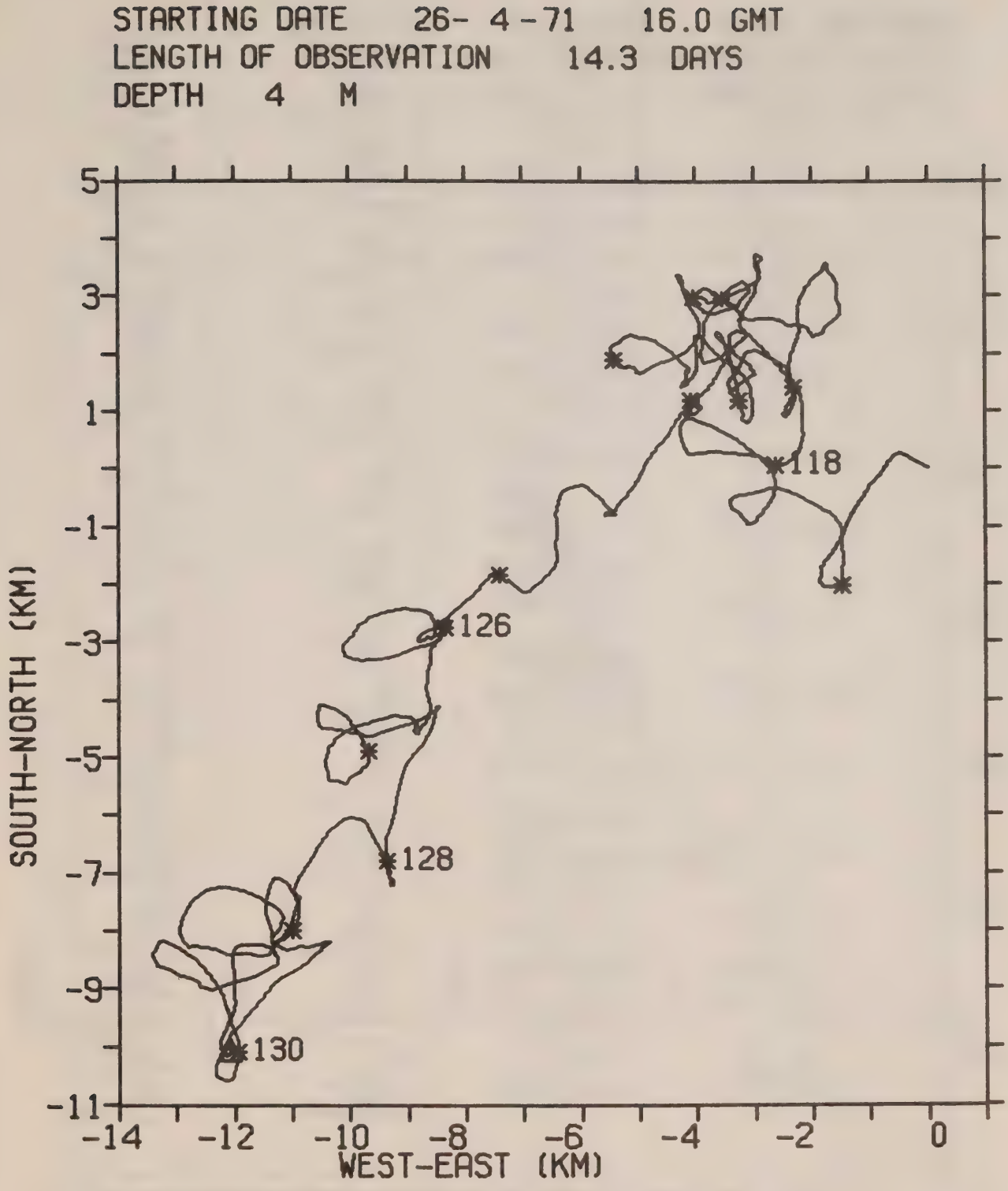

Figure 16 Vector trajectory plot of all the observations taken on the east side of channel.

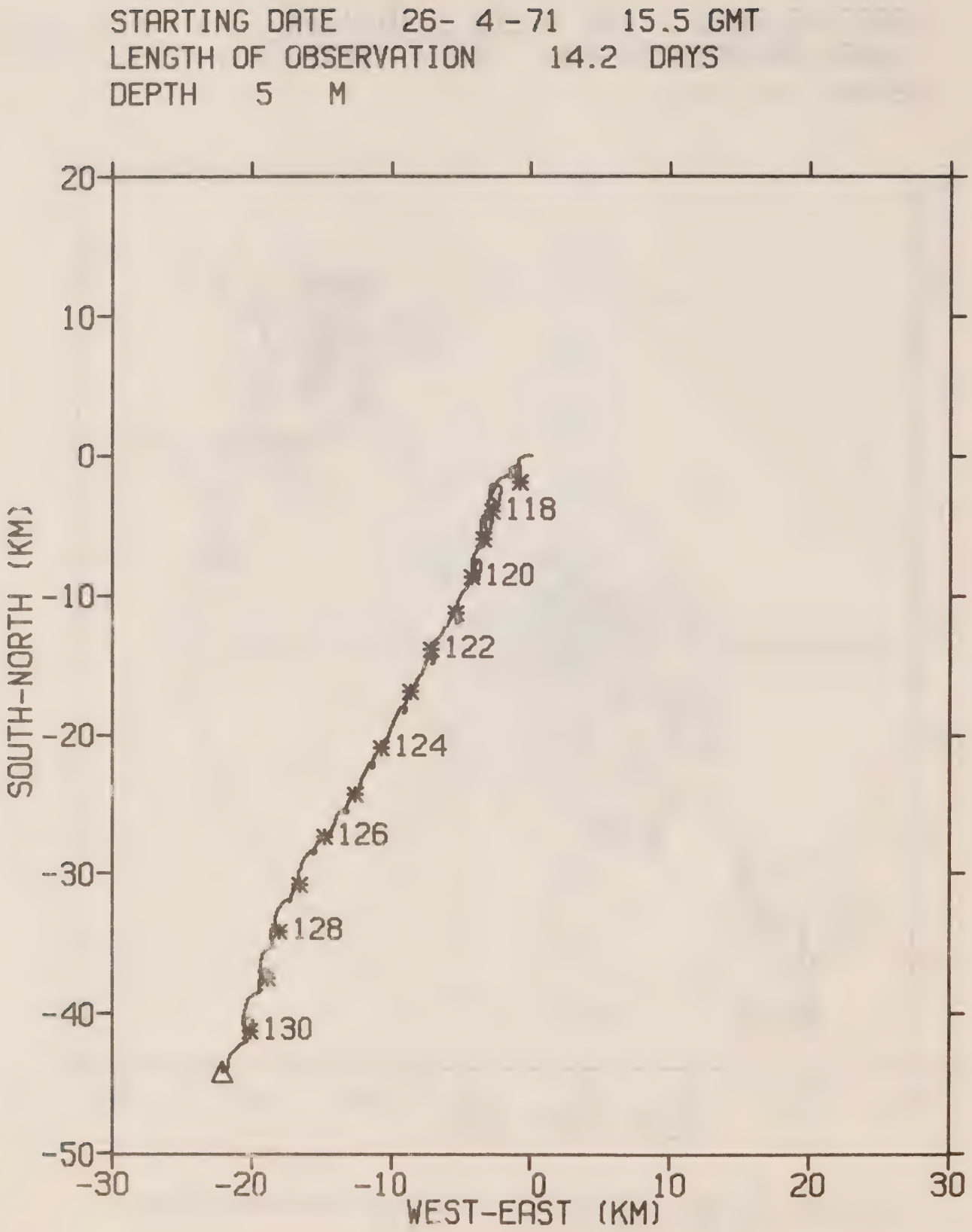

Figure 17 Vector trajectory plot of all the observations on the west side of the channel.

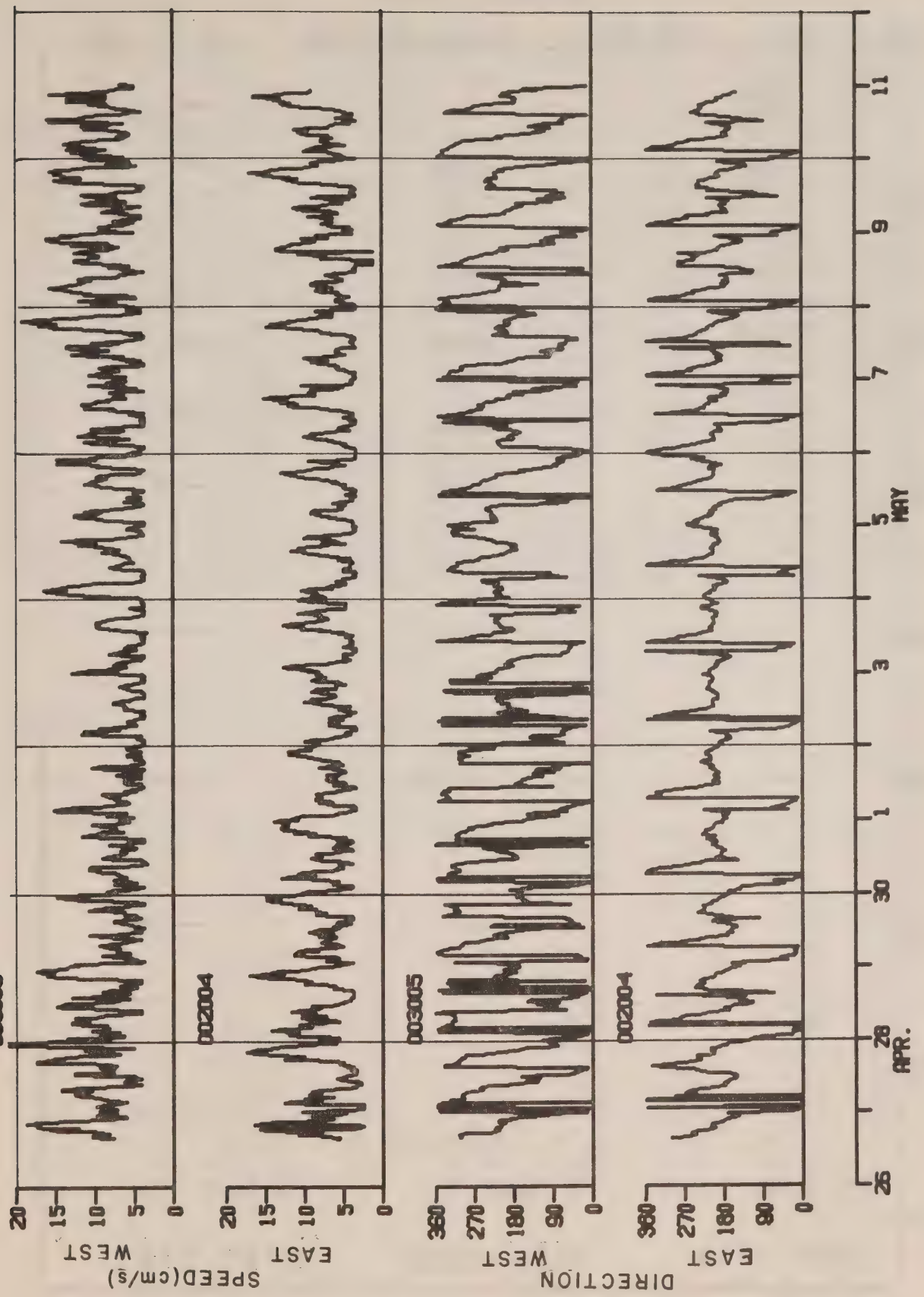

Figure 18 Speed and direction plots for the two sets of data collected on the east and west side of Robeson Channel.

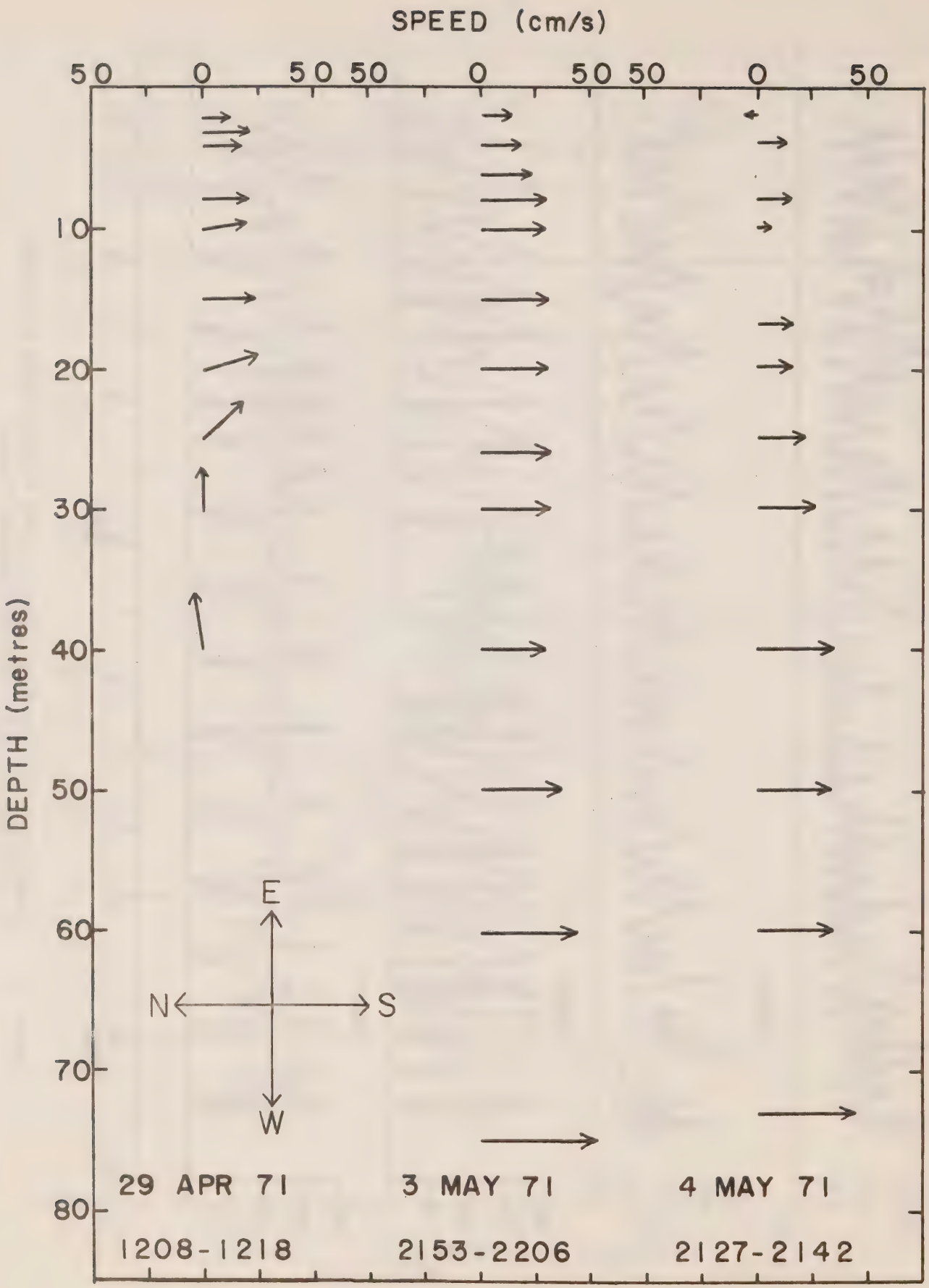

Figure 19 Examples of three speed and direction plots with depth observed through the ice at the mid-channel camps.

APPENDIX I

STATION ROB1 DATE 25/ 4/71
POSITION 81-54.0N, 62- 0.0W GMT 1944

PRESS	TEMP	SAL	DEPTH	SIGMA T	SVA	DELTA D	POT EN	SOUND VEL
2	-1.75	31.97	2	25.75	225.8	0.0	0.0	1437.
6	-1.74	31.98	6	25.75	225.7	0.09	0.00	1437.
10	-1.76	31.97	10	25.74	226.1	0.18	0.01	1437.
15	-1.74	31.98	15	25.75	225.6	0.29	0.03	1437.
20	-1.75	31.98	20	25.75	225.5	0.41	0.05	1437.
30	-1.64	31.98	30	25.75	225.4	0.63	0.10	1438.
50	-1.73	31.98	50	25.75	225.2	1.08	0.29	1438.
75	-1.58	32.41	75	26.10	191.7	1.60	0.61	1440.
100	-1.36	33.10	100	26.65	139.9	2.02	0.97	1442.
125	-1.18	33.51	125	26.97	108.9	2.33	1.32	1444.
150	-1.06	33.90	150	27.28	79.4	2.56	1.65	1445.
200	-0.53	34.09	200	27.42	66.8	2.93	2.29	1449.
300	-0.18	34.56	300	27.78	32.2	3.43	3.46	1453.
400	-0.08	34.68	400	27.87	24.0	3.71	4.44	1455.
500	0.21	34.74	500	27.91	20.8	3.93	5.46	1458.

STATION ROB2 DATE 3/ 5/71
POSITION 81-54.0N, 62- 0.0W GMT 1638

PRESS	TEMP	SAL	DEPTH	SIGMA T	SVA	DELTA D	POT EN	SOUND VEL
2	-1.76	32.09	2	25.84	217.1	0.0	0.0	1437.
6	-1.76	32.09	6	25.84	217.1	0.09	0.00	1437.
10	-1.76	32.09	10	25.84	217.0	0.17	0.01	1437.
15	-1.74	32.09	15	25.84	217.0	0.28	0.02	1437.
20	-1.73	32.09	20	25.84	216.6	0.39	0.04	1437.
30	-1.59	32.10	30	25.85	216.2	0.61	0.10	1438.
50	-1.75	32.10	50	25.85	215.5	1.04	0.27	1438.
75	-1.66	32.39	75	26.08	193.2	1.55	0.60	1439.
100	-1.49	33.11	100	26.66	138.2	1.96	0.96	1441.
125	-1.11	33.70	125	27.13	93.9	2.25	1.28	1444.
150	-0.79	34.10	150	27.44	64.6	2.45	1.55	1447.
200	-0.29	34.40	200	27.66	44.3	2.72	2.02	1450.
300	-0.07	34.46	300	27.70	40.2	3.15	3.09	1453.
400	0.05	34.70	400	27.88	23.0	3.46	4.17	1456.
500	0.15	34.72	500	27.89	22.3	3.69	5.20	1458.

STATION ROB3 DATE 8/ 5/71
POSITION 81-54.0N, 62- 0.0W GMT 1520

PRESS	TEMP	SAL	DEPTH	SIGMA T	SVA	DELTA D	POT EN	SOUND VEL
2	-1.74	31.99	2	25.76	224.7	0.0	0.0	1437.
10	-1.76	32.00	10	25.77	224.0	0.18	0.01	1437.
20	-1.73	32.00	20	25.77	223.8	0.40	0.05	1437.
30	-1.77	32.00	30	25.77	223.7	0.63	0.10	1437.
50	-1.76	32.01	50	25.78	222.3	1.07	0.28	1438.
75	-1.68	32.07	75	25.82	217.9	1.62	0.63	1439.
100	-1.41	33.22	100	26.75	130.4	2.06	1.01	1442.
125	-1.18	33.58	125	27.03	103.1	2.35	1.34	1444.
150	-0.72	34.10	150	27.43	65.5	2.56	1.62	1447.
200	-0.38	34.43	200	27.69	41.0	2.83	2.08	1450.
300	-0.10	34.61	300	27.82	29.0	3.18	2.94	1453.
400	0.10	34.70	400	27.88	23.3	3.44	3.86	1456.

STATION ROB4 DATE 10/ 5/71
POSITION 81-51.5N, 61-43.0W GMT 1326

PRESS	TEMP	SAL	DEPTH	SIGMA T	SVA	DELTA D	POT EN	SOUND VEL
2	-1.73	31.97	2	25.75	225.8	0.0	0.0	1437.
10	-1.75	31.97	10	25.74	226.2	0.18	0.01	1437.
20	-1.76	31.98	20	25.75	225.7	0.41	0.05	1437.
30	-1.74	31.98	30	25.75	225.5	0.63	0.10	1437.
50	-1.73	32.06	50	25.82	218.8	1.08	0.28	1438.
75	-1.51	32.50	75	26.17	185.2	1.58	0.60	1440.
100	-1.44	32.85	100	26.44	158.9	2.01	0.98	1441.
125	-0.81	33.92	125	27.30	78.4	2.31	1.30	1446.
150	-0.63	34.00	150	27.36	72.8	2.50	1.57	1447.
200	-0.44	34.36	200	27.64	46.2	2.79	2.08	1450.
300	0.04	34.70	300	27.88	23.0	3.14	2.90	1454.

STATION ROB5 DATE 11/ 5/71
POSITION 81-59.0N, 62-22.0W GMT 2037

PRESS	TEMP	SAL	DEPTH	SIGMA T	SVA	DELTA D	POT EN	SOUND VEL
2	-1.76	32.51	2	26.18	184.3	0.0	0.0	1438.
10	-1.73	32.49	10	26.16	186.4	0.15	0.01	1438.
20	-1.70	32.48	20	26.15	187.1	0.34	0.04	1438.
30	-1.69	32.49	30	26.16	186.4	0.52	0.09	1438.
50	-1.68	32.53	50	26.20	182.7	0.89	0.23	1439.
75	-1.51	32.96	75	26.54	150.2	1.31	0.49	1441.
100	-1.35	33.40	100	26.89	116.5	1.64	0.79	1442.
125	-0.98	33.93	125	27.31	77.0	1.88	1.06	1445.
150	-0.73	34.24	150	27.55	54.0	2.05	1.28	1447.

APPENDIX II

TEMPERATURE (T°C)

DEPTH (M)

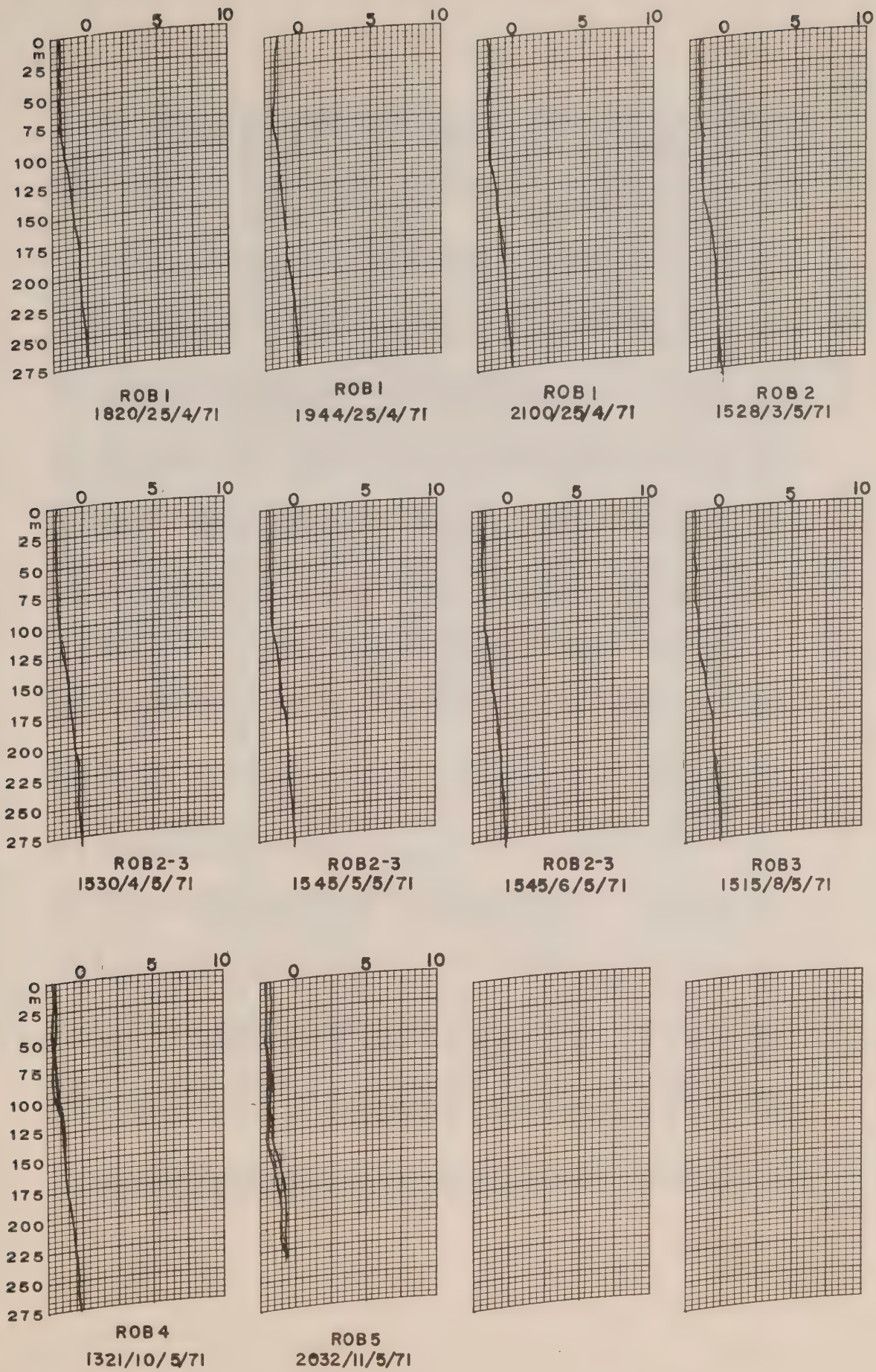

APPENDIX III

002005 3015260471 GMT 7072 1022 -78 ROBESON EAST 81515 61430 20 139 V2

	VEL	DIR	VEL	DIR	VEL	DIR	VEL	DIR	VEL	DIR	VEL	DIR	VEL	DIR	VEL	DIR
1	7.1	301	7.9	284	7.1	268	10.7	242	11.4	250	15.7	257	15.0	251	10.7	237
2	15.0	223	22.1	207	23.6	201	5.0	210	2.9	211	2.1	211	3.6	203	25.0	200
3	22.8	183	20.0	180	16.4	180	11.4	170	8.6	162	9.3	157	10.0	147	12.8	154
4	12.1	147	7.1	173	5.7	22	12.8	14	15.0	11	5.0	4	2.9	4	2.1	357
5	2.1	3	2.1	2	2.1	1	10.7	2	18.6	3	17.1	0	17.8	359	10.7	355
6	14.3	0	9.3	4	8.6	292	12.8	244	13.6	269	12.8	252	10.7	262	12.8	250
7	12.1	244	10.7	231	5.7	192	3.6	182	3.6	176	3.6	180	2.9	173	2.9	180
8	2.9	170	3.6	167	5.0	170	6.4	152	7.9	151	5.7	149	5.7	153	5.7	158
9	3.6	173	3.6	212	4.3	232	3.6	242	3.6	257	5.0	273	4.3	312	5.7	347
10	4.3	342	5.7	301	7.1	284	7.1	270	6.4	251	8.6	232	15.0	232	18.6	240
11	14.3	242	17.8	242	14.3	214	21.4	204	22.8	204	23.6	210	26.4	204	25.0	210
12	23.6	210	21.4	200	21.4	190	17.8	180	16.4	175	15.0	172	9.3	162	7.9	150
13	8.6	124	10.7	117	11.4	104	7.1	114	7.1	82	11.4	37	14.3	24	17.8	24
14	15.7	19	17.8	5	15.7	24	21.4	19	18.6	9	18.6	14	12.8	19	13.6	1
15	12.8	354	15.7	0	11.4	351	8.6	332	7.1	317	8.6	279	10.7	280	13.6	282
16	15.0	275	12.1	262	10.0	241	15.0	224	12.1	211	14.3	170	17.1	168	14.3	180
17	12.1	180	11.4	166	10.7	164	12.8	153	8.6	136	7.9	115	6.4	114	6.4	141
18	5.7	148	5.0	143	5.0	145	5.0	174	4.3	129	4.3	338	4.3	84	4.3	64
19	4.3	105	4.3	178	4.3	209	5.0	227	8.6	234	7.9	248	7.9	244	8.6	236
20	10.7	226	14.3	223	14.3	235	12.8	237	13.6	233	14.3	222	18.6	208	21.4	204
21	22.8	200	25.7	199	21.4	197	18.6	187	21.4	180	19.3	174	15.7	170	14.3	167
22	12.1	155	11.4	152	8.6	144	7.9	160	5.7	131	5.7	165	4.3	110	10.0	34
23	7.1	34	8.6	40	7.1	49	8.6	18	12.1	24	16.4	16	16.4	13	16.4	16
24	15.7	18	15.7	21	11.4	12	14.3	13	7.9	9	8.6	356	6.4	329	7.1	342
25	8.6	311	10.0	293	10.7	267	10.0	252	10.0	238	10.0	236	7.9	212	7.9	169
26	11.4	175	9.3	174	8.6	173	11.4	160	13.6	167	12.1	163	10.7	161	7.9	158
27	7.1	149	8.6	156	7.1	159	5.7	172	5.0	170	7.9	195	7.1	206	5.0	204
28	4.3	96	4.3	148	4.3	175	5.0	195	8.6	198	12.1	213	11.4	230	10.0	239
29	12.1	226	12.1	227	12.1	228	15.7	223	15.0	228	12.8	229	12.8	229	15.0	208

	VEL	DIR	VEL	DIR	VEL	DIR	VEL	DIR	VEL	DIR	VEL	DIR	VEL	DIR	VEL	DIR
30	19.3	209	19.3	203	20.7	198	22.1	194	19.3	189	21.4	186	22.1	181	16.4	173
31	17.8	179	14.3	169	15.0	164	13.6	169	11.4	160	7.9	142	5.7	142	5.0	140
32	4.3	140	5.0	85	7.1	54	8.6	40	7.9	46	7.1	66	7.1	20	11.4	16
33	14.3	9	19.3	6	17.1	9	15.0	9	12.1	5	15.7	359	14.3	358	11.4	351
34	8.6	354	7.9	339	6.4	320	7.9	318	6.4	281	6.4	264	7.1	246	4.3	234
35	5.7	232	7.9	214	10.0	147	12.1	157	12.8	199	12.1	197	10.7	186	10.7	186
36	12.1	186	9.3	184	7.1	183	5.7	177	4.3	182	5.0	185	5.7	190	8.6	198
37	7.1	197	7.9	207	7.1	208	5.0	208	4.3	197	5.0	203	7.1	209	7.9	220
38	5.7	217	12.1	199	13.6	217	12.1	229	12.1	226	16.4	221	13.6	224	18.6	224
39	17.1	212	19.3	207	19.3	205	17.8	204	18.6	204	18.6	200	18.6	194	17.8	182
40	20.7	185	19.3	182	15.7	181	17.1	174	15.7	180	14.3	179	9.3	185	7.1	171
41	7.1	166	5.7	173	5.0	196	4.3	226	3.6	29	3.6	74	3.6	58	5.0	39
42	8.6	39	8.6	29	11.4	26	8.6	22	9.3	14	12.1	12	12.1	9	10.7	357
43	10.7	350	11.4	324	11.4	330	12.1	334	8.6	337	7.9	327	7.9	309	5.0	287
44	5.7	253	3.6	247	4.3	227	7.9	224	8.6	220	5.7	191	6.4	191	7.9	202
45	9.3	207	10.0	197	7.9	191	9.3	200	8.6	197	10.0	202	7.1	196	7.1	190
46	5.7	198	5.7	196	6.4	199	7.9	207	9.3	212	11.4	208	7.9	205	6.4	213
47	6.4	214	7.1	222	7.1	235	10.7	222	10.7	210	11.4	210	13.6	210	13.6	212
48	14.3	209	17.8	219	17.8	222	15.7	223	17.8	218	12.8	208	15.7	212	12.8	204
49	12.8	198	13.6	195	12.1	189	11.4	189	12.1	185	11.4	189	14.3	184	12.1	172
50	10.0	170	8.6	165	7.9	172	7.1	166	5.7	175	5.0	172	5.7	187	5.0	194
51	5.0	214	3.6	77	3.6	61	3.6	47	4.3	30	6.4	30	9.3	28	7.1	18
52	7.9	18	9.3	13	7.9	2	6.4	355	9.3	358	9.3	1	7.9	340	6.4	323
53	5.0	316	5.0	299	4.3	287	3.6	277	5.7	245	7.1	230	7.1	220	7.1	212
54	5.0	205	5.7	202	10.7	204	11.4	208	13.6	204	14.3	207	12.1	206	12.8	204
55	10.7	195	8.6	193	7.9	193	8.6	195	8.6	194	10.0	199	12.1	206	12.8	202
56	12.1	209	12.1	218	7.9	220	7.9	213	7.9	213	7.9	215	5.7	215	7.1	209
57	7.9	213	11.4	206	12.8	206	11.4	204	12.1	206	10.0	208	11.4	210	10.7	230
58	12.1	214	12.1	213	11.4	214	13.6	210	12.8	214	17.8	205	18.6	201	18.6	196
59	15.7	193	12.8	199	9.3	193	9.3	192	6.4	196	5.7	186	5.0	179	5.7	171

002005 3015260471 GMT 7072 1022 -78 ROBESON EAST 81515 61430 20 139 V2

	VEL	DIR	VEL	DIR	VEL	DIR	VEL	DIR	VEL	DIR	VEL	DIR	VEL	DIR	VEL	DIR
60	5.7	163	6.4	165	6.4	172	6.4	202	4.3	213	4.3	267	3.6	359	3.6	57
61	3.6	62	3.6	52	5.7	24	6.4	27	5.0	22	4.3	17	5.0	16	5.0	358
62	4.3	337	5.0	318	5.0	299	5.0	284	5.7	282	5.0	288	4.3	242	6.4	235
63	7.1	231	6.4	223	11.4	206	10.7	209	15.0	207	14.3	212	15.0	208	17.8	207
64	18.6	206	15.7	203	15.7	199	12.8	205	10.7	203	9.3	203	9.3	203	10.0	207
65	11.4	197	10.7	198	10.7	200	14.3	198	15.7	195	12.8	200	11.4	210	7.9	220
66	5.7	230	5.7	235	5.7	229	5.7	209	5.7	206	5.7	192	7.9	203	12.1	205
67	15.7	211	14.3	214	11.4	220	10.0	224	10.7	228	12.8	224	11.4	222	12.1	211
68	13.6	209	13.6	213	15.0	199	12.1	201	8.6	199	10.0	197	8.6	194	7.1	204
69	5.7	191	5.7	173	7.9	170	6.4	170	6.4	180	6.4	184	5.7	195	3.6	204
70	3.6	238	3.6	17	4.3	39	3.6	53	4.3	39	6.4	39	6.4	34	5.7	25
71	5.0	17	5.0	5	5.0	357	5.0	351	5.0	327	4.3	316	5.0	293	6.4	263
72	7.1	252	5.0	241	5.7	227	8.6	221	10.0	215	12.8	207	12.8	204	14.3	205
73	15.7	205	17.1	207	14.3	205	15.0	204	15.7	210	12.1	206	9.3	201	10.7	204
74	5.7	192	8.6	195	7.9	186	7.9	191	9.3	189	12.8	194	14.3	195	13.6	198
75	7.1	207	5.7	211	5.0	194	4.3	197	3.6	208	3.6	203	3.6	195	4.3	221
76	3.6	241	4.3	241	4.3	262	4.3	255	4.3	265	4.3	237	5.0	248	5.0	243
77	6.4	238	9.3	226	9.3	225	10.7	212	11.4	208	12.8	203	12.8	212	12.8	202
78	12.1	211	8.6	208	6.4	198	7.1	204	7.1	197	6.4	200	5.7	182	5.7	191
79	8.6	187	5.7	177	4.3	157	4.3	153	4.3	87	5.0	76	3.6	59	4.3	42
80	5.7	29	4.3	30	4.3	31	3.6	14	3.6	334	5.0	321	5.7	306	6.4	287
81	0.4	285	5.7	276	5.7	268	8.6	252	7.1	254	8.6	242	10.0	229	12.1	225
82	13.6	214	15.0	206	16.4	205	17.1	203	17.8	199	19.3	202	17.1	202	15.0	203
83	12.8	199	12.1	200	9.3	213	8.6	213	7.1	207	5.7	192	8.6	182	8.6	207
84	13.6	218	10.7	222	4.3	241	3.6	255	3.6	229	3.6	224	3.6	263	3.6	313
85	3.6	335	3.6	356	3.6	349	3.6	338	3.6	327	4.3	310	4.3	299	5.7	277
86	5.7	271	6.4	264	5.7	244	7.9	230	9.3	223	8.6	212	10.7	200	13.6	201
87	13.6	204	14.3	203	12.1	203	12.8	206	12.1	209	7.9	202	7.1	200	5.0	184
88	5.7	183	5.7	191	7.1	189	5.7	195	4.3	190	3.6	192	3.6	199	3.6	87
89	5.0	50	3.6	51	4.3	30	0.4	35	5.7	33	4.3	19	4.3	4	4.3	338

	VEL	DIR	VEL	DIR	VEL	DIR	VEL	DIR	VEL	DIR	VEL	DIR	VEL	DIR	VEL	DIR
90	5.0	313	5.7	286	7.1	265	8.6	247	10.0	238	12.1	233	15.7	224	17.8	224
91	15.7	225	16.4	215	19.3	211	17.8	212	19.3	205	19.3	192	22.8	200	20.0	212
92	14.3	206	12.1	185	13.6	175	12.1	182	13.6	180	12.1	170	12.8	178	8.6	176
93	7.1	169	6.4	181	15.0	205	7.1	222	4.3	335	4.3	24	4.3	82	5.0	96
94	4.3	80	4.3	94	3.6	85	3.6	40	4.3	0	4.3	353	4.3	357	3.6	333
95	5.0	311	5.7	275	6.4	255	7.1	249	7.9	260	7.1	245	8.6	231	7.9	222
96	11.4	210	11.4	196	12.8	201	9.3	192	12.8	184	14.3	187	12.1	190	8.6	196
97	6.4	194	5.7	182	7.1	186	7.1	200	7.9	196	7.9	200	7.1	207	6.4	201
98	3.6	268	4.3	322	4.3	25	4.3	61	4.3	63	4.3	50	5.0	71	4.3	356
99	3.6	323	4.3	283	4.3	273	5.0	265	6.4	252	7.1	247	10.7	240	10.7	239
100	12.1	230	12.8	232	16.4	220	19.3	212	22.1	214	20.0	216	18.6	205	21.4	200
101	17.1	199	17.8	192	13.6	186	15.0	181	11.4	173	11.4	157	8.6	162	10.7	151
102	9.3	142	8.6	146	10.0	175	12.1	202	5.7	212	3.6	173	3.6	96	5.7	78
103	7.1	75	3.6	45	5.0	74	5.7	38	6.4	20	7.9	14	7.9	3	6.4	350
104	6.4	350	5.0	322	5.7	317	7.1	288	7.9	262	7.1	265	10.0	248	12.1	243
105	10.0	249	9.3	236	8.6	219	10.7	210	10.7	193	12.8	176	12.8	175	11.4	185
106	7.9	170	6.4	167	6.4	171	6.4	181	7.9	170	8.6	169	8.6	171	10.0	174
107	6.4	186	4.3	154	3.6	115	3.6	110	3.6	109	4.3	117	3.6	140	3.6	144
108	3.6	207	9.3	247	10.7	248	10.7	243	10.0	250	15.0	240	15.7	237	12.1	234
109	18.6	220	20.0	211	19.3	192	20.0	190	18.6	194	17.1	188	17.1	185	16.4	174
110	12.8	164	12.1	151	13.6	143	12.1	138	15.0	138	9.3	146	10.0	150	12.1	183
111	6.4	201	4.3	55	5.0	65	5.7	64	6.4	71	4.3	62	6.4	22	5.0	44
112	8.6	9	9.3	12	9.3	2	10.7	354	8.6	340	10.0	329	8.6	315	9.3	297
113	8.6	290	13.6	260	11.4	260	10.0	267	10.0	259	7.1	213	7.9	219	9.3	197
114	14.3	169	15.7	176	16.4	175	14.3	183	11.4	185	10.0	184	8.6	187	6.4	190
115	7.1	175	7.1	185	5.0	182	7.1	168	12.8	186	10.0	203	3.6	218	3.6	54
116	4.3	98	5.0	109	5.0	105	5.0	113	3.6	217	3.6	204	4.3	201	5.0	227
117	5.7	241	9.3	235	12.1	239	14.3	239	16.4	236	17.8	236	18.6	237	15.7	222
118	19.3	217	22.8	204	22.8	195	22.8	187	25.7	198	23.6	194	21.4	197	21.4	191
119	17.1	185	15.0	176	13.6	154	12.1	146	11.4	139	12.1	126	12.8	133	10.0	135

002005 3015260471 GMT 7072 1022 -78 ROBESON EAST 81515 61430 20 139 V2

	VEL	DIR	VEL	DIR	VEL	DIR	VEL	DIR	VEL	DIR	VEL	DIR	VEL	DIR	VEL	DIR
120	7.9	163	7.9	193	3.6	113	5.0	79	6.4	65	7.9	72	6.4	61	7.1	34
121	9.3	27	10.0	10	14.3	9	13.6	4	12.1	358	12.8	353	11.4	345	5.7	344
122	5.7	321	7.9	292	10.0	287	10.7	288	10.7	279	10.7	256	8.6	261	8.6	232
123	10.0	210	9.3	179	12.8	176	15.0	169	15.7	181	15.7	182	13.6	174	16.4	177
124	12.1	172	9.3	167	9.3	164	8.6	163	7.1	182	5.0	184	6.4	197	5.0	220
125	3.6	212	5.0	87	6.4	115	7.9	123	5.0	147	4.3	179	4.3	205	5.7	234
126	5.7	241	7.1	252	7.9	249	8.6	237	12.8	234	13.6	237	17.1	231	18.6	234
127	19.3	237	17.1	227	19.3	220	19.3	214	20.7	205	19.3	192	25.0	194	25.0	197
128	20.7	182	20.0	185	16.4	174	13.6	162	12.8	165	12.8	150				

WFIN

003004 0016260471 GMT 7072 1033 -78 ROBESON WEST 81590 62200 20 140 V2

	VEL	DIR	VEL	DIR	VEL	DIR	VEL	DIR	VEL	DIR	VEL	DIR	VEL	DIR	VEL	DIR
1	10.7	304	12.1	301	15.0	302	15.0	306	11.4	287	12.8	235	12.8	224	15.7	217
2	21.4	214	23.6	224	17.8	216	24.3	211	26.4	211	25.7	207	27.1	202	28.6	212
3	25.0	217	19.3	214	17.8	186	12.8	189	7.9	149	8.6	103	11.4	100	14.3	99
4	10.7	41	10.0	15	10.7	351	13.6	355	10.7	10	10.0	6	11.4	356	12.8	357
5	14.3	357	12.1	352	9.3	5	9.3	348	7.9	306	11.4	327	12.1	310	12.1	294
6	14.3	302	15.7	300	16.4	301	18.6	294	18.6	289	18.6	289	15.7	273	15.0	250
7	21.4	256	21.4	259	15.7	252	8.6	232	7.9	211	5.0	169	7.1	144	7.1	126
8	8.6	123	7.9	149	7.9	121	5.0	136	6.4	165	6.4	102	11.4	65	18.6	39
9	18.6	40	10.7	35	11.4	29	11.4	13	10.7	11	12.8	9	13.6	342	10.0	340
10	10.0	320	12.1	318	16.4	308	26.4	309	26.4	307	22.1	302	22.8	299	20.7	295
11	20.0	292	15.7	290	10.7	265	9.3	229	11.4	209	14.3	177	15.0	170	16.4	164
12	10.7	147	6.4	115	19.3	80	30.0	85	32.1	96	29.3	94	25.7	98	22.1	113
13	17.1	118	20.0	87	20.0	53	13.6	42	8.6	29	8.6	12	13.6	9	11.4	13
14	9.3	354	15.0	1	14.3	354	12.1	358	11.4	2	12.1	348	12.1	338	12.1	331
15	15.7	321	19.3	319	19.3	324	16.4	314	15.7	316	16.4	316	18.6	316	15.0	314
16	12.8	316	12.1	316	5.7	333	5.0	359	5.0	327	5.0	62	7.9	99	12.1	96
17	17.1	83	20.7	88	22.1	100	20.7	126	20.0	77	17.8	113	11.4	152	9.3	139
18	12.1	82	7.1	64	19.3	33	18.6	55	11.4	43	7.9	19	7.1	13	7.9	345
19	12.8	341	10.7	353	8.6	1	7.1	1	5.7	16	9.3	328	9.3	327	7.9	322
20	7.9	323	5.0	334	5.0	17	5.0	332	5.0	225	15.0	198	21.4	227	24.3	222
21	23.6	209	23.6	196	22.8	174	24.3	178	26.4	195	25.0	203	23.6	186	20.0	174
22	20.0	166	19.3	173	17.8	187	18.6	208	8.6	234	5.0	316	4.3	13	7.1	27
23	5.7	9	7.1	42	9.3	27	12.8	37	8.6	340	7.1	355	7.1	352	8.6	356
24	10.0	346	10.0	334	9.3	319	11.4	303	12.1	305	13.6	298	12.8	301	10.7	296
25	7.9	286	8.6	261	7.1	254	5.0	234	8.6	215	9.3	195	12.1	200	15.7	210
26	11.4	228	7.9	211	6.4	195	5.0	190	5.0	163	5.0	147	6.4	91	4.3	22
27	5.7	235	7.1	219	7.1	32	8.6	50	10.0	55	10.7	50	10.7	46	6.4	61
28	5.0	66	5.7	68	5.7	344	6.4	324	8.6	326	8.6	311	8.6	305	12.8	308
29	15.7	316	14.3	313	10.7	318	9.3	310	7.9	321	6.4	341	4.3	49	4.3	135

	VEL	DIR	VEL	DIR	VEL	DIR	VEL	DIR	VEL	DIR	VEL	DIR	VEL	DIR	VEL	DIR
30	6.4	158	15.0	155	16.4	159	19.3	164	22.1	161	17.1	173	15.7	163	17.8	172
31	12.1	175	10.0	166	12.1	160	10.7	164	7.9	192	6.4	140	4.3	146	5.0	66
32	7.1	35	10.7	24	7.1	6	5.7	4	7.9	355	10.7	358	9.3	343	7.9	356
33	7.9	0	8.6	334	9.3	325	10.0	329	10.7	319	12.1	314	14.3	303	13.6	305
34	15.7	310	15.7	314	15.0	322	10.0	324	5.0	323	3.6	307	4.3	282	4.3	277
35	5.0	238	5.0	201	9.3	176	12.8	172	11.4	180	12.1	175	9.3	182	8.6	184
36	7.9	202	7.9	212	9.3	220	7.1	224	6.4	234	5.7	249	7.1	10	11.4	47
37	7.9	359	7.9	353	5.0	162	4.3	19	4.3	41	4.3	6	5.0	314	10.7	308
38	17.1	310	12.8	314	15.7	310	12.1	304	12.8	300	8.6	292	11.4	286	10.7	275
39	10.0	284	10.7	284	12.1	251	15.0	228	11.4	240	8.6	222	7.9	181	7.1	158
40	9.3	159	8.6	141	9.3	122	6.4	125	12.1	78	11.4	110	8.6	149	7.9	126
41	22.1	56	20.0	58	22.8	76	20.0	69	18.6	51	13.6	57	12.1	42	7.9	32
42	7.9	27	7.1	9	8.6	0	9.3	355	10.0	338	10.7	328	9.3	334	11.4	332
43	12.1	335	12.8	344	7.9	348	8.6	340	5.7	340	8.6	326	5.7	331	5.0	329
44	4.3	91	5.0	137	5.0	162	5.0	168	7.9	177	8.6	165	8.6	160	7.9	159
45	7.9	153	5.0	141	5.0	131	7.1	115	10.0	119	7.9	121	5.0	136	5.0	87
46	5.0	130	4.3	128	10.7	74	15.0	71	12.8	76	8.6	80	6.4	92	4.3	4
47	4.3	303	4.3	296	5.0	299	5.7	303	6.4	308	5.0	307	5.0	280	7.9	293
48	7.9	304	6.4	307	5.0	308	5.0	307	6.4	270	7.9	240	7.1	223	7.9	223
49	5.0	233	5.0	224	4.3	352	4.3	63	4.3	95	4.3	97	4.3	104	5.7	94
50	5.0	137	5.7	144	5.0	130	9.3	75	17.1	64	15.7	69	16.4	72	13.6	66
51	9.3	62	9.3	52	13.6	68	7.9	50	7.1	15	5.7	345	6.4	339	7.1	344
52	7.9	334	6.4	354	6.4	11	5.0	343	4.3	57	5.0	114	4.3	130	5.0	179
53	5.0	209	5.0	216	4.3	187	5.0	148	8.6	173	8.6	193	7.9	188	8.6	193
54	8.6	196	9.3	192	10.7	211	10.7	208	8.6	216	7.1	207	7.1	212	5.7	220
55	4.3	221	4.3	154	4.3	107	4.3	2	4.3	299	5.0	336	5.0	318	6.4	340
56	7.9	12	7.9	33	8.6	39	9.3	45	7.9	41	5.7	2	5.7	324	4.3	327
57	5.0	328	4.3	286	4.3	240	5.0	230	4.3	234	4.3	264	5.0	251	14.3	224
58	19.3	220	17.1	217	15.0	219	12.8	216	10.7	214	7.9	190	8.6	179	10.0	181
59	10.7	200	7.9	183	10.0	183	8.6	195	5.7	179	5.0	178	5.0	167	4.3	155

	VEL	DIR	VEL	DIR	VEL	DIR	VEL	DIR	VEL	DIR	VEL	DIR	VEL	DIR	VEL	DIR
60	4.3	124	7.1	72	11.4	72	8.6	66	10.7	62	8.6	54	5.7	54	6.4	54
61	8.6	51	7.9	47	7.1	50	6.4	53	5.0	35	4.3	70	4.3	17	4.3	357
62	4.3	300	4.3	284	5.0	282	4.3	277	5.0	249	5.0	231	5.0	226	3.6	222
63	4.3	199	7.9	179	10.0	176	13.6	188	13.6	203	14.3	209	14.3	211	13.6	213
64	14.3	213	14.3	218	14.3	224	12.1	220	11.4	223	9.3	213	7.9	210	5.7	209
65	4.3	233	4.3	234	4.3	122	4.3	36	4.3	82	4.3	75	5.7	73	7.1	60
66	5.0	47	4.3	26	4.3	357	4.3	302	4.3	347	5.0	310	5.0	300	5.0	285
67	5.0	239	5.7	196	7.9	191	15.0	220	18.6	220	19.3	211	20.7	210	24.3	223
68	20.0	219	25.0	215	21.4	204	20.7	212	21.4	215	18.6	223	15.7	219	14.3	213
69	7.1	242	5.0	252	5.0	254	4.3	232	4.3	199	4.3	57	4.3	62	5.0	93
70	4.3	104	4.3	98	4.3	282	4.3	318	5.0	329	7.9	328	10.0	325	11.4	320
71	9.3	313	10.0	308	8.6	306	7.9	308	6.4	309	7.1	280	7.1	256	7.1	261
72	7.1	260	7.9	250	7.9	236	8.6	220	10.0	202	11.4	198	12.8	197	11.4	186
73	10.0	173	9.3	172	11.4	174	13.6	183	15.7	188	17.8	175	14.3	182	15.7	203
74	16.4	222	21.4	226	15.7	230	11.4	232	9.3	253	5.7	274	5.0	316	4.3	316
75	5.0	308	5.0	311	5.0	321	5.0	322	7.1	299	7.9	267	7.1	297	5.7	313
76	4.3	332	5.0	316	4.3	294	4.3	255	5.7	223	11.4	218	13.6	220	15.0	220
77	17.1	229	18.6	225	14.3	229	18.6	231	13.6	231	12.8	231	16.4	232	14.3	237
78	8.6	245	7.9	237	7.1	234	5.0	229	4.3	198	4.3	152	5.0	94	8.6	55
79	7.9	57	6.4	99	5.0	57	7.9	29	5.0	2	5.7	349	6.4	351	5.7	0
80	6.4	342	6.4	343	4.3	331	4.3	320	8.6	286	12.8	281	12.8	276	14.3	273
81	15.0	267	16.4	258	15.0	253	15.0	254	12.8	244	12.8	237	12.1	230	13.6	219
82	14.3	218	12.8	218	9.3	220	6.4	221	5.0	183	5.0	155	4.3	167	4.3	155
83	7.9	115	14.3	106	13.6	95	13.6	81	17.1	87	22.1	88	19.3	71	17.1	65
84	22.1	64	14.3	82	15.7	80	12.8	65	9.3	61	6.4	32	5.0	39	7.9	23
85	6.4	26	5.0	6	5.0	30	5.0	29	4.3	62	4.3	184	4.3	208	8.6	211
86	14.3	214	16.4	218	13.6	214	11.4	218	7.1	198	7.1	182	11.4	177	16.4	194
87	17.8	189	15.7	183	15.7	169	13.6	169	9.3	165	8.6	173	14.3	194	15.0	213
88	9.3	223	7.9	222	4.3	195	4.3	197	4.3	292	5.0	340	4.3	307	5.0	52
89	5.0	7	4.3	112	4.3	335	5.0	355	7.1	310	5.7	317	4.3	302	8.6	275

	VEL	DIR	VEL	DIR	VEL	DIR	VEL	DIR	VEL	DIR	VEL	DIR	VEL	DIR	VEL	DIR
90	8.6	274	11.4	279	10.7	250	16.4	256	15.7	254	16.4	247	17.1	259	15.7	249
91	14.3	246	14.3	238	11.4	224	12.1	217	10.0	220	7.9	200	10.7	188	8.6	194
92	8.6	187	8.6	156	11.4	161	6.6	181	4.3	130	8.6	98	8.6	91	5.7	136
93	10.0	95	15.7	33	8.6	59	12.1	59	12.1	45	10.0	46	7.9	32	9.3	355
94	9.3	7	7.9	342	12.1	331	15.7	328	12.1	328	14.3	326	12.1	323	9.3	325
95	11.4	308	10.0	296	13.6	293	10.7	295	5.7	300	4.3	281	4.3	242	5.0	212
96	6.4	195	7.9	193	5.0	181	7.9	174	10.7	169	8.6	129	12.8	97	19.3	94
97	15.0	105	15.0	104	15.0	92	11.4	117	15.7	89	19.3	66	20.0	64	20.0	75
98	17.1	77	12.1	70	9.3	73	15.0	61	9.3	58	7.1	57	5.0	51	5.0	30
99	4.3	35	4.3	73	4.3	172	7.1	227	5.0	212	7.9	192	9.3	193	15.0	198
100	19.3	206	22.8	213	22.1	221	25.7	212	24.3	204	22.1	192	27.1	194	26.4	188
101	29.3	200	25.0	200	20.7	183	17.8	182	17.1	174	12.1	170	9.3	160	7.9	127
102	5.0	132	7.9	177	5.0	269	7.9	352	7.9	356	5.0	343	7.9	2	7.9	347
103	11.4	338	15.0	340	10.0	323	17.8	336	14.3	327	14.3	332	10.7	333	5.7	352
104	6.4	307	8.6	287	16.4	280	15.0	259	19.3	240	19.3	228	19.3	220	22.1	211
105	23.6	212	22.8	214	20.0	211	19.3	210	18.6	192	17.1	122	16.4	208	15.7	198
106	15.0	199	17.8	198	15.7	207	10.0	216	9.3	243	9.3	259	5.7	261	7.1	1
107	4.3	11	8.6	28	7.1	55	7.1	42	11.4	17	11.4	21	7.1	351	10.7	321
108	15.0	313	15.7	297	18.6	302	18.6	294	15.7	290	15.7	284	15.0	281	13.6	270
109	13.6	260	15.0	252	16.4	239	16.6	227	16.4	218	15.0	213	11.4	198	11.4	189
110	9.3	210	11.4	178	19.3	156	11.4	127	12.1	85	20.0	101	22.8	96	24.3	117
111	22.1	86	24.3	88	19.3	106	21.4	80	20.0	34	15.0	42	12.8	44	6.4	41
112	13.6	72	12.1	24	11.4	21	12.1	9	13.6	11	9.3	344	8.6	337	7.9	353
113	6.4	322	7.9	325	10.7	332	7.1	319	6.4	309	5.0	298	5.0	289	5.0	281
114	5.7	255	9.3	214	8.6	198	12.8	201	11.4	199	8.6	187	10.7	182	7.9	182
115	5.0	182	11.4	158	15.7	166	17.1	172	13.6	173	7.9	145	8.6	92	10.7	123
116	10.0	123	11.4	70	16.4	62	17.1	103	10.0	72	11.4	74	9.3	71	7.1	65
117	5.0	95	5.0	80	5.0	197	4.3	239	4.3	239	7.9	228	7.9	219	17.1	229
118	20.7	229	22.8	231	20.7	244	17.1	242	17.8	234	19.3	218	21.4	218	21.4	220
119	22.8	223	21.4	221	23.6	224	22.1	206	21.4	202	16.4	213	16.4	192	8.6	185

003004 0016260471 GMT 7072 1033 -78 ROBESON WEST 81590 62200 20 140 V2

	VEL	DIR	VEL	DIR	VEL	DIR	VEL	DIR	VEL	DIR	VEL	DIR	VEL	DIR	VEL	DIR
120	5.7	166	7.9	128	12.1	108	7.9	94	7.1	61	10.0	20	15.0	5	16.4	21
121	13.6	8	8.6	4	12.8	355	17.1	339	15.7	342	19.3	340	15.7	342	12.1	342
122	20.0	345	14.3	327	18.6	326	17.8	326	19.3	318	20.7	311	18.6	310	18.6	303
123	15.7	298	11.4	291	9.3	290	8.6	241	10.0	205	7.9	206	7.1	217	7.1	182
124	8.6	149	9.3	155	9.3	118	14.3	108	16.4	118	12.8	122	17.1	94	17.1	118
125	13.6	143	8.6	119	15.0	103	23.6	65	21.4	75	24.3	75	19.3	73	16.4	63
126	16.4	58	12.1	65	9.3	56	7.9	10	6.4	336	5.0	333	7.1	328	8.6	317
127	10.0	302	10.7	278	12.1	270	15.7	270	12.1	268	12.1	242	17.1	208	20.0	177
128	18.6	174	20.0	179	12.1	179	15.7	175	12.1	179	17.8	190	23.6	209	16.4	201
129	13.6	203	11.4	199	11.4	180	8.6	139	6.4	123	6.4	157	6.4	62	9.3	14
130	7.9	10														

$FIN

CAI
EP321
-79R17

Government
Publications

Pacific Marine Science Report 79-17

FEB 5 1981

COPPER AND ZINC IN SEDIMENTS OF GEORGIA STRAIT, B.C. IN THE VICINITY OF TEXADA MINE

by

J.A.J. Thompson, D.W. Paton
and M. Timmons

INSTITUTE OF OCEAN SCIENCES, PATRICIA BAY
Sidney, B.C.

For further copies or additional information please write to:

Department of Fisheries and Oceans
Institute of Ocean Sciences
P.O. Box 6000
Sidney, B.C. CANADA
V8L 4B2

CA1
EP521
-79R17

Pacific Marine Science Report 79-17

COPPER AND ZINC IN SEDIMENTS OF GEORGIA STRAIT, B.C. IN THE VICINITY OF TEXADA MINE

by

J.A.J. Thompson, D.W. Paton
and
M. Timmons

Institute of Ocean Sciences, Patricia Bay
Sidney, B.C.
1979

ABSTRACT

The copper and zinc concentrations in sediments of Georgia Strait, B. C., adjacent to the inactive iron-copper mine on Texada Island, are reported. Copper concentrations in 32 samples from 16 μg g^{-1} to 1584 μg g^{-1} and exhibited a distribution pattern relating these elevated concentrations to the mine as source. No significant elevation of zinc in the samples (range 28-195 μg g^{-1}, dry weight) was observed although a statistically significant relationship between copper and zinc levels was established.

INTRODUCTION

Texada Mine, located on the northwest shore of Texada Island in Georgia Strait, B. C., closed down operations in September 1976. Since 1952, it had produced iron and copper concentrates for Japanese buyers. Until 1964, it was operated as an open pit. From 1966 on all operations were underground. A high grade of iron concentrate averaging 65% iron was produced. Copper concentrates averaged 0.055 percent. Usable amounts of sulfur and phosphorus were also mined.

Two factors were instrumental in bringing about the shut-down in 1976. The first and major one was the expiry of the Japanese contract on September 30. Secondly, the mine would have been required to install a submarine discharge pipe to eliminate pollution of neighboring beaches. The existing discharge line consisted of a wooden flume which terminated above the high-water line. Periodically, the flume was extended as the tailings accumulated on the beach.

Studies in 1971 (Goyette, personal communication, 1979) indicated that oysters (Crassostrea gigas) from the adjacent beaches were heavily contaminated with copper. Concentrations averaged 1,200 $\mu g\ g^{-1}$ (range 1,128-1,240 $\mu g\ g^{-1}$) for the specimens. The condition of the few oysters found in this area was extremely poor.

Discharge of solids to Georgia Strait averaged 3,266 tonnes per day (3,600 short tons) in 1970. Because of the high limestone content, a good deal of the tailings were used for cement manufacture and local road construction. There exists at present a large limestone deposit on the property which the company is now utilizing for similar purposes.

In January 1975, a cruise to collect samples of sediments on a grid in the Strait of Georgia was undertaken. This was part of a continuing program intended to study the chemistry of deposited tailings from various mines on the B. C. coast (Thompson and McComas, 1974; Thompson and Paton, 1975, 1976, 1978). We report here the data obtained for copper and zinc determinations for the 32 sediment samples that were collected.

METHODS

Sampling

Sampling stations and the area of study are shown in Figures 1 and 2. All samples were obtained with a Hydro Products Shipek grab. A vertical subsample was removed from the grab bucket with a plastic scoop, placed into a "Whirlpak" plastic bag and frozen immediately. Sampling was carried out from the C.S.S. Vector.

Analysis

In preparation for analysis the entire sub-sample was freeze-dried, pulverized in mortar and pestle and sieved through a 149 µm (100 mesh) screen.

Analysis was made only on the < 149 μm fraction.

An accurately weighed one gram sample was treated with hot aqua regia as described previously (Thompson and McComas, 1974). After dilution to 100 mL the extract was analyzed for copper and zinc by flame atomic absorption spectrophotometry. The instrument employed was a Jarrell-Ash, model 810. Instrument settings were primarily those recommended by the manufacturer. Data for copper and zinc were calculated as μg g^{-1} of dry sediment. Analytical precision was determined by replicate (10 analyses of U. S. National Bureau of Standards copper mine tails [SRM 331]). Means of 903 ± 6 (1σ) $\mu g.g^{-1}$ and 36.3 ± 5.9 (1σ) $\mu g.g^{-1}$ were obtained for copper and zinc respectively. The certified value for Cu is 910 ± 10 (1σ) $\mu g.g^{-1}$. Precision for three replicate determinations of copper in Texada samples was 16.4 ± 2.3 (1σ) μg g^{-1} (Station 28) and 1076 ± 21.9 (1σ) μg g^{-1} (Station 7).

RESULTS AND DISCUSSION

Copper and zinc concentrations for the 32 sediment samples are shown in Table 1. Spatial distributions have been plotted as isopleths shown in Figures 3 and 4.

Copper concentrations are highest in the vicinity of the mine outfall, reaching a maximum of nearly 1600 μg g^{-1}, dry weight at Station 4. From the isopleth diagram it is apparent that there was considerable alongshore drift northwestward. These values are the highest for any mine-derived materials studied by us. Southeast alongshore drift is indicated also, however data in this direction are not sufficient to indicate the extent of this distribution.

The structure of the isopleths in Figure 3 shows that a second transport component lies directly south of the mine. This component probably accounts for a major proportion of the waste materials which were released in the 24-year period of operations. The outer edge of mine-derived material detectable by chemical means lies between the 50 and 100 μg g^{-1} lines. A survey carried out by contractors for the mine in 1971 (Goyette, personal communication, 1979) delineated the distribution based upon visual observations. The outer limits as estimated have been reproduced in our scale in Figure 5. It can be seen that the direction of transport coincides well with our findings although as might well be expected the limits are one-quarter to one-fifth those determined chemically.

Figure 4 isopleths indicate no discernible trends in zinc distribution, and in particular, there are no contours which suggest that the mine was a source of this element. The copper-zinc ratio has been used previously (Thompson and McComas, 1974; Thompson and Paton, 1975) as an operational parameter to delineate mine tailings distribution. As an alternative to this graphic approach, which now appears to have limited applicability, we have plotted copper concentrations against the zinc values for each of the 32 stations (Figure 6). We obtained two regression lines using reduced major axis calculations (Till, 1974) which eliminate biases imposed by normal least squares regression. They are used where there is no apparent dependence of one parameter upon another. Inspection of the plot of all 32 data pairs indicated that stations 1 to 15 represented a different population that stations 16 to 32. This coincided roughly with the apparent zone of influence of the tailings

(Figure 3). After establishing a normal distribution of data by χ^2 applications two reduced major axis lines were generated (Figure 6) from data for stations 1-15 and 16-32. Both lines had highly significant correlation coefficients of $r = 0.57$ ($p < 0.02$) and $r = 0.90$ ($p << 0.001$), suggesting a strong geochemical relationship between these two elements in both mine-derived and natural sediments (i.e. Stations 16-32). Although there is strong evidence to suggest that these two data sets do represent different populations there were not sufficient grounds to warrant a comparison of slopes which would serve as a statistical demonstration that deposits of material different from naturally occurring sediments exist in Georgia Strait adjacent to the mine.

Most British Columbia coastal mines are located in fjords or inlets where water circulation is characteristically restricted. In cases where tailings have been released directly to the receiving waters (e.g. Howe Sound, Rupert Inlet, Alice Arm) the wastes have accumulated within a few km^2 of the discharge point. This type of situation in turn has created a potential or real source of heavy metal contamination due to diagenetic processes which serve to release the metals to interstitial and overlying waters. In the upper basin of Howe Sound, for example, we have observed enrichment of the water column and interstitial waters with copper (Thompson and Paton, 1978). There is some evidence also (Thompson, unpublished data) to suggest that pore waters in tailings deposited in Rupert Inlet may contain elevated concentrations of dissolved arsenic species because of the high arsenic content in the discharged materials.

Texada Mine and the small, now defunct operation at Jordan River on Vancouver Island (Ellis, 1975) share the distinction of being on open, well-flushed coastlines. This situation has served to distribute waste materials over a wide area, which might conceivably produce two opposing effects. On one hand this dispersal would prevent, except in the vicinity of the outfall, an accumulation of several centimeters of tailings which might be required before discernible chemical impact. However, on the other hand, if contaminants contained in the tailings were particularly mobile this dispersal may have the effect of distributing the contaminant over a larger area. Population diversity and the concentrations of some heavy elements (including both metals and metalloids) in organisms near industrial activity are often used as indicators of metal contamination. There are surprisingly few data available to indicate whether shoreline benthos on Texada Island have been affected. Goyette (1975) reported that oysters (Crassostrea gigas) collected within the tailings plume while the mine was still operating contained amounts of copper averaging 3,700 mg kg^{-1} (presumably dry wt.) and invertebrates dropped from 40 species in control areas to 2 species within the deposition area.

There are insufficient data however to indicate the extent of contamination in intertidal or subtidal invertebrates.

The entire question of metal concentrations derived from mining activities in benthos on this coast is one which begs an answer. It appears as if there may be a certain degree of site-specificity involved. This is suggested by data for oysters in particular. In Howe Sound this species (Goyette, 1975) contained up to 2,550 $\mu g\ g^{-1}$ (dry wt.) south of the mine outfall, one year after operations ceased. Concentrations are considerably greater than those found for any pristine inlet. Although the evidence suggests strongly that the Britannia Mine activity was the source of this excess copper there is a possibility that the contamination is the result of leaching from natural

mineral formations which contain the metal.

Waldichuk recently (1979) discussed the differences in metal content of biota from two dissimilar mining activities. Nine years of monitoring have yet to show evidence of increased tissue burdens of copper or zinc in shellfish in the Rupert/Holberg Inlet areas. However there were considerable increases of zinc in just one year of mining operation in mussel (M. Edulis) tissue from shore stations near the Marmorilik mine in Agfardlikavsa fjord in Greenland. Output of the latter mine is only 1400-1800 tonnes d^{-1} compared to 38,000 tonnes d^{-1} for the Island copper mine. The nature of mineralization is different, which may allow for a greater solubilization of lead and zinc.

Although there are no planned monitoring activities for the shoreline area of Texada Island it would nonetheless be of interest to see whether or not further uptake of copper by shellfish occurs in this area in spite of the non-restricted water movement.

CONCLUSIONS

The copper and zinc concentrations in marine sediments from Georgia Strait in the vicinity of a copper mine on Texada Island have been determined. Concentrations of up to approximately 1600 $\mu g\ g^{-1}$ (dry wt.) were found in nearshore stations within 1.8 km of the outfall. Concentrations decreased rapidly with distance from the mine, with background values being observed at about 9-18 km distance. Zinc concentrations showed no trends with distance.

ACKNOWLEDGEMENTS

The able-bodied assistance of Dr. Bob Olafson, as well as the officers and crew of C.S.S. Vector during the cruise in January 1975, is gratefully acknowledged. Miss B. Mathias typed the manuscript. D. Harrison assisted with additional analytical and statistical exercises. We thank D. Goyette of the Environmental Protection Service for providing historical information about the mine.

REFERENCES

Ellis, D.V. 1975. Pollution controls on mine discharges to the area. Int. Conf. Heavy Met. Environ. (Symp. Proc.) 1st 1975, Toronto. 2: 677-685.

Goyette, D.E. 1975. Marine tailings disposal - case studies. Paper presented at the Mining Effluent Regulations/Guidelines and Effluent Treatment Seminar, Banff, Alberta, Dec. 9-10. Unpublished manuscript.

Thompson, J.A.J. and F.T. McComas. 1974. Copper and zinc levels in submerged mine tailings at Britannia Beach, B. C. Fish. Res. Bd. Canada Tech. Rept. No. 473, 33 pp.

Thompson, J.A.J. and D.W. Paton. 1975. Chemical delineation of a submerged mine tailings plume in Rupert and Holberg Inlets, B. C. Fish. Mar. Serv. Tech. Rep. No. 506, 22 pp.

_____1976. Further studies of mine tailings distribution in Howe Sound, B. C. Fish. Res. Bd. Canada, Manuscript Rept. Series No. 1388, 14 pp.

_____1978. Copper in sediment interstitial waters and overlying waters of Howe Sound, B. C. Fish. Mar. Serv. Tech. Rep. 775: 29 pp.

Till, R. 1974. Statistical methods for the earth scientist. John Wiley and Sons, New York. 54 pp.

Waldichuk, M. 1979. Mine waste disposal into the sea and impact of metals on the biota: A comparison of two situations. Paper presented at the International Workshop on the Transfer of Pollutants in Two Southern Hemispheric Ocean Systems, Plettenberg Bay, Rep. of S. Africa, 23-25 April. Manuscript.

LIST OF FIGURES

Figure 1
The coastline of southern British Columbia. Hatched area indicates the location of the study.

Figure 2
Study area showing station locations.

Figure 3
Isopleths indicating copper concentrations in sediments in $\mu g\ g^{-1}$ (dry weight).

Figure 4
Isopleths indicating zinc concentrations in sediments in $\mu g\ g^{-1}$ (dry weight).

Figure 5
Delineation of tailing distribution obtained by visual identification, 1971 (Goyette, private communication).

Figure 6
Reduced major axis regression lines for copper vs zinc in sediment samples. Equation for --□-- Cu = 13.2 Zn - 937; r = 0.57.
--▲-- Cu = 1.00 Zn - 33.0; r = 0.90.

Table 1

Copper and Zinc Concentrations in Shipek Grab Samples of Georgia Strait Sediments near Texada Mine

Station	Cu[a] μg g^{-1}	Zn[a] μg g^{-1}
1	82	32
2	88	28
3	111	37
4	1584	195
5	1426	170
6	370	73
7	1076	130
8	714	130
9	265	90
10	504	148
11	89	92
12	281	106
13	279	142
14	187	104
15	238	139
16	139	146
17	112	138
18	105	143
19	66	125
20	85	138
21	42	88
22	95	139
23	68	121
24	32	73
25	21	45
26	55	64
27	44	76
28	16	28
29	41	89
30	58	98
31	31	59
32	26	56

a Dry Weight

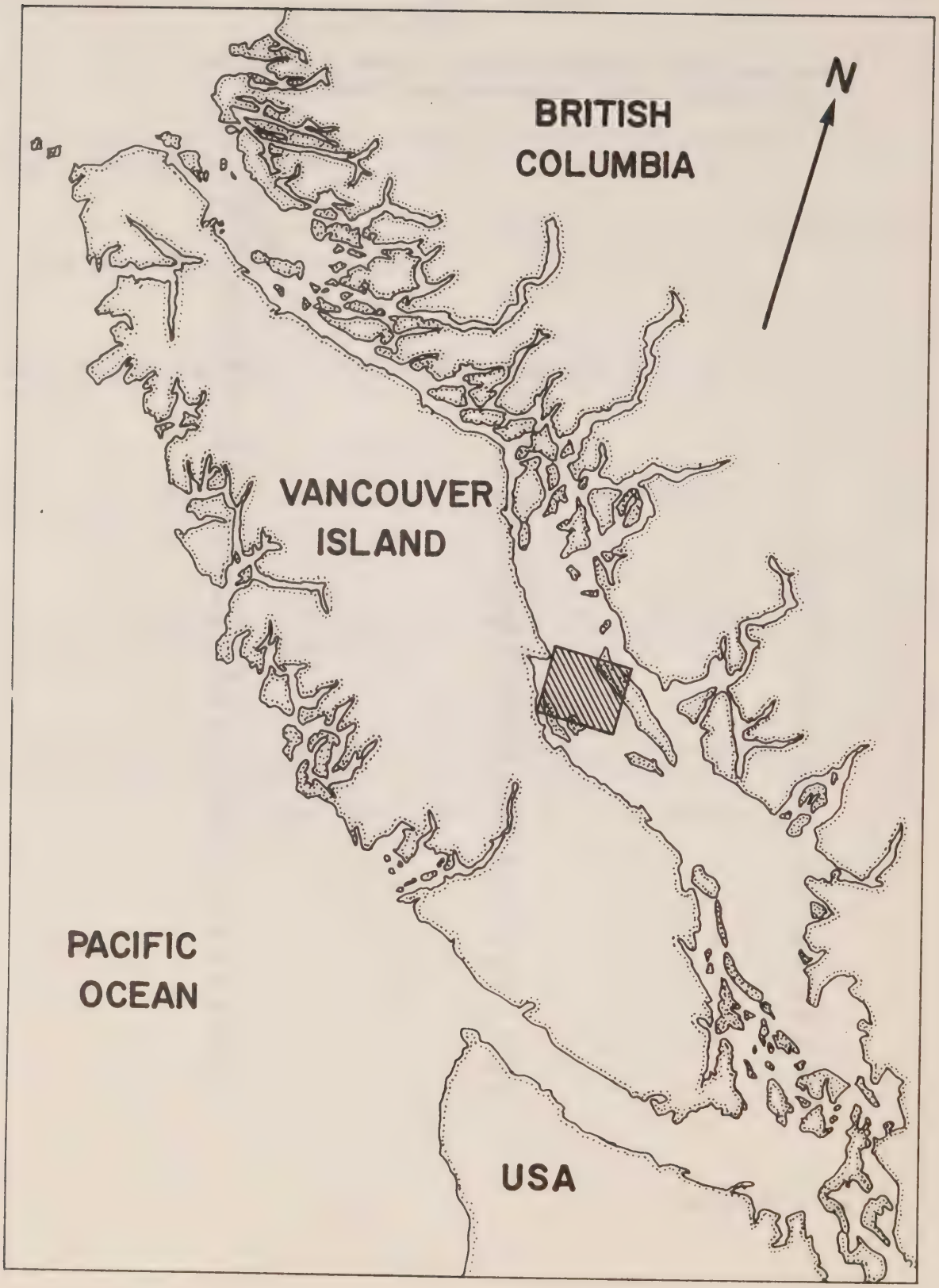

Figure 1

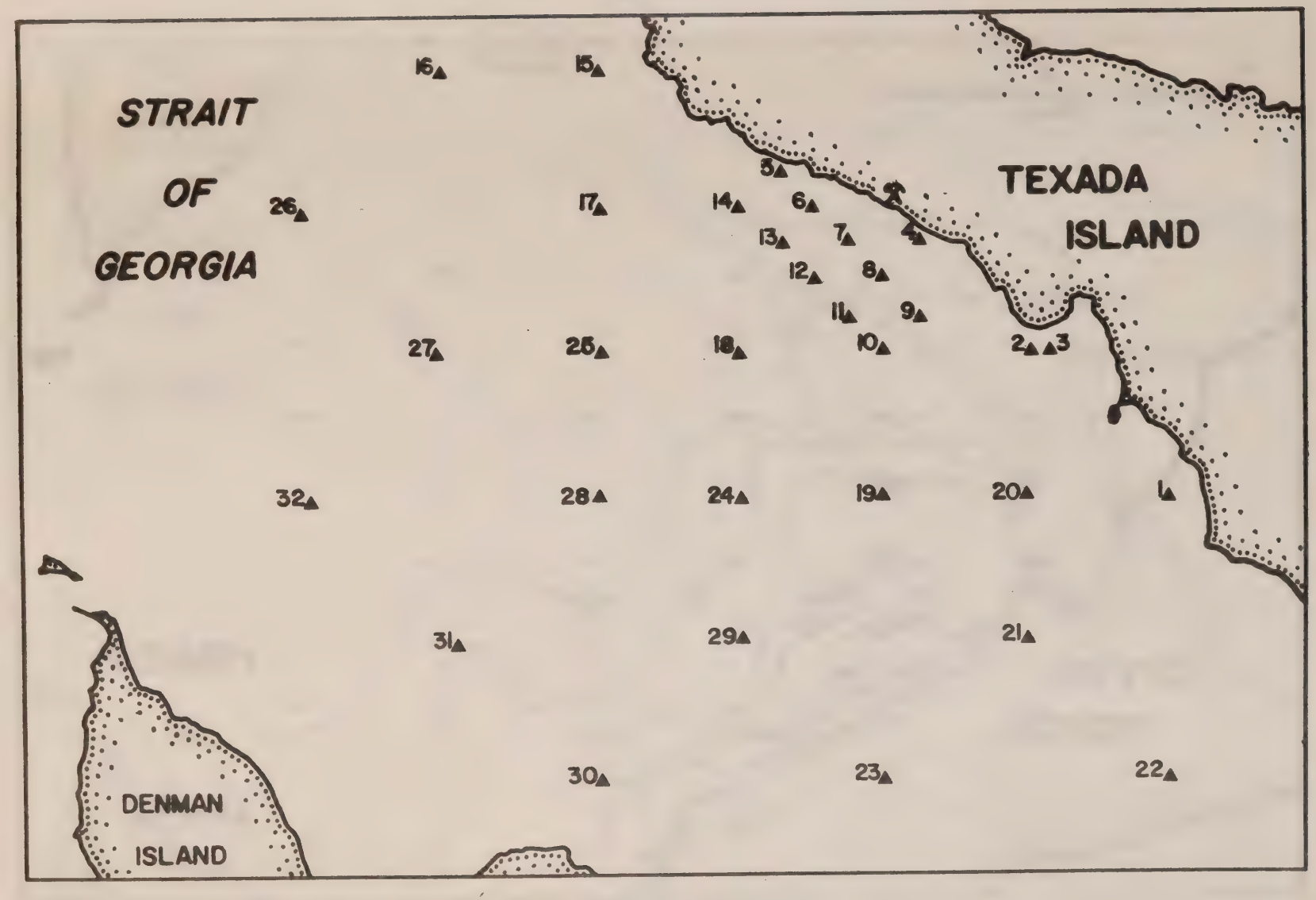
STRAIT
OF
GEORGIA
TEXADA
ISLAND
DENMAN
ISLAND
16
15
5
26
17
14
6
13
7
4
12
8
11
9
27
25
18
10
2
3
32
28
24
19
20
1
31
29
21
30
23
22

Figure 2

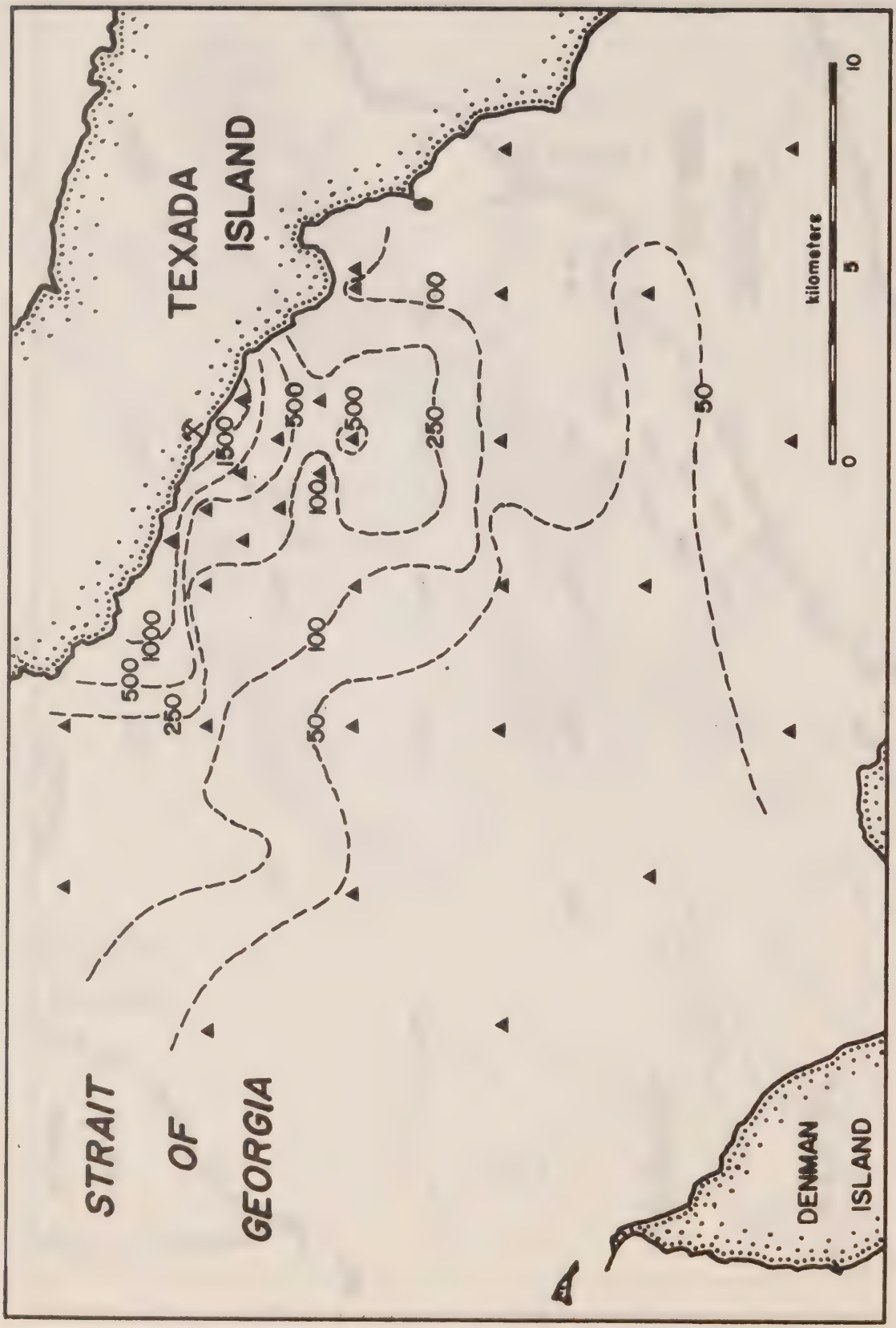
STRAIT
OF
GEORGIA
TEXADA
ISLAND
DENMAN
ISLAND
1500
1000
500
250
100
50
kilometers
0
5
10

Figure 3

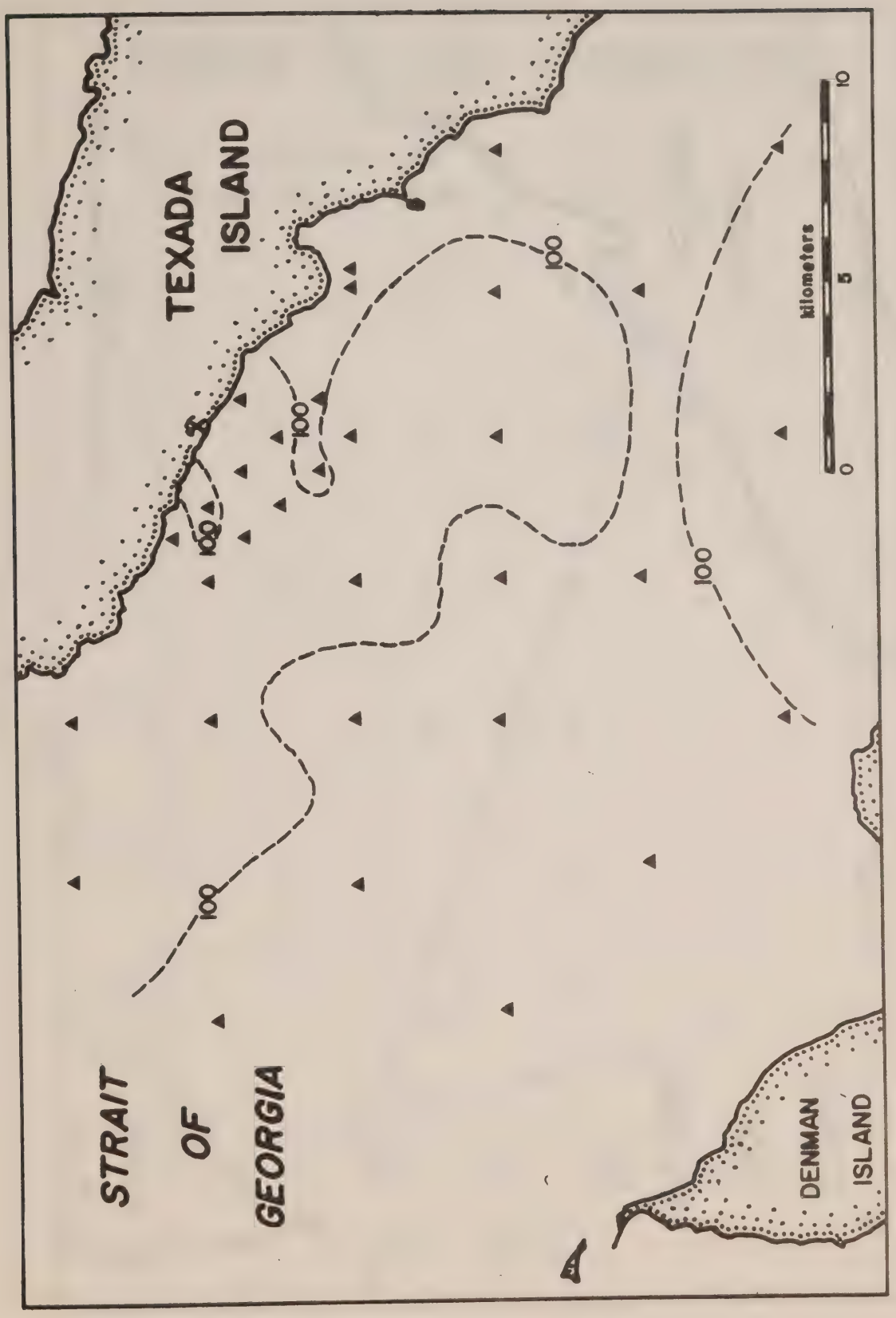
STRAIT
OF
GEORGIA
TEXADA
ISLAND
DENMAN
ISLAND
100
100
100
100
Kilometers
0
5
10

Figure 4

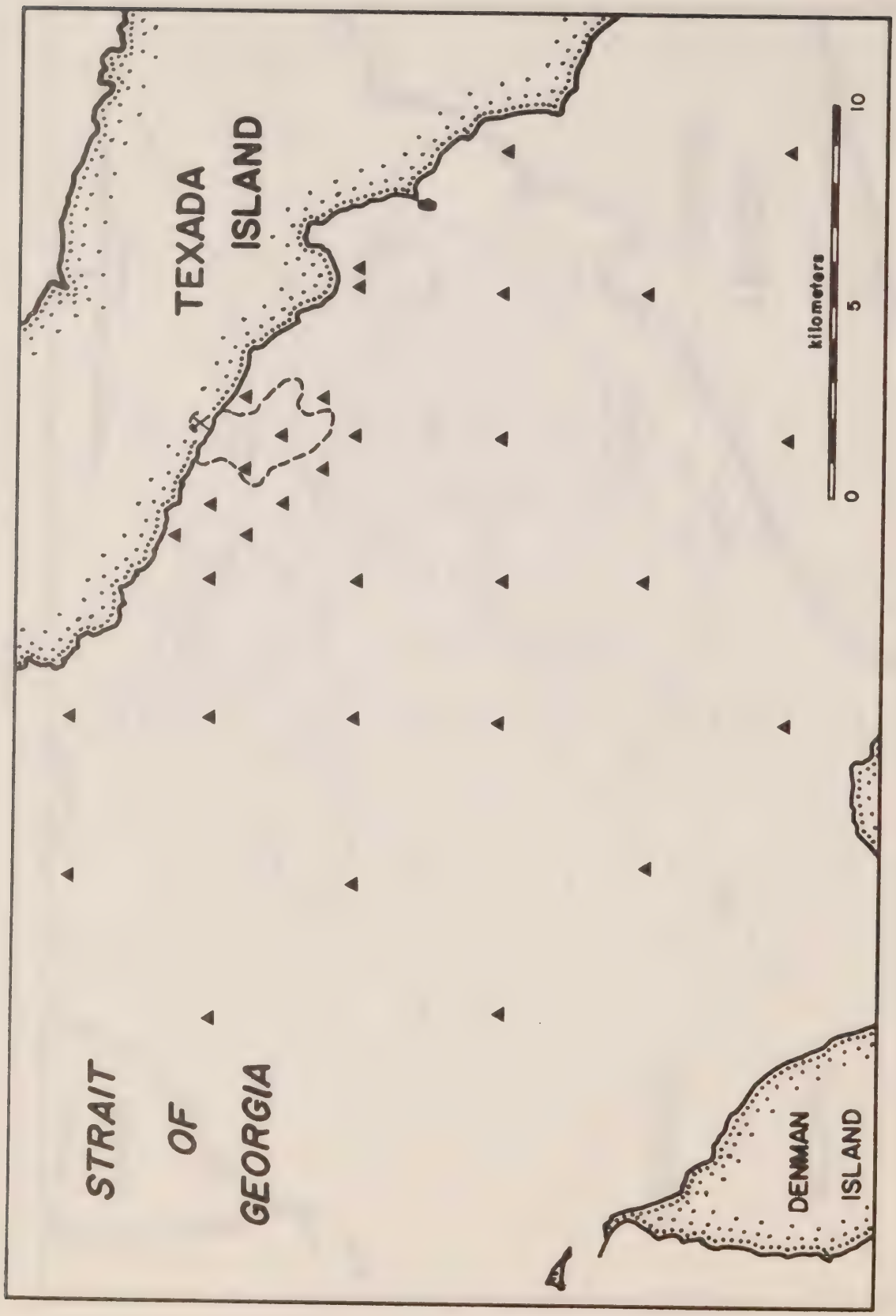
STRAIT
OF
GEORGIA
TEXADA
ISLAND
DENMAN
ISLAND
kilometers
0
5
10

Figure 5

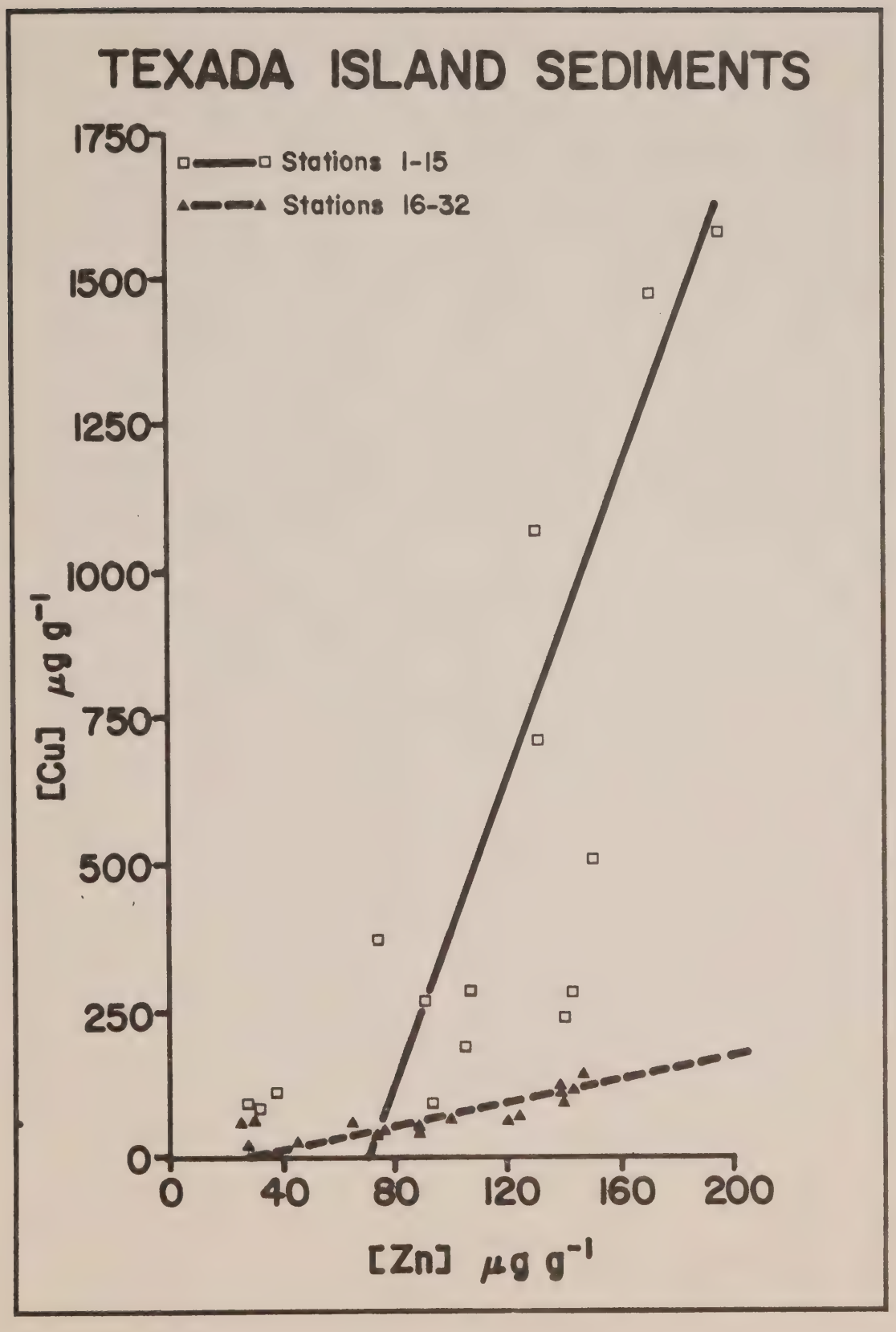
TEXADA ISLAND SEDIMENTS
Stations 1-15
Stations 16-32
1750
1500
1250
1000
750
500
250
0
[Cu] μg g⁻¹
0
40
80
120
160
200
[Zn] μg g⁻¹

Figure 6

Pacific Marine Science Report 79-18

CA1
EP321
-79R18

REPORT ON OCEAN DUMPING R AND D PACIFIC REGION DEPARTMENT OF FISHERIES AND OCEANS 1978-1979

Edited by

S.C. Byers

Dobrocky SEATECH Limited

and R.O. Brinkhurst

Institute of Ocean Sciences, Patricia Bay

for

Regional Ocean Dumping Advisory Committee (Pacific)

(R.O.D.A.C. (Pacific))

INSTITUTE OF OCEAN SCIENCES, PATRICIA BAY
Sidney, B.C.

For further copies or additional information please write to:

Department of Fisheries and Oceans
Institute of Ocean Sciences
P.O. Box 6000
Sidney, B.C. CANADA
V8L 4B2

CA1
EP 321
-79R18

Pacific Marine Science Report 79-18

REPORT ON OCEAN DUMPING R AND D
PACIFIC REGION
DEPARTMENT OF FISHERIES AND OCEANS
1978-1979

Edited by

S.C. Byers

Dobrocky SEATECH Limited

and

R.O. Brinkhurst

Institute of Ocean Sciences, Patricia Bay

for

Regional Ocean Dumping Advisory Committee (Pacific)
(R.O.D.A.C. (Pacific))

Institute of Ocean Sciences, Patricia Bay
Sidney, B.C.
1979

ACKNOWLEDGMENTS

We should like to express our thanks to the speakers and contractors who executed the bulk of the effort necessary for the workshop and the contents of this report. A special mention to C. D. Levings, the Technical Subcommittee Secretary, for his contributions and to L.S.C. Thomson for her editorial advice.

TABLE OF CONTENTS

		Page
I.	SUMMARY AND CONCLUSION.	1
II.	OBSERVATIONS OF TEMPORAL CHANGES IN BIOLOGICAL COMMUNITIES IN ALBERNI INLET. C.D. Levings	4
III.	DEVELOPMENT OF MEANINGFUL CRITERIA FOR OCEAN DUMPING. R.W. Macdonald	7
IV.	HEAVY METALS IN *Molpadia intermedia* FROM THE POINT GREY DUMPSITE. J.A.J. Thompson	16
V.	VARIABILITY OF CONTAMINANT CONTENT IN DREDGED SPOILS. R.W. Macdonald	20
VI.	METHYLATION OF LEAD IN MARINE SEDIMENTS. J.A.J. Thompson	23
VII.	AN EXAMINATION OF THE VARIABILITY OF UPWELLING AND ITS RELATIONSHIP TO THE FLUSHING OF ALBERNI INLET. J.A. Helbig	27
VIII.	AN EXAMINATION OF EVIDENCE FOR AN INTERNAL TIDE IN ALBERNI INLET. J.R. Buckley.	31
IX.	GROUP DISCUSSION ON FUTURE OCEAN DUMPING RESEARCH.	36
X.	FIGURES	37
XI.	TABLES.	47
XII.	APPENDICES.	53
	I. OCEAN DUMPING WORKSHOP ATTENDANCE LIST.	54
	II. 1978-1979 CONTRACTS	55
	III. LOCATIONS OF SCIENTIFIC AUTHORITIES	58
	IV. REPORTS FROM 1978-1979 CONTRACTS.	59

FIGURES

Page

1. IRON CONCENTRATIONS IN VICTORIA HARBOUR SEDIMENT 38

2. IRON CONCENTRATIONS IN FALSE CREEK SEDIMENT. 39

3. MANGANESE CONCENTRATIONS IN VICTORIA HARBOUR SEDIMENT. 40

4. MANGANESE CONCENTRATIONS IN FALSE CREEK SEDIMENT 41

5. ZINC CONCENTRATIONS IN VICTORIA HARBOUR SEDIMENT 42

6. ZINC CONCENTRATIONS IN FALSE CREEK SEDIMENT. 43

7. COLLECTION STATIONS FOR *Molpadia intermedia* AT THE POINT GREY DUMPSITE 44

8. PROFILES USED FOR THE MODEL TEST 45
   The sigma-t (σ_t) profile (a).
   Internal mode (———) and its corresponding
   vertical gradient (-----) for the first (b),
   second (c), and third (d) internal modes.

TABLES

Page

1. SUMMARY OF BENTHIC SAMPLING EFFORT. 48

2. SUMMARY OF LIFE HISTORY CHARACTERISTICS OF SOME ALBERNI INLET INFAUNA 49

3. SELECTIVE CHEMICAL EXTRACTIONS. 50

4. SUMMARY OF ANALYTICAL RESULTS FOR AROCHLORS OF VICTORIA HARBOUR DREDGE SPOILS 51

5. RESULTS OF STATISTICAL ANALYSIS OF THE PERCENTAGE OF VARIATION OF AROCHLORS DUE TO DIFFERENT CAUSES 51

I. SUMMARY AND CONCLUSION

This report summarizes the progress and results of the 1978-1979 studies contracted in support of Ocean Dumping legislation and reviews a workshop on ocean dumping research held on May 14, 1979 at the Institute of Ocean Sciences, Patricia Bay, Sidney, B.C.

Alberni Inlet has been the focus for extensive ocean dumping studies since the registration in Canada of the Ocean Dumping Control Act, 1975. The Inlet serves as an ideal location for a case study in that it receives relatively few other wastes, and has been studied intensively for its fisheries and for the environmental impact of a pulp mill and saw mills near its head. General explorations were made in the 1976-77 studies to obtain some understanding of the effect of disposal of wood wastes on the inner basin. The 1977-78 studies dealt with selected topics of dredge spoil impact on the Inlet with more emphasis on the oxygen budget of deep waters and the flux of oxygen to the sediments.

The Ocean Dumping Control Act specifies allowable limits for certain contaminants in materials to be dumped. Several contracts were designed to establish meaningful allowable levels of contaminants specifically applicable to the Pacific Coast marine environment. The 1978-1979 fiscal year saw the continuation and completion of these contracts and as a result, there has been a general progression away from using Alberni Inlet as a focal point for ocean dumping research.

Field studies investigating seasonal variation in the biological communities at the Port Alberni dumpsite have been completed. A preliminary review of the results demonstrates an interesting comparison between the control station and the dumpsite station. During the winter months and well into spring, when seasonal dumping occurs, the dumpsite contained fewer species and lower biomass than the control station. After May, and after dumping has ceased, the diversity at the dumpsite almost doubled; in some months the dumpsite had more species than the control station. Numbers of individuals at the dumpsite also increased in late spring and summer, but the biomass of the two communities remain relatively low throughout the summer period. It is apparent, that the dumpsite is quickly recolonized after dumping by such opportunistic species as *Axinopsida serricata, Capitella capitata, Dorvillea* spp., etc. Statistical analyses (contracted for 1979-80) will support a more definitive discussion of results.

A natural history study has been done on various species predominating the four "biotic provinces" as separated statistically from the 1976 dumpsite survey. Feeding strategy and mode of movement are the most available data in the literature. Two species of polychaetes, *Capitella capitata* and *Schistomeringos longicornis* inhabit the "dumpsite province" and exhibit life history characteristics which enable rapid colonization in degraded habitats. Wood-burrowing organisms, the mollusc *Xylophaga washingtona,* and the isopod *Limnoria lignorum,* were the prominent species in the "wood debris province".

Physical parameters influencing the renewal of oxygen to the deeper waters of the inner basin comprised the remaining topics of research done in Alberni Inlet. Evidence available suggests that upwelling off the west coast of Vancouver Island is a response to the relaxation of south-east winds. Upwelling of sufficient strength to induce renewal of water to the inner basin of Alberni Inlet is likely to occur every year. Consequently, deleterious effects due to oxygen demand should have no long-term accumulation. A mathematical model has been designed which reproduces much of the observed internal tide present in the inner basin. Several complications were encountered with respect to the geometrical simplifications of the model; however, it did substantiate that surface tides interacting with the sill at Sproat Narrows create internal waves of large amplitude.

Development of meaningful criteria for dumping of potentially harmful substances has been approached through a series of elutriate tests, release experiments, and extraction experiments to determine the rates and mechanisms of liberation of various metals from sediments. Contaminated sediments from Victoria Harbour and False Creek were used. The elutriate test is based on a water to sediment ratio of 4:1 while the release experiments use a much lower concentration. The release behaviour of iron is critically controlled by the dissolved oxygen, but this does not appear to be the case in the release pattern of the other elements. Elutriate tests on manganese, iron and zinc involved transfers to the dissolved phase of a very small percentage of the total amount of each element available in the sediment. These tests did not indicate, however, the amount of release which might take place at lower particulate concentrations in the environment.

The selective extraction scheme operates through six regimes: interstitial water, exchangeable, reducible, oxidizable, moderately reducible and residual. The two most important reservoirs in the sediments for all observed elements would be the oxidizable and residual compartments, in that order. The major location for mercury was the residual phase where there was no evidence of transfer from the particulate to dissolved phase. It is apparent that at low particulate levels during the release experiment, metals do become mobilized from the oxidizable compartment. Lead, copper and mercury appear not to mobilize from the sediment. Although cadmium demonstrates high mobilization, the water concentrations are likely not to venture much above background.

Earlier attempts have been made to use species of holothurians as a possible monitoring organism for heavy metals, mainly because of their size and abundance. Speciments of the holothurian, *Molpadia intermedia*, sampled from the Point Grey dumpsite near Vancouver did not provide adequate material to evaluate the utility of this species as a monitoring organism, at least at the analytical precision available. What evidence is available may indicate that there is no measurable effect of heavy metals on the benthos at the dumpsite.

Sampling variability determines the number of replicates required to characterize a material to be dumped. In continuation of work begun last year, determinations have been made of the sample to sample variability in polychlorinated biphenyls in dredged materials of Victoria Harbour. The arochlors measured in samples taken during the pre-dredge survey were, in all cases, higher than those measured for samples removed from the barges. Grab

samples obtained as part of the R.O.D.A.C. permit application correctly identified the levels of PCB present within the sampling and analytical error.

A study on lead methylation has been conducted on sediments from various locations on the B.C. coast. The results indicate that the discharge of lead-bearing particulates may not result in the mobilization of lead by biomethylation processes under anoxic conditions.

Future ocean dumping research will concentrate on two specific topics:

1. Continued efforts toward the development of meaningful criteria for maximum permissible concentrations of contaminants in dumped materials. This information could be used eventually for amendment of regulations under the Ocean Dumping Control Act.

2. Projects which will provide basic information to assist in the selection or relocation of dumpsites.

A list of participants in the workshop is given in Appendix I. Contracts for 1978-1979 are summarized in Appendix II. A complete list of the contracted studies for the coming year, 1979-1980 is not available.

Some of the references cited here are manuscripts produced under contract, and are not available for distribution. These reports as completed for the 1978-1979 program, have been listed in Appendix IV. For further information on any of the Institute of Ocean Sciences series of Contract Reports contact the listed Scientific Authority. The locations of the Scientific Authorities and a key to the research institution abbreviations can be found in Appendix III. Pacific Marine Science Reports (PMSR) are available for limited distribution from the Institute of Ocean Sciences, Patricia Bay.

This report was prepared by Dobrocky SEATECH Limited under contract to the Institute of Ocean Sciences Ref. DSS File No. 07SB.FP833-8-2465.

II. OBSERVATIONS OF TEMPORAL CHANGES IN BIOLOGICAL COMMUNITIES IN ALBERNI INLET

C.D. Levings

W.V.L.

Contractor: Dobrocky SEATECH Limited

This section covers two contracts dealing with the biological communities in Alberni Inlet. The major contract studying the benthic communities has been on-going for several years and is discussed first. The second and smaller contract acts as a literature search on infaunal life histories to supplement the data collected during the major contract. The results of this second contract are presented in the final paragraphs of this section.

Summary and Conclusions

Biological sampling in Alberni Inlet during the 1978-1979 fiscal year completed a project to document colonization of the dumpsite during and after the dumping season. This program, begun in November 1977 and conducted monthly until November 1978, was performed under contract by Beak Consultants Limited, and then, by Dobrocky SEATECH Limited (Byers and Brinkhurst, 1979).

Two stations were monitored throughout the study. The dumpsite station was located on the west shore of the upper basin of the Inlet about one mile south of Stamp Point at approximately 56 m depth; and the "control" station was in about 66 m depth, about 400 m south of the dumpsite. Triplicate benthic grabs were taken at each of the two stations using a 0.1 m^2 Smith-McIntyre grab. Sediment from each of the six replicates was analyzed for grain-size, loss-on ignition, and carbon/nitrogen ratios. Measurements of water characteristics (temperature, salinity, and dissolved oxygen) were taken 1 m from the bottom. Whenever bottom conditions permitted, oxygen comsumption of the benthos was measured with a tethered *in situ* respirometer.

Preliminary results of temporal differences in the fauna are shown in Table 1. Only mean values are indicated. These results are subject to revision until statistical analyses are complete. Conclusions regarding continued monitoring of the dumpsite in the Inlet, specifically, how many times per year and during what seasons, will be more apparent when the analyses are completed.

Literature Review of Some Infaunal Life Histories

Summary and Conclusions

A contract was let to Dobrocky SEATECH Limited for the purpose of examining the life histories of species featured in the statistical separation of four "biotic provinces" in the 1976 dumpsite survey (Brinkhurst, 1979). There were few available data in the literature on features such as life span, reproductive periodicity, and fecundity but the feeding strategy and mode

of movement had been examined in most of the 13 species. Table 2 presents a summary of the characteristics.

The "dumpsite province" was utilized by two species of polychaetes, namely *Capitella capitata* Fabricius and *Schistomeringos longicornis* (Ehlers). Both exhibit life history characteristics enabling rapid colonization and use of the degraded habitat. Such characteristics include relatively high fecundity (>1000 ova), planktonic dispersal of larvae, deposit feeding strategy, and known tolerance to hydrogen sulfide. Prominent species in the "wood debris province" were those that used wood for food and habitat, namely the mollusc *Xylophaga washingtona* and the isopod *Limnoria lignorum*, both wood-burrowing organisms. The species from the other "provinces" were relatively unknown biologically and hence generalizations were not possible.

GROUP DISCUSSION

Rob Macdonald inquired about the error bars involved with the respirometer results. Depending on weather and the condition of the substrate, an estimation of ±20-50% error was indicated: the mean deviation, though, was difficult to assess. The question was asked as to the comparability of the results from Alberni Inlet with a shallower area like Crofton (on the east side of Vancouver Island) and whether the two areas would demonstrate a similarity in species and/or statistics (Harbo, Anderson). If at all comparable, these 2 dumpsites might demonstrate a recolonization by similar opportunistic species but it was added that it was not unusual for a different arm in the same inlet to have a completely different community.

Levings was asked if, after the last three years of study, he had developed any strong feelings concerning the impact ocean dumping was having on the infauna at the head of the inlet (Hoos). His response was that the dumpsite should remain where it is, subject to monitoring. According to several studies on the oxygen budget for the deeper waters of the inner basin, the dumped wood waste is not a large sink of dissolved oxygen compared to the natural reservoirs. However, this needs confirmation by refining the terms in the oxygen budget.

References

Byers, S.C. and R.O. Brinkhurst, eds. 1979. Report on ocean dumping R and D Pacific Region, Fisheries and Environment Canada, 1977-1978. Pacific Marine Science Report. 79-5: 20-23.

Brinkhurst, R.O. ed. 1978. Report on ocean dumping R and D Pacific Region, Fisheries and Environment Canada, 1976-1977. Pacific Marine Science Report 78-9: 2-3.

III. DEVELOPMENT OF MEANINGFUL CRITERIA FOR OCEAN DUMPING

R.W. Macdonald

I.O.S.

Contractors: Can Test Limited
Seakem Oceanography Limited

Introduction

Monitoring for ocean dumping has been carried out both here and in other countries particularly since the "Convention on the Prevention of Marine Pollution by Dumping of Wastes and Other Matter" was approved in London, England in 1972. In that convention some substances were prohibited from being dumped, except as trace contaminants in other materials. The idea behind monitoring has been to prevent the dumping of "harmful" substances into the world oceans. What constitutes harmful and how to measure it has remained a rather intractable problem for many substances, including metals. Traditionally, metals in sediments have been determined by an acid digestion of a dried sample, this method being relatively simple, reproducible and inexpensive. Unfortunately this "total" metal content is very difficult to relate to possible environmental effects (Windom, 1975). It is, however, in continuing use and indeed, Canadian Ocean Dumping Regulations, where they specifically mention metals, refer to restrictive levels of total content above which a sediment may not be dumped.

More recently this obvious problem has been addressed by the use of an elutriate test (Keely & Engler, 1974). Although perhaps useful for estimating the effects of suction dredges, it does have serious limitations, some of which will be brought out later. Ideally, an inexpensive analytical technique is required which can identify the mobile fraction of metals in sediments, and recently Brannon et al. (1976) have investigated the use of selective chemical extraction to classify sediments. Basically, this approach compartmentalizes metals according to the chemical treatment required to liberate them from sediments. It has been emphasized that it is a purely operational technique and therefore depends on exactly how a particular sediment responds to a chemical treatment. Interpretation in terms of the form of metal binding must remain rather vague.

For our criteria study we have used the basic approach of Brannon et al. (1976) to examine the metal distribution in two local sediments, Victoria Harbour (VH) and False Creek (FC). We have also conducted 3-day release experiments in sea water with suspended sediments at approximately the 200 mg L^{-1} level. After the release experiment, the sediments were retrieved and again subjected to the selective extraction procedure, in order to see what internal rearrangements the metals had undergone during the release experiment.

Extraction Scheme

Extraction schemes for sediment have been available for some time, (Gupta & Chen, 1975, Nessenbaum, 1972, Chester and Messiha-Hanna, 1970). It was decided to follow the form developed by Brannon et al., (1976) since they had made the most extensive tests and their results were directly applicable to the ocean dumping problem. Their scheme operates in the following manner:

1. INTERSTITIAL WATER (IW)

   Care was taken to maintain anoxic conditions.

2. EXCHANGEABLE (E)

   Metals put into solution by 1 N ammonium acetate at the surface pH of the sediment. Solution is defined here as passing a 0.45 μ filter. In theory, metals located here are absorbed on organic or inorganic surfaces and will be mobilized in response to salinity changes. Release from this type of site should be rapid.

3. EASILY REDUCIBLE (ER)

   Metals put into solution by a 0.1 M hydroxylamine hydrochloride - 0.01 M hydrochloric acid solution. This phase consists of oxides, hydroxides and hydrous oxides of manganese and iron in the form of coatings or micro particles. Scavenged trace elements and phosphate may also be present (Brannon et al., 1976).

4. OXIDIZABLE (O)

   Metals put into solution by a 95^0C digestion with 30% hydrogen peroxide at a pH of 2.5. These metals originate largely from organic complexes and sulphides.

5. MODERATELY REDUCIBLE (MR)

   Metals put into solution by a sodium citrate - sodium dithionite solution. Metals released during this step are probably associated with hydrouns iron oxides which were not reduced during the "easily reducible" chemical treatment.

6. RESIDUAL (R)

   Essentially the metal that remains after the above extractions and determined by digestion with hot aqua regia. Metals located here tend to be bound in the matrix and so generally are not released except under extremely harsh conditions not normally encountered in the environment.

In addition to this selective extraction procedure, the sediments were subjected to several other determinations, including % organic carbon, size distribution, free and total sulphide, cation exchange capacity, pH and Eh. A total analysis for metals was also performed on a subsample of each homogenate in order to estimate the mass balance of the selective extraction scheme.

Results

Comparison between elutriate tests, release experiments and selective extraction is not possible unless some common base is used. For all of the metals, the data have been put into concentration units of $\mu g\ g^{-1}$ (dry weight). In that way, releases expressed in these units can be viewed directly in terms of the amounts of metal being transferred to the liquid phase during the elutriate test and also to the amounts of metals residing in each of the compartments as indicated by the selective extraction procedure. In actual fact, different solid to liquid ratios have been used: the elutriate test is based on a 4:1 (V:V) water to sediment ratio, whereas the release experiments performed here have used 40g (wet weight) of sediment in 200L of sea water. Nevertheless fluxes and concentrations expressed in terms of $\mu g\ g^{-1}$ dry weight sediment sediment should be directly comparable.

Iron

The results for iron are summarized in Figures 1 and 2. In referring to these it will be noted that for both Victoria Harbour (VH) and False Creek (FC) sediments, run #1 and run #2, which were supposed to be duplicate experiments, do not compare well. The reason for this is both revealing and simple. The cores, when collected, were kept sealed, and when delivered to Can Test were maintained under N_2 in a glove box, a procedure known to be essential for meaningful pore water measurements (Poldski & Glass, 1974). At this time subsamples were removed for various chemical tests and also a subsample was placed into a sealed polyethylene container and sent to Seakem for the release experiments. Anoxic integrity was maintained in this manner. At Seakem, subsamples were removed for run #1, weighed and added to the stirred 200L container. The remaining material was resealed in the polyethylene container and stored at 4^0C in the dark for a period of almost 2 weeks. Since the bottles were opened under a normal atmosphere, anoxic integrity was lost at this point. At the start of run #2, therefore, the sediments had been exposed to oxygen for a two week period.

In Figures 1 and 2 it can be seen that, for run #1, there is an initial period of 1-2 hours during which very little release takes place, and perhaps there is even a small amount of scavenging. With 4 hours, noticeable releases of iron took place for both sediments, with a maximum release ocurring after about one day. But within three days, the released iron had been scavenged and the dissolved levels returned to near background. Sediments which had already been exposed to oxic conditions for two weeks (run #2) behaved differently, initially releasing only a small amount of iron. The reproducibility of this effect between FC and VH sediments is excellent. Clearly, much of the process ocurring in the water column during run #1 was also ocurring in the material stored in the bottle and destined for run #2.

Of particular importance are the elutriate test results. These give no information on the longer term iron releases from anoxic sediments, and one might have predicted this since the test involves shaking the water-sediment mixture for only ½ hour. Furthermore the transfer of iron from the solid to the dissolved phase ($\mu g\ g^{-1}$ dry weight units) is very dependent on the concentration of particulate material. During the elutriate test only 0.81 $\mu g\ g^{-1}$ and 3.8 $\mu g\ g^{-1}$ was put into the water for the VH and FC sediment, respectively. Looking at Figures 1 and 2 it can be seen that these levels of

transfer hardly dip at all into the iron reservoir in the sediment. On the other hand, during the release experiment (run #1) as much as 1000 $\mu g\ g^{-1}$ transferred out of the solid phase, or approximately 4% of the iron reservoir was being affected.

Examination of the selective extraction data shows the comparison of before and after partitioning of iron. Releases occurring during run #1 cannot be derived from interstitial water (IW) or from the exchangeable portion (E). In both sediments, the easily reducible (ER) portion comes closer to the amount in question, and indeed for both sediments there is a significant depletion of iron from this compartment after the experiment. Analytical errors probably do not allow one to make any definitive statements about the remaining compartments since inter-core duplication was not observed. It should be noted that the bulk of the iron in both sediments is found in the oxidizable phase (sulphides and organics) and in the residence material.

Manganese

The behaviour of manganese is quite different from that of iron (Figures 3 and 4). In both the VH and FC sediments there was an immediate (1 hour) loss of dissolved manganese from the water. This was followed by a release from the sediments back into the dissolved state which continued throughout the rest of the experiment. Run #2 (keeping in mind the exposure of the sediments to oxygen) did not show the initial scavenging from the water, but the trend thereafter was for dissolved manganese to increase. In run #2 of the VH release experiments, the last data point (3 days) shows that the dissolved manganese had drastically decreased and was, in fact, below the initial background level. Whether or not this is genuine or an experimental error is difficult to say since it was not repeated in the other release experiments. What is interesting is that during three of the release experiments, the dissolved manganese levels approached those occurring initially in the interstitial water (21-23 mg L^{-1}). For comparison, the final concentrations of the four release experiments were 19.2, 7.6, 19.9 and 21.1 mg L^{-1}. To further emphasize the importance of this sediment: water ratio the elutriate test gave final dissolved manganese concentrations of 53 and 39 mg L^{-1}. Actual losses from solid to liquid during the elutriate test were, of course, remarkably small being only 0.46 $\mu g\ g^{-1}$ and 0.20 $\mu g\ g^{-1}$. The elutriate test therefore may have approximately reflected the water concentrations of manganese expected, but a detailed knowledge of the amount of manganese released cannot be known without information on the time - concentration path of the suspended sediments.

The selective extraction experiments showed that the bulk of the manganese was in the oxidizable portion and the residual portion of the sediments. Manganese concentrations in the interstitial water and in the elutriate test were generally low, and referring to Figures 3 and 4, the transfer of manganese to the water during the elutriate test must also be considered low. The exchangeable portion could have contributed sufficient manganese to produce the releases observed during the elutriate test. The release experiments cannot be explained so easily since at the end of the experiment a significant fraction of the manganese was in the dissolved phase. It would appear that portions of the oxidizable and/or residual manganese must have been mobilized during the three day release experiment.

Zinc

The behaviour of zinc appears to be more closely allied with that of manganese than that of iron. The similar trend of slow increase throughout the release experiment is evident in Figures 5 and 6. As was the case with manganese, the zinc concentration tended to approach a common level of 6-8 $\mu g\ L^{-1}$ in all four experiments. The results of the elutriate tests showed that more zinc was mobilized from the VH sediments than from the FC ones, and the reason for this may be that the VH sediments released the zinc faster. It is clear, however, that not much zinc is being transferred to the dissolved phase.

The majority of the zinc in both the VH and FC sediment appeared in the oxidizable portion with somewhat lesser amounts in the residual phase. Zinc mobilization during the release experiment can only be explained by proposing that much of the oxidizable portion of the zinc reservoir was being mobilized. Both mass balance during the release experiment, and comparison of the "before" and "after" distribution of zinc in both sediments bear this out. There is even evidence that some zinc is transferred from the oxidizable phase into the exchangeable and easily reducible phases of the sediment during the three day residence in oxic waters. For the elutriate tests the amounts of zinc being mobilized are so low that one does not require loss of the zinc from the oxidizable phase to explain the results. However it is interesting to note that some correlation ($r=0.516$) between the oxidizable phase and elutriate test results was observed by Brannon et al. (1976) based on several cores from different locations. The present results seem to give some very direct evidence that leaching of zinc from the oxidizable portion can take place.

Copper

The results of the selective extraction measurements for this element are presented in Table 3. The total levels of copper in VH sediments appears quite high, 196 $\mu g\ g^{-1}$, but falls into the range determined during the study (Byers and Brinkhurst, 1979). The copper levels are about half this in the FC core but in both cores the majority of material is located in the oxidizable phase with most of the remaining copper being accounted for by the residual phase.

The release experiments did not show any measureable amounts of copper being mobilized and, in fact, small amounts may even have been scavenged. Dissolved copper levels remained at or near detection levels after the sediment was mixed into the sea water. During the elutriate test detectable but very small amounts of copper appeared to be released with the scale of release being about 0.02 - 0.04 $\mu g\ g^{-1}$.

Cadmium

Table 3 includes the selective extraction data for cadmium and it is apparent that, like copper, the majority of the metal is found in the oxidizable portion. Due to the low levels (below detection limits) it was impossible to

assign the remaining cadmium more accurately, but the determination of total cadmium gave levels of about 1-1.2 μg g^{-1}, enough to prohibit dumping of the material.

The data obtained for cadmium during the release experiment were not good enough to make a case for either release from or adsorption onto suspended sediment. Detection limits and contamination are two problems which make the task of measuring dissolved cadmium difficult, if not impossible. However, it should be noted that the amount of cadmium remaining in the oxidizable phase after the release experiments was somewhat less than that at the beginning, a behaviour similar to that observed for zinc. On this basis, the evidence favours some loss of cadmium from the solid phase. The elutriate test gave no evidence of cadmium going into solution, even from these sediments which were relatively enriched in cadmium. In fact, all cadmium was below detection limits.

Lead

Selective extraction data for this element is also found in Table 3 where it can be seen that the lead levels in VH sediments are high but fall into line with previous determinations (Byers and Brinkhurst, 1979). Following the behaviour of copper, zinc and cadmium, the majority of lead was found in the oxidizable portion of the sediment. Most of the remaining lead was accounted for by the residual phase.

It is very difficult to demonstrate either release or adsorption of lead during the release experiment as was true of Cadmium, and lead remained below the μg L^{-1} level at all times. In any event it would seem that no more than 1% of the total lead was mobilized.

Arsenic

Results from the selective extraction procedure are presented in Table 3 and again it is apparent that levels are often at or below detection limits, making mass balances difficult to perform. Most of the arsenic appears in the oxidizable phase, and the residual compartment is of secondary importance. The release experiments did not yield any useful data for this element, but on the basis of the "before" and "after" selective extraction procedure, almost half of this element tied up in the oxidizable phase was lost, while the residual phase remained untouched. The behaviour of arsenic therefore seems to correlate with metals described above.

Mercury

Table 3 summarizes the data for this element which behaved somewhat differently from the other metals. The majority of this element was tied up in the residual phase and in keeping with this there was no evidence of transfer from the particulate to dissolved phase during the release experiment. In fact dissolved Hg levels tended always to drop slightly after the sediment was added to the sea water. In addition the elutriate test did not reveal any mercury mobilization.

Conclusions

Not all of the data obtained have been presented since this report is intended to present concisely the salient features, particularly as they apply to present methods of ocean dumping monitoring.

The first important point is the effect of storing sediments in contact with oxygen. Obviously, as Figures 1 and 2 clearly show, the behaviour of iron is controlled by this. However no clear evidence was found for any change in the release pattern of the other elements investigated, at least within the detection limits and precision involved in the respective measurements.

In view of the behaviour of manganese, iron and zinc, the elutriate test did not seem to be indicative of the amount of release which might take place at lower particulate concentrations in the environment. Transfers to the dissolved phase during the elutriate test generally involved very small percentages of the total amount of each element tied up in the sediment. One might therefore erroneously assume that much of the element in question was unavailable. An accurate picture of the time-concentration history of dredge spoils after dumping would be required before one could calculate the release budget. Maximum concentrations however might be quite successfully estimated by using the elutriate test, although the half-hour time period may prove to be rather arbitrary.

For all of the observed elements the two most important reservoirs in sediments would be the oxidizable and the residual compartments, generally in that order, except for manganese and perhaps iron. Mercury was different in that the major location for this element was the residual phase. Differences in concentration before and after the release experiment indicate that, at low particulate levels during the release experiment, metals do become mobilized from the oxidizable compartment. Actual amounts of metals found in the dissolved phase during the release experiment also indicate that the exchangeable and interstitial water phases do not contain enough of the elements to explain the results. In the case of lead and copper, mobilization does not appear to occur, or if it does it includes only a small percentage of the total metal contained in the sediment. Mercury also does not appear to be mobilized, in agreement with the fact that the majority of this element was found in the residual phase. Cadmium does, however, appear to be mobilized to an extent that perhaps 50% was lost during the three day experiment. Both the elutriate and release experiment though, indicated that water concentrations of cadmium are not likely to venture much above background.

Group Discussion

The results of the experiments identified Cd mobilization in sediments as being of possible concern. With respect to this, two attendees (Thompson, Waldichuk) asked if the elutriate tests conducted could be extrapolated to determine uptake from the interstitial water by animals. Apparently the tests could not, since such conditions would involve a totally different environment more closely linked with sedimentological work. Harbo asked how sediments containing a large amount of wood debris would compare to those sediments used for the experiments. The False Creek sediments, in fact, did contain wood

debris and the general tendency was towards mobilization of the metals. Since there could be a short-term depression of O_2 in the water column during and subsequent to dumping, Levings asked about the time frame of biological availability (concommitant with the release pattern of Fe in oxic conditions). After a typical dump, the metals would be available to planktonic organisms while the material was in the water column and could be released from these sediments up to 3 days afterwards; however, once the dumped material struck bottom a different biological and chemical process would be involved in reaching an equilibrium. What test, then, could be recommended as a means of determining biological uptake of these metals (Waldichuk)? A weak acid leach was suggested as a better method than the standard elutriate test for making the metals available (although the Eh and pH must be closely monitored). Young asked about the influence of reduced salinity such as that found in estuaries (eg. $5^{0}/_{00}$). Macdonald acknowledged that a change in salinity could cause an alteration in release times and a possibility of rescavenging of the element back to the solid phase. For example, Zn and Cu have been found to mobilize when the fresh water of the Fraser River encounters the salt wedge.

References

Brannon, S.M., R.M. Engler, J.R. Rose, P.G. Hunt and I. Smilt. 1976. Selective analytical partitioning of sediments to evaluate potential mobility of chemical constituents during dredging and disposal operations. Dred. Mat. Res. Prog. Vicksburg, M.S. Tech. Rep. D-76-7.

Byers, S.C. and R.O. Brinkhurst, eds. 1979. Report on ocean dumping R and D Pacific Region, Fisheries and Environment Canada, 1977-1978. Pacific Marine Science Report 79-5: 29-33.

Chester, R. and R.G. Messiha-Hanna. 1970. Trace element partition patterns in North Atlantic deep-sea sediments. Geochemica et Cosmochemica Acta 34: 1121-1128.

Gupta, S.K. and K.Y. Chen. 1975. Partitioning of trace metals in selective chemical fractions of nearshore sediment. Environmental Letters 10: 129-158.

Keely, J.N. and R.M. Engler. 1974. Discussion of regulatory criteria for ocean disposal of dredged materials: elutriate test rationale and implementation guidelines. Dred. Mat. Res. Prog. Vicksburg, M.S. Miscellaneous Paper D-74-14.

Nissenbaum, A. 1972. Distribution of several metals in chemical fractions of a sediment core from the sea of Okhotsk. Israel Journal of Earth Sciences 21: 143-154.

Poldoski, J.E. and G.E. Glass. 1974. Methodological considerations in western Lake Superior water - sediment exchange studies of some trace elements. Proceedings of the 7th Materials Research Symposium, N.B.S.

Windom, H.L. 1975. Heavy metal fluxes through salt-marsh estuaries. IN: L.E. Cronin, ed. Estuaries Research U.I. pp 137-153.

IV. HEAVY METALS IN *Molpadia intermedia* FROM THE POINT GREY DUMPSITE

J.A.J. Thompson
I.O.S.

Contractor: Can Test Limited

Introduction

In previous reports (Brinkhurst, 1978; Thompson and Paton, 1978) the use of the holothurian, *Molpadia intermedia* as a possible monitoring organism for heavy metals in the Point Grey Dumpsite area has been described. The previous study produced inconclusive results. Reasons for this were basically due to the lack of a uniform statistical sampling of the dumpsite, lack of sufficient samples, and, the questionable precision of the analytical data provided by the contractor.

In July 1977 a cruise to the dumpsite on the C.S.S. Vector provided samples of *M. intermedia* from the 17 stations shown in Figure 7. At least 5 specimens were collected from each station. Controls were obtained at station F off the Sechelt Peninsula ($49^0$21.6' N, $123^0$34.8' W).

Sampler casts at McCall Bank ($49^0$20.4' N, $123^0$35' W) and Satellite Channel ($48^0$42.5' N, $123^0$30' W) were unrewarding. Control comparability was seriously hampered for this reason.

All samples were obtained using a Smith-McIntyre grab (Kahlsico, San Diego). Sediments were passed through a 1.0 mm nylon mesh screen. Specimens were vigorously scrubbed to remove adhering sediment, weighed, and immediately after they were dissected in a clean-air hood. The longitudinal muscles were removed from each specimen and frozen in separate acid-washed vials. Preparatory to analysis, all samples were freeze-dried. The contractor was provided with a total of 83 coded samples, including NBS standard bovine liver and orchard leaves as analytical controls. Samples were digested in aqua regia and analyzed by flame or flameless atomic adsorption methods as required for Cu, Zn and Cd.

Results

Analytical results are summarized in the following table:

	Range [a] ($\mu g\ g^{-1}$ dry weight)	Control ($\mu g\ g^{-1}$ dry weight)
Copper	3.5 - 9.1	6.6
Zinc	121.0 - 146.0	129.0
Cadium	0.4 - 4.4	1.9

[a] Range indicates 5 or more determinations per station.

As was the case in the first study little can be concluded about trends in concentration in the dumpsite area for any of the metals studied. It should be noted that Cr and Pb were not determined in this present study because of financial restraints. These elements also provided the least precise data in the previous work.

Copper does exhibit a slight trend to increasing concentrations in the western sector; however, it is not significant. Moreover, the control lies midway in the range of dumpsite specimens.

An interesting aspect of the copper data is that the means are considerably lower than those obtained in the 1977 study. Overall copper mean for this work is 5.99 ± 1.75 μg g^{-1} dry weight against 26.0 ± 14.0 for the previous data. This significant difference may reflect greater care taken in sample preparation and/or greater analytical accuracy and precision. There is no *a priori* ecological reason for this decrease.

Zinc also exhibits a similar significant drop in the overall mean from 171.0 ± 55.0 to 137.0 ± 7.0 μg g^{-1} dry weight for 1977 and 1978, respectively. Here again the increase in precision may reflect the greater care in sample preparation and analysis.

Zinc is the only one of the three elements that exhibits noticeably higher data for the dumpsite when compared to the unfortunately scant control data. It is, however, not possible to indulge in a valid statistical exercise.

Data for cadmium are consistent with those obtained previously. Overall means for this and the earlier work are 1.4 ± 1.0 and 1.7 ± 1.4 μg g^{-1} dry weight, respectively.

Conclusions

Although analytical precision has improved it is still not possible to observe differences (if any) outside of the "noise" or background level of natural variability and analytical error. We were limited by the size of samples which were smaller than would be desired.

The holothurian *M. intermedia* does not fulfill expectations as a possible monitoring organism for several reasons;

1. it is insensitive to changes in sedimentary metal concentrations; or
2. there are no significant increases in sedimentary levels; or
3. it does not provide enough tissues from which valid data can be obtained.

If the first or third conclusions are true then it might be concluded further that another organism should be tested. An alternative observed in sufficient numbers was the sea urchin *Brisaster* sp.

If the second conclusion were correct it would be assumed that there is no measurable effect upon the benthos from dumping activities.

Group Discussion

Waldichuk mentioned that some of the cadmium levels in *Molpadia intermedia* were above those allowed by the Food and Drug Directorate for human consumption. This particular sea cucumber, however, was not expected to reach market value! In response to a question from Levings, Thompson mentioned that levels of copper had decreased between this study and the previous study done by E.P.S. where results from their routine sediment survey at Point Grey in 1978 (analyzed by Fletcher's techniques at the University of British Columbia) also indicated that metal values have all shown a reduction.

References

Brinkhurst, R.O. ed. 1978. Report on ocean dumping R and D Pacific Region, Fisheries and Environment Canada, 1976-1977. Pacific Marine Science Report 78-9: 32 pp.

Thompson, J.A.J. and D. W. Paton. 1978. Heavy metals in benthic organisms from Point Grey dumpsite - Vancouver, B.C. Pacific Marine Science Report 78-11: 21 pp.

V. VARIABILITY OF CONTAMINANT CONTENT IN DREDGED SPOILS

R.W. Macdonald

I.O.S

Contributors: C.S. Wong and P. Gregory

Contractor: Seakem Oceanography Limited

Introduction

During the last fiscal year, an examination of the reliability of sampling for ocean dumping monitoring was performed. As has already been reported (Byers and Brinkhurst, 1979) the sampling strategy involved obtaining seven grab samples at random locations throughout the dredge site before the commencement of dredging. In addition, four of the barges were sampled at seven randomly selected locations within each barge after it had been filled with spoil. Each sample was then split into three subsamples, stored in containers appropriate to the analysis to be performed and then randomly numbered so that the analyst would be unaware of replicates. This year the project was completed by examining the levels of polychlorinated biphenyls (PCB) in the 105 samples.

PCBs are a family of compounds consisting of over 200 individuals each being a particular chlorinated biphenyl generated by replacing the hydrogen at any combination of the positions numbered 2-6 and 2'-6' by chlorine. PCBs produced industrially are generally a mixture of many different PCB

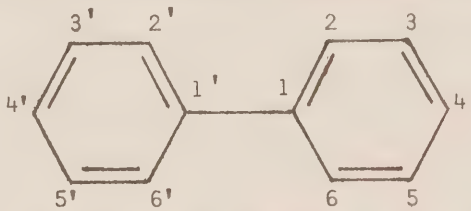

compounds and have been designated by referring to them as arochlors. A four figure number is added to indicate the number of carbon atoms involved and the percentage replacement of hydrogens by chlorine. For example, archlor 1254 contains 12 carbons (biphenyl) and has an average 54% replacement of the hydrogens. Quantitation of biphenyls is therefore difficult because, in principle, a single number is produced ($\mu g\ g^{-1}$) which covers a host of different compounds. Quantitation has been performed by using a set standard, arochlor 1242 for example, which comes closest to the distribution and range of compounds in the sample at hand (Harding et al., 1978). Although quantitation is not strictly accurate (it is like giving a grand number for the concentration of 100 different compounds each of which has not been calibrated), good precision can be achieved with a decent match between standard and sample. For the present results, quantitation was carried out by dividing the chromatogram into three areas each of which closely matched a particular arochlor. In addition decachlorobiphenyl was also quantitated and all of the results are summarized in Table 4. Levels of PCB determined last year by Willis, Cunliffe, Tait and Company Limited for E.P.S. permits (4443-0375) as

part of the normal R.O.D.A.C. permit process, are also included and show rather respectable agreement with the totals summarized here.

The 105 samples were decoded and subjected to analysis of variance, the results of which are presented in Table 5. For all of the arochlors, and the total, the between-replicate variability accounts for over 40% of the variation observed. The variation within each barge accounts for approximately a further 25% with the remaining variation being due to differences between barges. The ANOVA results show that variability within barges is significant only for the DCB fraction but differences between barges are real for all arochlors at the 99.9% confidence level. A point worth noting is that the arochlors measured in samples taken during the pre-dredge survey were, in all cases, higher than those measured for samples removed from the barges.

Conclusions

Due to the large number of different PCB compounds, exact quantification would be prohibitively expensive, and probably not necessary for ocean dumping monitoring unless a particular PCB compound was found to cause exceptional environmental problems. The ANOVA results show that there are genuine inter-barge differences but an examination of the data showed that in all cases the pre-dredge sampling programme provided samples with higher PCB levels than those found in the barges. Grab samples obtained as part of the R.O.D.A.C. permit application correctly identified the levels of PCB present within the sampling and analytical error.

Group Discussion

In response to a question from Levings, Hoos pointed out that PCB levels in Victoria Harbour were much lower than those reported from Puget Sound or Porpoise Harbour. Macdonald concluded the discussion by emphasizing the fact that the study on Victoria Harbour and False Creek sediments (PCB analyses completed this year and the trace elements and hydrocarbon analyses completed last year, 1978) demonstrated that adequate sampling done prior to dredging in a new area could reduce the monitoring required subsequently at the dumpsite.

References

Byers, S.C. and R.O. Brinkhurst, eds. 1979. Report on ocean dumping R and D Pacific Region, Fisheries and Environment Canada, 1977-1978. Pacific Marine Science Report 79-5: 29-33.

Harding, G.C.H., R.J. Leblanc, and W.P. Wass, 1978. Extended Abstracts, paper #31, International Symposium on Analysis of Hydrocarbons and Halogenated Hydrocarbons, Hamilton, Ontario, Canada.

VI. METHYLATION OF LEAD IN MARINE SEDIMENTS

J.A.J. Thompson

Contractor: Beak Consultants Limited

Introduction

It is known that a number of other elements besides mercury can form stable methylated compounds through biological activity in natural media. The mechanisms for the production of CH_3Hg^+ and $(CH_3)_2$ Hg are understood to some extent; however, little is known about the mechanisms and importance for the methylation of selenium, lead, arsenic and tin (among others).

Studies by Chau and coworkers at the National Water Research Institute in Burlington (Wong et al.,1975; Chau and Wong,1978), Jarvie in England and Huber in Germany have concentrated on the methylation of lead in lacustrine, and fluviatile sediments as well as in axenic bacterial cultures derived from them.

Contradicting results have been reported by Wong et al.(1975) and Jarvie et al.(1975). Recent work has clarified the situation to some extent. It is now known that both Pb(II) and Pb(IV) species can be methylated bacterially. Lead(II) methylation proceeds with difficulty, probably because an oxidative step is required. R_3Pb^+ cations, on the other hand, undergo facile methylation. Jarvie et al.(1975) first suggested that this reaction was abiotic (i.e. purely chemical). Studies by Chau et al.(1978) and Huber et al.(1978), however, clearly show that both biotic and abiotic reactions are extant with the latter being the dominant process.

Little is known about the importance of methylation of lead in marine ecosystems. Because total lead concentrations in sea water are extremely low (5-15 ng L^{-1}) it would not be expected (nor could it be easily determined) that methylation plays an important role in the water column. Lead in natural sediments is in a predominantly immobile phase and here again it might be predicted that little activity would be expected. (See pp. 12 of this report to identify mobility of lead).

Our interest in the lead methylation capability of sediments arose out of the studies on metals release from submerged mine tailings deposits in coastal inlets. We had found previously that ambient Hg in sediments is available for methylation, and were interested in whether lead may exhibit similar properties.

For this study, sediment samples from four locations on the B.C. coast were collected:

1. Burrard Inlet (English Bay).
2. Goletas Channel (Northern Vancouver Island).
3. Alice Arm (site of inactive molybdenum mine with high lead in tailings).

4. Granby Bay (site of abandoned copper mine at Anyox).

Methods

Collection was made with a Smith-McIntyre grab. A subsample from each grab was placed into a dark green plastic bag, purged of air, and sealed tightly. They were kept at 4^0C until needed for the experimental program.

A series of flasks containing sediment from each of the four areas was incubated anaerobically at 15^0 for periods up to 4 weeks. Sampling from the head-space gases was made with a septum at 0, 1, 7, 72, 168, 336 and 672 hours into the experiment. Three groups of 4 flasks were spiked with trimethyllead acetate, lead(II) nitrate and lead(II) acetate, respectively. A fourth set of 4 flasks served as controls. Each of the four flasks in all four groups contained solutions according to the following scheme:

1. 75 ml of unsterilized sea water
2. 75 ml of sterilized sea water
3. 75 ml of sea water, 1.0 ml of nutrient broth and 1.0 ml glucose
4. 75 ml of (3) with sterile sea water substituted.

Analysis for $(CH_3)_4$ Pb in head space gases was performed using a GLC with an electron capture detector. Confirmation of the presence of $(CH_3)_4$ Pb (TML) was made using a Finnigan GC/MS. Detection limit for the GLC method was 0.23 $\mu g\ L^{-1}$.

All samples were also analyzed for total lead (aqua regia and nitric acid extractable), total organic carbon, moisture and total sulphide.

Results and Conclusions

Results of the incubation experiments can be summarized as follows:

1. No TML was detected in the controls. This suggests that lead in sediments is unavailable to short-term methylation processes.
2. TML was produced readily in the presence of $(CH_3)_3Pb^+$. Over 90% of the available Pb was present in the head space as TML at the end of the experiment under all four conditions.
3. In the presence of $Pb(NO_3)_2$, TML was produced to a maximum of about 2.2 $\mu g\ L^{-1}$ or 0.026% of the available lead.
4. In the presence of $Pb(OAc)_2$, no TML was produced above the detection limit.
5. The presence of added nutrients had little effect upon methylation rate. Some slight differences in rates among the sediment types was noted. The sediment from Goletas Channel was the most productive in methylation of $Pb(NO_3)_2$; however, differences were not significant.
6. No methylation of $Pb(NO_3)_2$ or $(CH_3)_3Pb^+$ occurred in sterilized controls. Addition of Na_2S resulted in very rapid production of TML from $(CH_3)_3Pb^+$ but none from $Pb(NO_3)_2$.

Results of this study indicate that if methylation of lead occurs at all under natural conditions it must result in the production of very little TML. When it is considered that incubation temperatures were about three times greater than those encountered in coastal sediments, any methylation process would proceed very slowly.

The presence of lead in tailings-derived sediments from Alice Arm at levels up to 14 times those in the three other samples did not result in enhanced TML production. This would suggest that the lead (probably present as PbS) is not available to bacterial action in anoxic sediments. A recent report by Harrison and Laxen (1978) suggesting that tetraalkyllead in rural air was in part due to outgassing from intertidal mud flats, may indicate that oxygen exposure is required.

With respect to ocean dumping, our results would indicate that the discharge of lead-bearing particulates may not result in the mobilization of lead by biomethylation processes under anoxic conditions.

Group Discussion

Considerable discussion followed on lead and its various compounds. With little mobilization occurring with the Pb found in mine tailings, the question was raised whether other forms of Pb reacted in a similar manner (Hoos). Thompson replied that Pb in a more available form could behave quite differently. For example, in these experiments, all the sediments tested required the addition of lead before methylation was induced. It was postulated that lead compounds with a greater degree of covalency in the lead-anion bond might permit less or no methylation. In response to a question from Levings, Thompson indicated that Pb used for dating cores was actually a Pb isotope, not stable lead.

Waldichuk asked if this work was conclusive, but Thompson felt that better results could be obtained by means of a continuous flow apparatus where the carrier gas would collect everything that became mobilized, and in greater quantities. He also felt that more information was needed on the microbiology of methylation.

Young asked if the bugs were the means by which methylation occurs. In fact, this is true; however, organisms can also work as a means of demethylation depending on the strain of bacterium.

Waldichuk mentioned that the several compounds of lead have very different stabilities: $(CH_3)_4$ Pb (TML) is stable in sea water while $(CH_3)_2$ Pb is unstable. Also, lead oxides introduced to the sea via car exhausts are known to be quite non-reactive. Thompson acknowledged this and stated that Chau found this particular form of Pb didn't react because it was insoluble.

References

Brinkhurst, R.O. ed. 1978. Report on ocean dumping R and D Pacific Region, Fisheries and Environment Canada, 1976-1977. Pacific Marine Science Report 78-9: 32 pp.

Chau, Y.K. and P.T.S. Wong. 1978. Occurrence of biological methylation of elements in the environment. IN: Organometals and metalloids, occurrence and fate in the environment. American Chemical Society, Washington, D.C. ACS Symposium Series 82: 39-53.

Harrison, R.M. and D.P.H. Laxen. 1978. Natural source of tetraalkyllead in air. Nature 275: 738-40.

Huber, F., U. Schmidt, and H. Kirchmann. 1978. Aqueous chemistry of organolead and organolithium compounds in the presence of microorganisms. IN: Organometals and metalloids, occurrence and fate in the environment. American Chemical Society, Washington, D.C. ACS Symposium Series 82: 65-81.

Jarvie, A.W.P., R.N. Markall, and H.R. Potter. 1975. Chemical alkylation of lead. Nature 255: 217-218.

Thompson, J.A.J. and D.W. Paton. 1978. Heavy metals in benthic organisms from Point Grey Dumpsite - Vancouver, B.C. A preliminary report. Pacific Marine Science Report 78-11: 18 pp.

Wong, P.T.S., Y.K. Chau, and P.L. Luxon. 1975. Methylation of lead in the environment. Nature 253 (5489): 263-264.

VII. AN EXAMINATION OF THE VARIABILITY OF UPWELLING AND ITS RELATIONSHIP TO THE FLUSHING OF ALBERNI INLET

J.A. Helbig

Contractor: Beak Consultants Limited

General Introduction: W.H. Bell, I.O.S.

The dumping of dredge spoil in the inner basin of Alberni Inlet imposes an oxygen demand on the deep water of the basin. The evidence available to date suggests that flushing or renewal of this water occurs on an annual basis so that there has been no long-term accumulation of deleterious effects due to the oxygen demand. However, the question arises as to the invariability of the flushing and the consequences of a lack of renewal in any particular year. Failure of the renewal mechanism might require suspension of dumping permits in the Inlet for a certain period of time to avoid additional oxygen depletion problems.

The flushing of the Alberni Inlet system appears to result directly from upwelling on the west coast of Vancouver Island and is, therefore, related to the annual cycle of winds in the area. Beak Consultants Limited were awarded a contract to examine the problem and attempt an estimate of the likelihood of failure of the renewal mechanism. (Beak Report, 1979). The study was carried out by Dr. J. Helbig, who has summarized his results below. Dr. Helbig examined the relationship between coastal winds, surface sea water density and known renewal events in Alberni Inlet, insofar as the available data permitted. As a result of this examination, he suggests that upwelling is not so much due to the forcing of ocean circulation by north-west winds as it is a response to the relaxation of south-east winds. On the basis of a particularly strong upwelling event, which was responsible for basin water renewal in 1966, he establishes that there is some likelihood that an event of similar strength will not occur every year. However, he concludes that lesser events are adequate to cause renewal, in many instances, and one of sufficient strength for this purpose is almost certain to occur every year.

Introduction

That coastal upwelling might lead to the flushing of Alberni Inlet was first suggested by Tully (1949). Bell (1976) has clearly described how upwelling is related to deep water renewal and has argued on the basis of available, although scanty, data that the inner basin of the Inlet is replaced annually with oxygen "rich" water. Since local industry places a large biological oxygen demand on these waters, the importance of a failure in the presumed annual cycle is clear. This report summarizes an attempt to estimate the probability of a lapse in this cycle. Note that these ideas are not restricted to Alberni Inlet, but also apply to other inlets on the west coast of Vancouver Island.

The basic concept is deceptively simple. As the prevailing winds shift to southeastward in spring, the joint effect of the wind stress and Coriolis force is to drive surface waters away from the coast. To replace this water, deep (and more dense) water is upwelled from below. If the density of the upwelled water at sill depth exceeds that of the inlet, it will flow into the inlet and displace the resident water upwards.

There are three reasons why in any given year, the deep waters of Alberni Inlet may not be re-oxygenated: 1) the winds might be of improper direction or insufficient intensity or duration to induce sufficient upwelling; 2) the upwelled water could be too low in density; or,3) the upwelled water may be deficient in dissolved oxygen. Of these three, only the first is directly related to upwelling, and it is the only one examined here: the others are concerned with the "climate" of the offshore waters.

The available data consist of a relatively sparse set of oceanographic measurements taken in the two basins of Alberni Inlet and in the offshore zone; winds recorded at several locations on the west coast of Vancouver Island by the Atmospheric Environment Service; and a 41 year time series of surface temperature and salinity taken at the Amphitrite Point lighthouse station at the mouth of the Inlet. Included in the oceanographic data are the results of a series of 19 monthly cruises made in the inner basin in 1965-67.

Results and Conclusions

The wind stress calculated from winds at Tofino, the surface density computer from temperature and salinity fields at the Amphitrite Point lighthouse station, as well as the runoff from the Somass River have been examined to determine the relationship between coastal upwelling and renewal of the deep waters of Alberni Inlet. The major obstacle to the achievement of this goal is the severe lack of synoptic oceanographic data from Alberni, particularly from the outer basin which is directly connected to the Pacific Ocean. This deficiency of data prohibits the determination of the time and duration of renewal. The existing data are, however, consistent with an annual renewal of the deep waters of the inner basin beginning in late spring or summer. Obviously the outer basin is also flushed at least annually. Line P data clearly indicate the upwelling and downwelling of isopycnals.

Winds tend to blow down the coast (from the northwest) during the months of May through August and up-coast otherwise. Local topographic features can alter winds measured on land, particularly near inlets. For example, predominately southeastward winds tend to possess a positive onshore component. When the winds are strong, the alongshore component of the wind stress always greatly exceeds the onshore component. The comparison of winds measured at Tofino and at Estevan Point indicates that the wind field is comparatively homogeneous.

The linear correlation between the wind stress at Tofino and the surface density at Amphitrite Point is always small. This means that the long time series of surface temperature and salinity is of limited value in determining the relationship between upwelling and flushing. Several factors may contribute to the low correlation: fresh water runoff and its concomitant variation with the winds, local topographic modification of the winds, the depth of the mixed layer, non-linear effects, and wave-like disturbances that

are generated outside of and propagate into the region of interest.

Visual examination of the time series of wind stress, surface density, and river outflow reveals distinct upwelling - downwelling events. A comparison of these variables with density and dissolved oxygen content data from the inner basin of Alberni Inlet convincingly demonstrates that upwelling leads to flushing. The time scale for the onset of renewal following a shift to upwelling-favourable winds may be a week or less. Large scale flushing of the inner basin appears to take at least a month.

Based on the above comparison, estimates are made of the strength and duration of southeastward winds necessary to induce renewal. The probability for any one year period, that a 30-day interval will occur during which the average southeastward component of the wind stress will be of equal magnitude to the southeastward wind stress observed during May 1966 (when the renewal occurred) is about 75 percent. Since the most negative monthly and weekly averaged southeastward wind stress occurred during May, the calculated probability will tend to be underestimated and hence the likelihood of a lapse in the supposed annual renewal cycle is small. Based on 1965 values, this probability is essentially one.

Any future observation program relating to the flushing of Alberni Inlet or the other inlets on the west coast of Vancouver Island should include the mooring of current meters near all sills and in all connecting waterways to the ocean. Moreover these meters should be equipped with self recording conductivity and temperature sensors. This program should be supplemented by regular synoptic cruises. In addition, provision should be made for the adequate measurement of the winds.

Group Discussion

In response to an inquiry by Hoos, regarding the regularity of renewal of the inner basin of Alberni Inlet, Helbig indicated that there was a very strong probability that an upwelling event of sufficient strength to initiate flushing, would occur at lease once per year. Anderson pointed out, however, that the probability of flushing is not independent from year to year. For example, the filling of the inner basin with very dense water in one year might reduce the probability of flushing in subsequent years. To a query from Levings, Helbig replied that better temporal data on density would improve the capability for predicting the likelihood of renewal.

Buckley suggested that the data might be suseptible to cross spectral analysis as an alternative to correlation analysis. Helbig agreed, but advised that the scope of the project was not such as to allow it.

Young asked if every inlet along the west coast of Vancouver Island would flush in synchronism. Helbig stated that this would probably happen, with the possible exception of Quatsino Sound. Waldichuk asked whether a large wave (tsunami or seismic sea wave) would influence flushing, but the effect would apparently be dependent on the resonance period.

References

Beak Consultants Limited, 1979. Examination of the variability of upwelling on the west coast of Vancouver Island and its relationship to the flushing of Alberni Inlet. Sidney, Institute of Ocean Sciences. Contractor Report Series 79-3: 54 pp.

Bell, W.H. 1976. The exchange of deep water in Alberni Inlet. Pacific Marine Science Report 76-22: 19 pp.

Tully, J.P. 1949. Oceanography and prediction of pulp mill pollution in Alberni Inlet. Fish. Res. Board Can. Bull. No. 83.

VIII. AN EXAMINATION OF EVIDENCE FOR AN INTERNAL TIDE IN ALBERNI INLET

J.R. Buckley

Contractor: Seakem Oceanography Limited

General Introduction: W.H. Bell, I.O.S.

Time series measurements of water properties made in Alberni Inlet in 1977 revealed the existence of a large internal tide in the inner basin, a region which includes the designated dumpsite. The effect of such tides is to cause fluctuations in the water property data at a particular depth, the values obtained depending on the state of the tide at the time of the measurements. These fluctuations can make data interpretation very difficult, or even lead to mis-interpretation. This could be of considerable significance in examining the effects of ocean dumping at an existing dumpsite, or in selecting a location for a new dumpsite on the basis of historical data, in any area of non-homogeneous water structure.

A mathematical model of internal tides in fjords would be of great utility in evaluating their effect on water property data, especially an analytical model of simple application. Dr. Buckley's paper, summarized below, set out to determine the feasibility of developing such a model. He found several unavoidable complications, including difficulties with suitable geometrically-simple representations of the basin shape and with establishing suitable boundary conditions. While not completely successful in developing an applicable model, his efforts did point out some problem areas, indicated the likely region of generation of the internal tides, and substantiated the large amplitudes of motion to be expected with this phenomenon in waters structured like those of Alberni Inlet.

Introduction

The passage of the tide over the sill in a fjord may generate internal waves of significant amplitude. Such waves may move water tens of metres vertically within the water column and so could lead to erroneous interpretation of oceanographic data. Previous studies in Alberni Inlet have shown semi-diurnal isotherm excursions of up to 15 m in the inner basin (Buckingham, 1978). The present study was designed to provide an analytical model of this internal tide and to compare it to existing observations.

The model, based on an oceanic tidal model of Prinsenberg and Rattray (1975), simplified the basin geometry but uses the observed density distribution. Because of the geometrical simplifications, the model does not exactly reproduce the observed internal tide at all locations in the Inlet, but, as will be shown, it does reproduce much of the basic nature of the tide.

The Model

The basis of this internal tide model is the standard set of equations describing fluid flow. The equations are linearized, inviscid, and two dimensional with the effects of the earth's rotation neglected. These equations are solved in each of three straight-sided, flat-bottomed regions: the outer basin, the inner basin and the harbour. The deep inner and outer basins are joined at a shallow sill. There is no obstruction between the inner basin and the shallow harbour region. The solutions to the equations in the three regions are forced to be continuous at the junctions between the regions.

The fact that the regions are flat-bottomed allows the equations to be separated into two parts; one part containing all the horizontal variation and the other all the vertical variation. Each of these parts is solved independently. The vertical equation is solved by an infinite number of functions whose sum represent the total effect of the measured density profile. Each of the vertical functions (modes) has a horizontal equation associated with it. These horizontal equations are satisfied by simple wave solutions whose amplitudes are determined by the basin geometry, boundary conditions and region matching conditions. All of the equations for the wave amplitudes are solved simultaneously in one large matrix system. The matrices are, in principle, infinitely large, but in practice the solutions are approximated with a small number of modes.

Solutions in Alberni Inlet

Alberni Inlet was parameterized in three regions: an outer basin of 100 m depth and infinite length extending seaward, an inner basin of 100 m depth and 14 km length, and, a harbour region 15 m deep and arbitrarily long. A sill extending to 40 m from the surface is located at the junction between the inner and outer basins. In both the inner and outer basins, internal waves were assumed to travel both towards the head and the mouth of the Inlet; in the harbour region, no seaward progressing wave was assumed to exist.

The density profile used for the test of the model was the average of 25 profiles taken by Buckingham (1978) in a 25-hour period November 21-22, 1977. It is shown, along with the first three modes calculated from it, in Figure 8. Also shown are the vertical gradients of the first three modes. Horizontal currents are proportional to the modes while vertical displacements are proportional to the gradients of the modes. The proportionality constants are determined from the heights of the observed surface tidal constituents in the Inlet and from the tidal prism transports calculated from them. The following table shows the amplitudes of internal waves of the first three modes at 60 m depth for the two most important tidal contituents. The sum of amplitudes for each mode represents the amplitude of internal wave that would be observed if only the first three modes were important and is indicative of the magnitude of internal wave response. These results show that the observed isotherm displacements in Alberni Inlet can certainly be generated by the interaction of the surface tide with the bottom topography.

Tidal Constituents	Mode 1(m)	Mode 2(m)	Mode 3(m)	Sum (m)
M_2	9.34	-7.44	-12.73	-10.83
K_1	8.32	0.47	- 3.22	5.57

The solution to the horizontal equation indicates the source of the internal tides. Amplitudes of the horizontal waves for the M_2 tide are as follows:

Mode	Outer Basin		Inner Basin		Harbour
	up-inlet	down-inlet	up-inlet	down-inlet	up-inlet
0	1.00	-0.91	1.35	-1.26	29.36
1	0.00	-1.24	-0.62	-0.63	- 0.32
2	0.00	0.29	0.14	0.15	- 0.24
3	0.00	0.40	0.20	0.20	0.00

The fact that the up-inlet and down-inlet amplitudes in the inner basin are almost equal indicates that almost all the energy is reflected at the head of the inlet and therefore the flow of energy from the incoming surface (zeroth) mode to the higher modes is caused at the sill. This table also shows that the inlet responds more strongly to mode 3 than to mode 2. The reason for this result is that the gradient of mode 3 has a zero very near sill depth and that of mode 2 does not.

The horizontal and vertical results may be put together to generate a map of internal wave amplitude anywhere inside the model basin, but this was not done since there are no data to compare the map with.

The data that do exist show a tendency for the internal wave amplitude to increase with depth, while this model predicts exactly the opposite. A region with a sloping bottom has the property of increasing internal wave amplitude with depth, and may be a more suitable parameterization of the shape of the inner basin. Such a region, however, cannot easily be put into the sort of analytic model described here since the vertical and horizontal variations do not separate. Explicit inclusion of this shape of basin was therefore beyond the scope of the present study.

Conclusion

The model has shown that interaction of the surface tide with the sill can create internal waves of large amplitude, similar to the observed isotherm displacements. It did not predict, however, the correct amplitude variation in deeper water.

The model could be improved by the inclusion of a wedge-shaped region as the inner basin and by the calculation of a larger number of modes to better approximate the infinite sum solution. A more comprehensive set of measurements needs to be made to test the revised model effectively.

While the model developed here will not predict the characteristics of the internal tide at any specific locations in the inner basin of Alberni Inlet, it still will be useful in predicting how much energy is taken from the surface tide and distributed into the various internal modes under different stratification conditions.

Group Discussion

In considering inlets with a sloping bathymetry Macdonald asked if there was some area where the internal wave would break. Buckley responded that such an area likely exists but that the present linear model cannot be used to make any prediction about the location of the region. A non-linear model would be required for such a prediction. Levings questioned whether an internal wave would go through a narrow notch in a manner similar to the way it would go through a wide notch. By analogy to light travelling through a notch Buckley though that a three-dimensional model would be necessary as opposed to the two dimensional used in this study.

References

Buckingham, W.R. 1978. An oxygen budget of the deep waters in the inner basin of Alberni Inlet. Victoria, Dobrocky SEATECH Limited. Contract Report IOSPB-CR-22: 215 pp.

Prinsenberg, S.J. and M. Rattray Jr. 1975. Effects of continental slope and variable Brunt-Väisälä frequency on the coastal generation of internal tides. Deep-Sea Res. 22: 251-263.

IX. GROUP DISCUSSION ON FUTURE OCEAN DUMPING RESEARCH

A group discussion of future ocean dumping research trends followed the reporting of current projects.

Studies in Alberni Inlet were summarized and future research projects that developed from the Alberni work were noted. Biological data from the past few years will be collated and statistically analyzed as part of the 1979-1980 contracts. This will complete the studies on marine benthos communities in Alberni Inlet.

The chairman noted that there would be some support from the ocean dumping budget for the unsolicited proposal submitted to continue a more detailed study of the oxygen budget and internal tides of the inner basin of Alberni Inlet. This work could complete the need for any further physical oceanographic research in the Inlet.

Chemical research will continue to concentrate on the development of meaningful criteria and the establishment of realistic allowable concentrations or levels for the various chemical parameters as described in the Ocean Dumping Control Act.

The current status of dumping in Porpoise Harbour and the urgency of establishing a more environmentally suitable dumpsite near Prince Rupert were discussed. A site-specific examination of the Prince Rupert problem could provide information of general utility in the selection of dumpsites. The consensus of the group was that research on fish populations and/or communities should be supported by Ocean Dumping funds only when such studies were within the framework of studies considering all oceanographic and biological features of a study area, and related particularly to dumpsite selection or relocation.

The workshop was adjourned by Mr. Smith.

X.

FIGURES

FIGURE 1. IRON CONCENTRATIONS IN VICTORIA HARBOUR SEDIMENT

ELUTRIATE TEST 0.81 μg g^{-1}

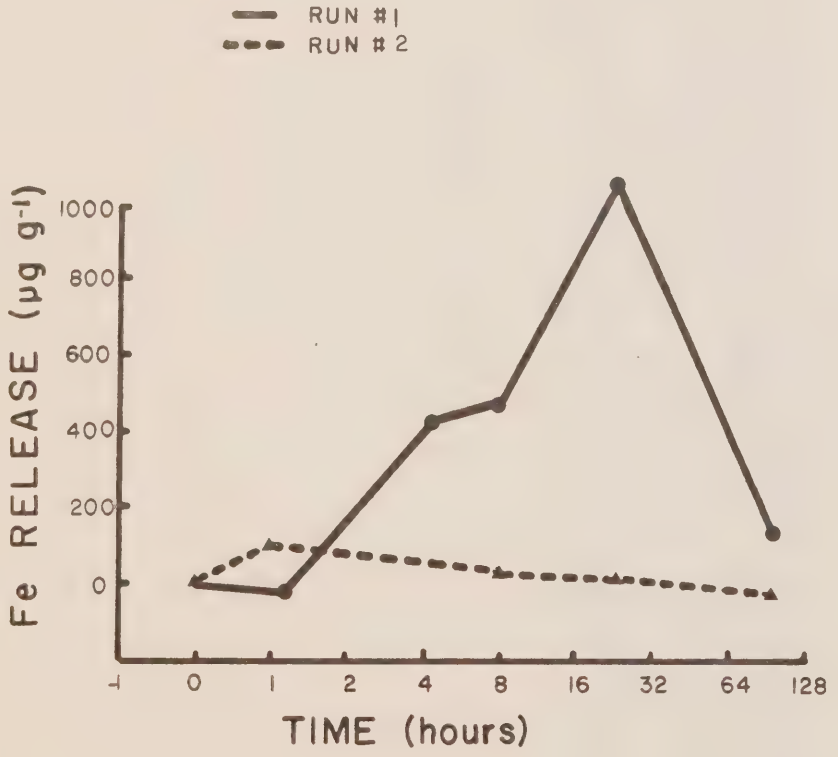

SELECTIVE EXTRACTION (μg g^{-1})

	BEFORE	AFTER
I W	.070 mg l^{-1}	.019 mg l^{-1}
EXCHANGE	6.6	1.1
EASILY RED	836	236
OXID	11892	12436
MOD RED	2297	1736
RESIDUAL	12050	6717
	27082	21126

FIGURE 2. IRON CONCENTRATIONS IN FALSE CREEK SEDIMENT

ELUTRIATE TEST 3.84 μg g^{-1}

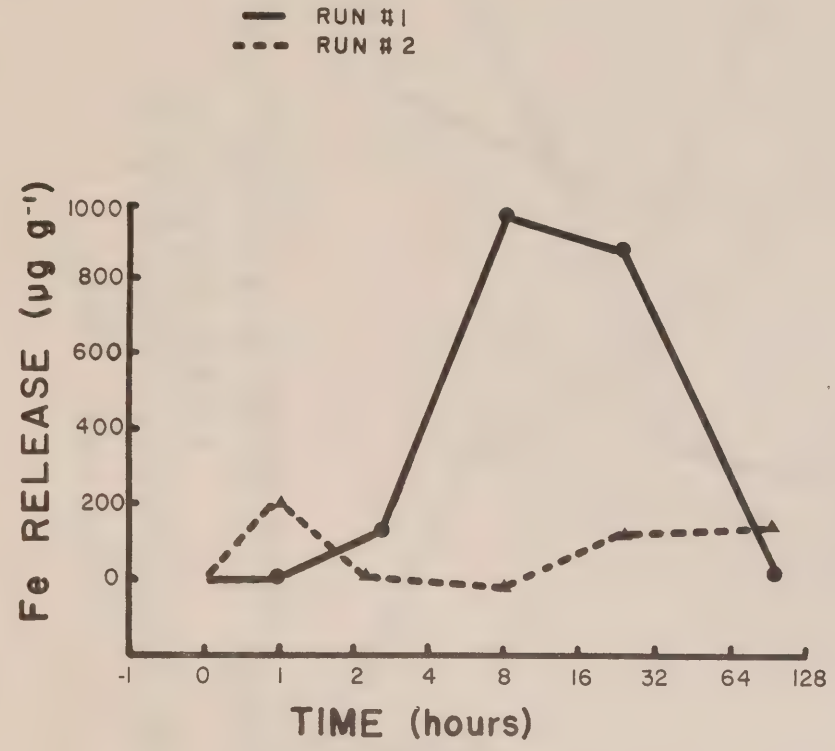

SELECTIVE EXTRACTION (μg g^{-1})

	BEFORE	AFTER
I W	.065 mg l^{-1}	.021 mg l^{-1}
EXCHANGE	1.4	< 0.8
EASILY RED	508	42
OXID	9483	455
MOD RED	3933	6609
RESIDUAL	11242	16312
	25167	23418

FIGURE 3. MANGANESE CONCENTRATIONS IN VICTORIA HARBOUR SEDIMENT

ELUTRIATE TEST 0.46 µg g^{-1}

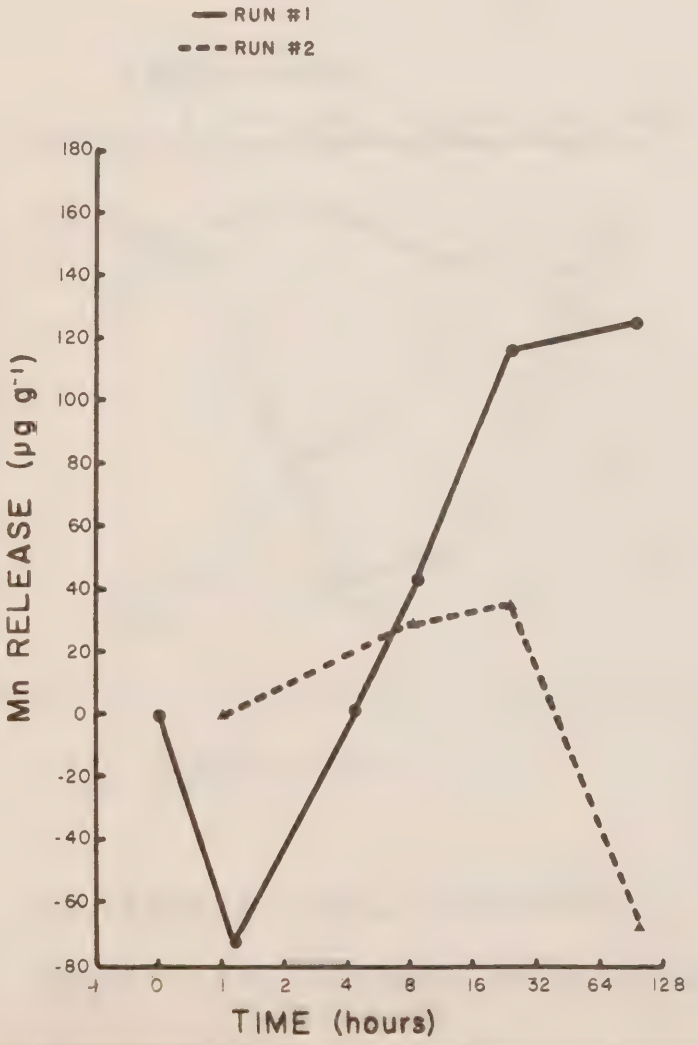

SELECTIVE EXTRACTION (µg g^{-1})

	BEFORE	AFTER
I W	.023 mg l^{-1}	.019 mg l^{-1}
EXCHANGE	< 0.3	< 1
EASILY RED	3.4	18.6
OXID	76.4	108
MOD RED	4.3	32
RESIDUAL	169	75
	253	235

FIGURE 4. MANGANESE CONCENTRATIONS IN FALSE CREEK SEDIMENT

ELUTRIATE TEST 0.20 µg g^{-1}

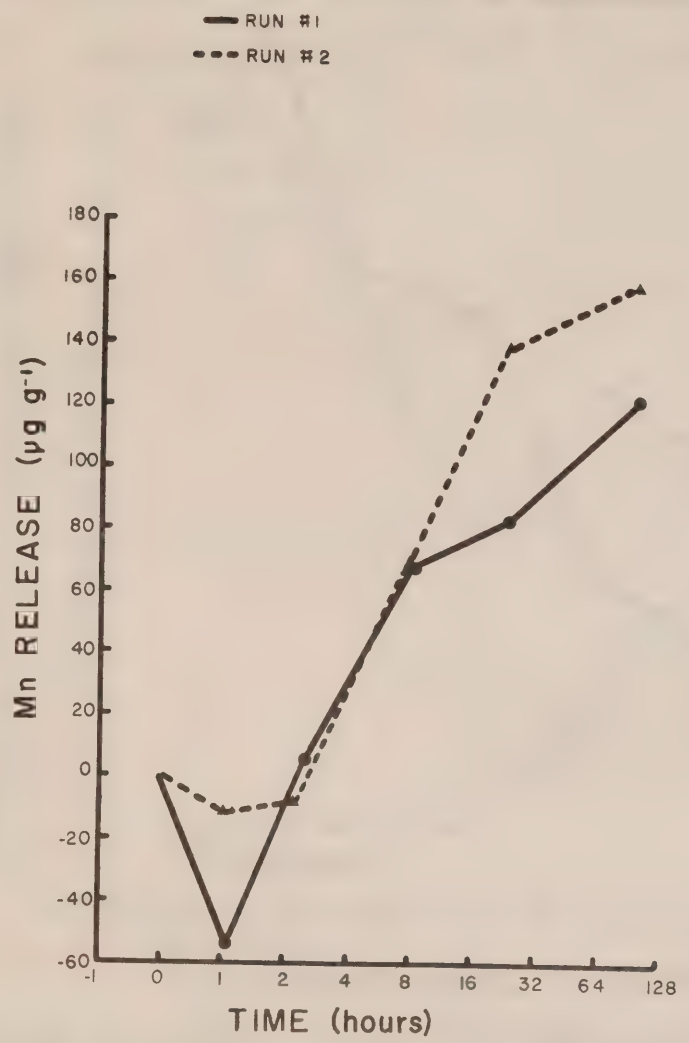

SELECTIVE EXTRACTION (µg g^{-1})

	BEFORE	AFTER
I W	.021 mg l^{-1}	.020 mg l^{-1}
EXCHANGE	4.6	1.2
EASILY RED	7.7	9.3
OXID	85.6	27.8
MOD RED	12.5	19
RESIDUAL	261	221
	371	278

FIGURE 5. ZINC CONCENTRATIONS IN VICTORIA HARBOUR SEDIMENT

ELUTRIATE TEST 0.46 µg g^{-1}

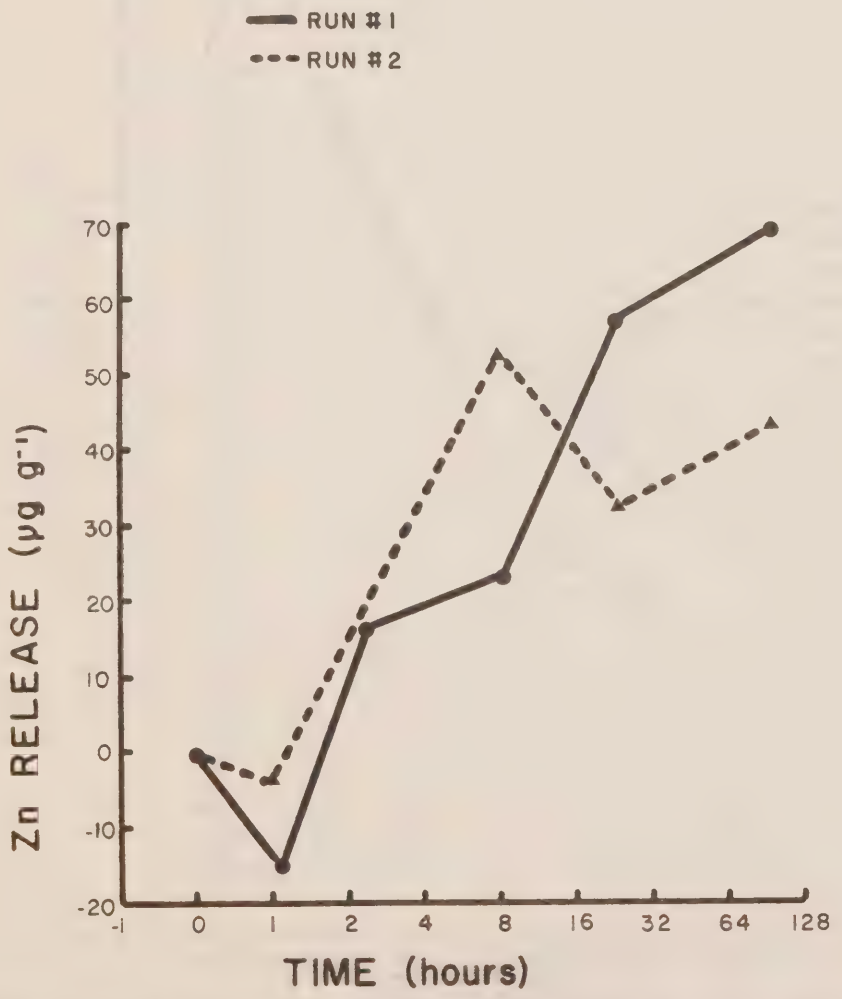

SELECTIVE EXTRACTION (µg g^{-1})

	BEFORE	AFTER
I W	<.001 mg l^{-1}	.006 mg l^{-1}
EXCHANGE	<.07	4.7
EASILY RED	2.3	27.6
OXID	203	137.4
MOD RED	<3.4	1.9
RESIDUAL	65.4	35.4
	274	207

FIGURE 6. ZINC CONCENTRATIONS IN FALSE CREEK SEDIMENT

ELUTRIATE TEST 0.05 µg g^{-1}

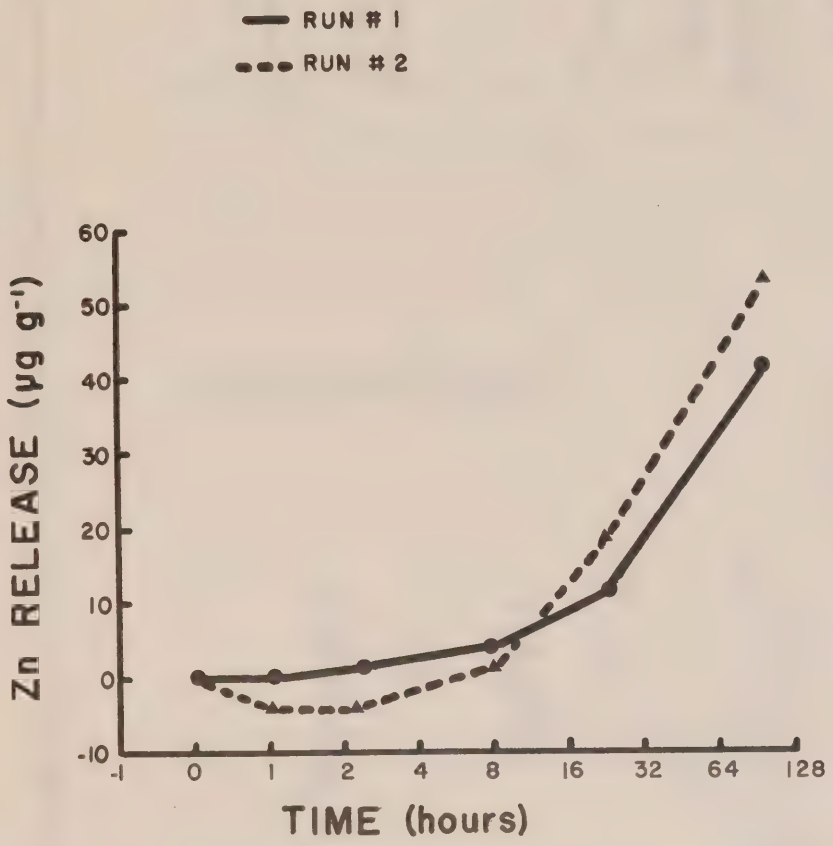

SELECTIVE EXTRACTION (µg g^{-1})

	BEFORE	AFTER
I W	.007 mg l^{-1}	.007 mg l^{-1}
EXCHANGE	<.07	3.6
EASILY RED	5	8.2
OXID	179	37.0
MOD RED	2.5	-
RESIDUAL	60.3	70.8
	247	120

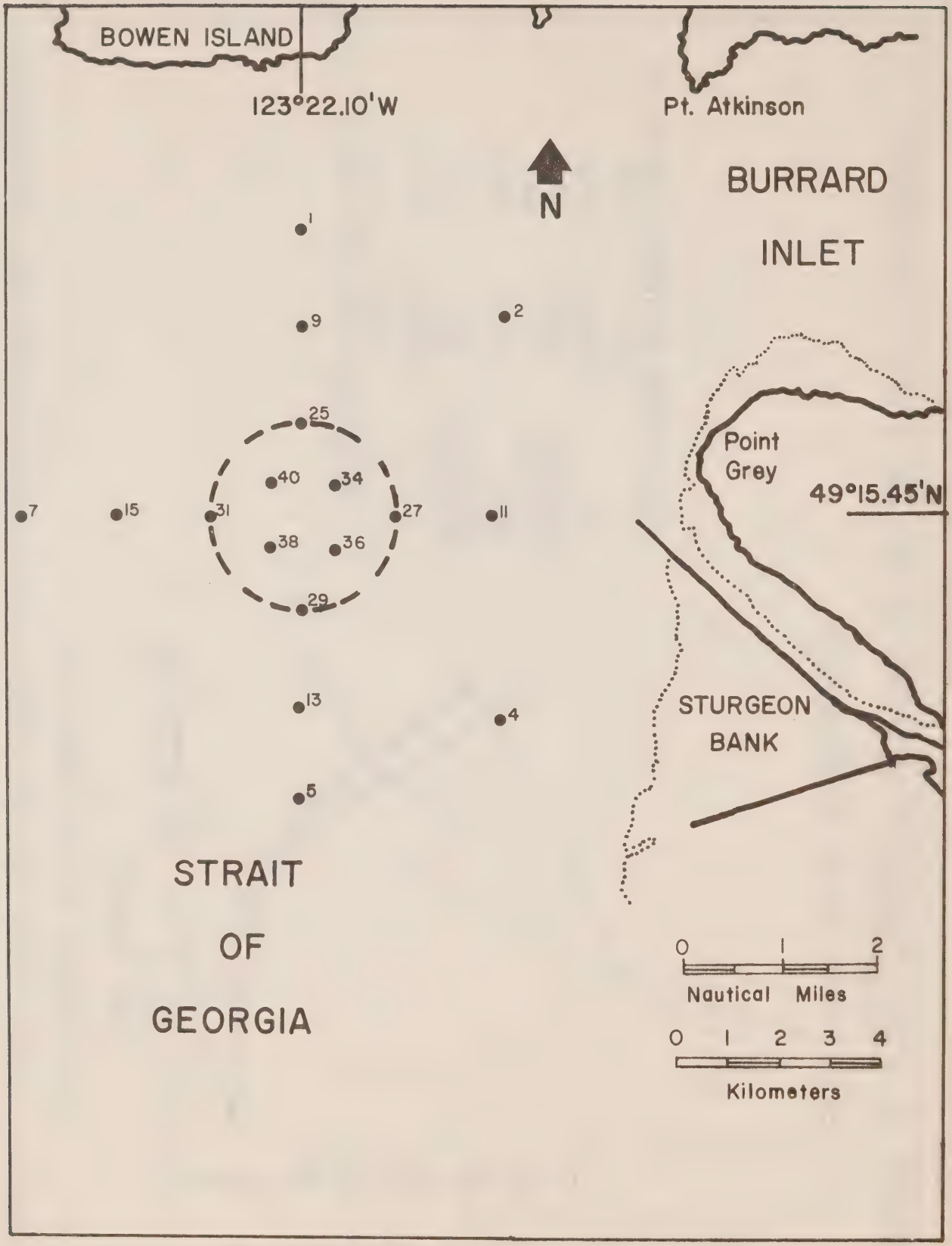

FIGURE 7. COLLECTION STATIONS FOR *Molpadia intermedia* AT THE POINT GREY DUMPSITE.

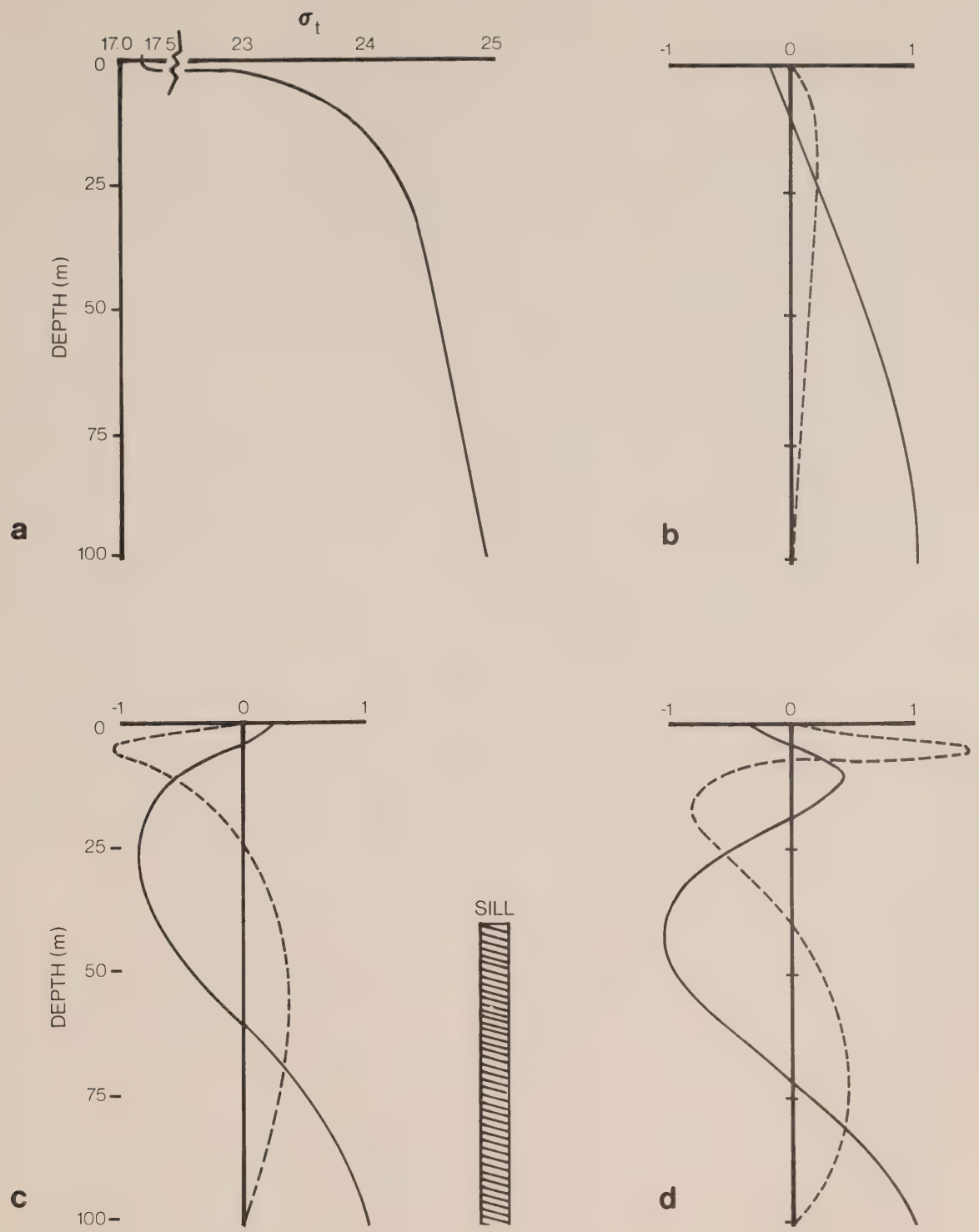

FIGURE 8. PROFILES USED FOR THE MODEL TEST:
The sigma-t (σ_t) profile (a).
Internal mode (———) and its corresponding vertical gradient (-----) for the first (b), second (c), and third (d) internal modes.

XI.

TABLES

TABLE 1

SUMMARY OF BENTHIC SAMPLING EFFORT

		Dumpsite			Control Site		
DATE	TRIP NUMBER	TAXA	INDIVIDUALS (m^{-2})	BIOMASS (mg m^{-2})	TAXA	INDIVIDUALS (m^{-2})	BIOMASS (mg m^{-2})
Nov. 15/77	1	7	813	302	10	566	121
Nov. 28/77	2	10	4803	1951	18	1356	574
Dec. 13/77	3	5	1213	282	18	3023	4235
Dec. 20/77	4	15	3096	1980	13	793	5061
Jan. 25/78	5	9	1396	135	14	1026	870
Feb. 21/78	6	8	913	649	14	1193	1820
Mar. 09/78	7	7	473	169	13	816	1342
Mar. 21/78	8	n.d.			15	2143	364
Apr. 20/78	9	5	513	85	12	1220	247
May 18/78	10	8	2993	798	10	783	16
July 04/78	11	15	383	851	16	1180	915
July 31/78	12	19	2120	594	12	620	418
Aug. 28/78	13	18	2650	1229	10	400	1493
Sept. 20/78	14	12	1060	421	15	920	1511
Oct. 18/78	15	16	2060	868	18	970	1337
Nov. 15/78	16	16	3910	1994	12	1070	1204
Grand Means (n=16)		11	1774	745	14	1129	1345

TABLE 2. SUMMARY OF LIFE HISTORY CHARACTERISTICS OF SOME ALBERNI INLET INFAUNA

CHARACTERISTICS:	1	2	3	4	5	6	7	8
Central Province Fauna								
Macoma carlottensis	PE	10^3	1	+	MN	SF	BU	TO?
Axinopsida serricata	?	?	?	+?	?	?	BU	TO?
Scoloplos pugettensis	PE	10^3	1	+?	DA?	DF	BU	TO?
Aricidea lopenzi	?	?	?	+?	DA?	DF	BU	?
Eudorella pacifica	AN?	10^1	1-2	-?	NP?	EP	FS	IN?
Heterophoxus oculatus	?	10^1	?	-?	NP?	EP	FS	IN?
Wood Debris Fauna								
Xylophaga washingtona	PE	10^4	1?	+?	MN?	WO	BO	TO?
Nebalia pugettensis	?	?	?	?	?	SC	FS	TO?
Limnoria lignorum	PE	10^1	1?	-?	NP	WO	BO	TO
Oradarea sp. A	?	10^1	?	-?	NP?	SC	FS	?
Dumpsite Fauna								
Schistomeringos longicornis	PE	10^3	1	+	WK	DF	BU	TO
Capitella capitata	PE	10^2-10^4	3	- or +	NP/WK	DF	BU	TO
Dumpsite Fringe Fauna								
Trochochaeta multisetosa	PE?	?	?	?	?	DF	BU	TO?

COLUMN CODES: 1. AN = lives for one year; PE = lives for more than one year. 2. Fecundity: given by orders of magnitude. 3. Number of reproductive periods in one year. 4. With (+) or without (-) a larval dispersal stage. 5. Approximate time spent in the plankton: NP = not planktonic; DS = days; WK = weeks, MN = months. 6. Feeding strategy: DF = depostit feeder, SF = suspension feeder, epistratial feeder = EP, scavengers = SC, wood eaters = WO. 7. Mode of movement: BU = burrower, BO = borer; FS = free-swimmer. 8. Tolerance to oxygen deficiency. TO = tolerant, IN = intolerant. A question mark standing alone (?) indicates that the characteristic for that particular species is unknown. Entries followed by a ? indicate guesses based on notes presented in Section 4.

TABLE 3

SELECTIVE CHEMICAL EXTRACTIONS

Metal concentrations ($\mu g\ g^{-1}$ dry weight) in the different compartments before and after the release experiment. Compartments were defined according to the selective extraction scheme used by Brannon et al.,1976.

COPPER

	VICTORIA HBR.		FALSE CREEK	
	Before	After	Before	After
IW	<0.001*		0.002*	
E	0.019	0.47	0.015	1.7
ER	<0.07	0.13	<0.05	0.09
O	133	144	66.7	16.5
MR	2.9	1.1	0.71	<0.17
RE	29.4	47	19.7	40.7
Σ	165	193	87	59.2

CADMIUM

	VICTORIA HBR.		FALSE CREEK	
	Before	After	Before	After
IW	<0.001*		<0.001*	
E	<0.007	0.14	<0.005	0.14
ER	0.068	0.18	<0.05	0.14
O	1.67	0.84	1.47	0.50
MR	<0.068	<0.11	<0.5	<0.08
RE	<0.74	<0.55	<0.58	<0.31
Σ	<2.56	<1.82	<2.61	<1.17

LEAD

	VICTORIA HBR.		FALSE CREEK	
	Before	After	Before	After
IW	<0.001*		<0.001*	
E	1.03	<2.3	<0.5	<1.65
ER	0.09	0.22	<0.05	<0.02
O	167	170	38.2	9.2
MR	<6.7	5.1	<5	1.7
RE	23.2	44.3	29.4	49.3
Σ	198	222	67.6	62

ARSENIC

	VICTORIA HBR.		FALSE CREEK	
	Before	After	Before	After
IW	0.01*		<0.005*	
E	0.072	<0.11	<0.025	<0.08
ER	<0.34	0.16	<0.25	<0.08
O	3.67	1.63	1.85	1.00
MR	<0.34	<0.11	<0.25	<0.08
RE	0.62	0.53	0.80	1.88
Σ	<5.06	<2.55	<3.18	<3.12

MERCURY

	VICTORIA HBR.		FALSE CREEK	
	Before	After	Before	After
IW	<0.0005*		<0.0005*	
E	<0.004	<0.11	<0.003	<0.08
ER	<0.034	<0.11	<0.03	<0.08
O	<0.034	<0.11	<0.03	<0.08
MR	-	<0.11	<0.03	<0.08
RE	2.14	2.98	0.51	0.56
Σ	<2.21	<3.42	<0.56	<0.88

KEY

IW Interstitial Water
E Exchangeable
ER Easily Reduced
O Oxidizable
MR Moderately Reducible
RE Residual
* Interstitial water units mg L^{-1}

TABLE 4

SUMMARY OF ANALYTICAL RESULTS FOR AROCHLORS
OF VICTORIA HARBOUR DREDGE SPOILS

ANALYSIS	MEAN ng g^{-1} DRY WEIGHT	RANGE ng g^{-1} DRY WEIGHT
Arochlor 1242	85.8	0 - 1210
Arochlor 1254	205.4	0 - 1950
Arochlor 1260	57.4	0 - 458
Decachlorobiphenyl	11.4	0 - 87
Total	360	0 - 3640
Total (E.P.S. permit application 4443-0375)	390,84	

TABLE 5

RESULTS OF STATISTICAL ANALYSIS OF THE PERCENTAGE
OF VARIATION OF AROCHLORS DUE TO DIFFERENT CAUSES

Measurement	Variation accounted for within sub-samples from the same grab sample on the barge	Variation accounted for between samples taken from the same barge		Variation accounted for between samples taken from different barges	
	(In %)	(In %)	P<	(In %)	P<
Arochlor 1242	44.8	26.8	0.25	28.5	0.001
Arochlor 1254	40.6	22.0	0.25	37.5	0.001
Arochlor 1260	44.2	26.4	0.25	29.4	0.001
Decachloro-biphenyl	41.5	45.1	0.001	13.4	0.001
Total	40.0	24.7	0.10	35.2	0.001

XII.

APPENDICES

APPENDIX I

OCEAN DUMPING WORKSHOP ATTENDANCE LIST

G.R. Smith, Ocean Engineering I.O.S. (Workshop Chairman)
C.D. Levings, W.V.L., West Vancouver (Workshop Secretary)

E.P. Anderson, Dobrocky SEATECH Limited, Victoria
W.H. Bell, Coastal Zone Oceanography, I.O.S
I. Birtwell, Habitat Protection, D.F.O., Vancouver
W.R. Buckingham, Dobrocky SEATECH Limited, Victoria
J.R. Buckley, Seakem Oceanography Limited, Sidney
S.C. Byers, Dobrocky SEATECH Limited, Victoria
J.A. Crerar, Beak Consultants Limited
L. Dawson-Burns, MacMillan Bloedel Limited, Vancouver
R. Deverall, Can Test Limited, Vancouver
R. Harbo, Habitat Protection, D.F.O., Vancouver
J. Helbig, Beak Consultants Limited, Richmond
R.A.W. Hoos, E.P.S., Vancouver
R.W. Macdonald, Ocean Chemistry, I.O.S.
E. McGreer, E.V.S. Consultants Limited, North Vancouver
D. Morse, Chemex Labs Limited, North Vancouver
J. Park, Can Test Limited, Vancouver
S. Steele, D.F.O., Vancouver
P. Thomas, Econotech Services Limited, New Westminster
J.A.J. Thompson, Ocean Chemistry, I.O.S.
M. Waldichuk, W.V.L. West Vancouver
C.S. Wong, Ocean Chemistry, I.O.S.
R. Young, MacMillan Bloedel Limited

See Appendix III for details of the research institution abbreviations.

APPENDIX II

1978-79 CONTRACTS

A. Biology

[1] Ref. DSS File No. 08SS. KF833-7-1210 $27,000.00

[2] Ref. DSS File No. 08SB. KF833-8-0248 $29,010.00

Marine biological sampling and observations of temporal changes in benthic communities and benthic respiration at a dumpsite in Port Alberni.

Scientific Authority: C. D. Levings, W.V.L.

Contractors: [1]Beak Consultants Ltd.
[2]Dobrocky SEATECH Ltd.

Ref. DSS File No. 08SB. KF833-8-0248
Amendment $ 1,372.00

(a) Review literature on the reproductive ecology of selected invertebrates from a dumpsite in Alberni Inlet.

(b) Verify identification of invertebrates performed by others working at Alberni Inlet and compare identification with current studies.

Scientific Authority: C. D. Levings, W.V.L.

Contractor: Dobrocky SEATECH Ltd.

B. Chemistry

Ref. DSS File No. 07SB. KF833-8-0590 $ 6,300.00

Analysis of sediment samples for polychlorinated biphenyls.

Scientific Authority: R. W. Macdonald, I.O.S.

Contractor: Seakem Oceanography Ltd.

Ref. DSS File No. 07SB. KF833-8-0591 $ 7,358.00

Determination of the lead methylating capacity of Pacific coastal marine sediments.

Scientific Authority: J. A. J. Thompson, I.O.S.

Contractor: Beak Consultants Ltd.

Ref. DSS File No. 07SB. KF833-8-0592-1 $10,421.15

Development of a meaningful criteria for ocean disposal of dredged or sedimentary material - Part I.

Scientific Authority: R. W. Macdonald, I.O.S.

Contractor: Can Test Ltd.

Ref. DSS File No. 07SB. KF833-8-0592-2 $10,241.25

Development of a meaningful criteria for ocean disposal of dredged or sedimentary material - Part II.

Scientific Authority: R. W. Macdonald, I.O.S.

Contractor: Seakem Oceanography Ltd.

Ref. DSS File No. 08SB. KF833-8-1577 $ 1,377.00

Analyses of samples of marine holothurian, *Molpadia intermedia* for the determination of copper, zinc and cadmium.

Scientific Authority: J. A. J. Thompson, I.O.S.

Contractor: Can Test Ltd.

C. Physics

Ref. DSS File No. 07SB. KF833-8-0594 $ 7,980.60

Examination of the variability of upwelling on the West Coast of Vancouver Island and its relationship to the flushing of Alberni Inlet.

Scieitific Authority: W. N. Bell, I.O.S.

Contractor: Beak Consultants Ltd.

Ref. DSS File No. 07SB. KF833-8-0593 $ 4,402.00

Examination of evidence for an internal tide in Alberni Inlet.

Scientific Authority: W. N. Bell, I.O.S.

Contractor: Seakem Oceanography Ltd.

D. Administration

Ref. DSS File No. 07SB. KF833-8-0459 $ 8,435.00

Support for the West Coast dumping program.

Scientific Authority: R. O. Brinkhurst, I.O.S.

Contractor: Dobrocky SEATECH Ltd.

For H.Q. Office $ 2,500.00

Annotated bibliography of Canadian papers and reports bearing on Ocean Dumping. Part II: Pacific Region.

Scientific Authority: D. S. Bezanson (Bedford Institute of Oceanography)

Contractor: Catherine Moyse

APPENDIX III

LOCATIONS OF SCIENTIFIC AUTHORITIES

1979

E.P.S. Environmental Protection Service
Kapilano 100, Park Royal
West Vancouver, B.C.
V7T 1A2

D.F.O. Department of Fisheries and Oceans

I.O.S. Institute of Ocean Sciences
P.O. Box 6000
9860 West Saanich Road
Sidney, B.C.
V8L 4B2

W.V.L. West Vancouver Lab
(formerly P.E.I. Pacific
Environment Institute)
4160 Marine Drive
West Vancouver, B.C.
V7V 1N6

Habitat Protection Directorate
1090 West Pender Street
Vancouver, B.C.
V6E 2P1

APPENDIX IV

REPORTS FROM 1978-1979 CONTRACTS

Anderson, E.P., S.C. Byers, G.W. O'Connell. 1978. Observations of temporal changes in benthic communities and benthic respiration at a dumpsite in Port Alberni, June to November, 1978. Victoria, Dobrocky SEATECH Ltd. Contract Report IOSPB-CR-34: 78 1.

Beak Consultants Ltd. 1978. An examination of the variability of upwelling on the West Coast of Vancouver Island and its relationship to the flushing of Alberni Inlet. Vancouver. Sidney, Institute of Ocean Sciences, Patricia Bay. Contractor Report Series 79-3: 54 pp.

Beak Consultants Ltd. 1979. Determination of the lead methylating capacity of Pacific coastal marine sediments. Vancouver. Contract Report IOSPB-CR-31: 24 1.

Buckley, J.R. 1979. A model of the internal tide in the inner basin of Alberni Inlet. Sidney, Seakem Oceanography Ltd. Contract Report IOSPB-CR-26: 44 1.

Byers, S.C. and R.O. Brinkhurst. ed. 1979. Report on ocean dumping R and D Pacific Region, Fisheries and Environment Canada, 1977-1978. Pacific Marine Science Report 79-5: 76.

Can Test Limited. 1979. Benthic organisms. Vancouver. Contract Report IOSPB-CR-28: 9 1. (contract involving analyses of samples of marine holothurian, *Molpadia intermedia* for the determination of copper, zinc, and cadmium).

Can Test Ltd. 1979. Development of meaningful criteria for ocean disposal of dredged or sedimentary material - PART I. Vancouver. Contract Report IOSPB-CR-29: 26 1.

Clements, A.J. and D.J. Thomas. 1979. Development of meaningful criteria for ocean disposal of dredged or sedimentary material - PART II. Sidney, Seakem Oceanography Ltd. Contract Report IOSPB-CR-30: 38 1.

Conlan, K.E. 1979. The biological effects of ocean dumping: a selected, annotated bibliography. S.C. Byers, ed. Sidney, Institute of Ocean Sciences, Patricia Bay. Contractor Report Series 79-2: 208.

McFarland, M. 1979. Analysis of sediment samples for polychlorinated biphenyls. Sidney, Seakem Oceanography Ltd. Contract Report IOSPB-CR-32: 25 1.

O'Connell, G.W. 1979. Notes on the life histories of some benthic infauna from Alberni Inlet, including remarks on some previous identifications. Victoria, Dobrocky SEATECH Ltd. Contract Report IOSPB-CR-33: 37 1.

CA1
EP321
-79R19

Pacific Marine Science Report 79-19

Publication

FEB 5 1981
University of Toronto

SATELLITE OBSERVATIONS OF SEA SURFACE TEMPERATURE PATTERNS OFF THE PACIFIC COAST OF CANADA

by

S. Tabata

and

P.M. Kimber

INSTITUTE OF OCEAN SCIENCES, PATRICIA BAY
Sidney, B.C.

For further copies or additional information please write to:

Department of Fisheries and Oceans
Institute of Ocean Sciences
P.O. Box 6000
Sidney, B.C. CANADA
V8L 4B2

CA1
EP321
-79R19

Pacific Marine Science Report 79-19

SATELLITE OBSERVATIONS OF SEA SURFACE TEMPERATURE PATTERNS OFF THE PACIFIC COAST OF CANADA

by

S. Tabata and P.M. Kimber

Institute of Ocean Sciences, Patricia Bay

Sidney, B.C.

1979

ABSTRACT

Infrared satellite imagery of the waters off the Pacific coast of Canada for the five-year period, July 1974 through July 1979, has been examined in order to delineate sea surface temperature patterns in the area. A series of charts depicting oceanic thermal fronts is compiled. The source data consist of enhanced VHRR, NOAA satellite infrared imagery in photographic-print format, obtained mostly from the National Satellite Data Services Branch of the National Climatic Center (NOAA) and some from its field station (San Francisco, California) and also from the Arctic Weather Centre of the Atmospheric Environment Service of Canada (Edmonton, Alberta). Some are based on original data acquired from the San Francisco field station and the Arctic Weather Centre. With regularly-obtained imagery in photographic-print format only two shades of the grey-tone variations of the sea surface can generally be delineated successfully by an optical device. However, with suitably enhanced imagery made from original data, at least six shades of these variations can be differentiated. Unless enhancement is made consistent from image to image it is possible to misinterpret locations of weak fronts. In order to track fronts successfully from day to day it is desirable to use original satellite data. Comments are made to explain the occurrence of certain water types at various locations.

Introduction

Sea surface temperatures obtained by the infrared radiation sensors aboard satellites have been applied, since 1968, to depict a number of oceanographic features and processes. The scientific applications range from studies of upwelling (e.g. La Violette and Chabot, 1968; La Violette, 1974; Stumpf, 1975) to those of ocean circulation (Vukovich, 1974); eddies (e.g. Gotthardt and Potocsky, 1974) and oceanic fronts (Wyrtki, 1977). Techniques for processing satellite data have advanced sufficiently to a stage that now daily or weekly charts of distribution of sea surface temperatures over wide oceanic areas are compiled routinely and used operationally by countries such as Japan (Hanzawa, 1979) and the U.S.A. (Pichel et al, 1979). Moreover, detailed charts of fishing areas are produced regularly by France (Noel, 1979), Japan (Hanzawa, 1979) and the U.S.A. (Jurick, 1977) and made available to commercial fishermen as aids to their fish-catching effectiveness.

Over the past five years (1974-1979) well over 100 infrared satellite images of the waters off the Pacific coast of Canada and northern U.S.A., for relatively cloud-free conditions have been acquired. Inspection of these revealed that less than one half of the total number possessed sufficient definition of sea surface thermal features necessary to map oceanic thermal fronts in the area. The present report is primarily a compilation of charts depicting major oceanic fronts off the Pacific coast of Canada (Figure 1) based on these images. It also contains some discussion on data quality and on oceanic events deduced from the examination of the imagery.

Data

Satellite data obtained by the very high resolution radiometers (VHRR) of the spacecrafts, NOAA-3, NOAA-4, NOAA-5 and TIROS-N, were utilized. The visual and infrared imagery based upon these data are reported to have a spatial resolution of one kilometre at subpoint. The full sensitivity of the infrared sensors aboard these satellites is $\pm$ 0.5^{o}C (Koffler, 1976). The majority of the data were procured from the National Satellite Data Services Branch of the National Climatic Center, NOAA (Washington, D.C.) while the rest were obtained from its San Francisco Field Service Station (Redwood, California). A limited number was obtained from the Arctic Weather Centre of the Atmospheric Environment Service (Edmonton, Alberta). The imagery are available in 25 cm x 25 cm size photographic-print format. Examples of these, in reduced size, are shown in Figures 2 and 3. The imagery is essentially photographic prints produced by a computer-interfaced Muirhead-type facsimile recorder. The visible data (Figure 3a) are displayed over the full range of the reflective surface brightness, the white and black representing respectively the light and dark colour of the surface. The infrared data (Figures 2 and 3b) cover a large range of infrared radiation temperatures. Because of this, neither the sensitivity of the photographic paper nor the eyes will be able to perceive small changes of temperature, say, a degree. In order to overcome this deficiency usually a narrower range is selected to give an "enhanced" image covering, for example, the range 0 to 20°C in grey-tone levels. Light tones represent lower temperatures; darker tones represent higher temperatures. The white and black on these prints now represents, respectively, the temperatures less than and greater than those assigned as limits. In the imagery obtained routinely from the Climatic Data Center, even the enhanced data are not all suitable for a local area on account of the choice of larger range to cover greater oceanic

areas. Generally, imagery obtained from the field station contained better definition of the sea surface features than did that from the Climatic Data Center - a reflection of the difference in enhancement made at the two data sources.

A limited amount of original satellite information which had been digitized and recorded on magnetic tapes at the San Francisco Field Service Station and the Arctic Weather Centre was obtained and the data processed locally. A few examples of these are included in this report to show the superiority of these products over regularly-obtained photographic prints.

Data Analysis

The visual and infrared imagery were viewed in pairs (in the case of daytime observation) to determine the extent of cloud-free oceanic areas. Only such areas were considered for further examination. Cloud-free areas for nighttime imagery were determined from interpolation of two successive daytime observations, one before and the other after the observation in question. Data that presented difficulty with this interpolation on account of possible fog or low cloud formation during the night were excluded from the analysis. Areas that did not possess distinguishable surface features as a result of poor data quality, such as inadequate imagery enhancement and/or "noisy" scan-lines, etc., also were excluded from analysis.

An optical device, the Zoom Transfer Scope (Bausch and Lomb), was utilized to transfer the thermal surface features, such as an oceanic front, in the imagery, to a base chart. This device can readily reduce or enlarge imagery to an appropriate scale and its anamorphic system can compensate for geometric distortion in the imagery due to relief, earth curvature, print shrinkage, etc., thereby allowing a feature on a print to be superimposed onto a chart or map. When control points on the imagery are clearly distinguishable, such as small islands, sharp points or capes of coastline, positions of sea surface features in their general vicinity can be transferred to a base chart with an estimated accuracy of a few kilometres. In areas far removed from such control points the accuracy is expected to drop considerably, by up to an order of magnitude.

In some prints the area under study was located at the edge or corner of the prints where large distortion of the earth's surface was present. In such a case the Zoom Transfer Scope is incapable of correcting the spatial distortion. For these a transparent grid overlay supplied by NOAA and containing latitude and longitude lines was used to obtain positions of sea surface features. The error in the determination of the positions using this method may be as large as 30 km (Stevenson and Kirkham, 1977).

The original data sets recorded on magnetic tape were processed with the aid of a Hewlett-Packard 2100S minicomputer and Versatec 1100A printer-plotter. The selected parts of the digitized radiance information were printed as grey-tone variations on a printer-plotter. The image was geometrically corrected for the strong side-to-side distortion and several adjacent pixels (picture elements) were averaged to reduce effects of noise and banding. Averages of 2 x 4 and 7 x 8 pixels were made, the latter providing information averaged over an area of 6 km x 7 km. Oceanographic data collected approximately at the time of satellite observations were used to "field-calibrate" the latter. An example of the data used for calibration is shown in Figure 4 (Tabata and Gower,

1979). It is evident from these data that the satellite data are capable of yielding sea surface temperatures to within 0.5°C, a figure which is better than that of the routinely-observed satellite temperatures of ± 2°C (Brown, 1975).

Results

In Figure 5-1 through 5-52 are shown illustrations depicting areas of warm and cool waters and their associated fronts off the Pacific coast of Canada and northern U.S.A. They were interpreted from infrared satellite imagery available in photographic-print format.

As is evident from these illustrations, during spring through autumn, cooler waters were present adjacent to Vancouver Island at three locations: at the approaches to and in Juan de Fuca Strait, at the approaches to and in Queen Charlotte Strait and in the vicinity of Scott Islands (e.g. 28 April 1976 - Fig. 5-29; 31 May 1978 - Fig. 5-44; 30 July 1974 - Fig. 5-1; and 20 October 1977 - Fig. 5-42). The few sets of data for winter show that during this season the waters at these locations were warmer than in their immediate vicinity (e.g. 5 January 1979 - Fig. 5-47) except on 31 December 1977 (Fig. 5-43) when it was cooler. The contrast between the cool and warm water is most striking during summer and autumn and least in winter and spring.

The waters present along the west coast of Vancouver Island were usually cooler than those lying immediately offshore (e.g. 5 January 1979 - Fig. 5-47; 4 August 1974 - Fig. 5-3 and 20 October 1977 - Fig. 5-42). However, from time to time isolated areas of warm water occurred adjacent to the coast (e.g. 28 April 1976 - Fig. 5-29; 31 May 1978 - Fig. 5-44; and 9 September 1975 - Fig. 5-20).

Generally, the warm water that lay offshore occurred in a band of few hundred kilometres breadth at latitude 49°N (e.g. 10 September 1976 - Fig. 5-20). In one example, however, the band was as narrow as 50 km (31 December 1977 - Fig. 5-43). Landward of this band of warm water was a well-defined tongue of cool water with its source along the west coast of Vancouver Island and its leading edge directed southward. This tongue was most easily recognized during summer and autumn (e.g. 14 July 1979 - Fig. 5-52 and 9 September 1975 - Fig. 5-18).

One of the more interesting features of the sea surface temperature pattern off the coast, especially off Vancouver Island, is the presence of a number of well-defined plumes or tongues of cool water (in most cases) and of warm water with their axes lying perpendicular to the coast. They occurred during all seasons (e.g. 5 January 1979 - Fig. 5-48; 1 June 1978 - Fig. 5-45; 4 August 1974 - Fig. 5-3; and 9 September 1975 - Fig. 5-18). The separation between the axes of the tongues was typically 100 to 150 km. Some of the tongues of cool water extended seaward, intercepting Line P at Stations 3 and 4.

The cool water of Juan de Fuca Strait often spread northwestward until it finally lost its identity as it merged with the other cool water lying off Amphitrite Point (e.g. 26 August 1974 - Fig. 5-5 and 18 October 1976 - Fig. 5-32). Occasionally one branch of this water spread to northwestward while another branch backed and spread southward upon leaving the Strait (e.g. 5

January 1979 - Fig. 5-47 and 1 June 1978 - Fig. 5-45). At other times this northwestward "flow" continued to the vicinity off Amphitrite Point, then backed and "flowed" southward, intercepting Line P in the vicinity of Station 2 and occasionally Station 1 (e.g. 23 August 1975 - Fig. 5-16; 21 September 1975 - Fig. 5-26; and 20 October 1977 - Fig. 5-42).

The cool water lying off the mouth of Columbia River in winter (6 February 1976 - Fig. 5-27) and warm water there in summer (31 May and 1 June 1978 - Figs. 5-44 and 5-45; and 14 July 1979 - Fig. 5-52) is likely to be associated with the Columbia River plume.

The Queen Charlotte Sound - Hecate Strait area is usually cloudier than the southern areas and consequently there are less data available there. From the few sets of data available it appears that a large tongue of warm water with its source in the offshore region further south, intruded the area (e.g. 9 September 1975 - Fig. 5-18; 20 October 1977 - Fig. 5-42 and 14 July 1979 - Fig. 5-52). Offshore of McInnes Island the water was frequently cooler than the adjacent waters during all seasons (e.g. 5 January 1979 - Fig. 5-47; 1 June 1978 - Fig. 5-45; 29 August 1974 - Fig. 5-7 and 20 October 1977 - Fig. 5-42).

An example of the distribution of sea surface temperatures of the study area produced from the original data in digital form is shown in Figure 6. The series of numerals in Fig. 6a represent the grey-scale levels of the infrared radiation from the earth's surface. By making use of the calibration curve (Fig. 3), these levels in turn can be converted into equivalent sea surface temperature levels from which appropriate isotherms can be drawn. Fig. 6b shows the detailed sea surface temperature distribution for 9 September 1975 as derived from the data indicated in Fig. 6a. Another example from 10 September 1975 is shown in Fig. 7. Despite the fact that the above pair of observations was made from two separate spacecraft, the former by NOAA-3 and the latter by NOAA-4, the temperatures for the two consecutive days are remarkably similar.

Discussion

Only one half of the total of more than one hundred infrared satellite imagery in photographic-print format on hand possessed sufficient definition of sea surface temperature patterns required for mapping oceanic fronts. Of this some still presented difficulty with imagery interpretation due to fuzzy definition and "noisy" scan lines. The fact that some of the imagery contained featureless sea surface does not necessarily imply that features were absent. Rather, it would appear that this could be the result of the degree of enhancement made on each data set. Imagery obtained from the Climatic Data Center seems generally to be enhanced over a relatively large temperature range. This type of enhancement is not desirable for certain local areas where more effective enhancement can be made over a narrower temperature range. In the results presented in Fig. 5 it is noted that most of the fronts shown for successive days are generally consistent from day to day. On the other hand, there are some that portrayed appreciable variations such as during 26 - 28 November 1976 (Fig. 5-34 to 5-39). Some of the variations might be real, due to day to day changes in surface conditions, but others are believed to be due to the degree of enhancement made on each set which would have the effect of shifting the position of the fronts.

It was initially thought that it should be possible to delineate at least four shades of the grey-tone variations in the photographic-print imagery employing optical devices. However, this proved to be more difficult than was originally assumed. For most, only two shades could be delineated properly. In contrast to this, with imagery that had undergone enhancement to suit local conditions it was possible to differentiate at least six shades of the grey-tone variations, as has been possible for the data of 14 July 1979 (Fig. 5-52).

The few examples of detailed sea surface temperatures obtained from the analysis of raw data demonstrate the effectiveness of using original data to map local sea surface temperature patterns. The remarkable similarity between the patterns obtained from NOAA-3 during its nighttime pass of 9 September 1975 (Fig. 6b) and that derived from NOAA-4 during its daytime pass of 10 September 1975 (Fig. 7) is an indication of its effectiveness over patterns derived from routinely-obtained imagery from the data centre.

The imagery revealed a variety of features in the distribution of sea surface temperatures off the coast upon which some comments can be made.

The occurrence of cool water along the Pacific coast of North America during the summer months is usually attributed to the effect of upwelling (Sverdrup et al, 1942). The northerly winds that prevail along the Pacific coast during spring through autumn result in the divergence of surface water adjacent to the coast as a result of the offshore Ekman transport. In order to compensate for the surface offshore drift, cold and saline water is upwelled from greater depth. Off Oregon upwelling can occur as soon as early spring but off the Pacific coast of Canada it does not appear until late spring (Bakun, 1973). Studies conducted over the continental shelf of Oregon indicate that the region of upwelling is restricted to a very narrow band of approximately 10 km from the edge of the coast (Halpern, 1974; Moores et al, 1976). For the mean oceanographic conditions over the continental shelf off Vancouver Island the Rossby baroclinic radius of deformation is approximately 40 km; consequently, the region of upwelling here is likely to extend further offshore (Yoshida, 1955).

The frequent occurrence of a band of cool water adjacent to Vancouver Island and the Washington-Oregon coast, as determined from satellite imagery, can in many cases, be explained in terms of upwelling. For example, the persistent occurrence of cool water during 30 July - 5 August 1974 (Figs. 5-1 to 5-4) is almost certainly due to the effect of upwelling as the upwelling indices for the area were favourable during the one month between late July and late August (Bakun, in preparation). During other periods upwelling conditions were not as persistent for extended duration. Such were conditions during late August and September 1974. The rather "spotty" occurrence of cool water adjacent to the coast during this period (26-29 August 1974 - Figs. 5-5 to 5-7; 10-13 September 1974 - Figs. 5-8 to 5-11; and 19-20 September 1974 - Figs. 5-12 to 5-14) is probably a reflection of irregular upwelling along the coast. Some of the imagery showed that, even when upwelling condition was favourable, as indicated by the indices for latitude 48°N, longitude 125°W and latitude 51°N, longitude 131°W, the band of cool water did not extend continuously from Vancouver Island to the Oregon coast (28 July 1975 - Fig. 5-15; 23 August 1975 - Fig. 5-16; 8-12 September 1975 - Figs. 5-17 to 5-22;

and 18-21 September 1975 - Figs. 5-23 to 5-26). The reason for this discrepancy may be attributed either to the indices not being representative for the local area or else to certain areas having experienced local heating.

The occurrence of cool water along the coast during the winter (31 December 1977 - Fig. 5-43; 5-7 January 1979 - Figs. 5-47 to 5-49 and 21 January 1979 - Fig. 5-50) is unlikely to be due to the upwelling effect. For the case of 31 December 1977, it may be due to cooling from excessive heat loss to the atmosphere that was associated with the local atmospheric circulation at that time. Starting on 29 December very cold continental air was blowing offshore for more than a week (Atmospheric Environment Service, private communication). In such a situation it can be assumed that the largest cooling over water occurs closest to the land. It is also possible that mist, which might give misleading sea surface temperature in the infrared imagery, could have formed over the water, but none of the coastal weather stations reported it. For the other two periods in January 1979, cooling due to heat loss is also suspected as upwelling condition was not favourable during these periods (Bakun, in preparation).

The cool water associated with the tongues has lower salinity than does the adjacent water (Tabata and Gower, 1979) and therefore can be considered as the water that originated near the coast. This would imply that the cool, brackish coastal waters are advected seaward as relatively narrow jets rather than in a broader diffused flow.

The cool waters that are present during spring through autumn and warm waters there during winter at the approaches to and in Juan de Fuca Strait and Queen Charlotte Strait and in the vicinity of Scott Islands can be attributed to tidally-induced vertical mixing. These areas are characterized by the presence of strong tidal currents with their speed exceeding 1½ m/sec at certain parts within them (Environment Canada, 1976). Even in areas where tidal currents are not as strong, there appears to be recognizable tidal influence on sea surface temperatures observed in inland seaways due to tidal mixing (Herlinveaux, 1957). During late spring through early autumn the coastal waters are generally warmer at the surface than immediately below and vice-versa in winter (Herlinveaux and Giovando, 1969). The consequence of tidal mixing would then be to reduce the surface temperature during spring through autumn and to raise it during winter. It is to be noted that wind mixing could achieve the same results also.

Vertical mixing capable of overcoming stratification of coastal waters need not be restricted only to waters adjacent to land. Indeed, such mixing can be effective in more open waters of the continental shelf if the current speeds there are sufficiently large. In this regard, Simpson and Hunter (1974) have proposed that the transition between stratified and mixed regimes can be represented by a mixing parameter based on the ratio of potential energy required for complete vertical mixing to the rate of dissipation of energy of the tidal currents. Where the buoyancy term remains relatively constant the parameter simplifies to H/U^3, where H is the water depth and U is the amplitude of the tidal current. This, of course, assumes that other currents are of minor importance. For the continental seas off the United Kingdom, complete vertical mixing was found to occur when the value of this parameter was less than 50-100 sec^3/m^2.

We can apply this criterion if we assume comparable tidal friction and water column stability for the waters off the Canadian coast. Over the continental shelf off Vancouver Island, the amplitude of the tidal current is about 50 cm/sec, based on only one series of observations off Tofino (Huyer, et al, 1976). From a very limited number of observations in Queen Charlotte Sound-Hecate Strait (Canadian Joint Committee on Oceanography, 1955) it would appear that the amplitude of the tidal currents herein is of the same order of magnitude as off Vancouver Island. Given an amplitude of 50 cm/sec, only areas with depth less than approximately 10 m would experience complete mixing upon applying the criterion. Since very little area of the shelf off Vancouver Island and Queen Charlotte Sound-Hecate Strait is as shallow as 10 m, tidal currents with the above amplitude would be ineffective in destroying the stratification necessary to lower the surface temperature in summer and raise it in winter. However, if the tidal amplitude had been underestimated and if we can assume that the amplitude can be 50% greater than quoted above, areas with depth less than 30-40 m should experience complete mixing, even in the absence of other currents, or of wind or convective mixing. Such an area is present along the western half of northern Hecate Strait and a small area (15 km x 20 km) located about 80 km south of McInnes Island. The occasional occurrence of cool water along the western side of Hecate Strait (e.g. 19-20 September 1974 - Figs. 5-12 to 5-14 and 9 September 1975 - Fig. 5-18) could have been due to tidally-induced vertical mixing. No evidence of cool water in summer has been found for the area south of McInnes Island. Probably the tidal current there is not sufficiently strong to overcome stratification.

The presence of cool water at the approaches to Juan de Fuca Strait can be explained on the basis of other than wind-induced upwelling and tidal mixing mentioned earlier. It can also be a consequence of local upwelling associated with the behaviour of the seaward flow of Juan de Fuca water (Tully, 1942). This follows from the assumption that the seaward flow is in the form of a "wake stream" or a jet. This stream, in northern hemisphere, should veer to the right and a counter current should occur along the left side of the wake stream (Rossby, 1937-38). Such a current system could result in a formation of a zone of upwelling between these two currents.

In order to ascertain which processes are responsible for the occurrence of cool water at the approaches, other supporting information such as salinity would be required. As has been shown recently (Tabata and Gower, 1979), only with salinity data was it possible to interpret the cool water there on 9-10 September 1975 (Figs. 5-19 and 5-20) as being due to local upwelling.

The Columbia River water, before entering the ocean, is warmer than the ocean water at the river mouth in the summer and cooler during the winter, by a few Celsius degrees in both cases (National Ocean Survey, 1970). Accordingly, during these seasons at least, the Columbia River plume should be clearly distinguishable from the oceanic waters. Yet, of the 27 images that included the area off the mouth of Columbia River only a few indicated its presence with any certainty. The reason for its absence in the imagery for the summer months is not clear. One possible explanation is that the warm river water upon entering the ocean is rapidly cooled by mixing with the cool, upwelled waters along the coast. It is also possible that the degree of enhancement was insufficient to delineate the plume from the surrounding waters.

During the winter the Columbia River plume appears to flow northward in a

narrow band of few tens of kilometres off the coast (Budinger et al, 1964). Accordingly, even if the plume water were cooler than the surrounding waters it will be difficult to delineate the plume from the other coastal waters that might have been cooled by other means, such as heat loss to the atmosphere. The band of cool water present along the Washington coast during 31 December 1977 (Fig. 5-43) and 5 January 1979 (Fig. 5-48), at least for the portion close to the river mouth, might have been the plume but from temperature data alone it will be difficult to ascertain this. Salinity data should be able to resolve this question.

The occurrence of a number of tongues of cool or warm water with their axes frequently oriented perpendicular to the coast and spaced regularly (e.g. Fig. 5-18) suggests the presence of wave-like phenomena. Mysak (1977) has examined the above feature and proposed that the observed pattern may be due to the baroclinic instability of the California Undercurrent. Detailed analysis of satellite data obtained during the two days in early January 1979 has provided further evidence that the cellular pattern evident in the satellite imagery is consistent with the model of baroclinically unstable waves (Emery and Mysak, 1979). Whether or not such pattern can definitely be attributed to this effect would require additional supporting data.

Conclusions

Only one half of a set of satellite imagery obtained from the Climatic Data Center could be interpreted adequately. The lack of features of the sea surface does not necessarily imply that the sea surface was featureless. Instead, the absence of features is almost certainly to be due to the degree of enhancement applied to each set of data. Unless the degree of enhancement is consistent from image to image it is even possible to misinterpret the sequence of features; for example, difference in enhancement can shift positions of some of the less well-defined fronts. With the regularly-obtained imagery from the Climatic Data Center generally only two shades of the grey-scale level could be delineated with a conventional optical device. On the other hand, it is possible to differentiate at least six shades of the grey-scale level in a suitably-enhanced image. Due to difficulty associated with enhancement, daily monitoring of movement of fronts from successive imagery could be misleading. For any detailed analysis of sea surface temperature pattern, especially for the tracking of the movement of fronts and eddies in local areas, such as the continental shelf, analysis of original data is preferable as the enhancement can be made consistent for any sequence of imagery or it can be varied to suit the task on hand. For coastal waters the use of satellite imagery alone to interpret oceanographic processes can be misleading as there may be a number of processes that may change water temperature. Other properties of water, such as salinity would be required to validate the interpretation.

The oceanic region off the Pacific coast of Canada is frequently cloud covered. For about 90% of the time either clouds or fog are present. As a result useful infrared satellite coverage over the area is limited. However, despite this, from the examination of satellite imagery obtained over the past five years it has been possible to get some better insight into the nature of circulation off the coast. With improved access to the original satellite data it should be possible to use the data effectively, in "real time", not only as aids to the study of oceanographic processes and events

and even in the planning of oceanographic surveys, but also as a guide to commercial fishermen searching fishing grounds and to those involved in coastal pollution study and pollutant cleanup.

Acknowledgements

We are indebted to Messrs. L. Breaker and E. Daghir of the San Francisco Field Service Station of the National Environmental Satellite Service (NOAA) and Messrs. D. Fraser and G. Schram of the Arctic Weather Centre of the Atmospheric Environment Service for providing us with well-enhanced satellite imagery and also for making arrangements to provide us with the original data received from the satellites; to Mr. D. Faulkner of the Atmospheric Environment Service (Vancouver, B.C.) for giving local weather conditions for certain periods when presence of mist or fog was suspected and to Mr. Dawson Truax for processing the original data. We further wish to thank Dr. J.F.R. Gower for his helpful comments and for reviewing the manuscript.

References

Bakun, A., 1973: Coastal upwelling indices, west coast of North America, 1946-71. NOAA Tech. Rept. NMFS SSRF-671, National Marine Fisheries Service, NOAA, U.S. Dept. Commerce, Seattle, Washington, 102 pp.

Bakun, A., in preparation: Daily and weekly upwelling indices, west coast of North America, 1974-79. Unpublished manuscript report, NOAA/NMFS Pacific Environmental Group, Monterey, California, 90 pp.

Brown, S.R., 1975: SST quarterly report, April-June 1975. Unpublished manuscript report, NOAA/NESS, U.S. Dept. Commerce, Wash., D.C., 2 pp.

Budinger, T.R., L.K. Coachman and C.A. Barnes, 1964: Columbia River effluent in the northeast Pacific Ocean, 1961, 1962; Selected aspects of physical oceanography. Univ. Wash., Dept. Oceanogr. Tech. Rept. No. 99 (ref. M63-18). 78 pp.

Canadian Joint Committee on Oceanography, 1955: Data Record, Current measurements, Hecate Strait 1954. Manuscript Rept., Pacific Oceanographic Group, Fish. Res. Bd. Canada, Nanaimo, B.C., 54 pp.

Emery, W.J. and L.A. Mysak, 1979: Dynamic interpretation of satellite sensed thermal features off Vancouver Island. Submitted to the J. Phys. Oceanogr.

Environment Canada, 1976: Sailing directions British Columbia coast (South portion). Volume 1, tenth edition, Fisheries and Marine Service, Victoria, B.C., 339 pp.

Gotthardt, G.A. and G.J. Potocsky, 1974: Life cycle of a Gulf Stream anticyclonic eddy observed from several oceanographic platforms. J. Phys. Oceanogr., 4, 131-134.

Halpern, D., 1974: Variations in the density field during coastal upwelling. Tethys, 6, 363-374.

Hanzawa, M., 1979: Preparation of sea-surface temperature charts based on data from GMS. Papers submitted to the Joint IOC/WMO Seminar on oceanographic products and the IGOSS data processing and services system, Intergovernmental Oceanographic Commission, Workshop report no. 17 - supplement, 175-179.

Herlinveaux, R.H., 1957: On tidal currents and properties of the sea water along the British Columbia coast. Prog. Rept. of the Pacific Coast Stations, Fish. Res. Bd. Canada, No. 18, 7-9.

Herlinveaux, R.H. and L.F. Giovando, 1969: Some oceanographic features on the inside passage between Vancouver Island and the mainland of British Columbia. Tech. Rept. 142, Fish. Res. Bd. Canada, 48 pp.

Huyer, A., J. Gagnon, and S. Huggett, 1976: Observations from current meters moored over the continental shelf off Vancouver Island, 28 November 1974 to 8 April, 1975, and related oceanographic and meteorological data. Tech. Rept. No. 4, Marine Environmental Data Service, Ottawa, 54 pp.

Jurick, F., 1977: Space age technology makes job easier for west coast fishermen. Sea Grant '70, 1(6), 3-5.

Koffler, R., 1976: Digital processing of NOAA's very high resolution radiometer (VHRR) data. International Astronautical Federation, 27th. Congress, Ref. No. 76-209, 7 pp.

La Violette, P.E. and P.L. Chabot, 1968: Nimbus II satellite sea surface temperature vs. historical data in a selected region, a comparative study. Deep Sea Res., 15, 617-622.

La Violette, P.E., 1974: A satellite-aircraft thermal study of the upwelled waters off Spanish Sahara. J. Phys. Oceanogr., 4, 676-684.

Moores, C.N.K., C.A. Collins and R.L. Smith, 1976: The dynamic structure of the frontal zone in the coastal upwelling region off Oregon. J. Phys. Oceanogr., 6, 3-21.

Mysak, L., 1977: On the stability of the California Undercurrent off Vancouver Island. J. Phys. Oceanogr., 7, 904-917.

National Ocean Survey, 1970: Surface water temperature and density, Pacific Coast, North and South America and Pacific Ocean Islands. NOS Publication 31-3, third edition, NOAA, 88 pp.

Noel, J.A.H., 1979: On-line use of infrared data from the geostationary satellite ("Meteosat") for both scientific and industrial purposes. Papers submitted to the Joint IOC/WMO Seminar on Oceanographic products and IGOSS data processing and services system, Intergovernmental Oceanographic Commission, Workshop report no. 17-supplement, 319-322.

Pichel, W.G., F.E. Kniskern and R.L. Brower, 1979: NOAA/NESS operational satellite oceanographic products. Papers submitted to the Joint IOC/WMO Seminar on Oceanographic products and the IGOSS data processing and services system, Intergovernmental Oceanographic Commission, Workshop report No. 17-supplement, 369-389.

Rossby, C.G. 1937-38: On the mutual adjustment of pressure and velocity distributions in certain simple current systems. J. Mar. Res., 1, 15-28.

Simpson, J.H. and J.R. Hunter, 1974: Fronts in the Irish Sea. Nature, 25, 404-406.

Stevenson, N.R. and R.G. Kirkham, 1977: Coastal zone and open ocean observations from NOAA satellite very high resolution radiometers. Final Report, Inter-American Tropical Tuna Commission, La Jolla, California, 88 pp.

Stumpf, H.G., 1975: Satellite detection of upwelling the Gulf of Tehuantepec, Mexico. J. Phys. Oceanogr., 5, 388-393.

Sverdrup, H.U., R.H. Fleming and M.W. Johnson, 1942: The oceans, their physics, chemistry and general biology. Prentice-Hall Inc., New York, 1087 pp.

Tabata, S. and J.F.R. Gower, 1979: A comparison of ship and satellite measurements of sea surface temperatures off the Pacific coast of Canada. Submitted to J. Geophys. Res.

Tully, J.P., 1942: Surface non-tidal currents in the approaches to Juan de Fuca Strait. J. Fish. Res. Bd., Canada, 5, 398-409.

Vukovich, F.M., 1974: The detection of nearshore eddy motion and wind-driven currents using NOAA 1 sea temperature data. J. Geophys. Res., 79, 853-864.

Wyrtki, K., 1977: Advection in the Peru Current as observed by satellite. J. Geophys. Res., 82, 3939-3943.

Yoshida, K. 1955. Coastal upwelling off the California coast. Records of Oceanogr. Works in Japan, 2, 8-20.

List of Figures

Figure 1. Chart showing general area of study. The weathership observational line, Line P, and associated station numbers are indicated.

Figure 2. Very high resolution radiometer (VHRR) NOAA-3 infrared imagery of western Canada and U.S.A. and of the waters off their Pacific coast, based on data taken during the nighttime overpass at 0339 GMT, 9 September 1975. The imagery has been enhanced to accentuate sea surface thermal features. The lighter and darker tones of the ocean are associated with cooler and warmer waters, respectively.

Figure 3. Very high resolution radiometer (VHRR) NOAA-4 satellite imagery of western Canada and U.S.A. and of the waters off their Pacific coast, based on data taken during the daytime overpass at 1709, GMT, 10 September 1975:

(a) Visual imagery, showing among other things, the cloudy and cloudfree areas. The white and black represents respectively the light and dark colour of the earth's surface.

(b) Infrared imagery (enhanced). The lighter and darker areas of the ocean are associated with cooler and warmer waters, respectively.

Figure 4. Plots of satellite-derived sea surface temperatures against shipborne and shore-station sea surface temperature. The satellite data were taken at 0339 GMT, 9 September 1975; shipborne and shore-station data were collected within one day of the satellite observation. The location of shore-stations (Race Rocks, Amphitrite Point, Kains Island and Pine Island) is shown in Fig. 1. Shipborne data were collected near latitude 48°N and within 500 km of the coast.

Figure 5. Chart of the ocean off the Pacific coast of Canada and northern U.S.A. showing areas of relatively warm and cool waters and the fronts associated with them, as deduced from satellite imagery. The continuous and dashed lines delineating the warm and cool water represent strong and weak fronts, respectively. The blank space can be considered either as an area of no data coverage or where the definition of features was poor. Each illustration has annotated data: time (hours, minutes, seconds, GMT), date, orbit number and spacecraft identification.

Figure 5-1.	17:23:00	30 July 1974	3279	NOAA-3
Figure 5-2.	17:47:20	01 August 1974	3322	NOAA-3
Figure 5-3.	17:26:15	04 August 1974	3359	NOAA-3

Figure 5-4.	18:32:00	05 August 1974	3372	NOAA-3
Figure 5-5.	18:05:00	26 August 1974	3632	NOAA-3
Figure 5-6.	17:20:00	27 August 1974	3644	NOAA-3
Figure 5-7.	17:44:00	29 August 1974	3669	NOAA-3
Figure 5-8.	18:10:59	10 September 1974	3818	NOAA-3
Figure 5-9.	17:30:00	11 September 1974	3830	NOAA-3
Figure 5-10.	18:39:40	12 September 1974	3843	NOAA-3
Figure 5-11.	17:54:40	13 September 1974	3855	NOAA-3
Figure 5-12.	17:13:45	19 September 1974	3929	NOAA-3
Figure 5-13.	19:03:00	19 September 1974	3930	NOAA-3
Figure 5-14.	18:19:00	20 September 1974	3942	NOAA-3
Figure 5-15.	18:56:57	28 July 1975	3194	NOAA-4
Figure 5-16.	17:53:20	23 August 1975	3519	NOAA-4
Figure 5-17.	17:14:01	08 September 1975	3719	NOAA-4
Figure 5-18.	03:38:36	09 September 1975	8322	NOAA-3
Figure 5-19.	18:08:01	09 September 1975	3732	NOAA-4
Figure 5-20.	17:09:00	10 September 1975	3744	NOAA-4
Figure 5-21.	17:05:00	12 September 1975	3769	NOAA-4
Figure 5-22.	18:52:34	12 September 1975	3770	NOAA-4
Figure 5-23.	18:39:25	18 September 1975	3845	NOAA-4
Figure 5-24.	17:44:00	19 September 1975	3857	NOAA-4
Figure 5-25.	18:37:36	20 September 1975	3870	NOAA-4
Figure 5-26.	17:39:36	21 September 1975	3882	NOAA-4
Figure 5-27.	17:43:00	06 February 1976	5610	NOAA-4
Figure 5-28.	17:44:00	27 April 1976	11192	NOAA-3
Figure 5-29.	18:52:31	28 April 1976	11205	NOAA-3
Figure 5-30.	17:38:01	19 September 1976	644	NOAA-5

Figure 5-31.	18:01:01	07 October 1976	867	NOAA-5
Figure 5-32.	03:41:35	18 October 1976	996	NOAA-5
Figure 5-33.	17:42:00	18 October 1976	1003	NOAA-5
Figure 5-34.	04:08:17	26 November 1976	1479	NOAA-5
Figure 5-35.	18:13:00	26 November 1976	1486	NOAA-5
Figure 5-36.	03:26:00	27 November 1976	1491	NOAA-5
Figure 5-37.	17:29:00	27 November 1976	1498	NOAA-5
Figure 5-38.	04:37:00	28 November 1976	1504	NOAA-5
Figure 5-39.	18:38:00	28 November 1976	1511	NOAA-5
Figure 5-40.	17:48:01	11 September 1977	5063	NOAA-5
Figure 5-41.	04:18:36	12 October 1977	5440	NOAA-5
Figure 5-42.	14:17:11	20 October 1977	5539	NOAA-5
Figure 5-43.	17:53:49	31 December 1977	6437	NOAA-5
Figure 5-44.	17:47:01	31 May 1978	8306	NOAA-5
Figure 5-45.	04:49:00	01 June 1978	8312	NOAA-5
Figure 5-46.	17:25:00	03 June 1978	8343	NOAA-5
Figure 5-47.	04:04:59	05 January 1979	1010	NOAA-5
Figure 5-48.	18:01:27	05 January 1979	1017	NOAA-5
Figure 5-49.	04:33:13	07 January 1979	1035	NOAA-5
Figure 5-50.	17:55:09	21 January 1979	1215	NOAA-5
Figure 5-51.	23:06:06	11 July 1979	3829	TIROS-N
Figure 5-52.	22:33:47	14 July 1979	3871	TIROS-N

Figure 6. Sea surface temperatures derived from original infrared satellite data of 0330 GMT, 9 September 1975 (these data were used by NOAA to produce the imagery shown in Figure 2).

(a) Grey-scale digitized imagery. The numerals represent the averages of 7 x 8 pixels (equivalent to average temperatures of an area 6 km x 7 km), the lower and higher numerals representing the lower and higher temperatures, respectively. The area covered in this illustration is shown as the small bordered portion in Fig. 2.

Figure 6. (continued) (b) Isotherms (^{o}C) constructed from data shown in Fig. 6a. The dashed lines over the ocean represent the cruise track of CFAV *Endeavour* (19 August - 10 September 1975).

Figure 7. Sea surface temperatures (^{o}C) derived from original infrared satellite data of 1709 GMT, 10 September 1975 (these data were used by NOAA to produce the imagery shown in Fig. 3).

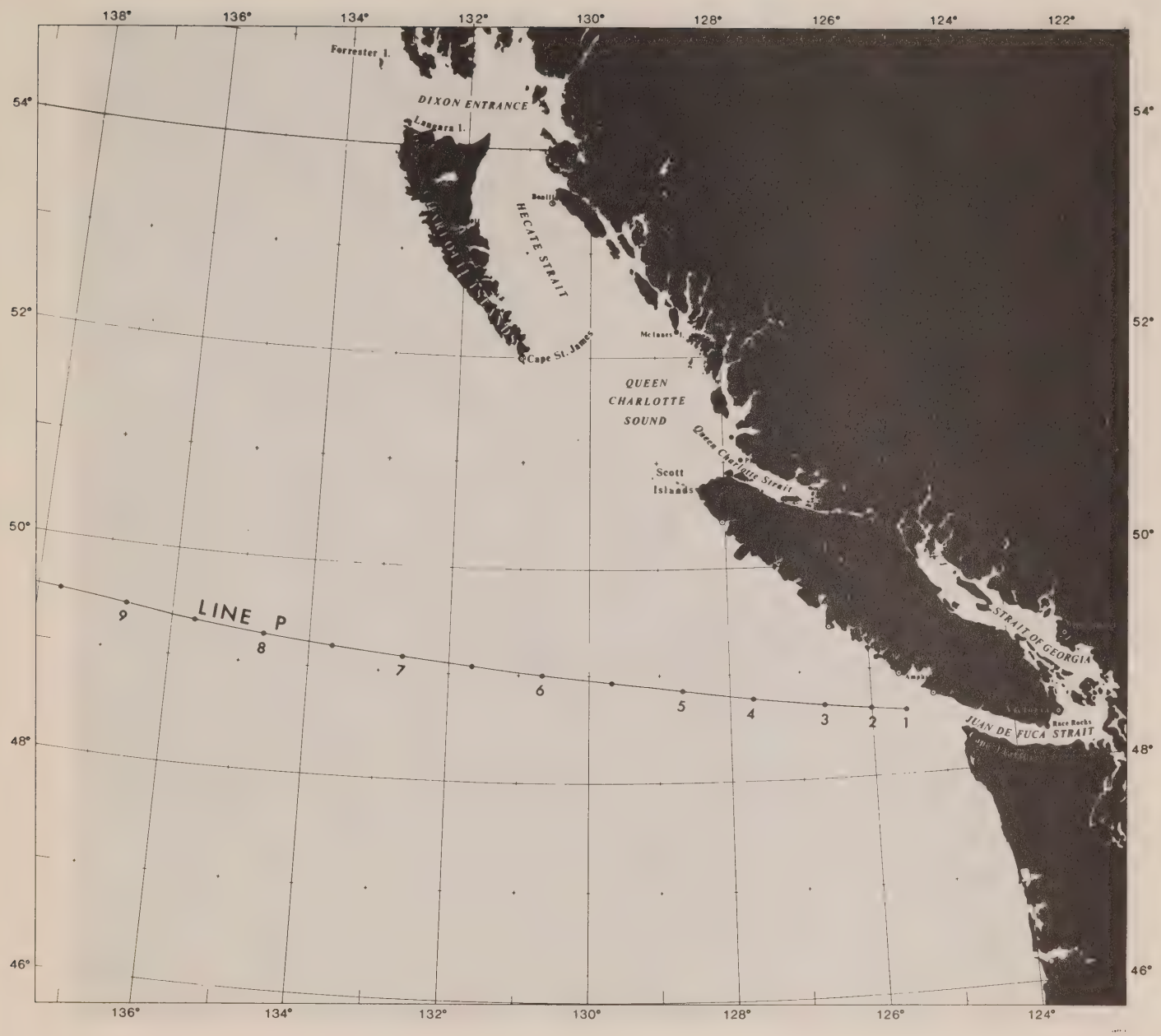

Figure 1. Chart showing general area of study. The weathership observational line, Line P, and associated station numbers are indicated.

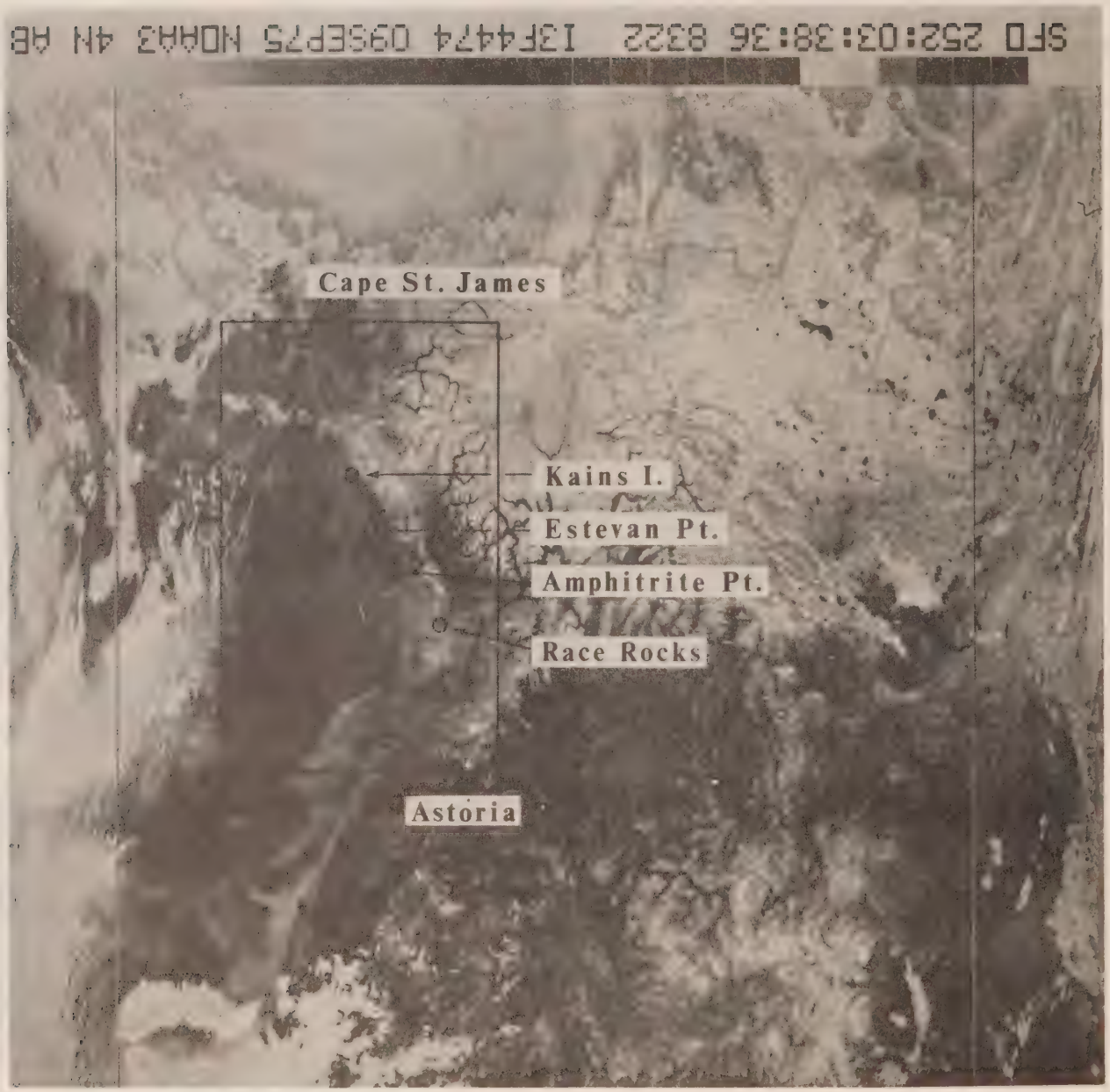

Figure 2. Very high resolution radiometer (VHRR) NOAA-3 infrared imagery of western Canada and U.S.A. and of the waters off their Pacific coast, based on data taken during the nighttime overpass at 0339 GMT, 9 September 1975. The imagery has been enhanced to accentuate sea surface thermal features. The lighter and darker tones of the ocean are associated with cooler and warmer waters, respectively.

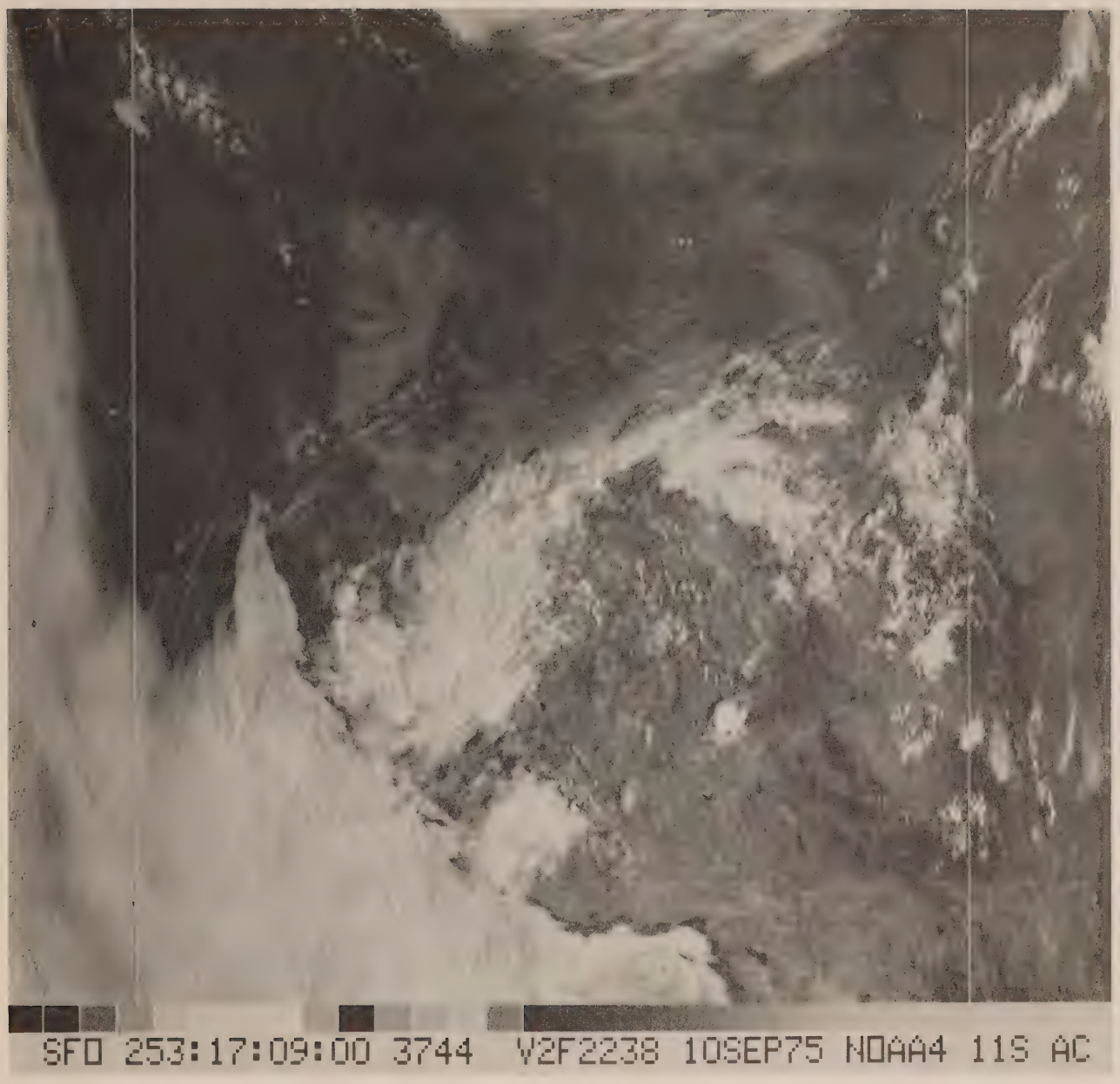

Figure 3. Very high resolution radiometer (VHRR) NOAA-4 satellite imagery of western Canada and U.S.A. and of the waters off their Pacific coast, based on data taken during the daytime overpass at 1709, GMT, 10 September 1975:

(a) Visual imagery, showing among other things, the cloudy and cloudfree areas. The white and black represents respectively the light and dark colour of the earth's surface.

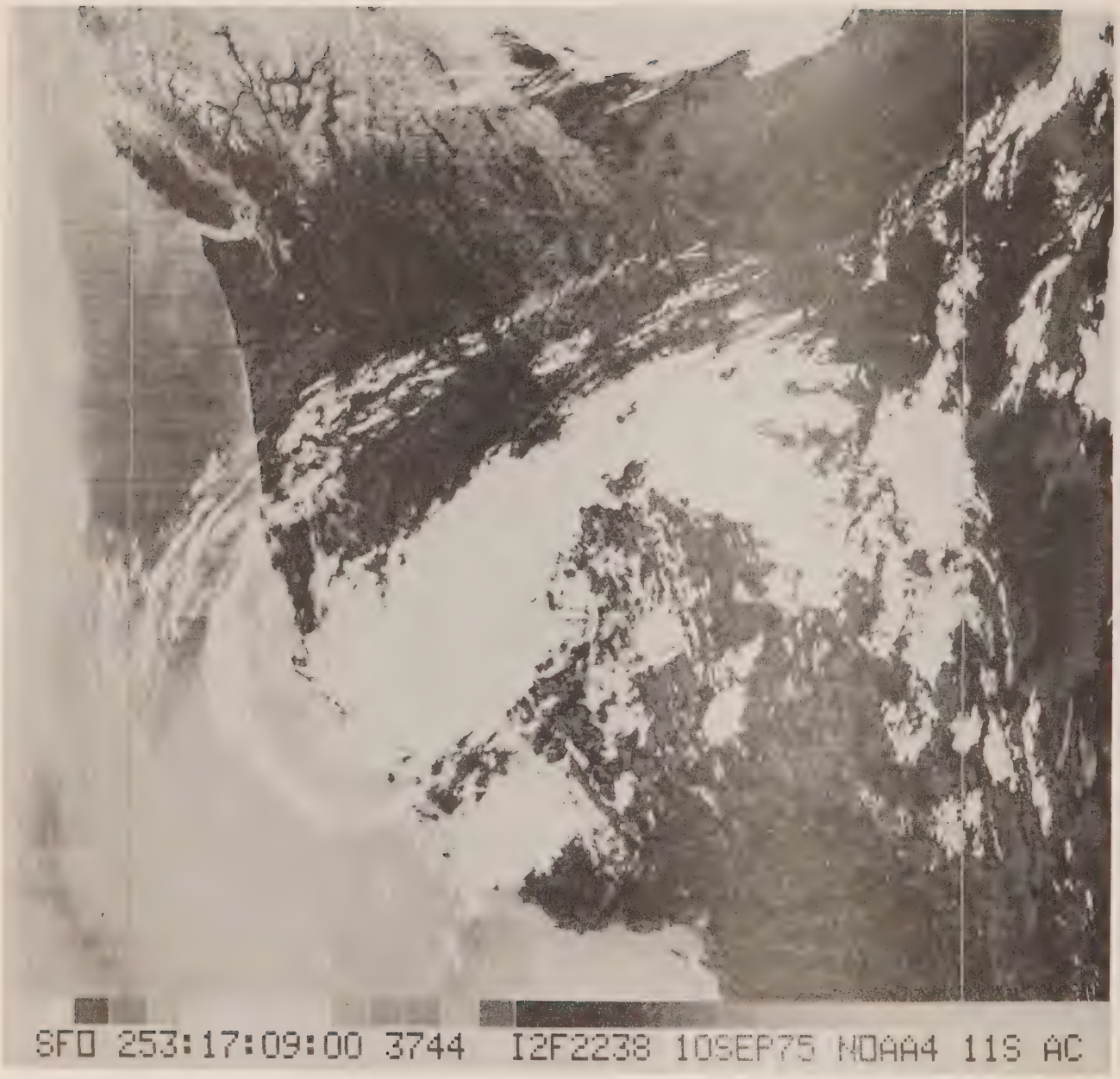

Figure 3. Very high resolution radiometer (VHRR) NOAA-4 satellite imagery of western Canada and U.S.A. and of the waters off their Pacific coast, based on data taken during the daytime overpass at 1709, GMT, 10 September 1975:

(b) Infrared imagery (enhanced). The lighter and darker areas of the ocean are associated with cooler and warmer waters, respectively.

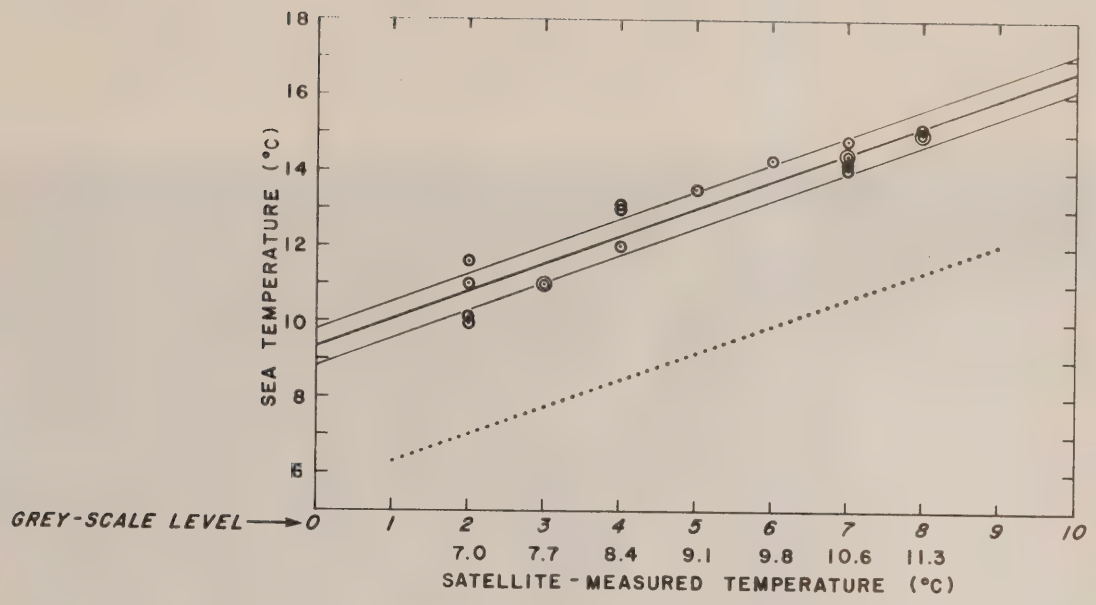

Figure 4. Plots of satellite-derived sea surface temperatures against shipborne and shore-station sea surface temperature. The satellite data were taken at 0339 GMT, 9 September 1975; shipborne and shore-station data were collected within one day of the satellite observation. The location of shore-stations (Race Rocks, Amphitrite Point, Kains Island and Pine Island) is shown in Fig. 1. Shipborne data were collected near latitude 48°N and within 500 km of the coast.

Figure 5. Chart of the ocean off the Pacific coast of Canada and northern U.S.A. showing areas of relatively warm and cool waters and the fronts associated with them, as deduced from satellite imagery. The continuous and dashed lines delineating the warm and cool water represent strong and weak fronts, respectively. The blank space can be considered either as an area of no data coverage or where the definition of features was poor. Each illustration has annotated data: time (hours, minutes, seconds, GMT), date, orbit number and spacecraft identification.

FIGURE 5-1. 17:23:00 30 JULY 1974 3279 NOAA 3

FIGURE 5-2. 17:47:20 01 AUGUST 1974 3322 NOAA 3

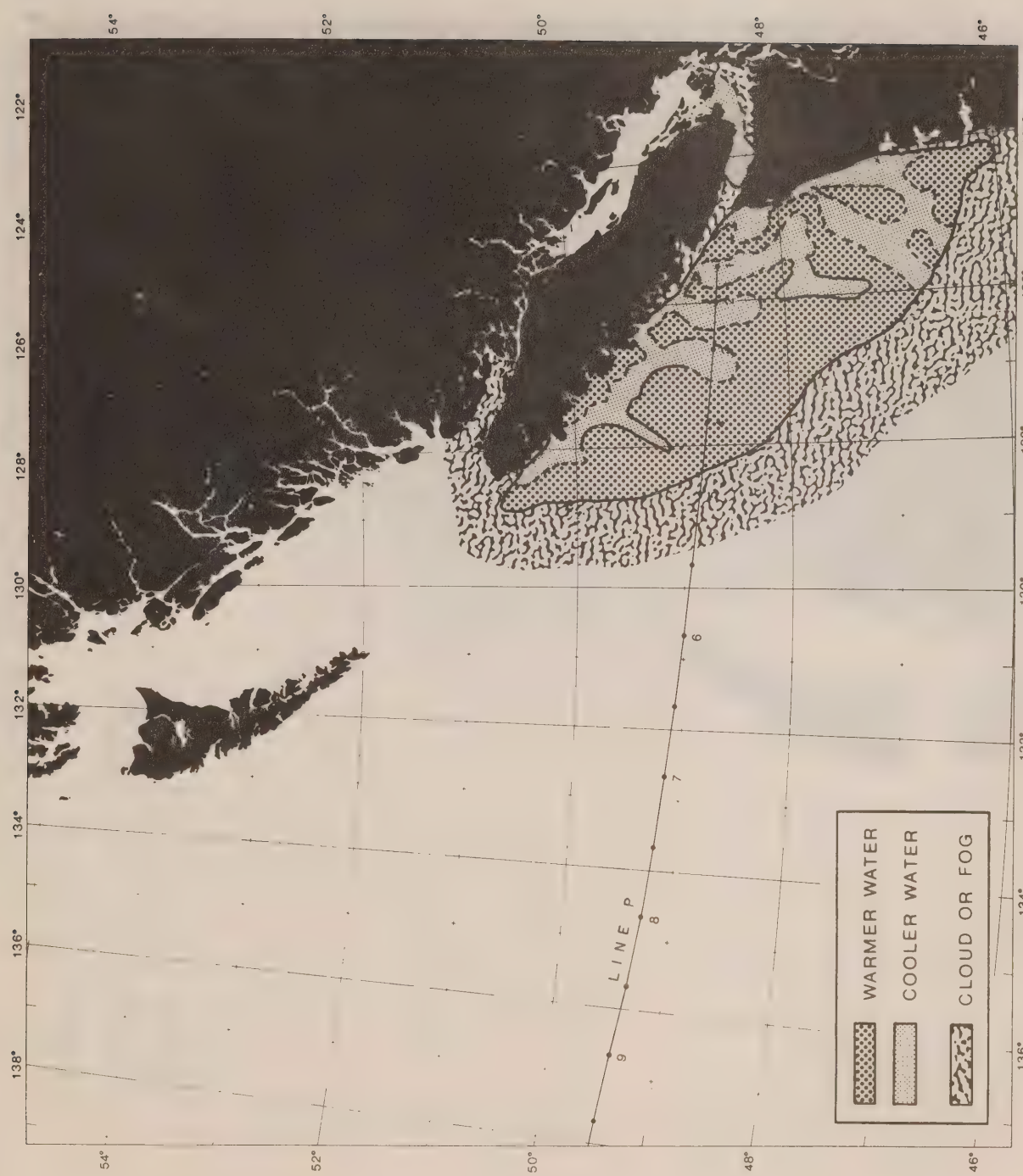

FIGURE 5-3. 17:26:15 04 AUGUST 1974 3359 NOAA 3

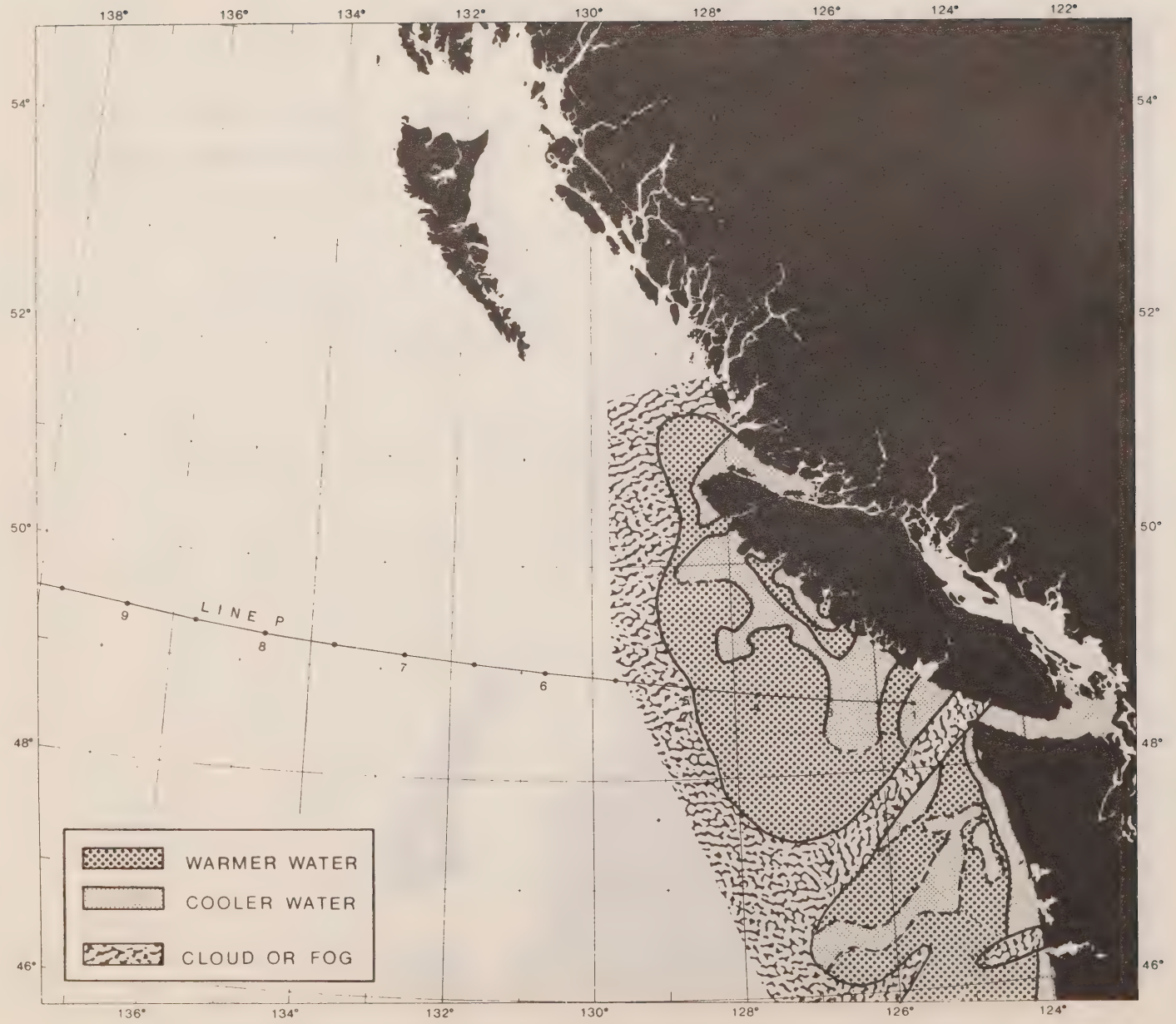

FIGURE 5-4. 18:32:00 05 AUGUST 1974 3372 NOAA 3

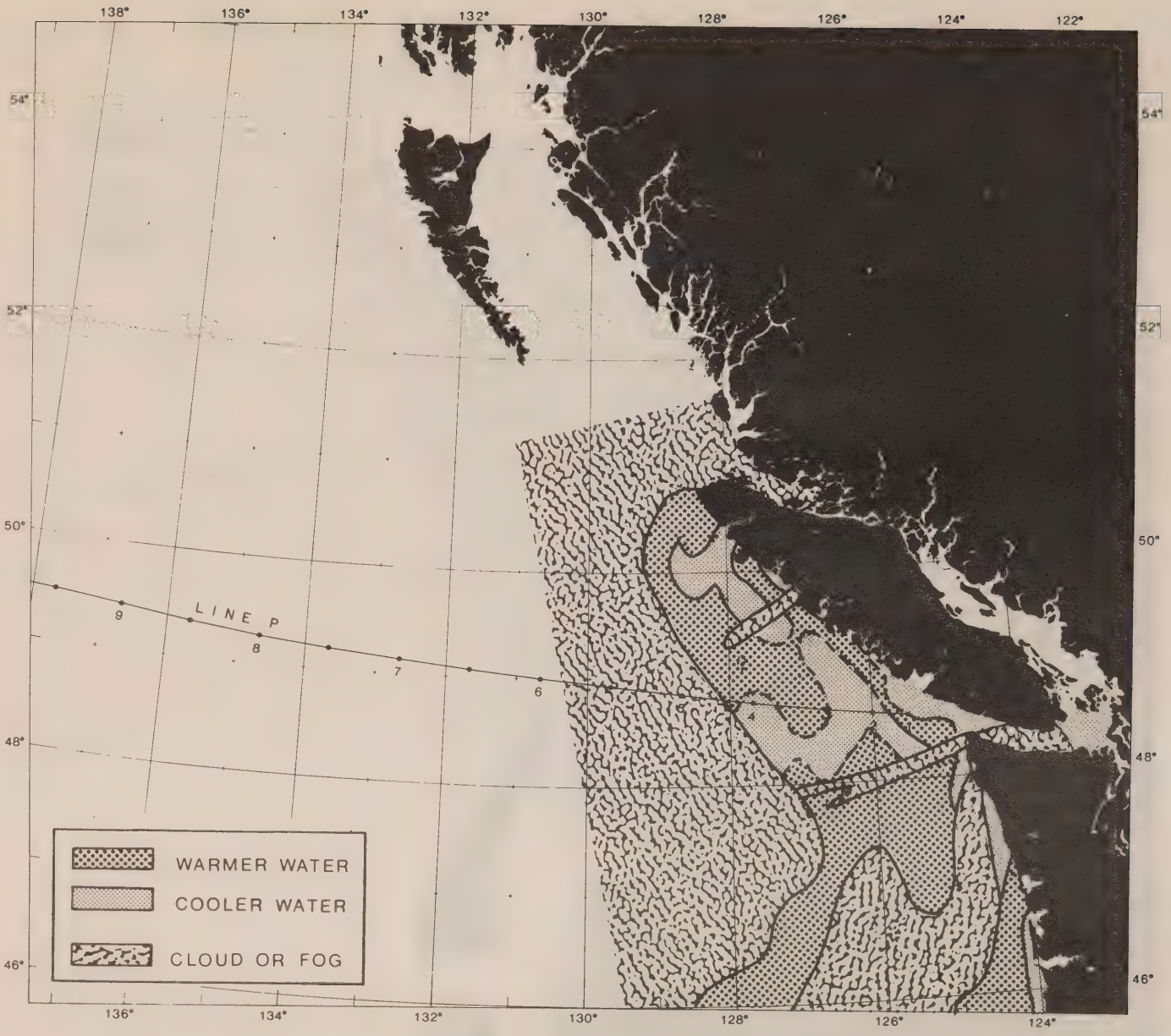

FIGURE 5-5. 18:05:00 26 AUGUST 1974 3632 NOAA 3

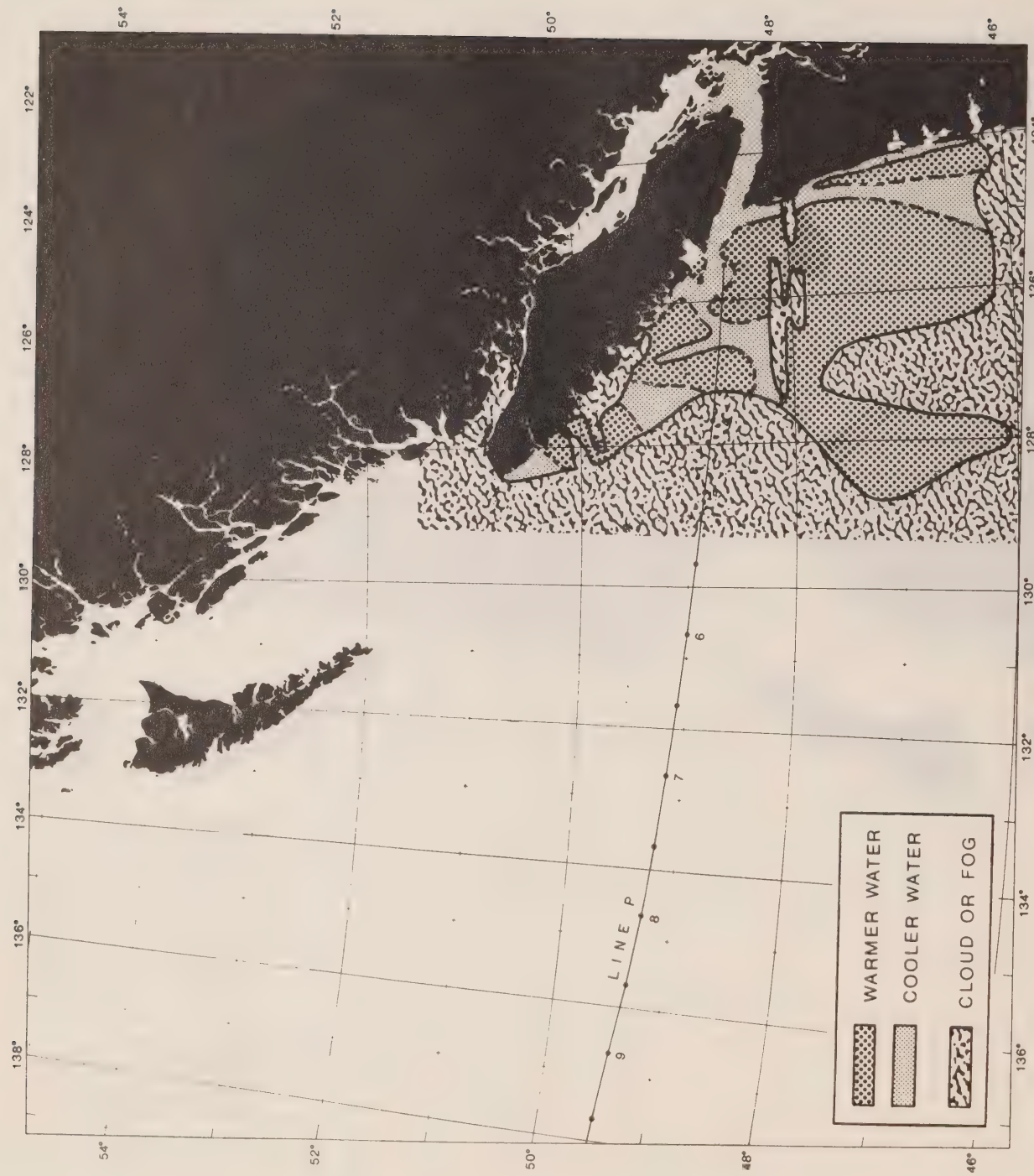

FIGURE 5-6. 17:20:00 27 AUGUST 1974 3644 NOAA 3

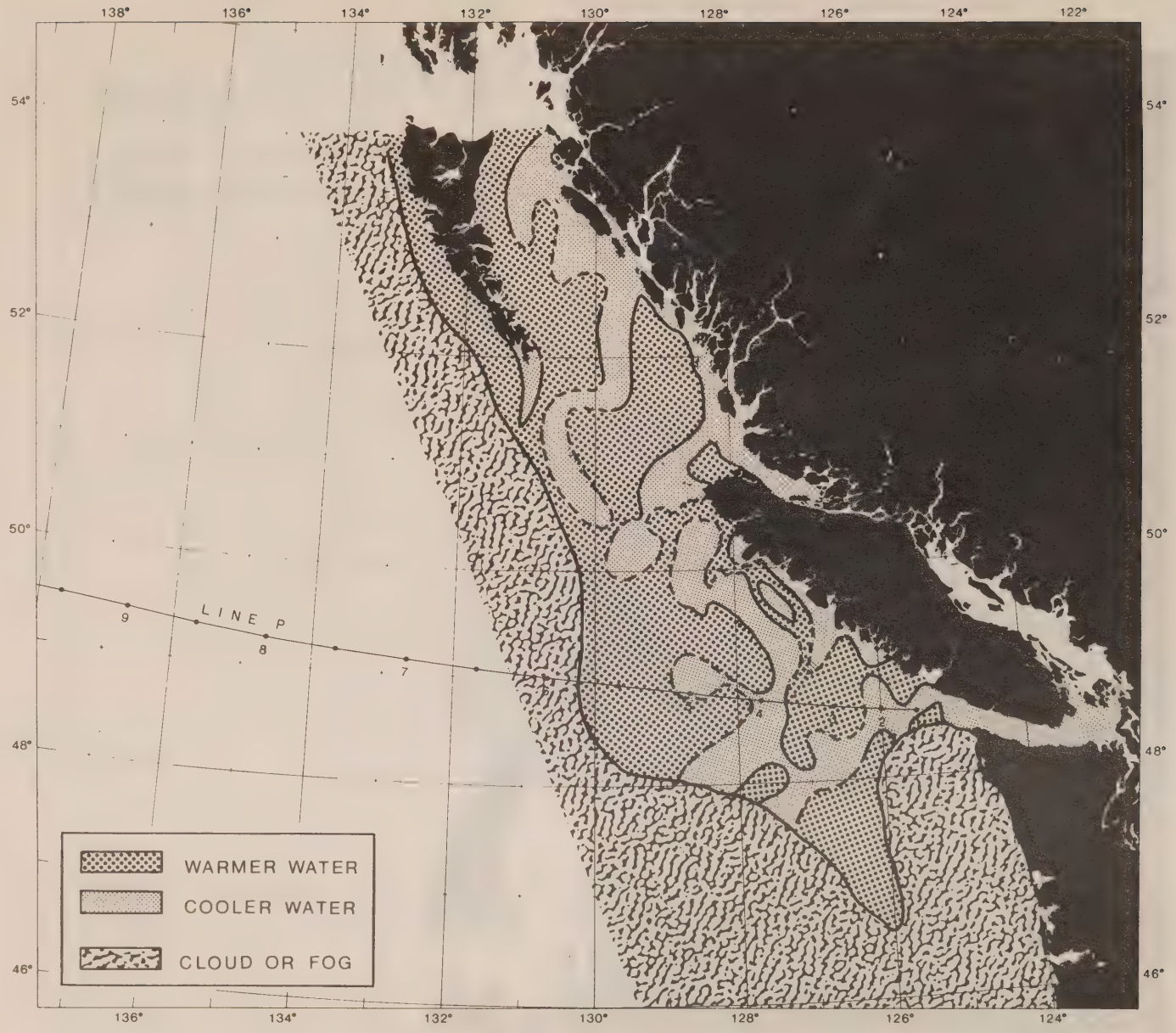

FIGURE 5-7. 17:44:00 29 AUGUST 1974 3669 NOAA 3

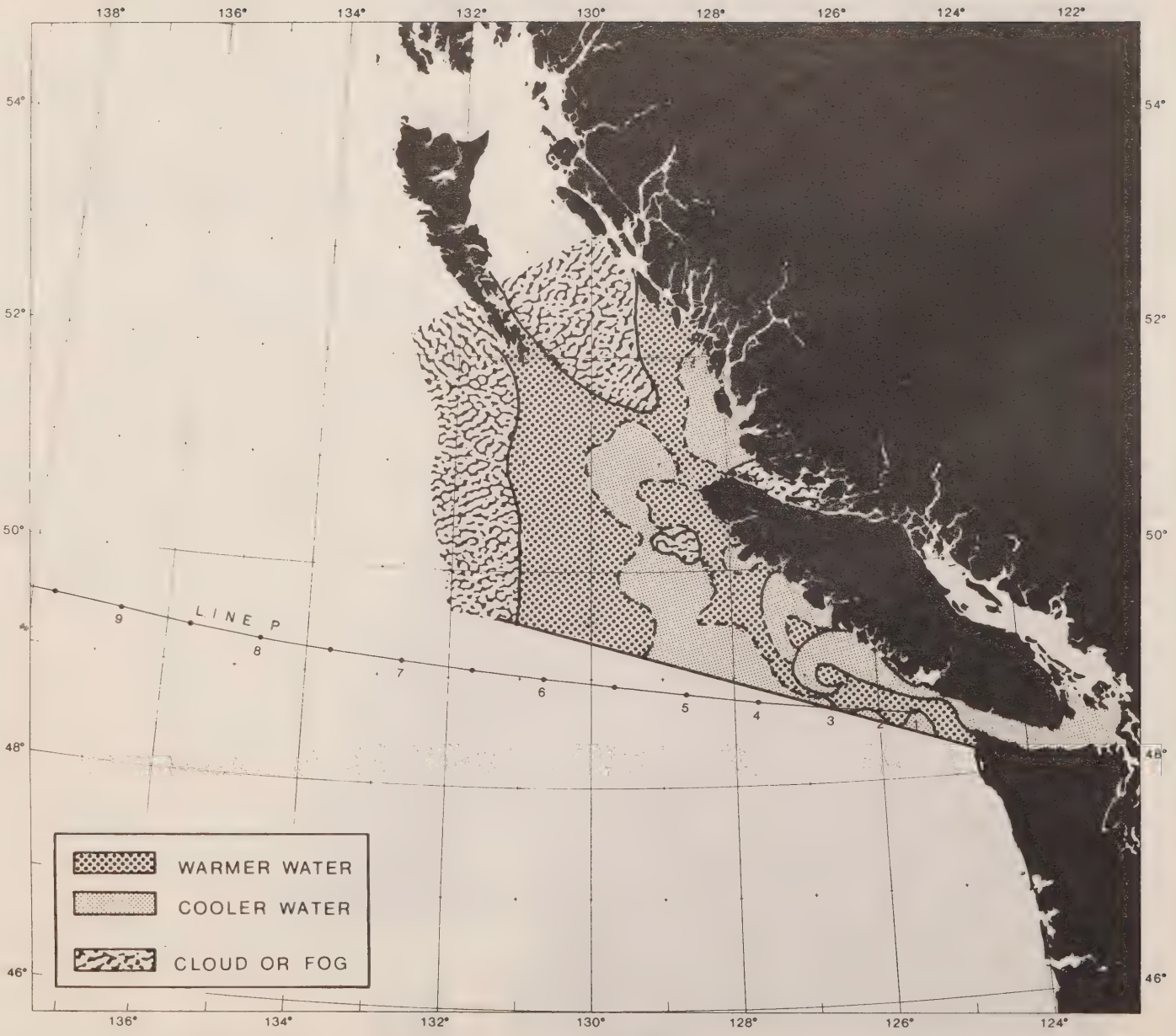

FIGURE 5-8. 18:10:59 10 SEPTEMBER 1974 3818 NOAA 3

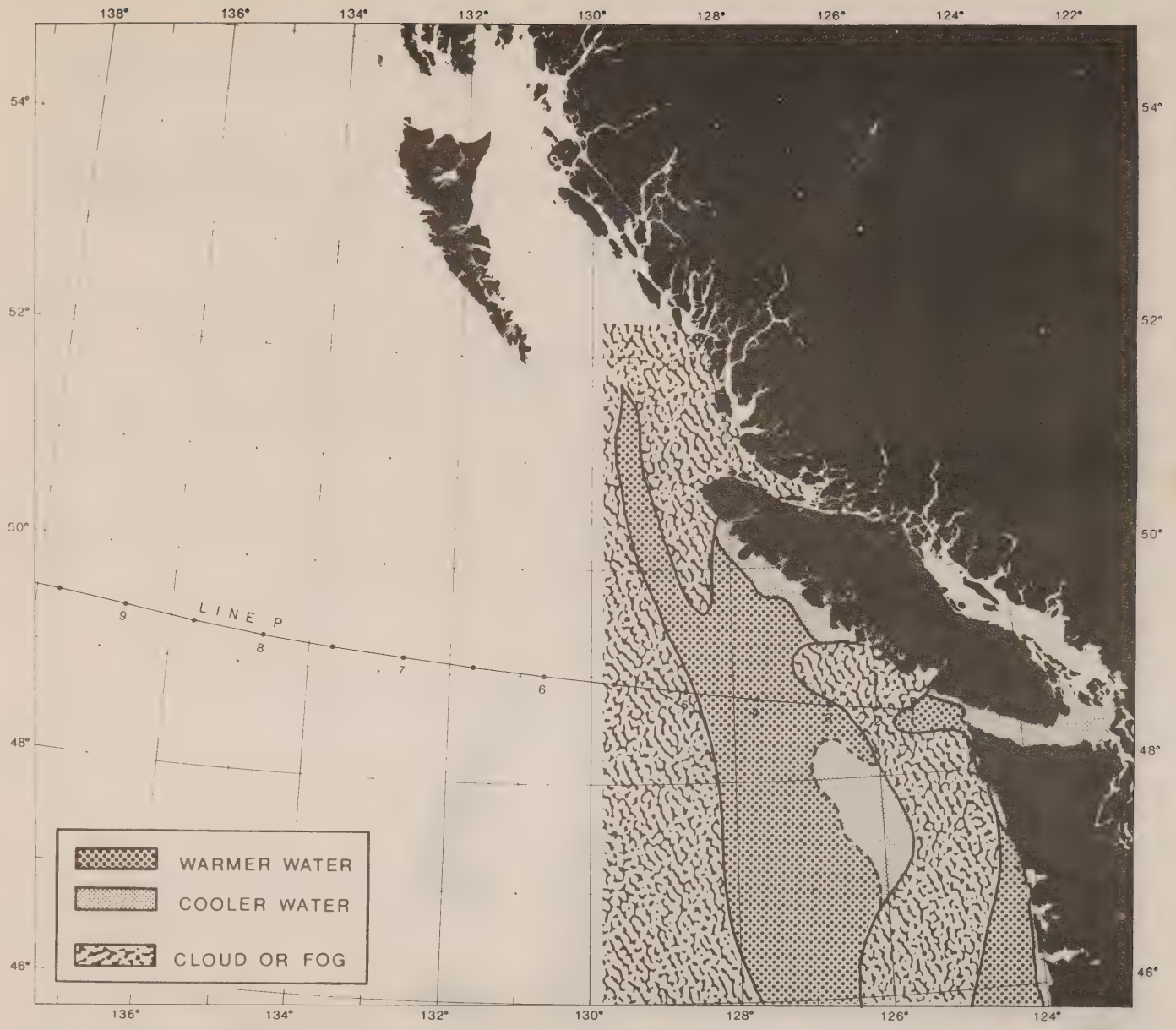

FIGURE 5-9. 17:30:00 11 SEPTEMBER 1974 3830 NOAA 3

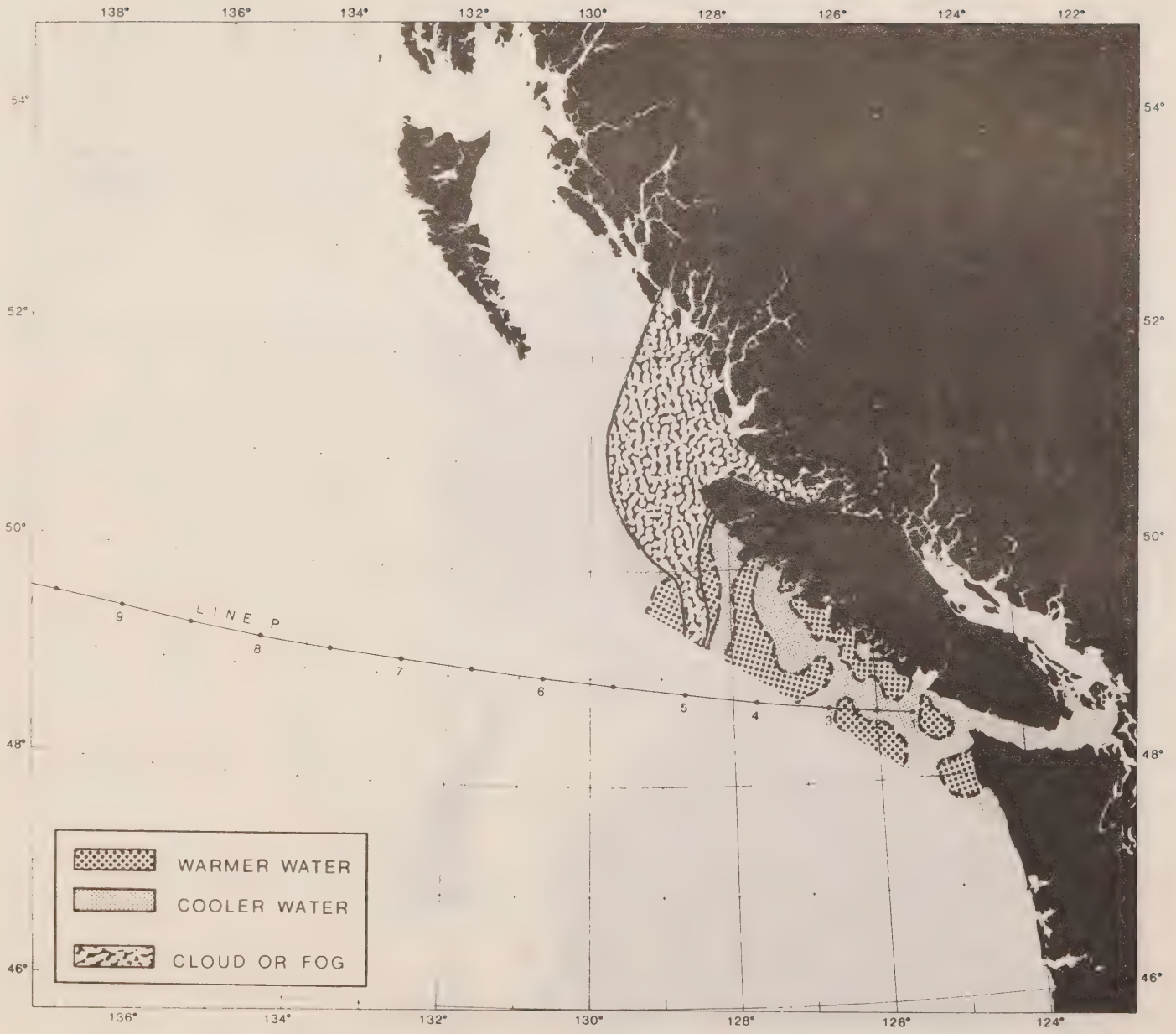

FIGURE 5-10. 18:39:40 12 SEPTEMBER 1974 3843 NOAA 3

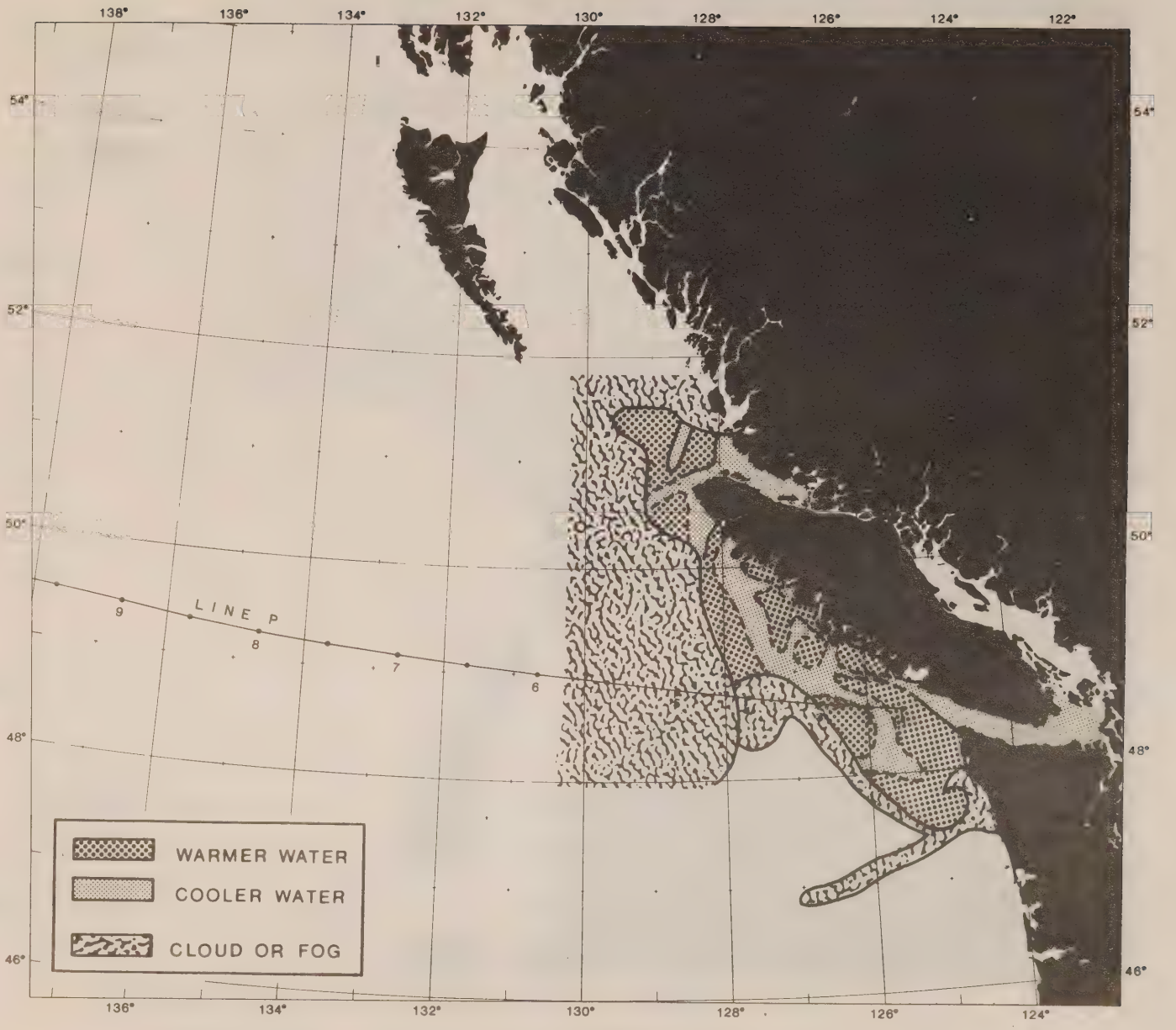

FIGURE 5-11. 17:54:40 13 SEPTEMBER 1974 3855 NOAA 3

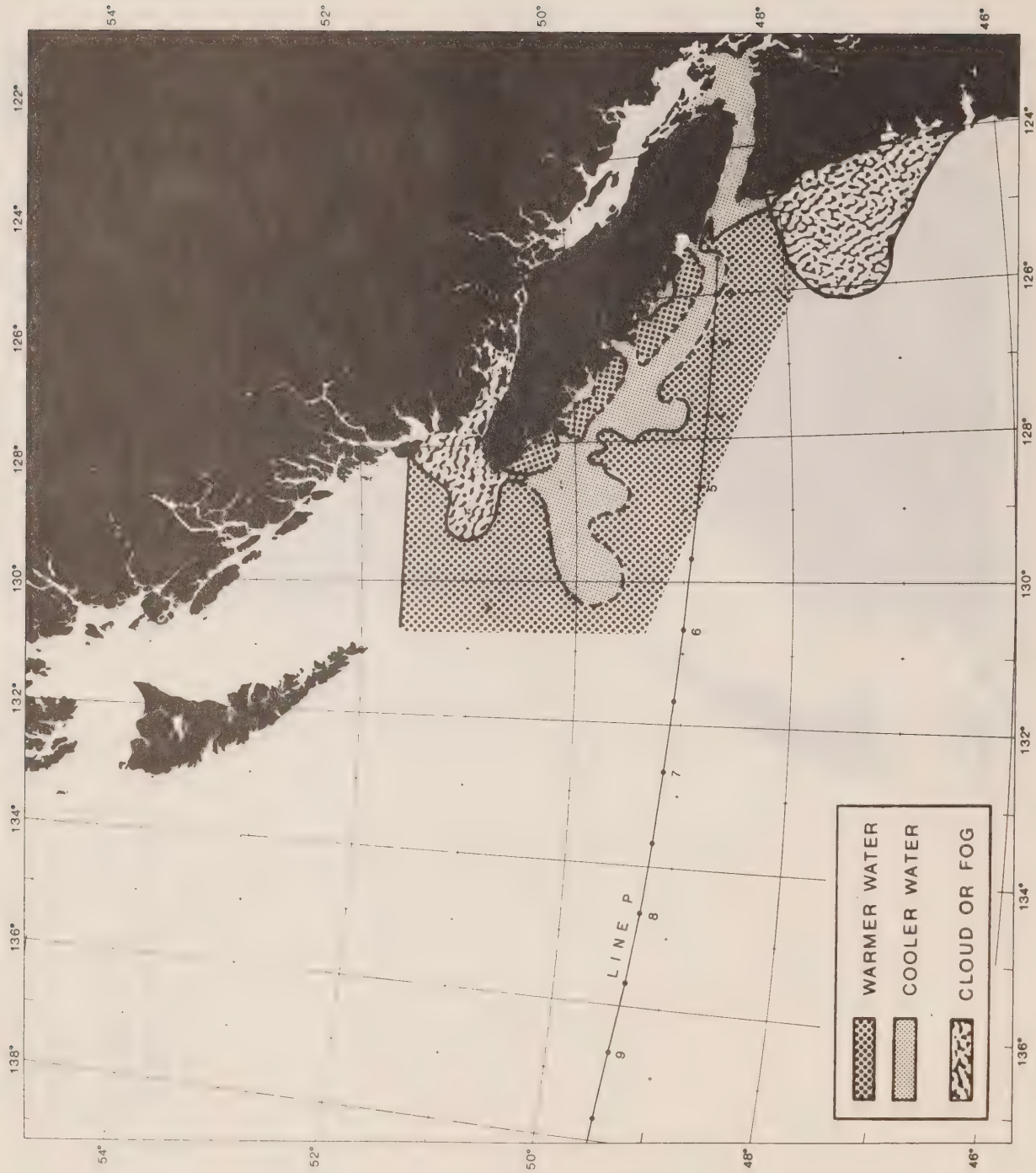

FIGURE 5-12. 17:13:45 19 SEPTEMBER 1974 3929 NOAA 3

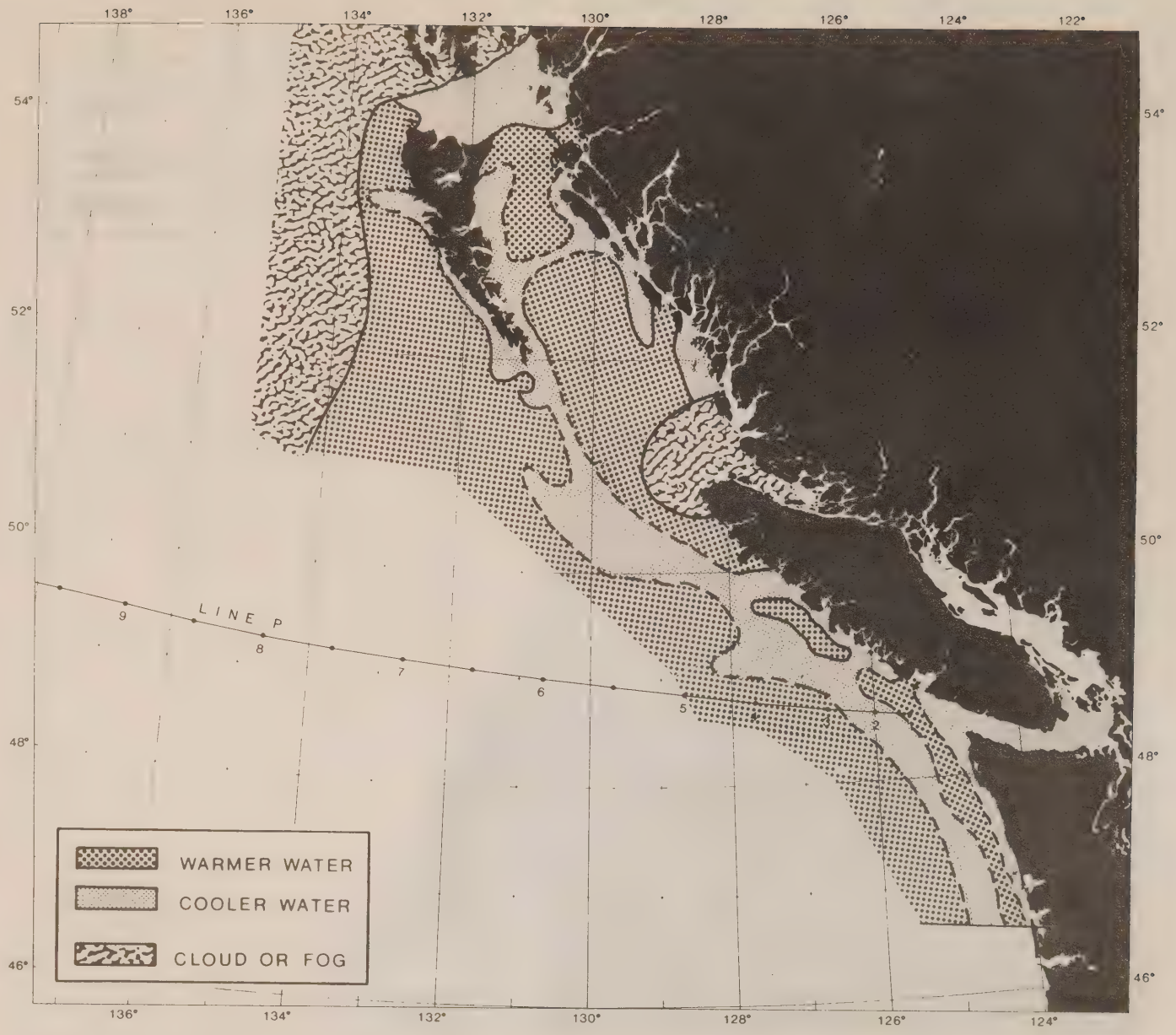

FIGURE 5-13. 19:03:00 19 SEPTEMBER 1974 3930 NOAA 3

FIGURE 5-14. 18:19:00 20 SEPTEMBER 1974 3942 NOAA 3

FIGURE 5-15. 18:56:57 28 JULY 1975 3194 NOAA 4

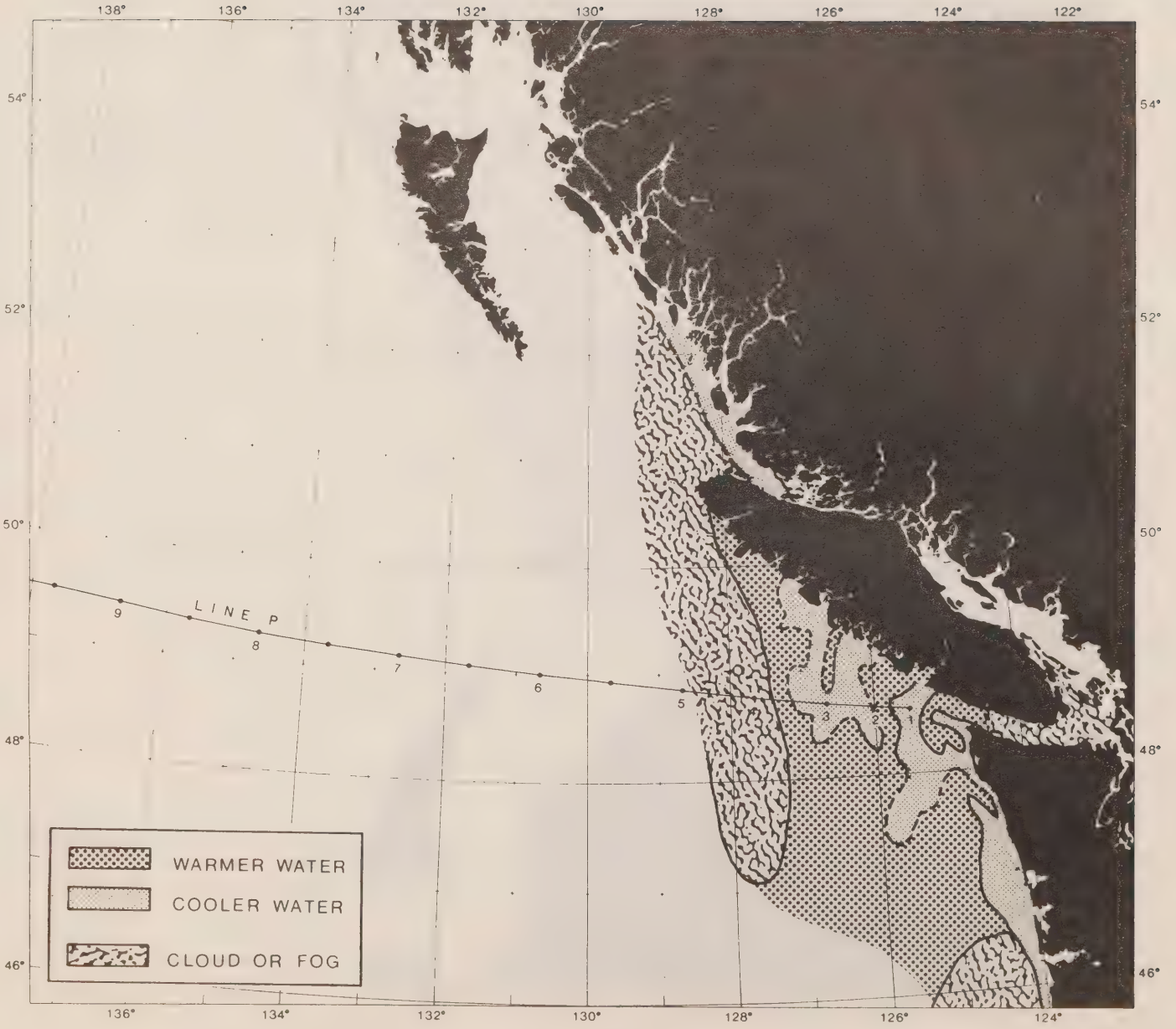

FIGURE 5-16. 17:53:20 23 AUGUST 1975 3519 NOAA 4

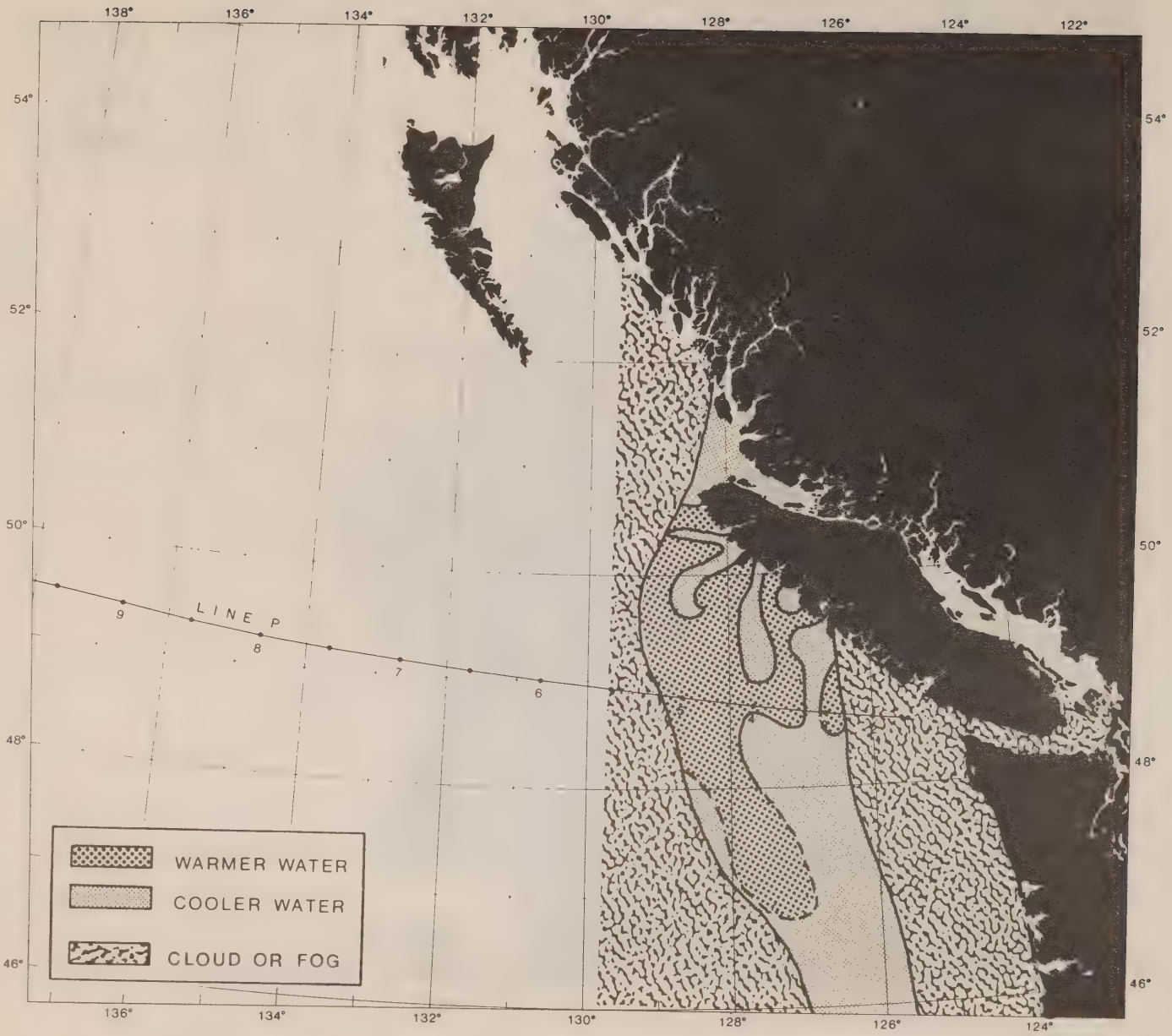

FIGURE 5-17. 17:14:01 08 SEPTEMBER 1975 3719 NOAA 4

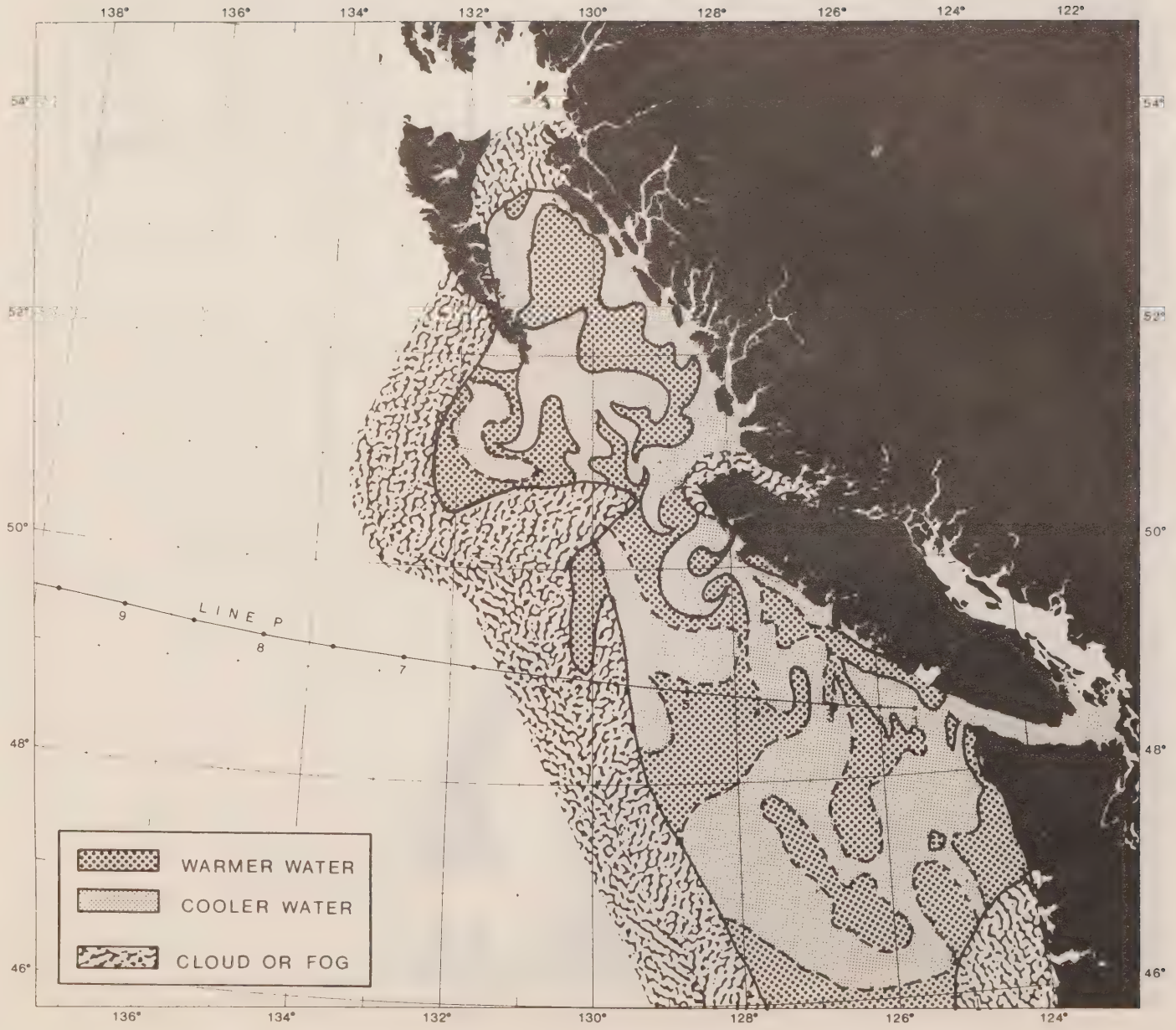

FIGURE 5-18. 03:38:36 09 SEPTEMBER 1975 8322 NOAA 3

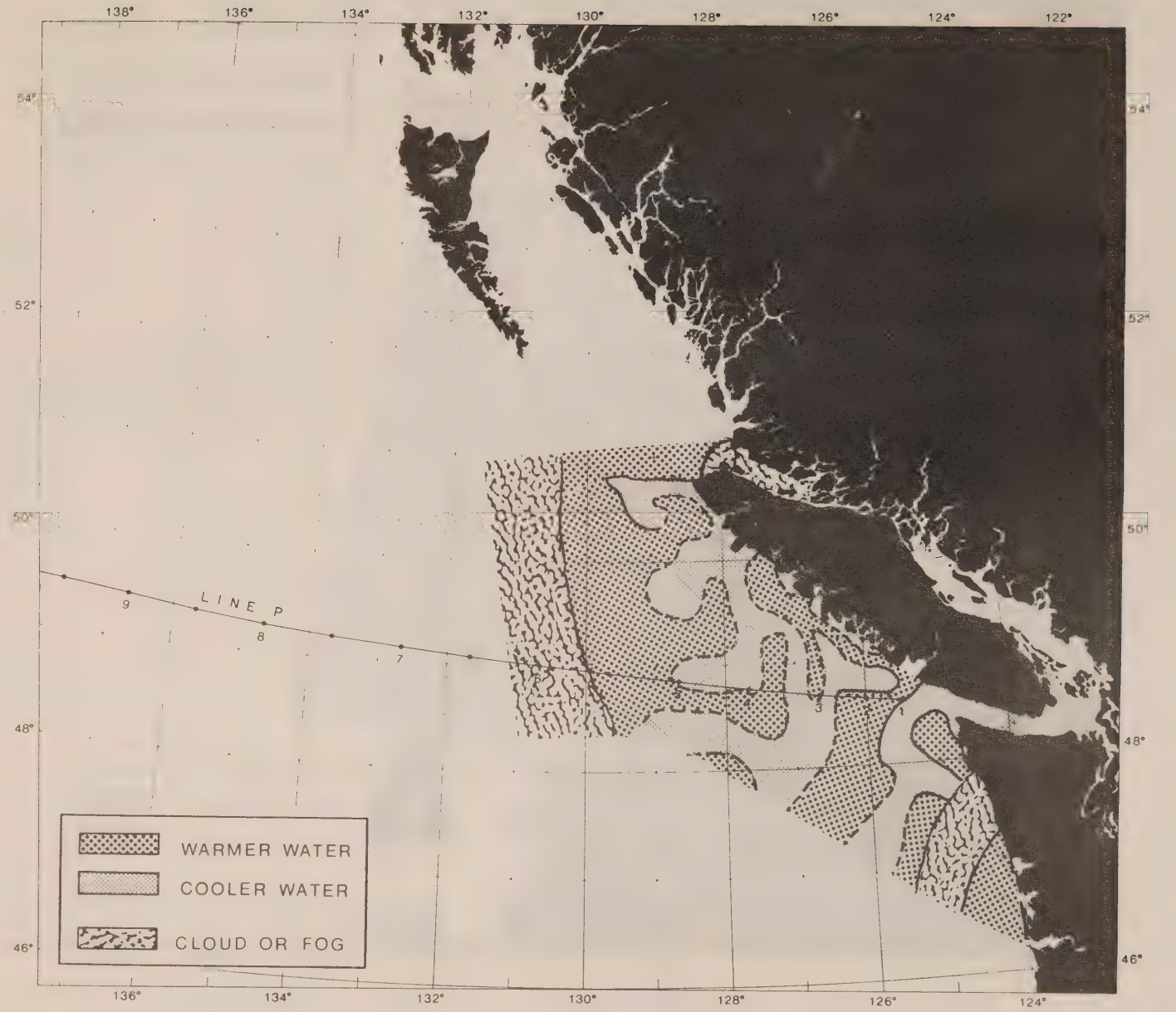

FIGURE 5-19. 18:08:01 09 SEPTEMBER 1975 3732 NOAA 4

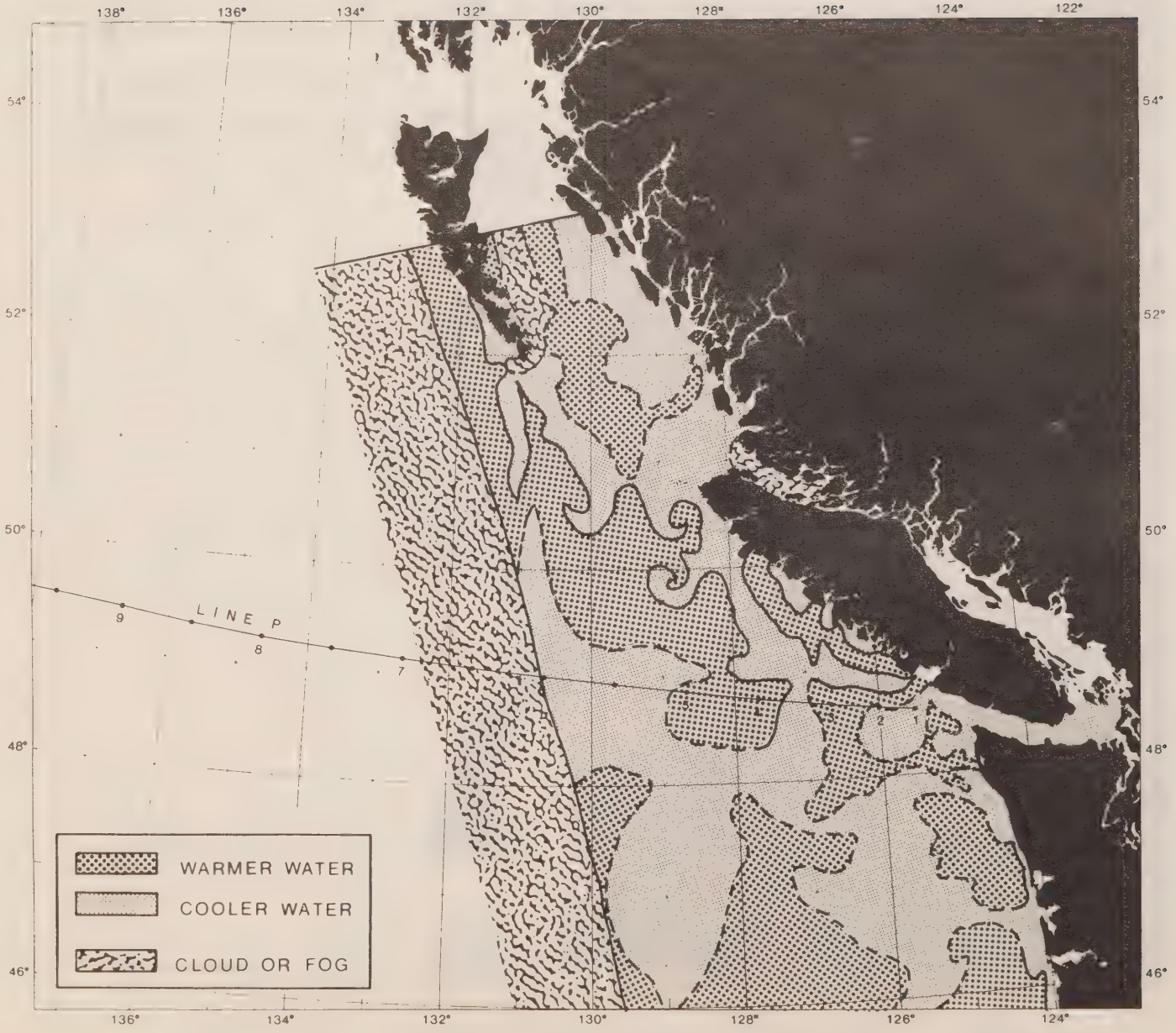

FIGURE 5-20. 17:09:00 10 SEPTEMBER 1975 3744 NOAA 4

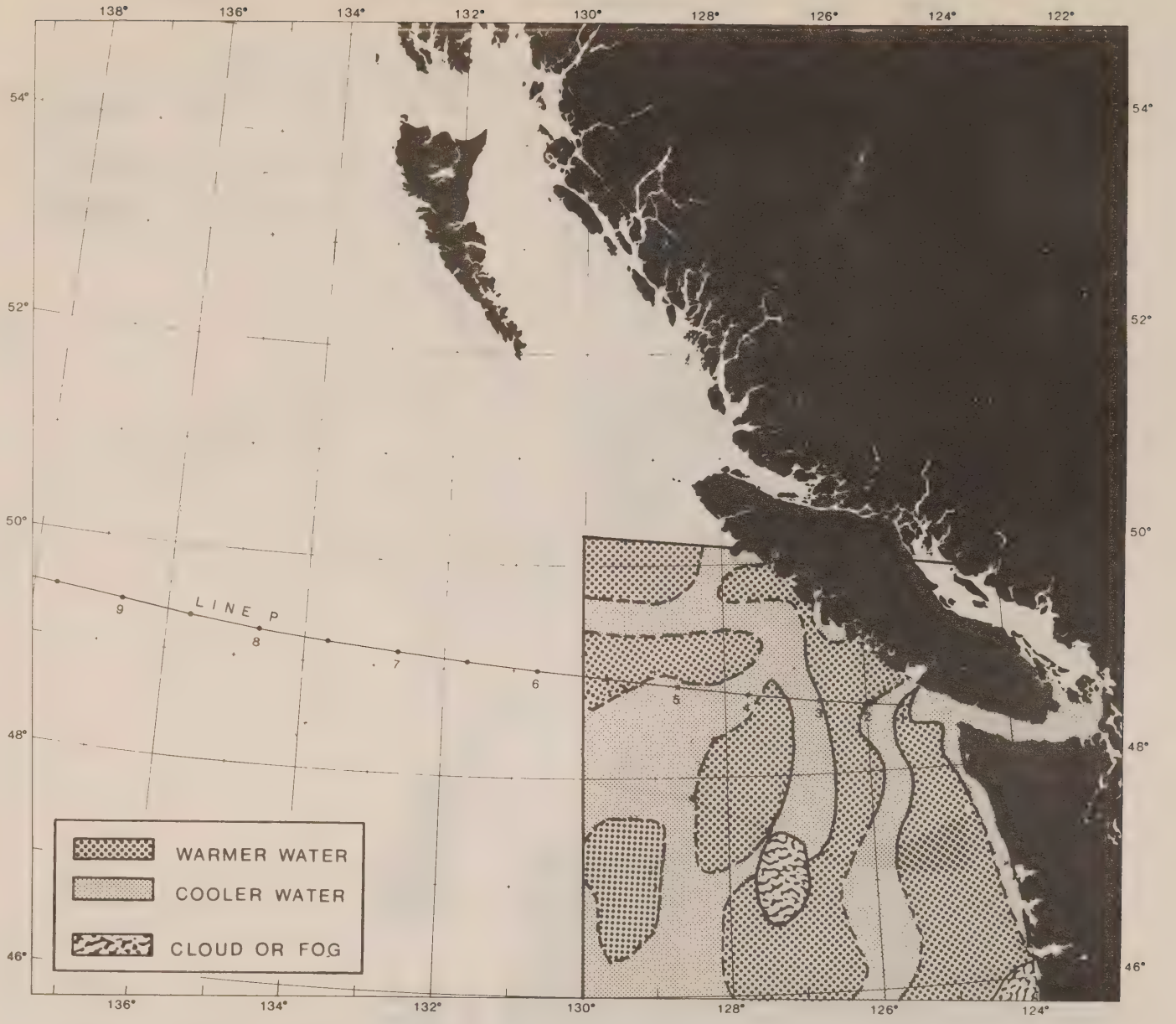

FIGURE 5-21. 17:05:00 12 SEPTEMBER 1975 3769 NOAA 4

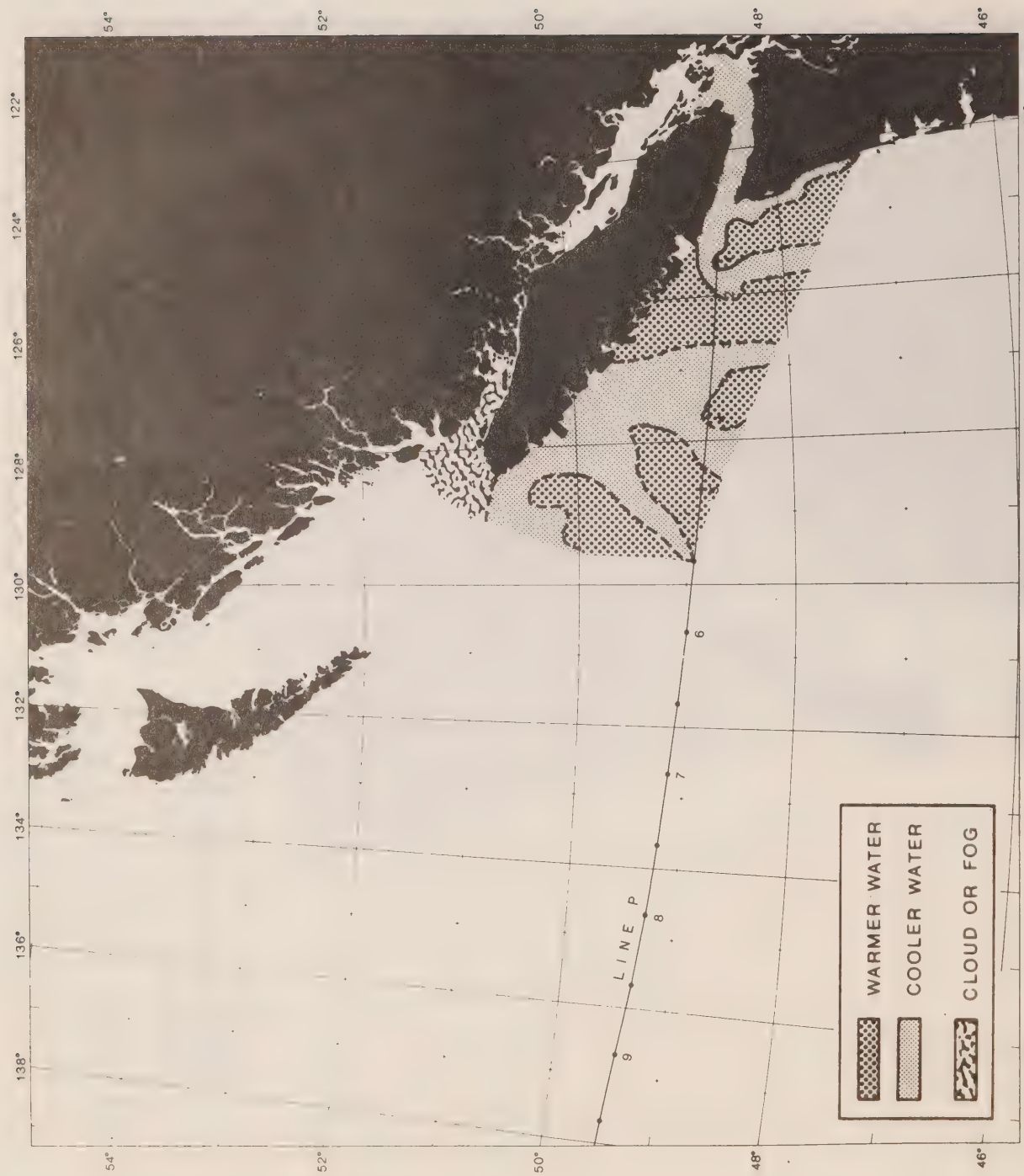

FIGURE 5-22. 18:58:10 12 SEPTEMBER 1975 3770 NOAA 4

FIGURE 5-23. 18:39:25 18 SEPTEMBER 1975 3845 NOAA 4

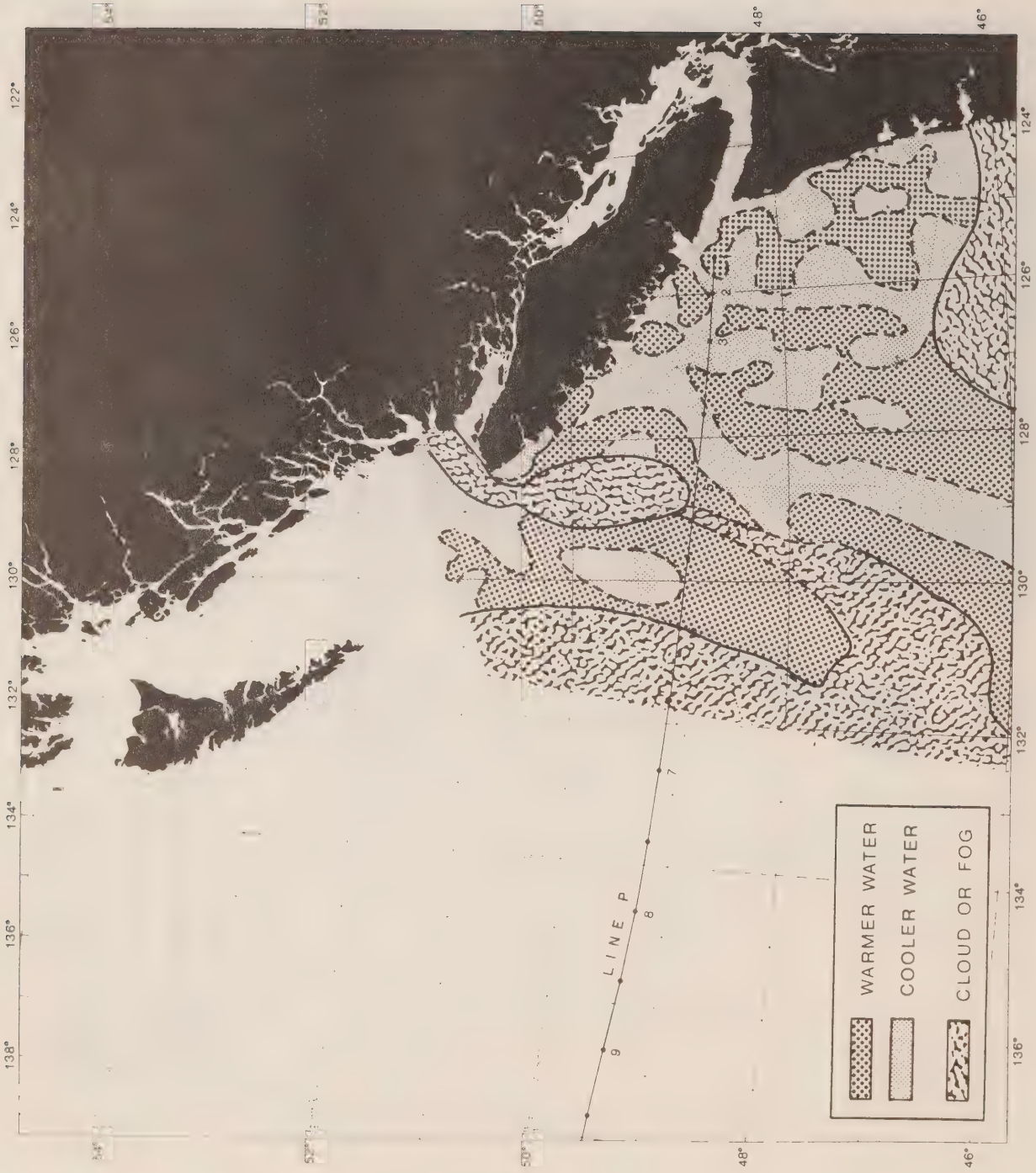

FIGURE 5-24. 17:44:00 19 SEPTEMBER 1975 3857 NOAA 4

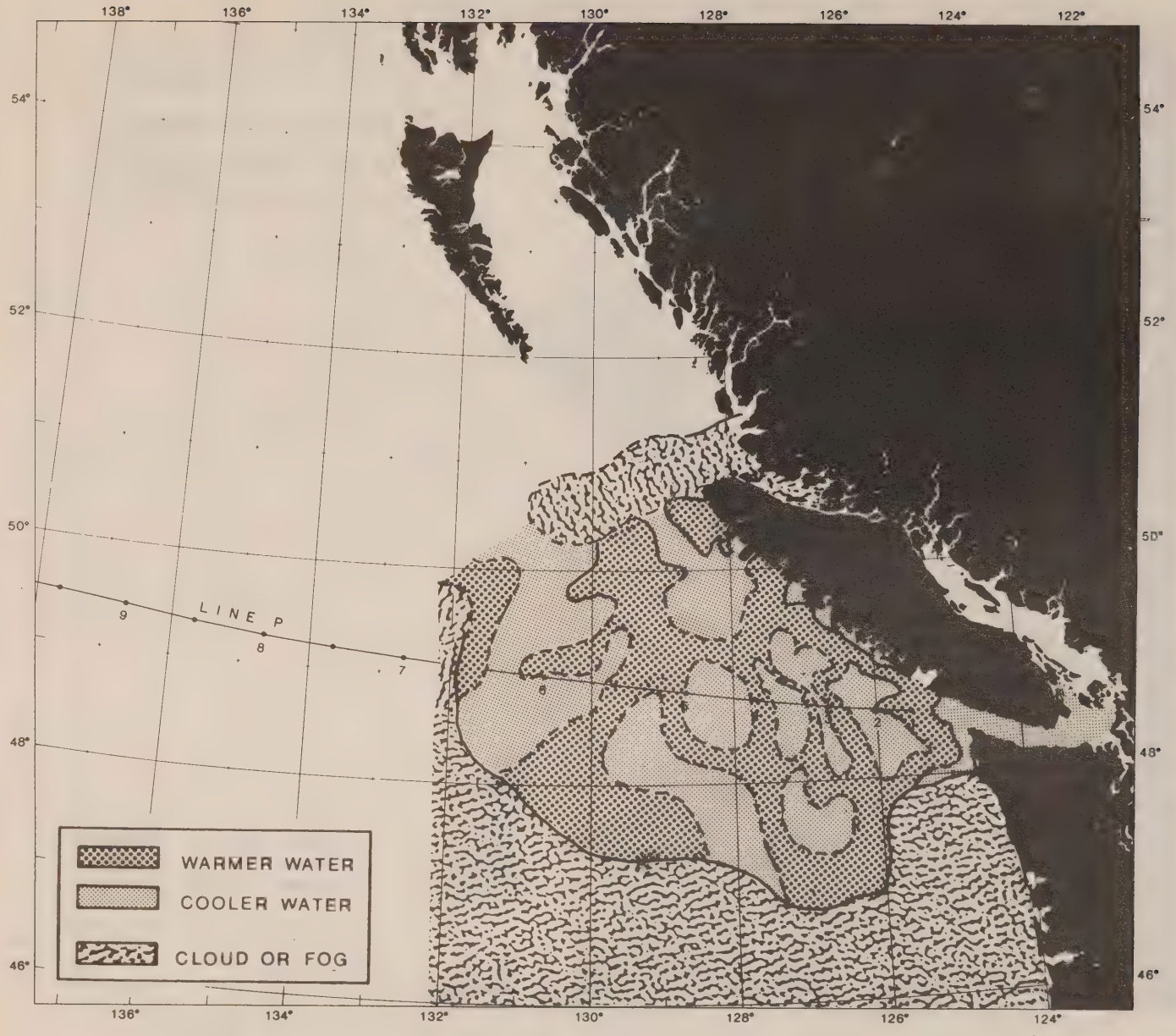

FIGURE 5-25. 18:37:36 20 SEPTEMBER 1975 3870 NOAA 4

FIGURE 5-26. 17:39:36 21 SEPTEMBER 1975 3882 NOAA 4

FIGURE 5-27. 17:43:00 06 FEBRUARY 1976 5610 NOAA 4

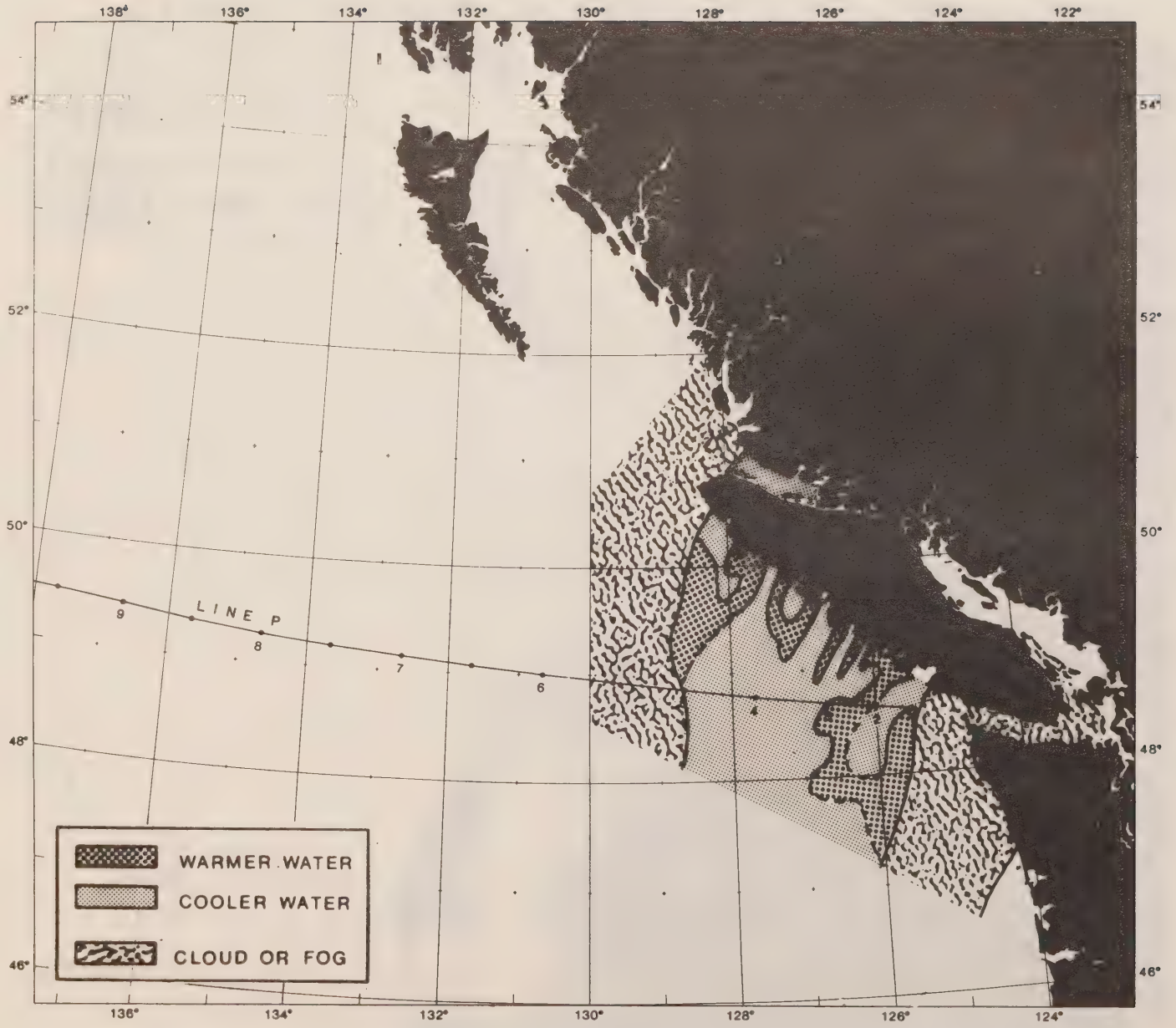

FIGURE 5-28. 17:44:00 27 APRIL 1976 11192 NOAA 3

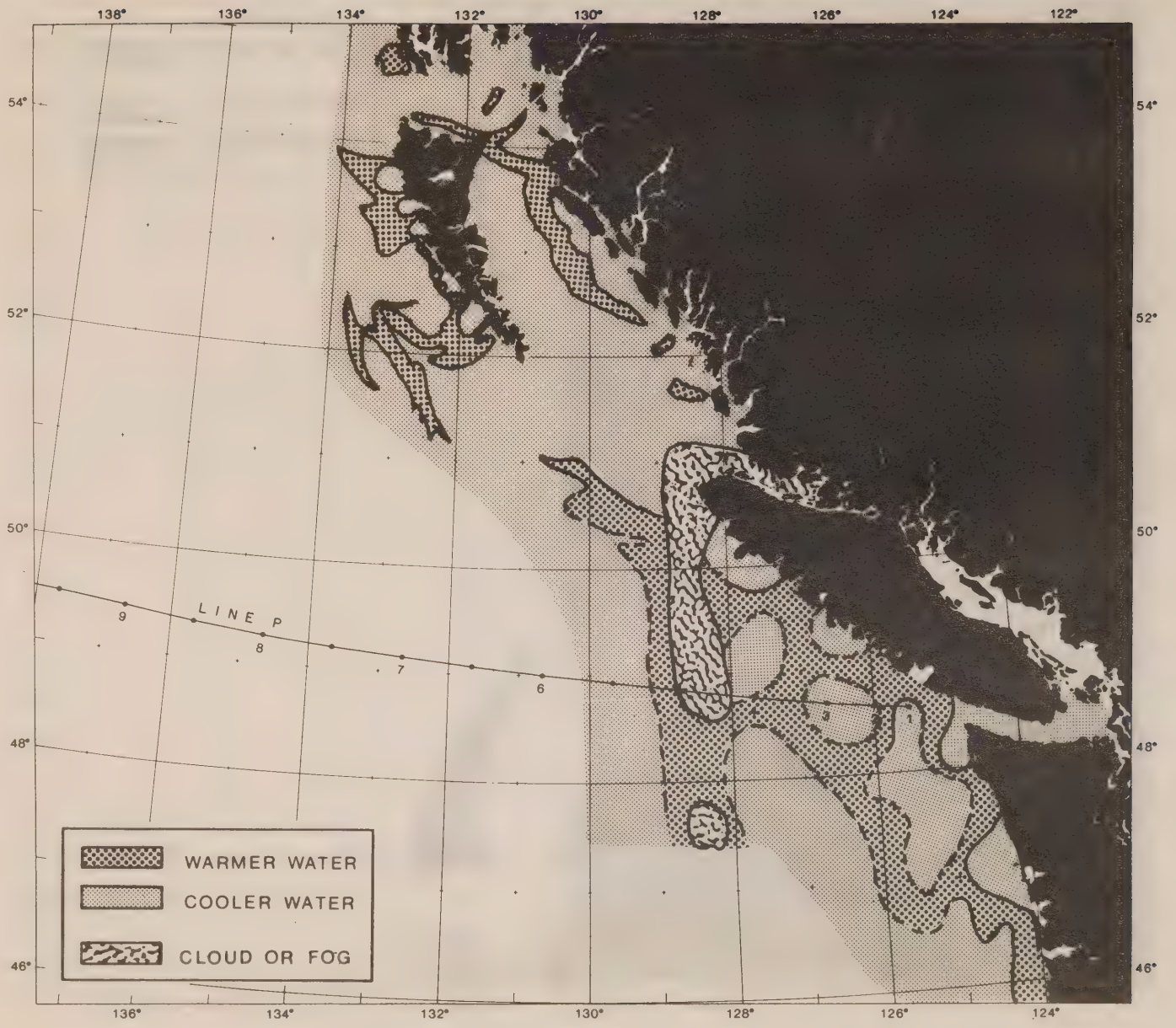

FIGURE 5-29. 18:52:31 28 APRIL 1976 11205 NOAA 3

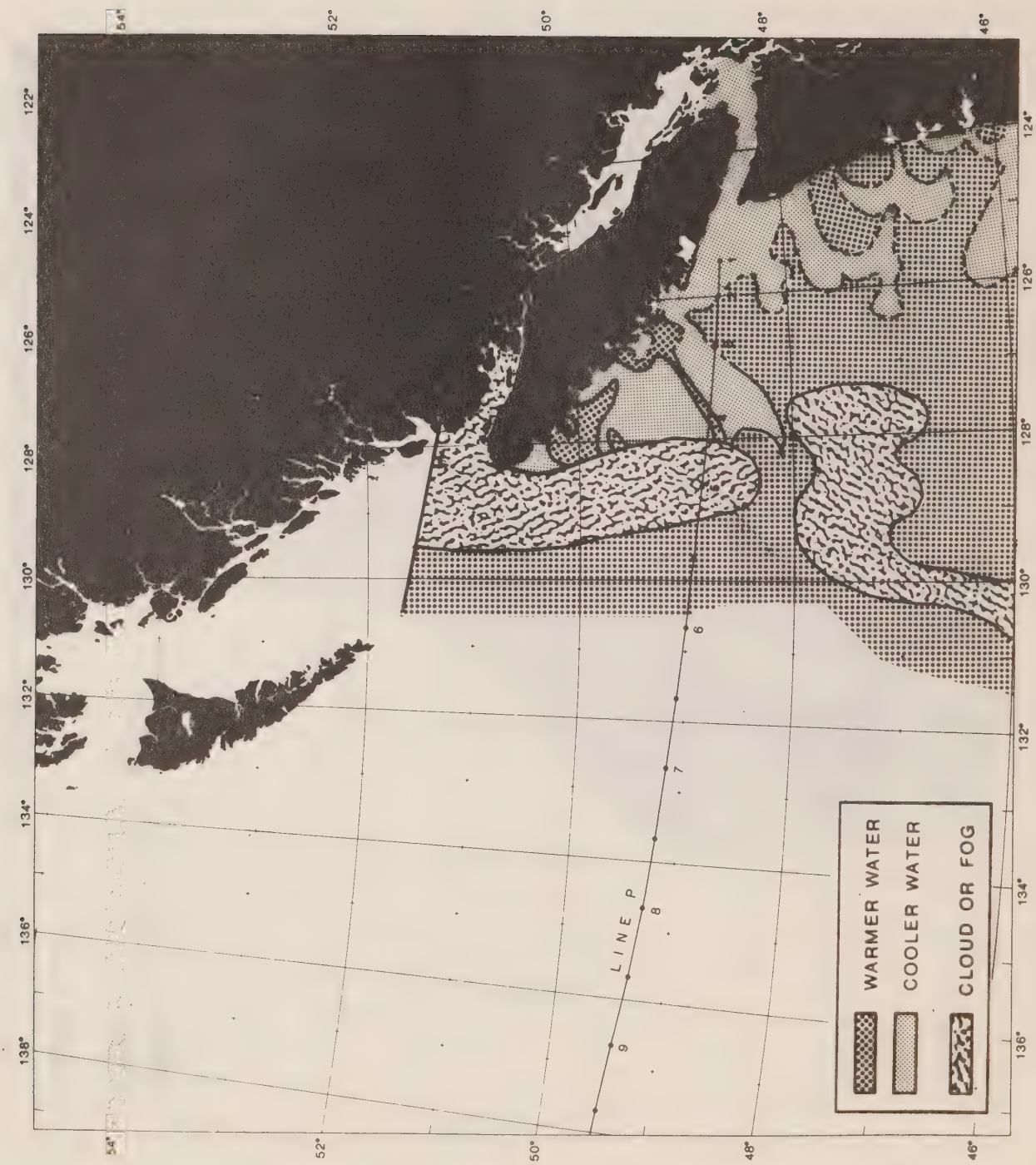

FIGURE 5-30. 17:38:01 19 SEPTEMBER 1976 644 NOAA 5

FIGURE 5-31. 18:01:01 07 OCTOBER 1976 867 NOAA 5

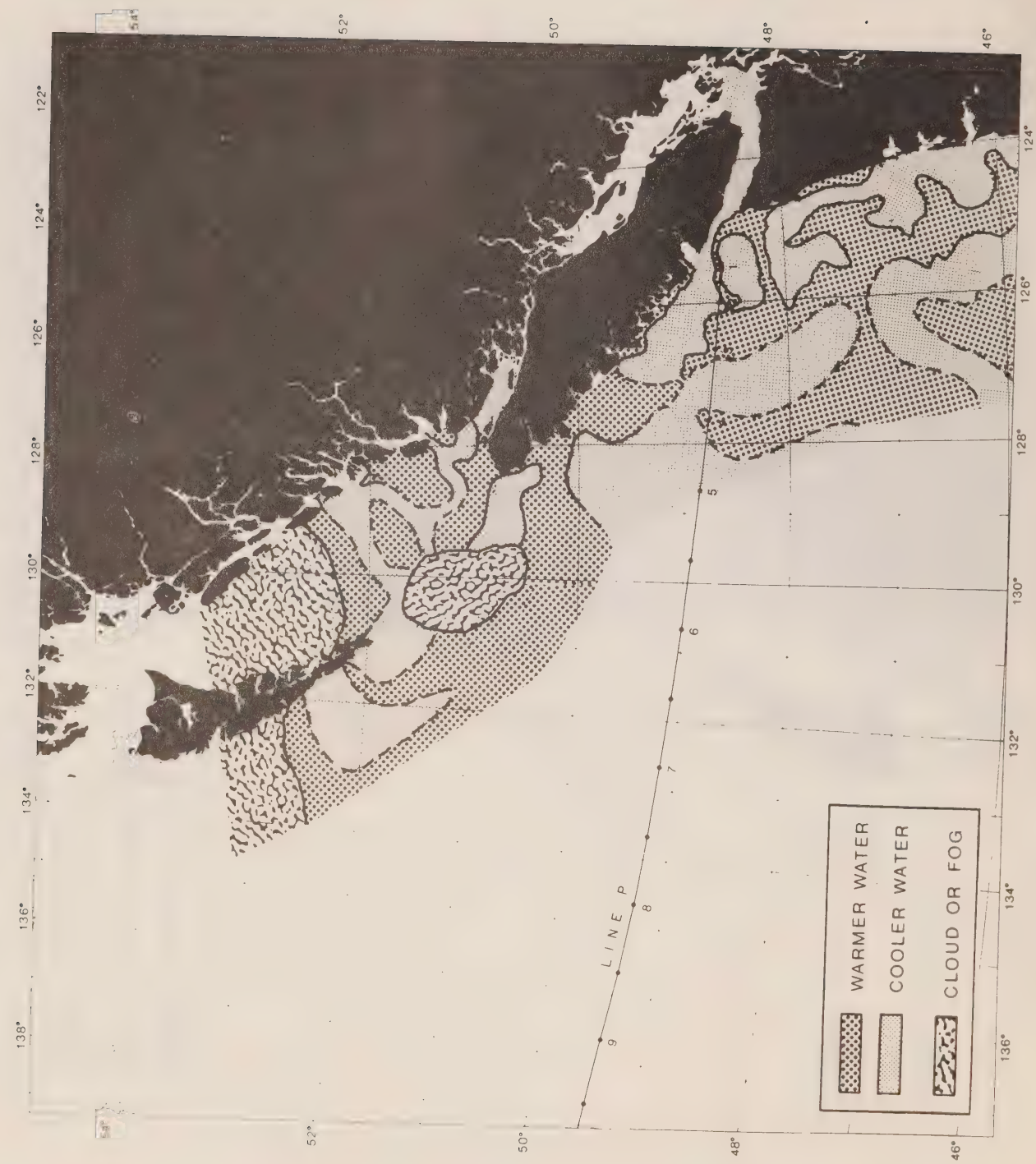

FIGURE 5-32. 03:41:35 18 OCTOBER 1976 996 NOAA 5

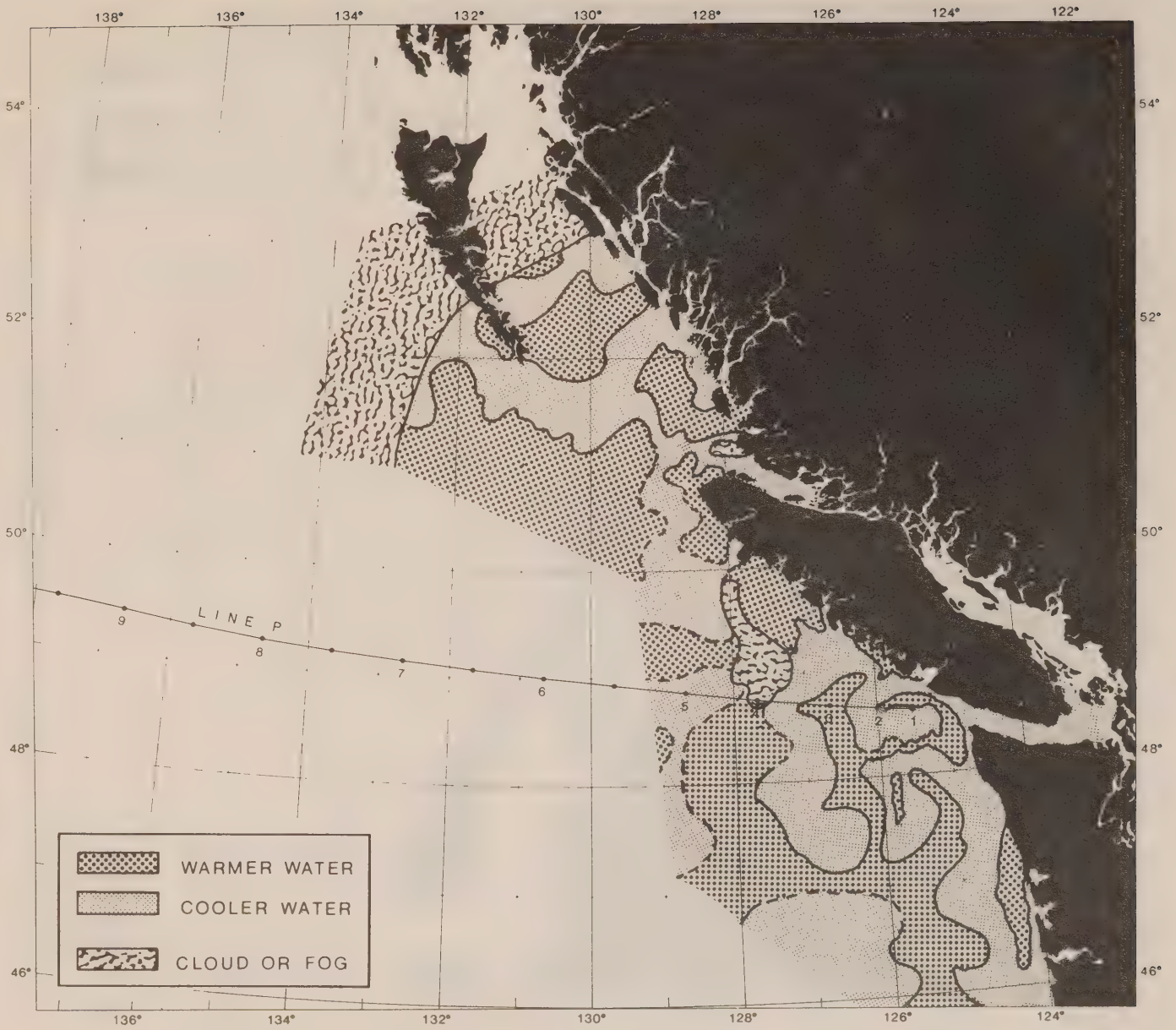

FIGURE 5-33. 17:42:00 18 OCTOBER 1976 1003 NOAA 5

FIGURE 5-34. 04:08:17 26 NOVEMBER 1976 1479 NOAA 5

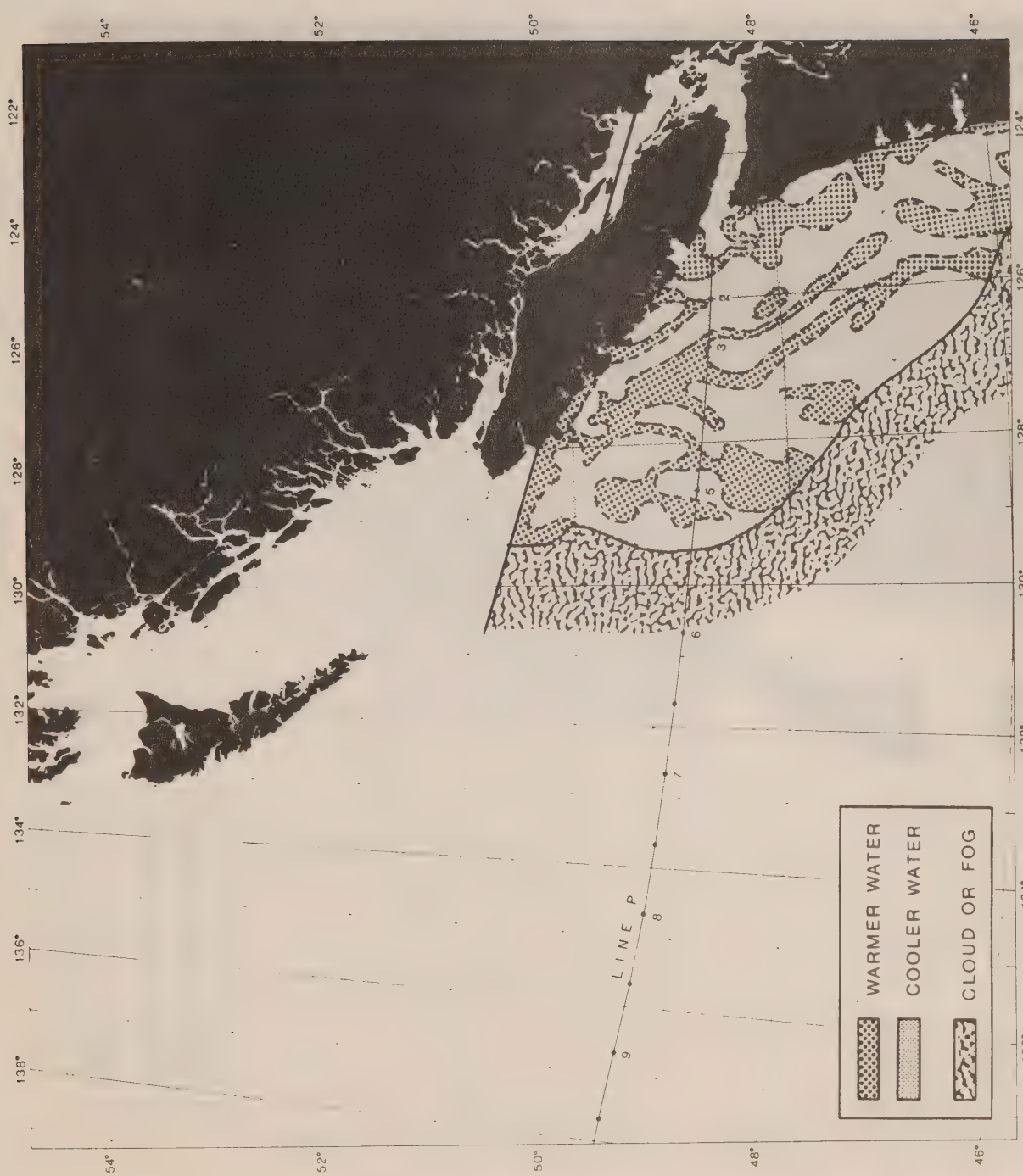

FIGURE 5-35. 18:13:00 26 NOVEMBER 1976 1486 NOAA 5

FIGURE 5-36. 03:26:00 27 NOVEMBER 1976 1491 NOAA 5

FIGURE 5-37. 17:29:00 27 NOVEMBER 1976 1498 NOAA 5

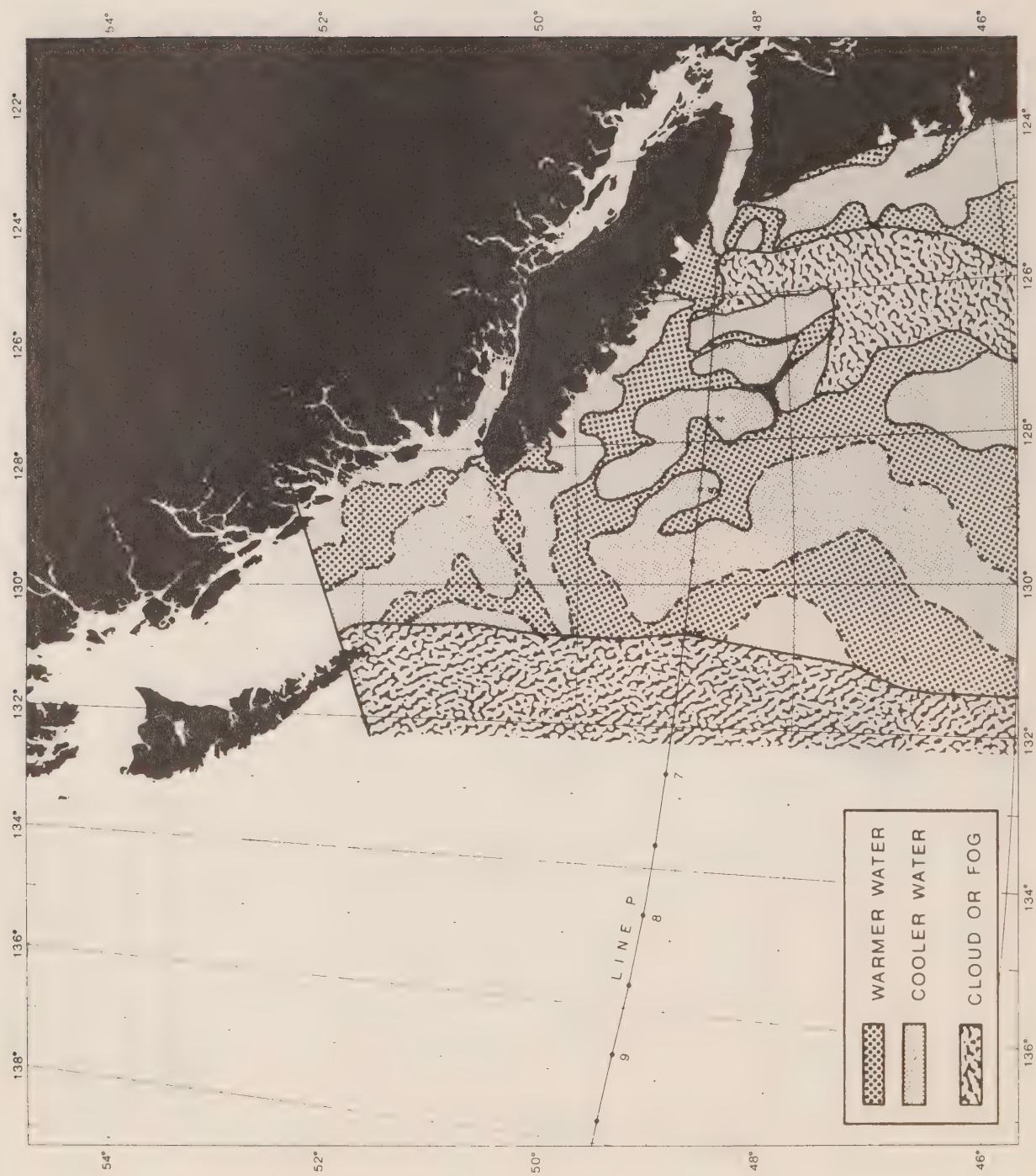

FIGURE 5-38. 04:37:00 28 NOVEMBER 1976 1504 NOAA 5

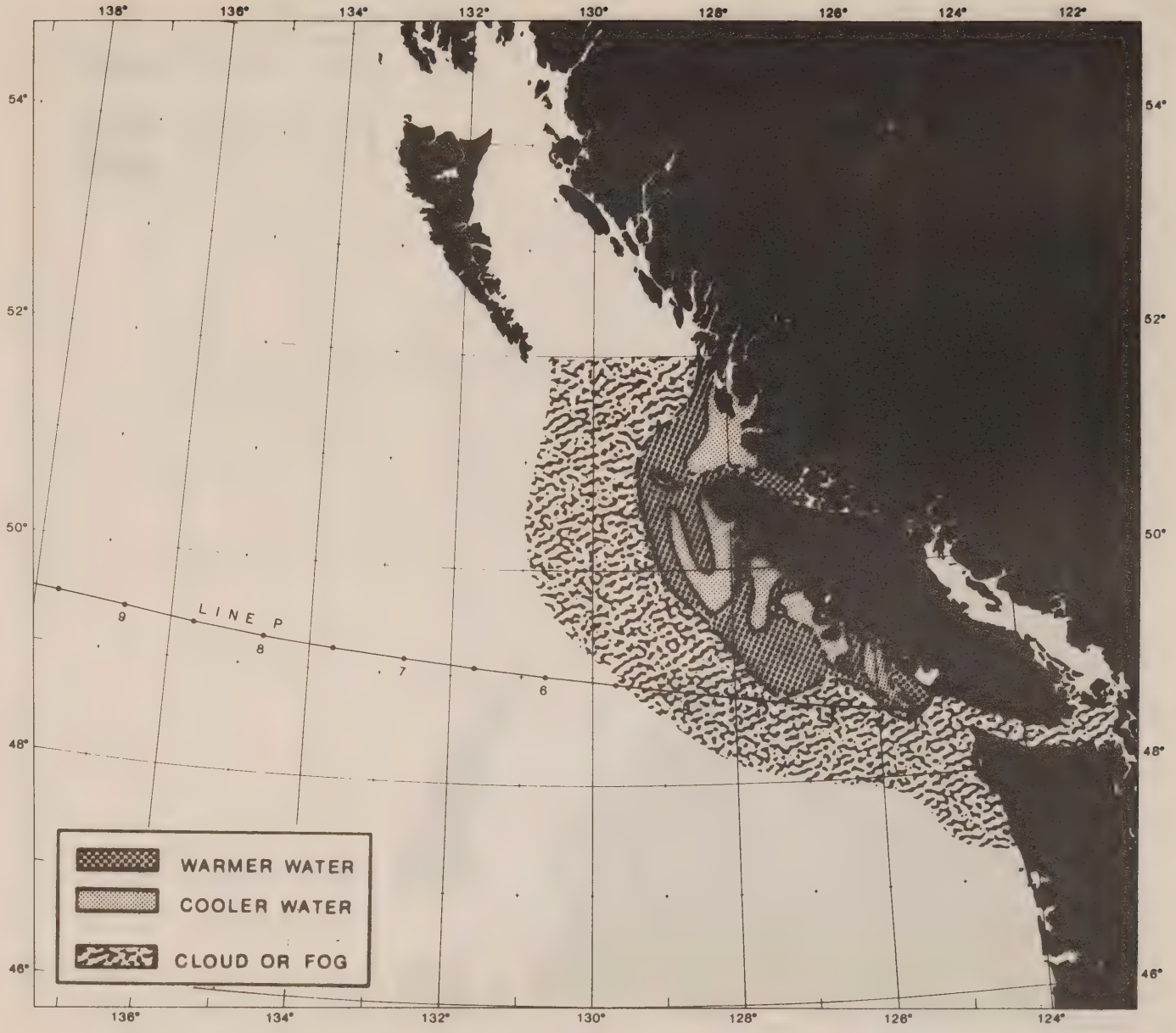

FIGURE 5-39. 18:38:00 28 NOVEMBER 1976 1511 NOAA 5

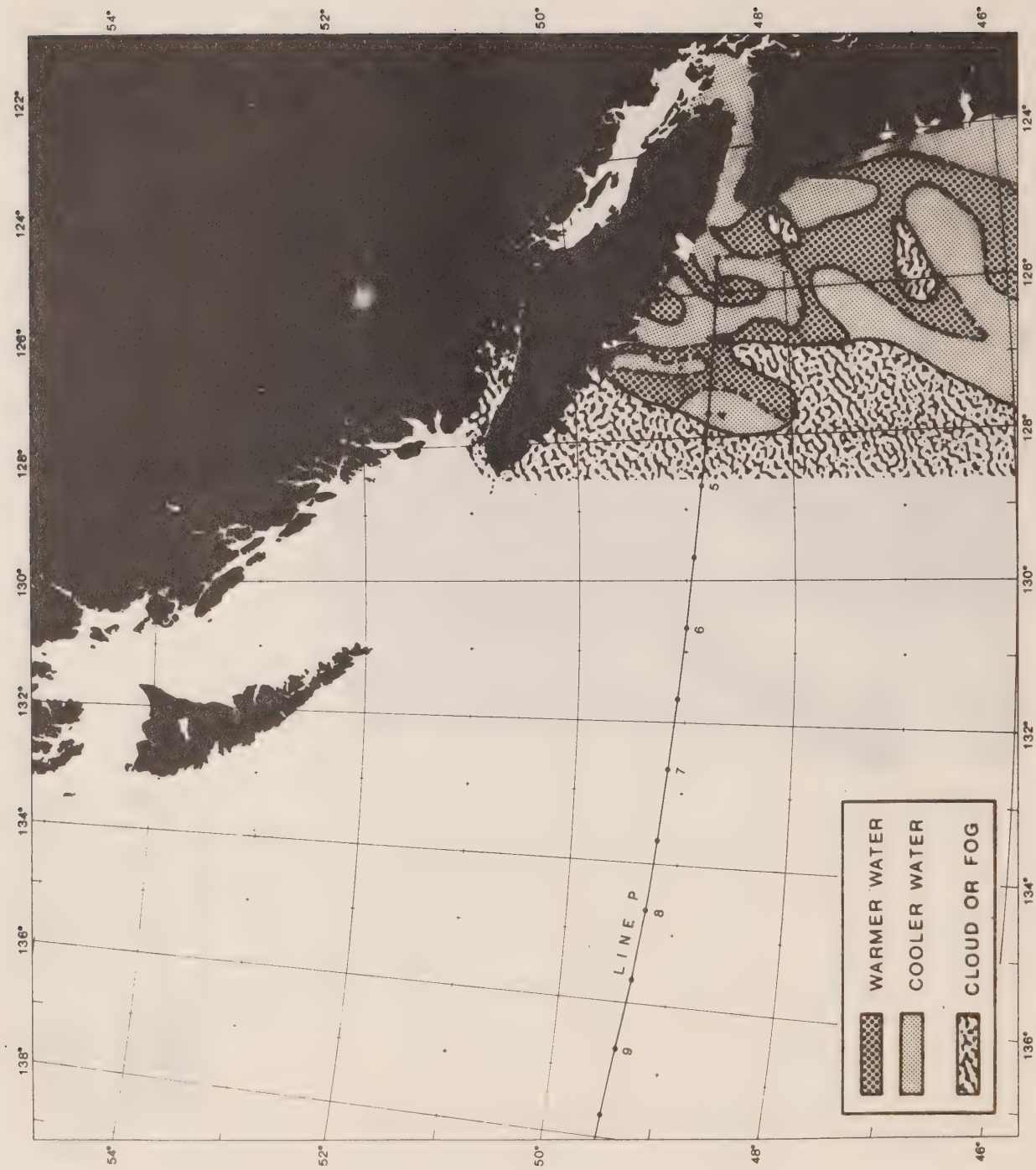

FIGURE 5-40. 17:48:01 11 SEPTEMBER 1977 5063 NOAA 5

FIGURE 5-41. 04:18:36 12 OCTOBER 1977 5440 NOAA 5

FIGURE 5-42. 04:17:11 20 OCTOBER 1977 5539 NOAA 5

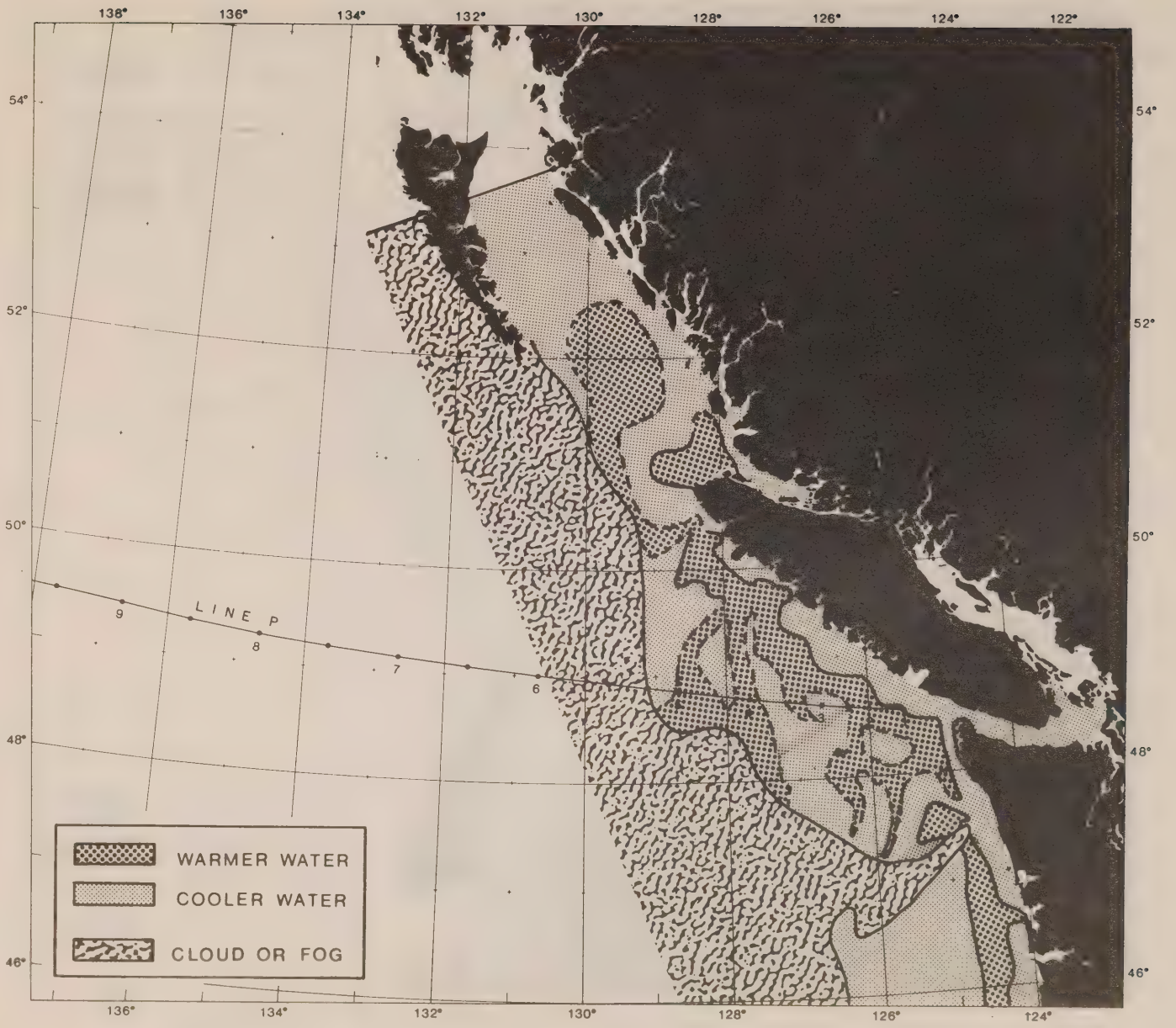

FIGURE 5-43. 17:53:49 31 DECEMBER 1977 6437 NOAA 5

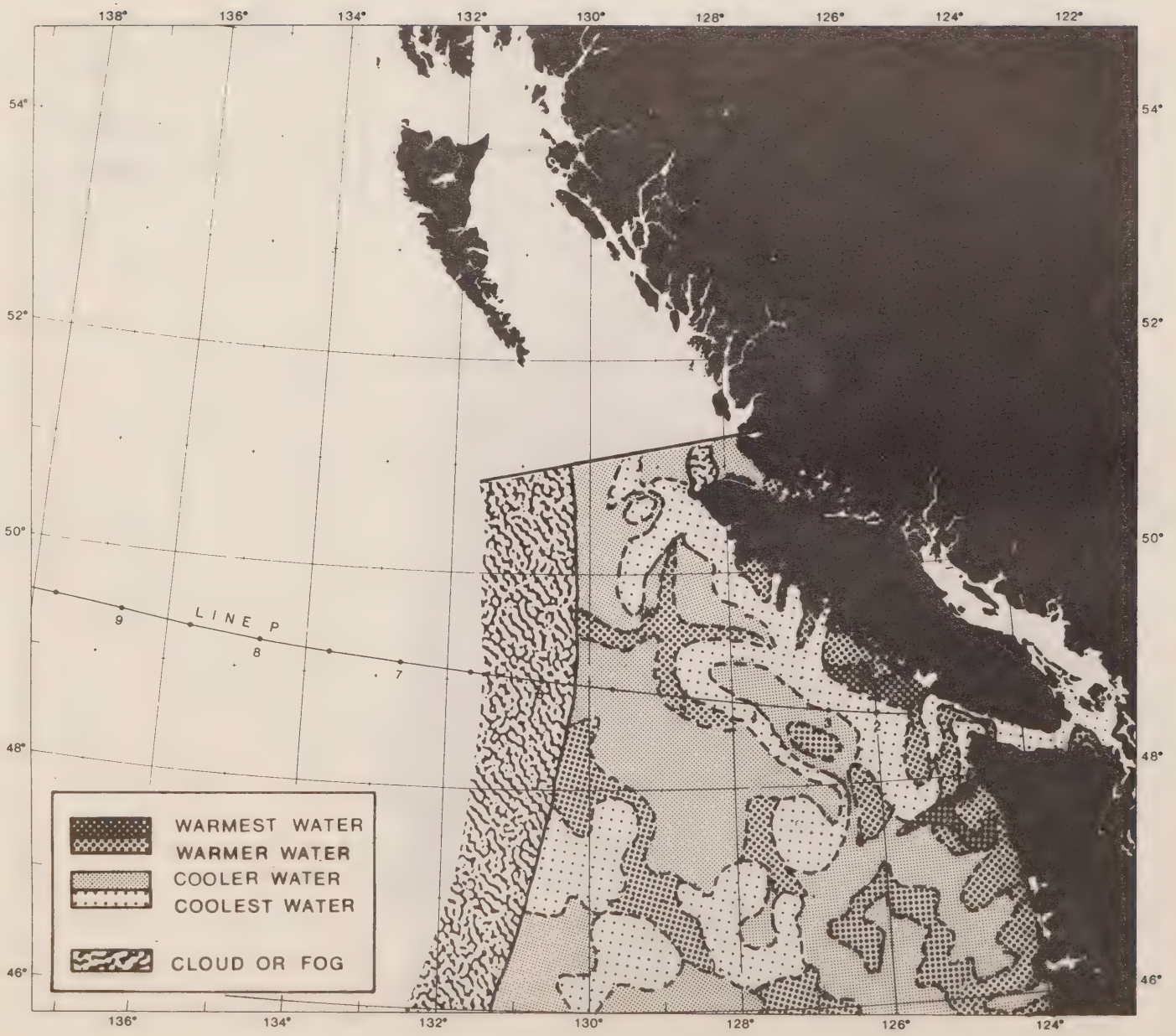

FIGURE 5-44. 17:47:01 31 MAY 1978 8306 NOAA 5

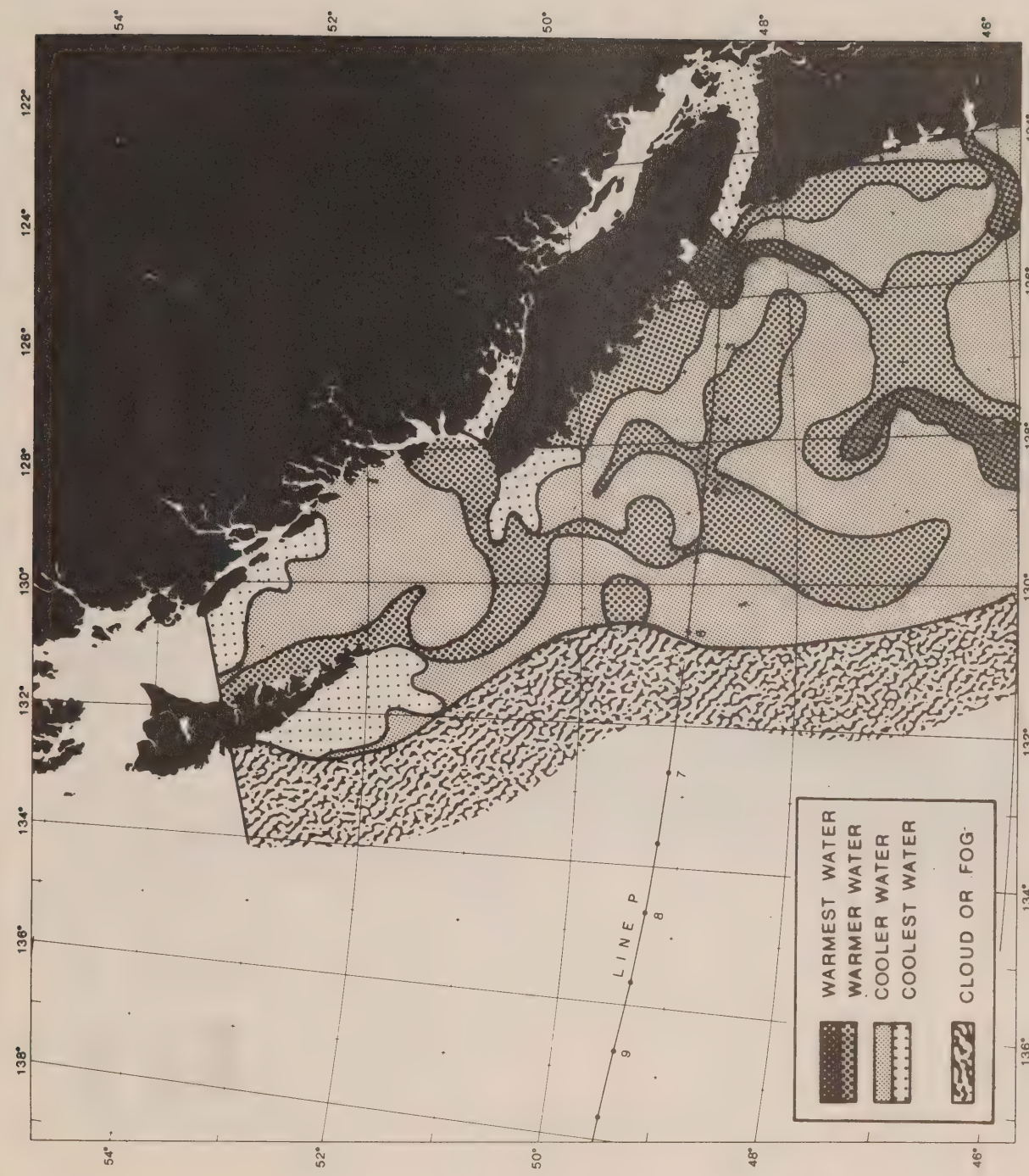

FIGURE 5-45. 04:49:00 01 JUNE 1978 8312 NOAA 5

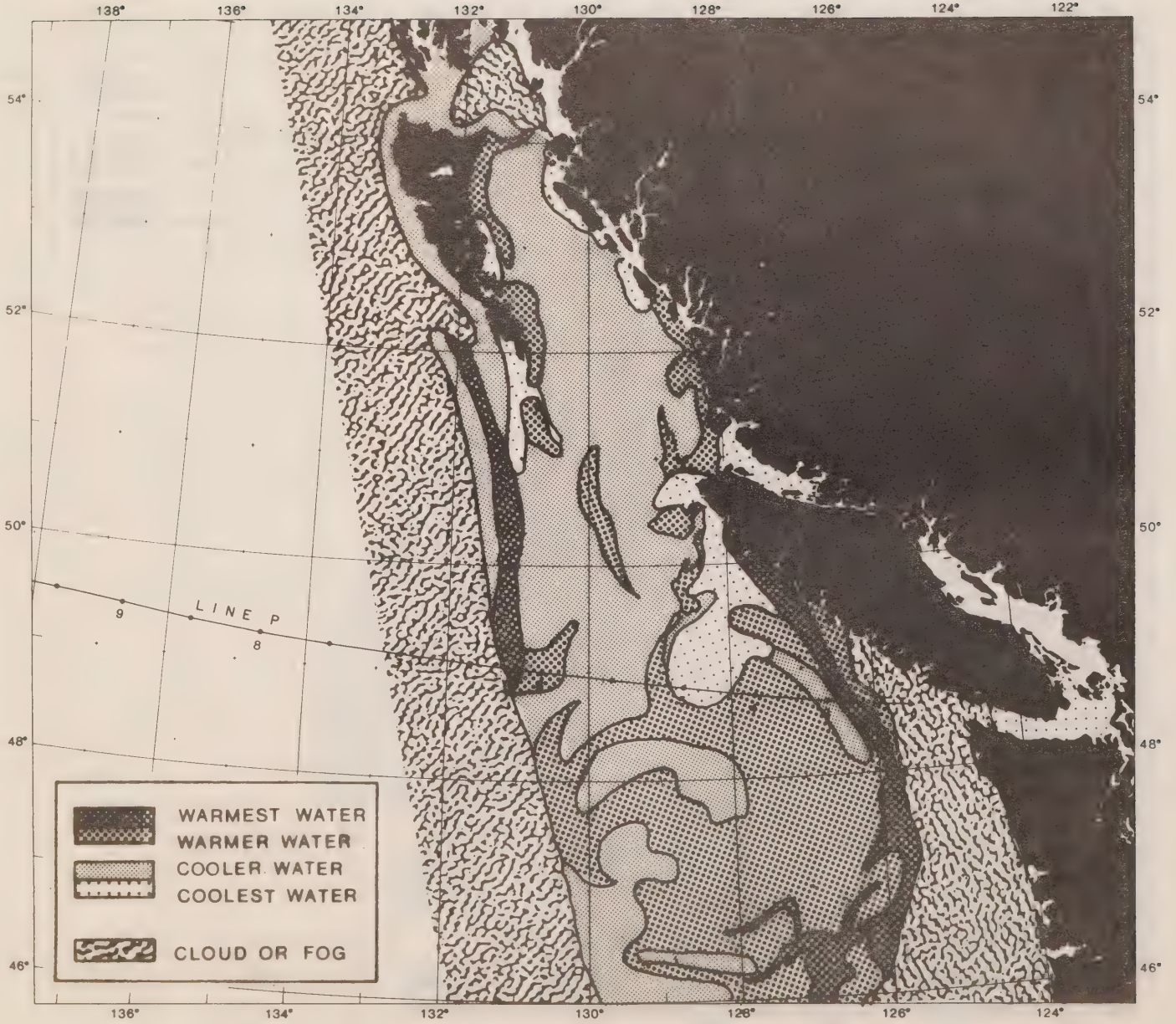

FIGURE 5-46. 17:25:00 03 JUNE 1978 8343 NOAA 5

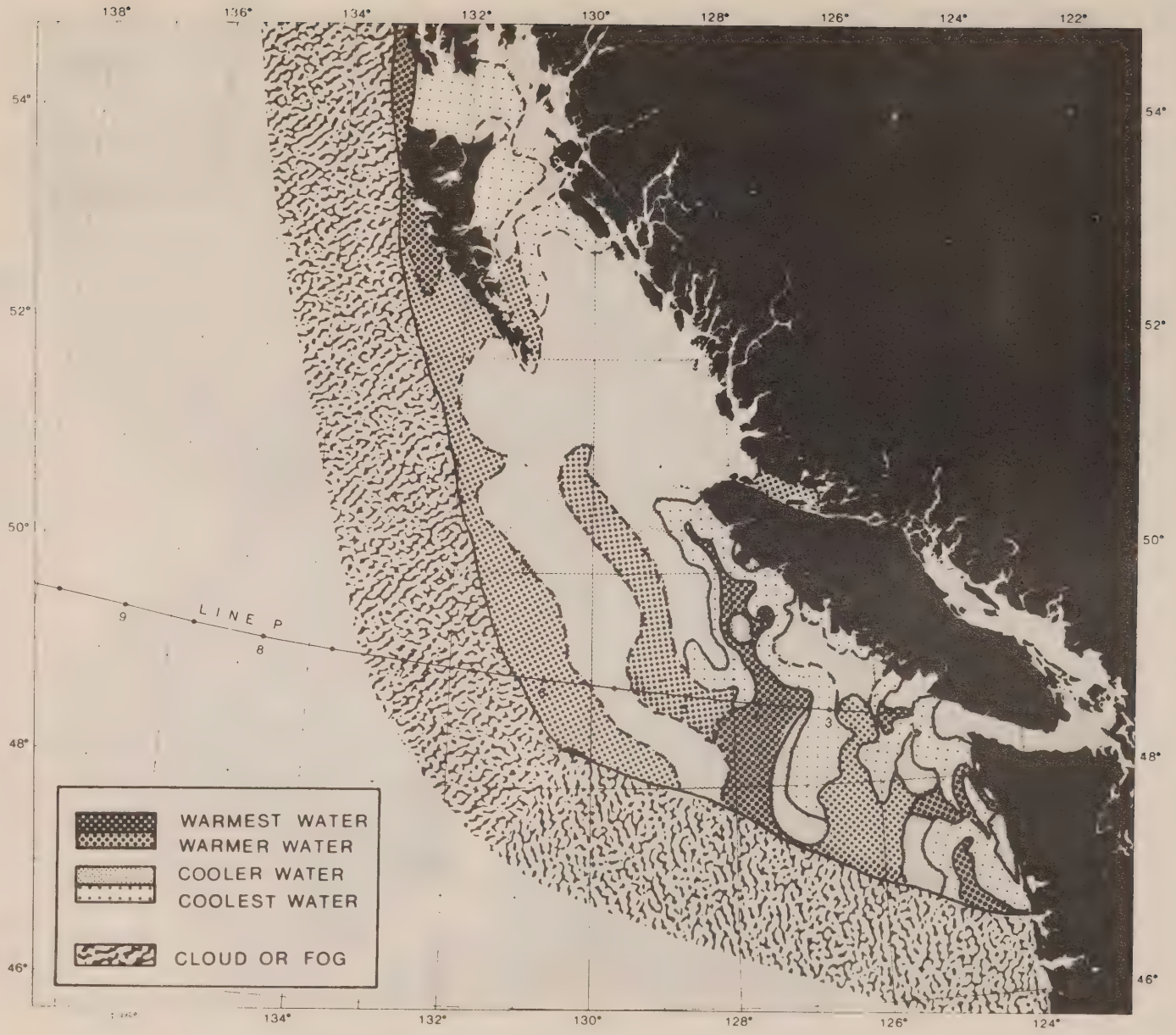

FIGURE 5-47. 04:04:59 05 JANUARY 1979 1010 NOAA 5

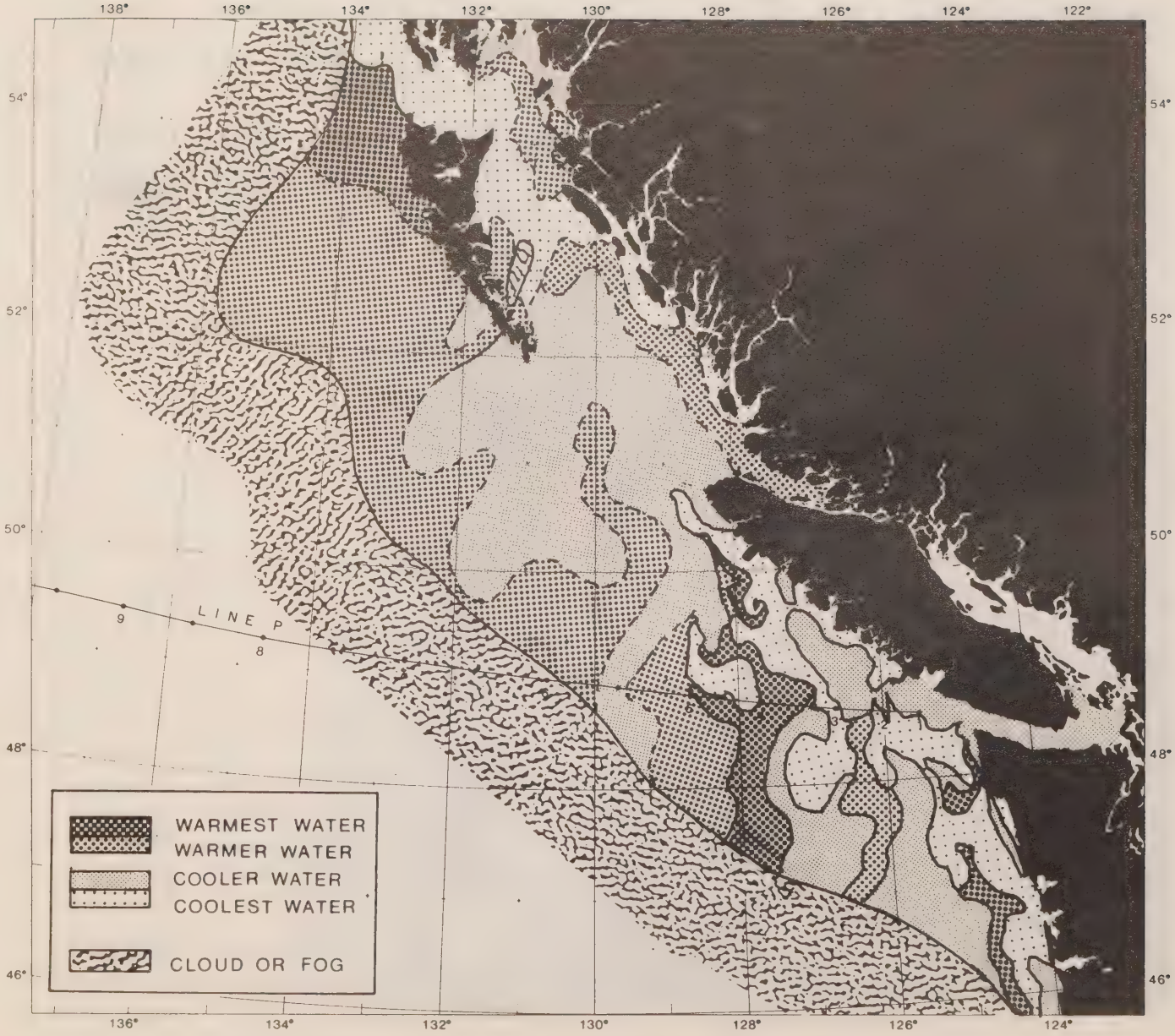

FIGURE 5-48. 18:01:27 05 JANUARY 1979 1017 NOAA 5

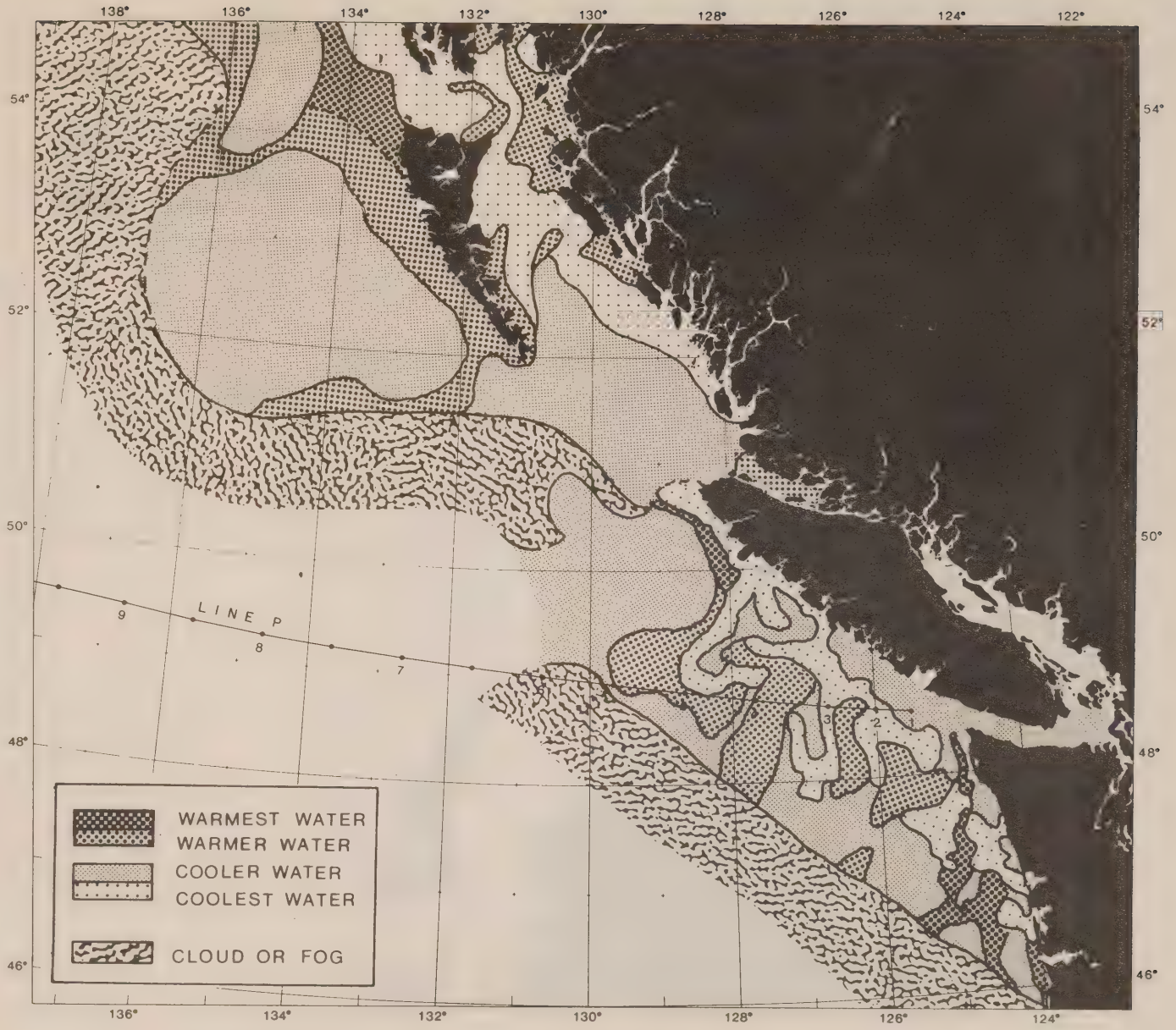

FIGURE 5-49. 04:33:13 07 JANUARY 1979 1035 NOAA 5

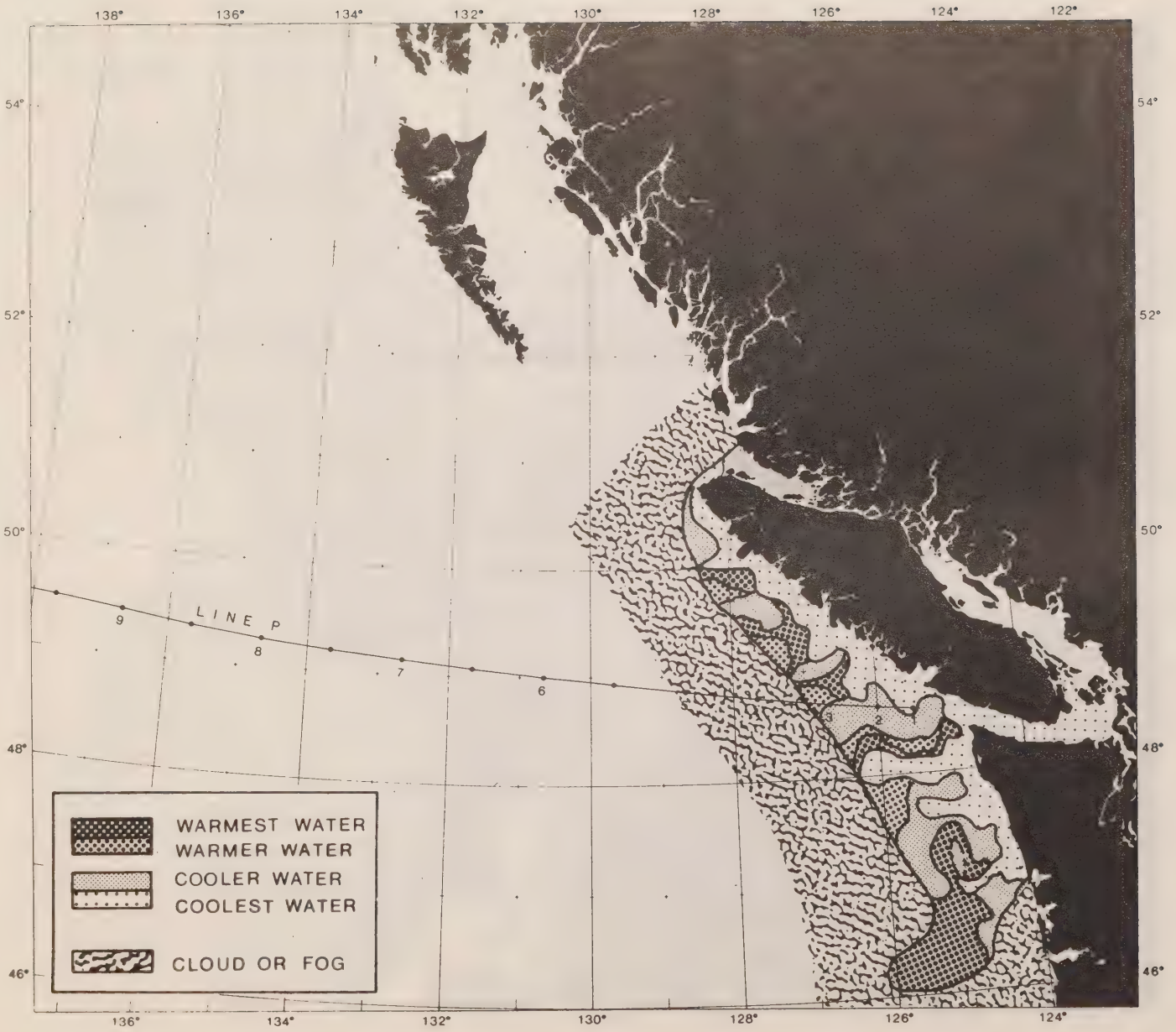

FIGURE 5-50. 17:55:09 21 JANUARY 1979 1215 NOAA 5

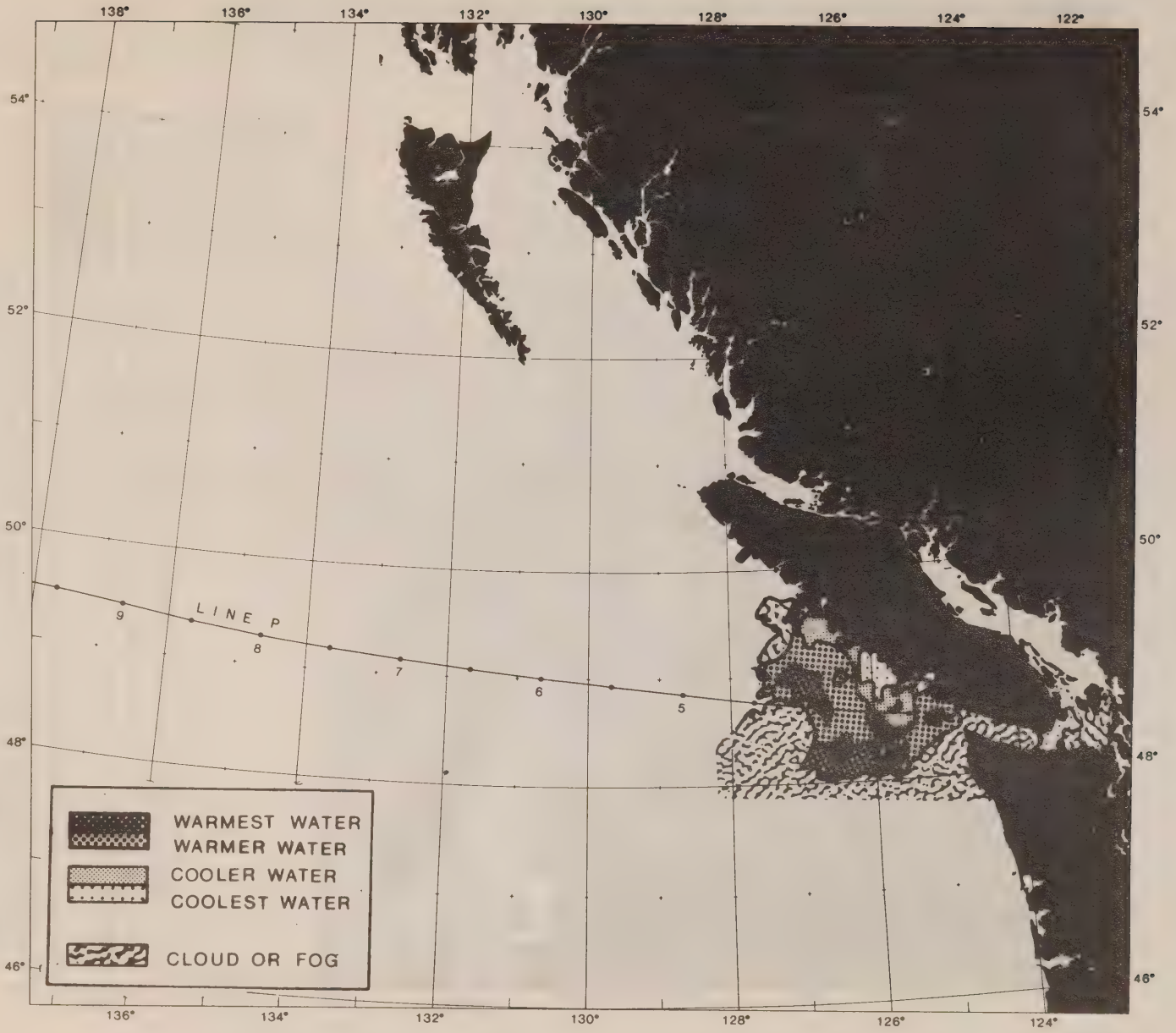

FIGURE 5-51. 23:06:06 11 JULY 1979 3829 TIROS-N

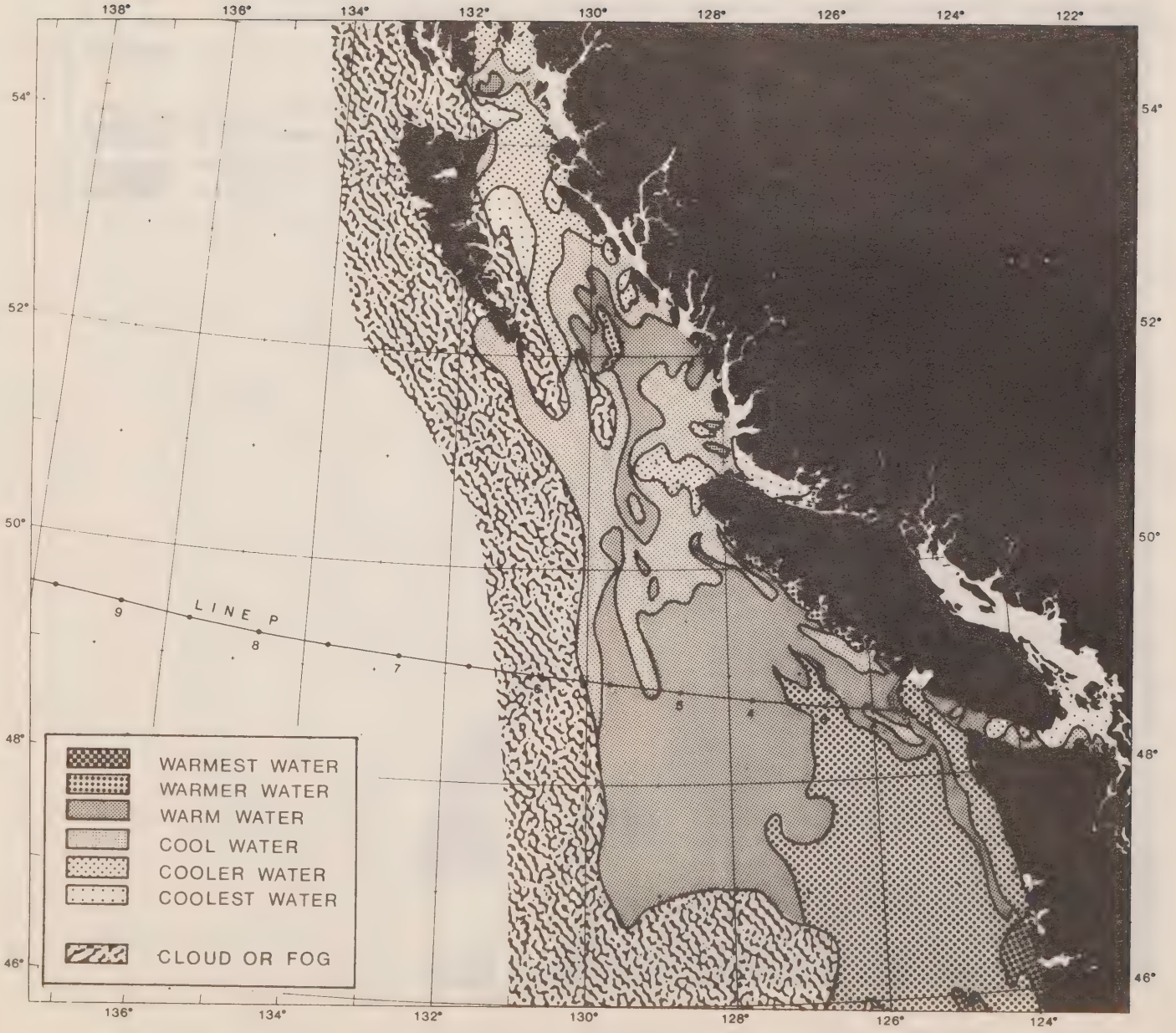

FIGURE 5-52. 22:33:47 14 JULY 1979 3871 TIROS-N

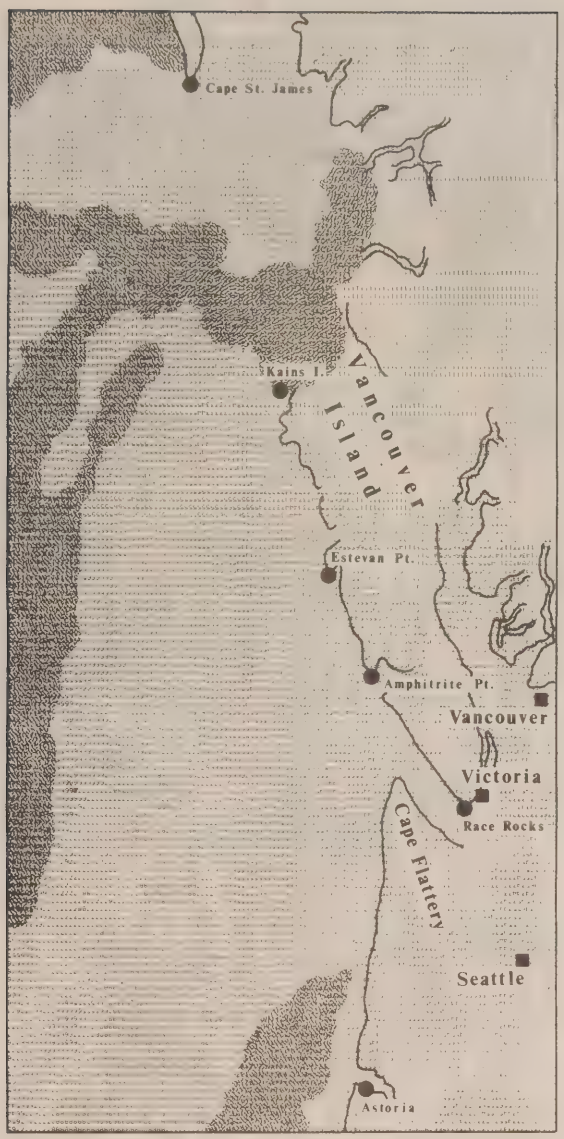

Figure 6. Sea surface temperatures derived from original infrared satellite data of 0330 GMT, 9 September 1975 (these data were used by NOAA to produce the imagery shown in Figure 2).

(a) Grey-scale digitized imagery. The numerals represent the averages of 7 x 8 pixels (equivalent to average temperatures of an area 6 km x 7 km), the lower and higher numerals representing the lower and higher temperatures, respectively. The area covered in this illustration is shown as the small bordered portion in Fig. 2.

Figure 6. Sea surface temperatures derived from original infrared satellite data of 0330 GMT, 9 September 1975 (these data were used by NOAA to produce the imagery shown in Figure 2).

(b) Isotherms (^{o}C) constructed from data shown in Fig. 6a. The dashed lines over the ocean represent the cruise track of CFAV *Endeavour* (19 August - 10 September 1975).

Figure 7. Sea surface temperatures (^{o}C) derived from original infrared satellite data of 1709 GMT, 10 September 1975 (these data were used by NOAA to produce the imagery shown in Fig. 3).

CA1
EP321
-79R20

Pacific Marine Science Report 79-20

Publication

FEB 5 1981
University of Toronto

A THREE-DIMENSIONAL SUBSURFACE MOORING MODEL

by

W.H. Bell

INSTITUTE OF OCEAN SCIENCES, PATRICIA BAY
Sidney, B.C.

For additional copies or further information please write to:

Department of Fisheries and Oceans
Institute of Ocean Sciences
P.O. Box 6000
Sidney, B.C. CANADA
V8L 4B2

C41
EP 321
-79R20

Pacific Marine Science Report 79-20

A THREE-DIMENSIONAL SUBSURFACE MOORING MODEL

by

W.H. Bell

Institute of Ocean Sciences, Patricia Bay

Sidney, B.C.

1979

ABSTRACT

A static single-point mooring model is developed for use in the analysis of moored instrument array geometry and for the interpretation of collected data. The model incorporates the steady three-dimensional hydrodynamic forces exerted by a space-varying velocity field acting on a moored system comprised of a subsurface buoy, a stretchable cable and various instrument packages. The system equations are solved by piecewise integration down the cable. The computer program provides a comprehensive listing of coordinates, angles, forces, etc.

CONTENTS

	Page
Abstract	i
Contents	ii
Introduction	1
Theoretical Analysis of the Buoy-Cable System	1
A. The Buoy	1
B. The Cable	5
C. The Instruments	11
D. Method of Solution of System Equations	13
Computer Solution of the Buoy-Cable System	13
A. The Buoy	13
B. The Instrument	13
C. The Cable	14
D. The Velocity Profile	15
E. The Iteration Procedure	15
F. Program Output	16
G. Verification	16
Conclusion	16
References	17
Appendix A - Sample Computation	18
Appendix B - Program Source Listing	25

FIGURES

Figure 1.	Cable segment in the principal reference frame	3

TABLES

Table I.	FORTRAN Coding Form For Mooring Program Example.	19
Table II.	Output Listing For Mooring Program Example.	21

Introduction

The Coastal Zone Oceanography Group at the Institute of Ocean Sciences, located at Sidney, B.C., makes frequent use of moored instrument arrays for the measurement of ocean currents and seawater properties. The moorings are usually single-point taut-line types, often supported by subsurface buoys. Some time ago, it was found expedient to develop a static two-dimensional model to aid in the design of the moored systems and in the analysis of the data obtained therefrom. This development was described in Pacific Marine Science Report 77-12 (Bell, 1977), entitled *Static Analysis of Single-Point Moorings*. The two-dimensional model has proved to be a valuable design tool, but has sometimes been inadequate for problems of the "hindcasting" type because the data are, very often, three-dimensional in nature. Therefore, it was decided to revise the model to provide a three-dimensional capability, as reported herein.

Certain material included in PMSR 77-12, pertaining to the utility of models, mooring cable elasticity and hydrodynamic drag, is not repeated. We suggest that a perusal of that report might be a worthwhile preliminary to a study of the present one. Although not a prerequisite for proper application of the three-dimensional model given here, it could provide some additional insight into the problem. The capability for using either a surface or subsurface buoy, which was incorporated into the computer program for the two-dimensional mooring model, has not been retained in the new model. In retrospect, it appeared simpler to write and apply separate routines for the two cases. The three-dimensional model does include such details as elastic cable, varying cable types along the length of the mooring line, instrument or buoyancy packages attachable along the line and a space-varying velocity profile.

Theoretical Analysis of the Buoy-Cable System

A. The Buoy

No particular buoy geometry has been assumed in the development of the model. In practice, the shape of the buoy may result in the generation of lift forces, or moments of forces, and no account of such complications is taken here. The simplest case only is considered, the basic assumptions being:

1. The line of action of all forces is through the centre of gravity of the buoy.

2. There are no cross-flow forces, i.e. no lift or kiting forces.

3. There is no change in drag coefficient with a change in buoy aspect.

The justification for retaining as much simplicity as possible is that the mooring system configuration is primarily determined by weight and buoyancy forces and by cable drag, buoy drag usually being a relatively unimportant feature.

To begin, flow velocity components U, V and W are specified in a Cartesian coordinate system (called here the principal reference frame) along the directions of the X, Y and Z axes, respectively, where Z is vertical and positive upwards. The components (Fig. 1) have a resultant velocity vector R whose orientation is defined by the angle ϕ in the vertical plane and γ in the horizontal plane, and whose magnitude is given by:

$$R^2 = U^2 + V^2 + W^2 \tag{1}$$

Therefore:

$$R = \frac{U}{\sin\phi \sin\gamma} = \frac{V}{\sin\phi \cos\gamma} = \frac{W}{\cos\phi} = \frac{(U^2 + V^2)^{\frac{1}{2}}}{\sin\phi} \tag{2}$$

and

$$\phi = \cos^{-1}\left(\frac{W}{R}\right) \tag{3}$$

$$\gamma = \tan^{-1}\left(\frac{U}{V}\right) \tag{4}$$

The angle ϕ is here called the current tilt and γ is the current direction.

The buoy is considered as a free body, with the various force components acting through its centre of gravity. It is assumed that the buoy drag coefficient C_{DB} is independent of the aspect presented to the current, as stated above. The cross-sectional area of the buoy is A_B. The drag force is given by:

$$D_B = C_{DB} \frac{\rho}{2} A_B R|R| \tag{5}$$

with components:

$$\begin{aligned} D_{BX} &= D_B \sin\phi \sin\gamma \\ D_{BY} &= D_B \sin\phi \cos\gamma \\ D_{BZ} &= D_B \cos\phi \end{aligned} \tag{6}$$

The weight force W_B and buoyancy force B_B have components in the Z-direction only, so that the gravitational force components are:

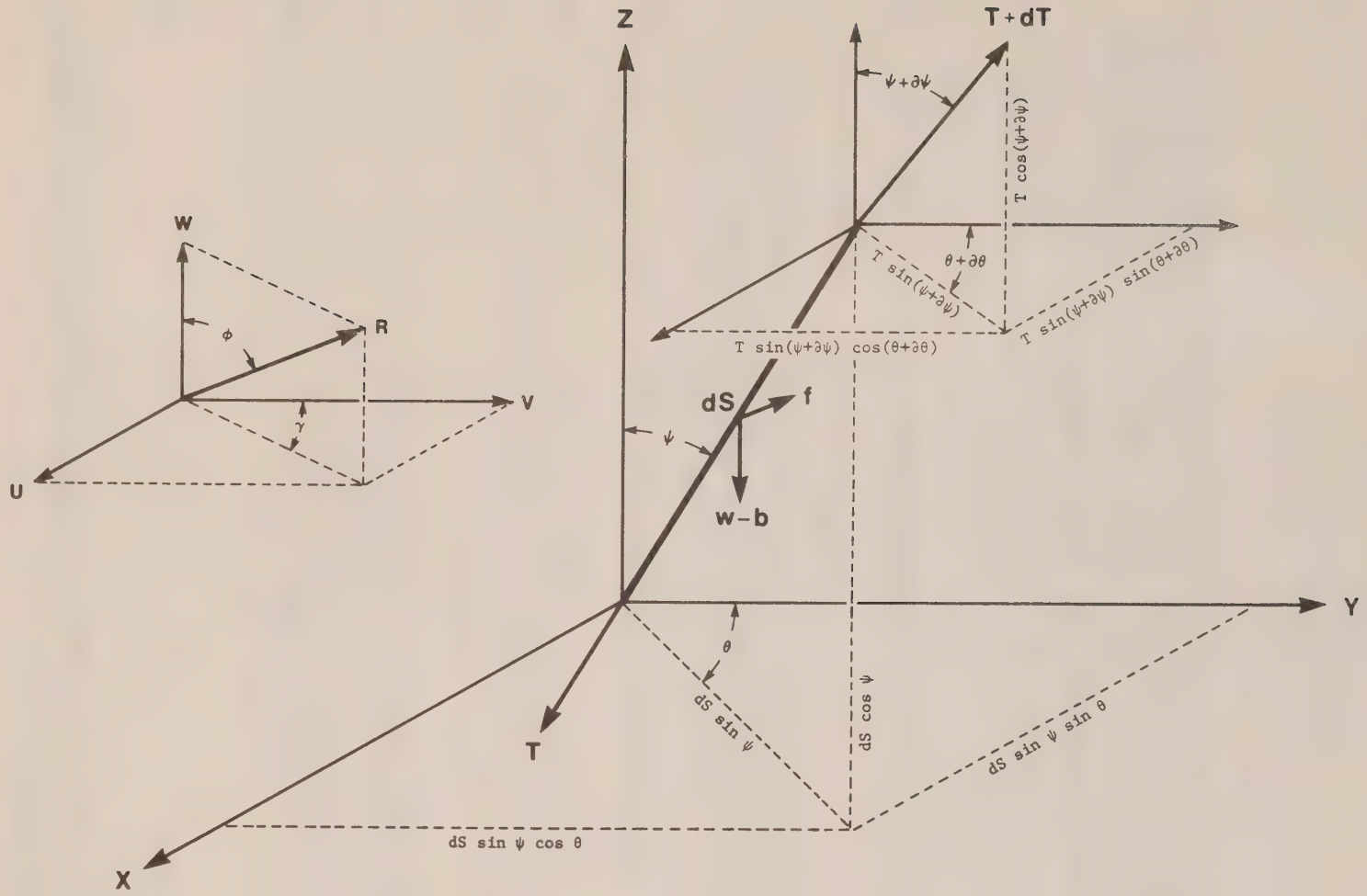

Figure 1. Cable segment in the principal reference frame

$$G_X = G_Y = 0$$
$$G_Z = B_B - W_B \tag{7}$$

Tension components, due to the reaction of the mooring cable at the point of attachment, must also be taken into account. The orientation of the cable (Fig. 1) is defined by the angles θ and ψ, where θ lies in the horizontal plane and is here called the cable azimuth, and ψ is in the vertical plane and is called the cable angle. The tension components are:

$$T_X = -T \sin \psi \sin \theta$$
$$T_Y = -T \sin \psi \cos \theta \tag{8}$$
$$T_Z = -T \cos \psi$$

Summing forces in the three component directions, one obtains:

$$-T \sin \psi \sin \theta + D_B \sin \phi \sin \gamma = 0 \tag{9}$$

$$-T \sin \psi \cos \theta + D_B \sin \phi \cos \gamma = 0 \tag{10}$$

$$-T \cos \psi + D_B \cos \theta + (B - W) = 0 \tag{11}$$

From Equations (9) and (10):

$$\tan \theta = \tan \gamma \tag{12}$$

therefore:

$$\theta = \gamma \tag{13}$$

(which was to be expected because the horizontal components of the drag force, resulting from the horizontal velocity components, determine the direction of the tension force at the buoy).

From Equations 10, 11 and 13:

$$\psi = \tan^{-1}\left[\frac{\sin\phi}{(B-W)/D_B + \cos\phi}\right] \tag{14}$$

and:

$$T = D_B \frac{\sin\phi}{\sin\psi} \tag{15}$$

Equations 3, 4, 5, 13, 14 and 15 are solved to provide values of θ, ψ and T at the buoy. These, together with coordinate values (X, Y, Z), provide the initial conditions at the upper end of the mooring cable.

B. The Cable

Assumptions made in modelling the mooring cable are as follows:

1. The cable is flexible and extensible.

2. The cable diameter is not significantly reduced when stretching occurs, i.e. radial strain is neglected. This has implications for the drag cross-sectional area and for the displaced volume, but the effect is minute, for steel cables at least.

3. Cable drag can be separated into normal and longitudinal components.

4. No strumming occurs explicitly, although its effect can, perhaps, be simulated by means of a larger-than-normal drag coefficient.

The solution of the cable free-body equations is more easily accomplished in a system of cable coordinates, rather than in the principal reference frame. This system is defined by first rotating the XY-plane (Fig. 1), through the angle θ about the Z-axis, to bring the Y-axis into coincidence with the tangent to the projection of the cable on the XY plane. One now has a new set of axes x', y' and z', say, where:

$$\begin{aligned} x' &= X\cos\theta - Y\sin\theta \\ y' &= X\sin\theta + Y\cos\theta \\ z' &= Z \end{aligned} \tag{16}$$

Next, rotate the y'z'-plane through the angle ψ about the x'-axis to bring the z'-axis into coincidence with the tangent to the projection of the cable on the y'z'-plane. Now one has the cable coordinate axes x, y and z, where:

$$\begin{aligned} x &= X \cos\theta - Y \sin\theta \\ y &= X \sin\theta \cos\psi + Y \cos\theta \cos\psi - Z \sin\psi \\ z &= X \sin\theta \sin\psi + Y \cos\theta \sin\psi + Z \cos\psi \end{aligned} \tag{17}$$

This is more readily expressed in matrix form as:

$$C = AI \tag{18}$$

or:

$$I = A^{-1}C \tag{19}$$

where C is the column matrix of any vector quantity in the cable coordinate system and I is the column matrix of the corresponding vector quantity in the principal reference frame. The transformation matrix A and the inverse matrix A^{-1} are given by:

$$A = \begin{bmatrix} \cos\theta & -\sin\theta & 0 \\ \sin\theta\cos\psi & \cos\theta\cos\psi & -\sin\psi \\ \sin\theta\sin\psi & \cos\theta\sin\psi & \cos\psi \end{bmatrix} \tag{20}$$

and:

$$A^{-1} = \begin{bmatrix} \cos\theta & \sin\theta\cos\psi & \sin\theta\sin\psi \\ -\sin\theta & \cos\theta\cos\psi & \cos\theta\sin\psi \\ 0 & -\sin\psi & \cos\psi \end{bmatrix} \tag{21}$$

The matrix relationships can be used to obtain the cable system velocity components, namely:

$$\begin{aligned} u &= U \cos\theta - V \sin\theta \\ v &= U \sin\theta \cos\psi + V \cos\theta \cos\psi - W \sin\psi \\ w &= U \sin\theta \sin\psi + V \cos\theta \sin\psi + W \cos\psi \end{aligned} \tag{22}$$

The magnitude of the resultant velocity is:

$$u^2 + v^2 + w^2 = R^2 \tag{23}$$

and its orientation in the cable system is defined by the angles η in the xz-plane and λ in the xy-plane. The following relationships hold:

$$R = \frac{u}{\sin\eta \sin\lambda} = \frac{v}{\sin\eta \cos\lambda} = \frac{w}{\cos\eta} = \frac{(u^2 + v^2)^{\frac{1}{2}}}{\sin\eta} \tag{24}$$

so:

$$\eta = \cos^{-1}\left(\frac{w}{R}\right) \tag{25}$$

$$\lambda = \tan^{-1}\left(\frac{u}{v}\right) \tag{26}$$

An element of cable length dS is considered. This element lies in the direction of the z-axis and its location in the principal reference frame can be found by integrating along the cable length S over the directional derivatives:

$$\begin{aligned} \frac{dX}{dS} &= \sin\theta \sin\psi \\ \frac{dY}{dS} &= \cos\theta \sin\psi \\ \frac{dZ}{dS} &= \cos\psi \end{aligned} \tag{27}$$

In considering the hydrodynamic drag forces on the cable, the Independence Principle of fluid dynamics is assumed to apply (Schlichting, 1960), i.e. the normal drag force depends only on the normal velocity (the component in the xy-plane). This force comprises both pressure drag and skin friction. The longitudinal drag force consists solely of skin friction, with the stress proportional to the longitudinal velocity. Thus, two independent forces exist:

$$\begin{aligned} f_N &= (f_x^2 + f_y^2)^{\frac{1}{2}} \propto (u^2 + v^2) \\ f_L &= f_z \propto w^2 \end{aligned} \tag{28}$$

If q, r and s are drag forces per unit length in the x, y and z directions, respectively, then:

$$\begin{aligned} f_x &= q\, dS \\ f_y &= r\, dS \\ f_z &= s\, dS \end{aligned} \tag{29}$$

To solve for q, r and s, the usual convention is followed of assigning a non-dimensional drag coefficient as the proportionality constant in Equations 28. Thus:

$$f_N = C_D \frac{\rho}{2} (u^2 + v^2) D \, dS \tag{30}$$

where D is the cable diameter and C_D incorporates the effects of both pressure drag and normal skin friction. C_D can be written as:

$$C_D = C_P + C_{FN} \tag{31}$$

where the pressure coefficient C_P is measured at $\eta = 90°$, and the skin friction coefficient C_{FN} is a function of Reynolds number R_e. Also:

$$f_L = C_{FL} \frac{\rho}{2} R^2 \pi D \, dS \tag{32}$$

where the longitudinal skin friction coefficient is a function of both the angle η and R_e, as:

$$C_{FL} = k R_e^{\frac{1}{2}} \cos \eta \sin^{\frac{1}{2}} \eta \tag{33}$$

The constant k is determined empirically. The appropriate form for skin friction coefficients is open to some conjecture. For a fuller discussion of cable drag, the reader is referred to Bell (1977). Now the drag components per unit length can be determined from the foregoing equations, as follows:

$$q = \frac{f_x}{dS} = \frac{f_N \sin \lambda}{dS} = C_D \frac{\rho}{2} D R^2 \sin^2 \eta \sin \lambda$$

$$r = \frac{f_y}{dS} = \frac{f_N \cos \lambda}{dS} = C_D \frac{\rho}{2} D R^2 \sin^2 \eta \cos \lambda \tag{34}$$

$$s = \frac{f_z}{dS} = \frac{f_L}{dS} = C_{FL} \frac{\rho}{2} \pi D R^2$$

Gravity forces on the cable consist of a weight force w per unit length and a buoyancy force b per unit length. The combination acts in the Z-direction, with a magnitude of (b-w)dS on each elemental length of cable. Resolving this in the cable coordinate system:

$$
\begin{aligned}
g_x &= 0 \\
g_y &= (w-b) \sin \psi \, dS \\
g_z &= -(w-b) \cos \psi \, dS
\end{aligned}
\tag{35}
$$

Tension components at the upper end of the cable are, in the principal reference frame:

$$
\begin{aligned}
T_X &= (T+dT) \sin(\psi+d\psi) \sin(\theta+d\theta) \\
T_Y &= (T+dT) \sin(\psi+d\psi) \cos(\theta+d\theta) \\
T_Z &= (T+dT) \cos(\psi+d\psi)
\end{aligned}
\tag{36}
$$

Transforming to the cable coordinate system by use of the previous matrix relationships, and ignoring second order quantities, one obtains:

$$
\begin{aligned}
t_{Ux} &= T \, d\theta \sin \psi \\
t_{Uy} &= T \, d\psi \\
t_{Uz} &= T+dT
\end{aligned}
\tag{37}
$$

At the lower end of the cable:

$$
\begin{aligned}
t_{Lx} &= t_{Ly} = 0 \\
t_{Lz} &= -T
\end{aligned}
\tag{38}
$$

Summing all of the foregoing components in each of the cable coordinate directions gives a set of three equations:

$$\frac{d\theta}{dS} = \frac{-q}{T \sin \psi}$$

$$\frac{d\psi}{dS} = -\frac{1}{T} \{r + (w-b) \sin \psi\} \qquad (39)$$

$$\frac{dT}{dS} = -s + (w-b) \cos \psi$$

These three equations, together with the defining equations for the drag force components, and with Equations 27, are solved simultaneously to obtain all of the required cable parameters.

An inextensible cable has been assumed in the foregoing. If an elastic cable is desired, then it is necessary to make the following substitutions, where ε is the elongation per unit length:

$$dS \rightarrow dS\ (1+\varepsilon)$$
$$(w-b) \rightarrow (w-b)/(1+\varepsilon) \qquad (40)$$

Here, the implication is that the weight of one foot of stretched cable is $w/(1+\varepsilon)$ so there is no change in total weight. Further, the buoyancy per foot of stretched cable happens also to be taken as $b/(1+\varepsilon)$, so that some compensation for the effect of radial strain on the displaced water volume is included, although not in the correct formal manner. Any error in this term is small compared to the other forces involved, so it was not considered necessary to formalize it. Also, the effect of radial strain on the drag force term is neglected, again because of its relative insignificance. To approximate the elastic characteristics of various cable materials, it is convenient to use a second-order curve:

$$1 + \varepsilon = a_0 + a_1 T + a_2 T^2 \qquad (41)$$

where T is the tension and a_0, a_1, a_2 are constants to be determined from the material specifications supplied by the cable manufacturers. An expanded discussion of this subject is available in Bell (1977). The set of equations for a stretchable cable is, then:

$$\frac{d\theta}{dS} = \frac{-q(1+\varepsilon)}{T \sin \psi}$$

$$\frac{d\psi}{dS} = -\frac{1}{T} \{r(1+\varepsilon) + (w-b) \sin \psi\}$$

$$\frac{dT}{dS} = -s(1+\varepsilon) + (w-b) \cos \psi \qquad (42)$$

$$\frac{dX}{dS} = (1+\varepsilon) \sin \theta \sin \psi$$

$$\frac{dY}{dS} = (1+\varepsilon) \cos \theta \sin \psi$$

$$\frac{dZ}{dS} = (1+\varepsilon) \cos \psi$$

C. The Instruments

Instrument packages of various shapes and sizes may be attached to the cable at various locations along its length. Here, as for the buoy, only the simplest case is considered. All of the forces act through the centre of gravity and the drag coefficient is not a function of aspect. The instrument has a weight W_I in air, a buoyancy B_I, a drag coefficient C_{DI} and a cross-sectional area A_I. Its presence in the system causes incremental changes, at the point of attachment, in line angle, line azimuth and tension, given by $\Delta\psi$, $\Delta\theta$ and ΔT, respectively. The drag on the instrument is given by:

$$D_I = C_{DI} \frac{\rho}{2} A_I R|R| \qquad (43)$$

In the principal reference frame, the drag force components are:

$$D_{IX} = D_I \sin \phi \sin \gamma$$

$$D_{IY} = D_I \sin \phi \sin \gamma \qquad (44)$$

$$D_{IZ} = D_I \cos \phi$$

The tension components at the upper cable attachment point are:

$$\begin{aligned} T_{UX} &= T \sin\psi \sin\theta \\ T_{UY} &= T \sin\psi \cos\theta \\ T_{UZ} &= T \cos\theta \end{aligned} \tag{45}$$

At the lower cable attachment point, they are:

$$\begin{aligned} T_{LX} &= -(T-\Delta T) \sin(\psi+\Delta\psi) \sin(\theta+\Delta\theta) \\ T_{LY} &= -(T-\Delta T) \sin(\psi+\Delta\psi) \cos(\theta+\Delta\theta) \\ T_{LZ} &= -(T-\Delta T) \cos(\psi+\Delta\psi) \end{aligned} \tag{46}$$

The gravity force is:

$$\begin{aligned} H_X &= H_Y = 0 \\ H_Z &= B_I - W_I \end{aligned} \tag{47}$$

Summing the components in the three coordinate directions, and solving the resulting equations, gives the new cable azimuth, angle and tension due to the presence of the instrument as:

$$\theta+\Delta\theta = \tan^{-1}\left[\frac{D_{IX} + T \sin\psi \sin\theta}{D_{IY} + T \sin\psi \cos\theta}\right] \tag{48}$$

$$\psi+\Delta\psi = \tan^{-1}\left[\frac{D_{IY} + T \sin\psi \cos\theta}{\cos(\theta+\Delta\theta)\ \{D_{IZ} + T \cos\psi + B_I - W_I\}}\right] \tag{49}$$

$$T-\Delta T = \frac{D_{IZ} + T \cos\psi + B_I - W_I}{\cos(\psi+\Delta\psi)} \tag{50}$$

Some instrument packages may be very buoyant or very heavy, so the simplifying approximations for small changes in angle cannot be made here.

D. Method of Solution of System Equations

The equations for the complete buoy-cable system are first-order non-linear and form a boundary-value problem requiring boundary conditions at each end of the cable. The buoy boundary condition is satisfied by assuming an elevation for the buoy. This, in turn, fixes the velocity and permits calculation of the conditions at the upper end of the cable. The anchor boundary condition is that the elevation of the anchor must coincide with that of the sea bottom, within acceptable limits. The governing equations are solved for the unknown coordinates, angles and tension, by a step-wise integration along the cable, beginning at the buoy end, to a point of discontinuity resulting from the concentrated loads caused by the presence of an instrument package. The effect of the forces on the package is added to the cable forces and the integration is continued in a similar fashion until the lower end of the cable is reached. If the anchor boundary condition is not satisfied within the specified error limits, then a new buoy position is chosen and the procedure is repeated.

Computer Solution of the Buoy-Cable System

A. The Buoy

No specific geometry having been used in formulating the model, the only buoy-related input data required by the computer program is the weight in air of the buoy, the gross buoyancy (i.e. the weight of water displaced) and the product of the drag coefficient and the cross-sectional area presented to the flow. If a characteristic dimension is also included in the input data, then the Reynolds number will be calculated. An initial elevation is assigned to the buoy to fix its position with respect to the velocity field and to the bottom. This elevation is assumed to coincide with the bottom of the buoy, which is the point of attachment of the cable. Calculation of the boundary conditions for this end of the cable can then be carried out directly. Here, and elsewhere throughout the program, numerous tests are incorporated to avoid divide-by-zero situations and similar problems.

B. The Instrument

The program permits various kinds of instrument packages, including floats for additional buoyancy, to be inserted in the system. However, they are represented simply as point forces and should be positioned at multiples of the basic cable segment length used for integration along the cable (discussed in the next section). The instrument locations, in length units along the cable from the buoy, are read into the computer, converted into an integer number of cable segments and stored in an array capable of holding fifteen different values. Because of the conversion, the instrument locations are still correct when the cable is stretched. Other data which must be provided are the weight in air, the gross buoyancy, the cross-sectional area presented to the flow and the drag coefficient. Any shackles or other fittings located near an instrument should have their weights accounted for by including them in the instrument weight. Before each integration is made, the program checks to see if there is an instrument at the upper end of the cable segment. If so, the velocity is determined and the instrument drag calculated. Then the resulting increments in cable tension and angles are combined with the preceding values of these variables.

C. The Cable

The integration along the cable is carried out over a series of cable segments which are of equal length when unstretched, this length being a sub-multiple of the total cable length. The choice of segment size depends on the problem parameters, such as the complexity of the velocity profile, the number and location of instrument packages, etc. The integration routine uses the Runge-Kutta method with error control. An external subroutine specifies the functions required for the evaluation of the derivatives given in Equations 42. The integration routine also requires the specification of an error tolerance on the integral, a step size, and a value of the independent variable at the end point of the integration. Double precision is used throughout to reduce the possibility of cumulative rounding errors.

For a stretchable cable and step-wise integration, the end point must correspond to the strained length of each cable segment. This requires that the independent variable be stretched as well, i.e. Equation 42 is divided through by the quantity $(1+\varepsilon)$, giving $(1+\varepsilon)dS$ as the independent variable instead of dS. In the program, the strained unit length $(1+\varepsilon)$ is represented by the function STRCH. It is calculated on the basis of the tension at the upper end of a cable segment. For greater accuracy, this tension could include one-half of the tension increment for the previous segment. Generally speaking, however, the increment is usually no more than a few tenths of one percent of the tension, so this correction is ignored here. If required, the accuracy can be improved by reducing the segment length. Any necessity for this is easily checked by running the model for two different segment lengths.

The boundary conditions for the first cable segment are provided by the buoy calculations, and for subsequent segments by the results of the integration over the preceding cable segment. The velocity used for calculating cable drag is that which occurs at the midpoint of the segment, the midpoint elevation being estimated on the basis of the cable angle for the preceding segment. An iteration on the cable angle would result in a slightly more accurate midpoint location and, therefore, a slightly more accurate velocity (only when the velocity profile is not uniform). This was not deemed worthwhile since, for the calculation of drag, the midpoint velocity is assumed to apply over the whole segment in any case. One could incorporate a varying velocity (when such is the case) throughout the integration over a cable segment, but at the expense of a considerable increase in program complexity. Again, if concern is felt about the outcome of the procedure as presently used, especially when the velocity is changing rapidly with depth, the program can be run with small segment lengths. Some trial runs in which the segment lengths were varied by factors of two or more, all other variables remaining unchanged, showed no variation in the results. Thus, the indication is that the simple procedure used to obtain the velocity for the drag determination is adequate. Also, while only an average velocity value is used in the drag calculation, the dependence of the drag on the actual cable angle is included throughout the integration along a cable segment since the angle is one of the dependent variables.

The mooring line used in the model is not restricted to one size or one kind of material throughout its length. Presently, ten different cable types can be incorporated. Information on these, including the distance from

the buoy of the lower end of each type, is read into an array. Then (as is done for the instruments), the end position is converted into an integer number of cable segments, the conversion permitting an easy check on type changes as well as allowing cable stretch without causing any additional problems. The form of the longitudinal drag equation used with each type is optional, the choice being either that for smooth cable, for wire rope, or no axial drag at all. The selection is made by assigning an appropriate logical flag in the input data.

D. The Velocity Profile

Provision is made in the model for incorporating a three-dimensional velocity field around the cable in terms of the components U, V and W. The speed versus depth relationships for the components are represented by first-order profile segments of the form:

$$\begin{aligned} U &= a_1 + b_1 Z \\ V &= a_2 + b_2 Z \\ W &= a_3 + b_3 Z \end{aligned} \tag{51}$$

where Z is the elevation above the sea floor. Up to ten such segments can be pieced together for each component, permitting the simulation of a fairly complex velocity field. The profile segments can be any convenient size and do not have to correspond to multiples of the cable segment length. In the program, the velocity profile information is stored in an array, the first element in each row being the lower depth limit of applicability (measured from the sea floor) of the three-dimensional segment whose coefficients (a_1, b_1, a_2, b_2, a_3, b_3) are given by the other elements of that row. A conditional branch on the depth is used in the various calculations to obtain the correct velocity at a given depth.

E. The Iteration Procedure

The solution of the buoy-cable model is based on making an estimate of the buoy position with respect to the bottom and, proceeding from there, integrating along the cable to the anchor. If the anchor elevation doesn't coincide with the bottom elevation, within specified limits, the estimate of the buoy position is modified and another integration is performed. A simple additive modification of the buoy position is made for the first iteration, using the error in the anchor location. Subsequent iterations use a procedure which is, perhaps, more complex than necessary for subsurface moorings since it is a carry-over from the two-dimensional model, where the complexity was required for truculent cases involving surface floats. It does seem to provide a more rapid convergence to the correct solution than does any simpler scheme tried. The program halts when more than fifteen iterations are required, but subsurface moorings seldom take more than one or two.

F. Program Output

The first portion of the program output lists information associated with the integration and iteration routines. In particular, the various estimates of buoy elevation and the resulting anchor position are given for each iteration. Following this there is a listing of all pertinent input and output data about the buoy-cable system and the velocity profile, including items such as instrument package drag and position coordinates.

Next, a printer plot of the coordinate system is given as in *aide-memoire* when perusing the various angular quantities in the tabulation which follows. This table gives the coordinates, tensions, forces and velocities corresponding to the solution of the system equations for each cable segment. The cable drag values given in this table are for unit cable length. The drag value listed in the j-th row applies to the segment whose lower-end coordinates are also listed in the j-th row.

G. Verification

The model has been exercised in all eight octants with the same contrived three-dimensional data set and appropriate symmetrical results obtained. This implies that there were no basic programming errors in implementing the three-dimensional equations since, if errors had been made, one might expect some asymmetries to appear. The model has also been applied to field data previously used to verify the two-dimensional program and identical results obtained. Taken together, the results of these tests have inspired confidence in the use of the model for three-dimensional predictions although, as yet, no adequate field data set has been available for a proper three-dimensional verification. In particular, adequate velocity profile information is required because of the square law dependence of drag on flow speed.

Conclusion

A model of a static single-point subsurface mooring system has been developed for predicting system geometry in a three-dimensional velocity field. It incorporates a flexible, extensible cable whose characteristics may be varied over different portions of the system and it permits the inclusion of instrument packages at various locations along the cable. The accuracy of results obtained from the model depends in large measure on the provision of accurate velocity information.

References

Bell, W.R. 1977. Static Analysis of Single-Point Moorings. Pac. Mar. Sci. Rept. 77-12. Institute of Ocean Sciences, Patricia Bay, Victoria, B.C.

Schlichting, H. 1960. Boundary Layer Theory. McGraw-Hill, N.Y.

Appendix A - Sample Computation

The program is here applied to a system comprising a subsurface float, two instrument packages and a 100 ft length of cable which is mainly wire rope with a short segment of nylon line at the lower end. The FORTRAN coding form for this example is given in Table I.

The first data card provides the buoy specifications, with ten columns allotted for each of the following: the gross buoyancy (weight of water displaced - 600 lbs in this instance), the buoy weight in air (300 lbs), the diameter (3 ft) or some other characteristic length, and the product of drag coefficient and cross-sectional area presented to the flow (4.2 sq ft).

The next cards in sequence provide information on the cable. Here, two different types are used. The second data card is for ¼" diameter wire rope whose lower end is at a distance of 90 ft along the cable from the buoy, as shown in Column 1-7. The next five sets of seven columns each are used to specify, in the order given, cable gross buoyancy per unit length (0.022 lbs/ft), weight in air per unit length (0.100 lbs/ft), diameter (0.021 ft), drag coefficient (1.4) for flow in a direction normal to the cable and drag coefficient (0.0) for flow parallel to the cable axis. Beginning in Column 43, there are three sets of ten columns each which can contain the coefficients for a second-order fit to the fractional stress-strain relationship for the cable. In this instance, since wire rope is being used, Hooke's Law is obeyed so only first-order coefficients are required (1.0, 2.4×10^{-6}, 0.0). Columns 73-75 contain logical variables used for selecting the form of the longitudinal drag equation. If a "T" appears in Column 73, a form appropriate to smooth wire is used; if in Column 74, the form is for rough wire; if in Column 75, longitudinal drag is ignored altogether (as here). The third data card represents a segment of ½" diameter nylon line whose lower end is 100 ft from the buoy. Buoyancy, weight, diameter and drag coefficients are, respectively: 0.045 lbs/ft, 0.050 lbs/ft, 0.036 ft, 1.4, 0.1. The stress-strain coefficients are 1.045, 1.125×10^{-4} and 1.389×10^{-8}, as determined from a graph supplied by the manufacturer of the line. The "T" in Column 74 shows that the rough wire longitudinal drag equation is being used for this case. Up to ten different cable types may be represented in the model, each with its own data input card. If the number of types used is less than ten, the sequence must be terminated with an end-of-file indication. Hence, the fourth card here contains @ EOF.

Next, the instrument package data is supplied. The fifth and sixth cards contain, in Columns 1-10, the locations of the instruments in distance along the cable from the buoy. Instruments must be positioned at multiples of the basic segment length, as mentioned in the text. In this example, the length is 5 ft and the instruments are at 85 and 90 ft. Then Columns 11-20 of each card contain the gross buoyancy (50 lbs and 20 lbs, respectively, for the two instruments), Columns 21-30 show the weight in air (15 and 50 lbs), Columns 31-40 hold the cross-sectional area for the drag calculation (0.8 and 1.5 sq ft) and Columns 41-50 contain the drag coefficient (0.6 and 1.1). Since the number of instrument data cards is less than the maximum number of fifteen, the next card must be an end-of-file indicator.

TABLE I. FORTRAN CODING FORM FOR MOORING PROGRAM EXAMPLE

IBM

FORTRAN CODING FORM

Form GX09-0011-0 U/M050
Printed in Canada

PROGRAM: MOORING PROGRAM EXAMPLE
PROGRAMMER: W.H. BELL
DATE: 20/10/79
PUNCHING INSTRUCTIONS: GRAPHIC / PUNCH
PAGE 1 OF 1
CARD ELECTRO NUMBER*

Card No.	COMM	STATEMENT NUMBER	CONT	FORTRAN STATEMENT	IDENTIFICATION SEQUENCE
1.				600. 300. 3. 4.2	
2.				90. .022 .100 .021 1.4 .0 1. 2.4 E-06	FFT
3.				100. .045 .050 .036 1.4 .1 1.045 1.125 E-04-1.389E-08	FTF
4.				@EOF	
5.				85. 50. 15. .8 .6	
6.				90. 20. 50. 1.5 1.1	
7.				@EOF	
8.				60. 2. 0. 5. 0.	
9.				50. -13. .25 5. 0.	
10.				40. -13. .25 -9. .28	
11.				25. -3. 0. -9. .28	
12.				0. -3. 0. -2. 0.	
13.				@EOF	
14.				20. 100. 100. .25 .01 F	

1 2 3 4 5 6 7 8 9 10 11 12 13 14 15 16 17 18 19 20 21 22 23 24 25 26 27 28 29 30 31 32 33 34 35 36 37 38 39 40 41 42 43 44 45 46 47 48 49 50 51 52 53 54 55 56 57 58 59 60 61 62 63 64 65 66 67 68 69 70 71 72 73 74 75 76 77 78 79 80

* A standard card form, IBM electro 888157, is available for punching statements from this form.

Following on, another five cards are used to provide the velocity profile information. Each card specifies a particular segment of the profile by giving, firstly, the lower limit of applicability of the segment in distance above bottom and, secondly, the coefficients for a linear velocity *vs* depth equation for each component. Thus, the eighth card indicates a uniform velocity, at elevations in the water column greater than 60 ft above bottom, having a U-component of 2 ft/sec, a V-component of 5 ft/sec and no W-component. The ninth card shows that, between 50 and 60 ft above bottom, the velocity components are U = -13 + 0.25 Z, V = 5, W = 0, and similarly for cards ten through twelve. The easiest way of determining the coefficients is to graph each component of the desired velocity profile, for clarity, then obtain a zero or first-order fit to each segment separately. Ten velocity profile segments are provided for in the program; if fewer than this are used, an end-of-file indication must be inserted.

The fourteenth, and final, data card contains the desired number of cable segments (20) in Columns 1-10, the cable length (100 ft) in Columns 11-20 and the initial guess for the buoy elevation (100 ft) in Columns 21-30. The initial guess can be any reasonable value because the iteration procedure usually ensures a rapid closure on the correct position. The permissible iteration error, which is the position accuracy for the anchor end of the cable, is provided in Columns 31-40. Here it is 0.25 ft. The integration subroutine requires the specification of an integration error tolerance, given here as 0.01 in Columns 41-50. Generally, a value of 0.01 to 0.1 has been satisfactory in all of the modelling done to date. Finally, Column 51 contains a logical variable which, if given as "T", will result in the printing of various data as a diagnostic aid, when required.

When the program is run, various listings are produced, as shown in Table II for the present example. These listings are self-explanatory.

TABLE II. OUTPUT LISTING FOR MOORING PROGRAM EXAMPLE

```
NO. OF CABLE SEGMENTS =        20.

INTEGRATION ERROR TOLERANCE =     .01000

PERMISSIBLE ITERATION ERROR =        .25   FT

INITIAL GUESS FOR BUOY POSITION =    100.00   FT ABOVE BOTTOM

     ZED          Y(6)          ZMAX          ZLOW          YMAX          YMIN

   100.00         10.24
    89.76         10.24         100.00         79.51         10.24        -10.24

    89.76          -.66
    90.38          -.66         100.00         89.76         10.24          -.66

    90.38           .00

 NO. OF ITERATIONS REQUIRED WAS    2 .
```

VELOCITY PROFILE :

LOWER LIMIT (FT ABOVE BOTTOM)	U	V	W
60.	2.00 + .00000*Z	5.00 + .00000*Z	.00 + .00000*Z
50.	-13.00 + .25000*Z	5.00 + .00000*Z	.00 + .00000*Z
40.	-13.00 + .25000*Z	-9.00 + .28000*Z	.00 + .00000*Z
25.	-3.00 + .00000*Z	-9.00 + .28000*Z	.00 + .00000*Z
0.	-3.00 + .00000*Z	-2.00 + .00000*Z	.00 + .00000*Z

TABLE II. (continued)

```
BUOY PARAMETERS :

GROSS BUOYANCY =   600.000   LBS
WEIGHT IN AIR =   300.000   LBS
DIAMETER =     3.000   FT
CROSS-SECTIONAL AREA X DRAG COEFFICIENT =     4.200   SQ FT
BUOY COORDINATES (     14.30 ,     42.17 ,     90.38 ).
VERTICAL EXCURSION =      9.62  FT
BUOY DRAG =    121.80  LBS


CABLE PARAMETERS - TYPE 1 :

GROSS BUOYANCY =      .0220   LBS PER FT
WEIGHT IN AIR =      .1000   LBS PER FT
DIAMETER =      .0210   FT
NORMAL DRAG COEFFICIENT =     1.4000
AXIAL DRAG COEFFICIENT =      .0000
ELASTIC COEFFICIENTS: A0= .1000+001  ; A1= .2400-005  ; A2= .0000
LENGTH =    90.000   FT


CABLE PARAMETERS - TYPE 2 :

GROSS BUOYANCY =      .0450   LBS PER FT
WEIGHT IN AIR =      .0500   LBS PER FT
DIAMETER =      .0360   FT
NORMAL DRAG COEFFICIENT =     1.4000
AXIAL DRAG COEFFICIENT =      .1000
ELASTIC COEFFICIENTS: A0= .1045+001  ; A1= .1125-003  ; A2=-.1389-007
LENGTH =    10.000   FT


TOTAL LENGTH OF CABLE =   100.000   FT.


INSTRUMENT PARAMETERS - NO. 1 :

DISTANCE ALONG UNSTRETCHED CABLE FROM BUOY =     85.   FT
BUOYANCY =    50.000   LBS
WEIGHT IN AIR =    15.000   LBS
CROSS-SECTIONAL AREA =      .800   SQ FT
DRAG COEFFICIENT =      .600
INSTRUMENT DRAG IS      6.24  LBS
INSTRUMENT COORDINATES (      1.08 ,      6.33 ,     14.44 ).
VERTICAL EXCURSION =       .56  FT


INSTRUMENT PARAMETERS - NO. 2 :

DISTANCE ALONG UNSTRETCHED CABLE FROM BUOY =     90.   FT
BUOYANCY =    20.000   LBS
WEIGHT IN AIR =    50.000   LBS
CROSS-SECTIONAL AREA =     1.500   SQ FT
DRAG COEFFICIENT =     1.100
INSTRUMENT DRAG IS     21.45  LBS
INSTRUMENT COORDINATES (       .55 ,      4.32 ,      9.89 ).
VERTICAL EXCURSION =          .11 FT
```

TABLE II. (continued)

AN ATTEMPT TO ILLUSTRATE THE COORDINATE SYSTEM USED FOR THE 3-D MOORING MODEL IS PRESENTED BELOW. THE ANGLES ASSOCIATED WITH THE CABLE VECTOR ARE *ANGLE* & *AZIMUTH*, AND WITH THE CURRENT VECTOR ARE *TILT* & *DIRECTION*. NORTH LIES IN THE DIRECTION OF THE Y-AXIS AND EAST IN THE DIRECTION OF THE X-AXIS.

TABLE II. (continued)

CABLE FUNCTIONS :

X (FT)	Y (FT)	Z (FT)	CABLE LENGTH (FT)	ANGLE (DEG)	AZIMUTH (DEG)	TENSION (LB)	NORMAL DRAG (LB/FT)	AXIAL DRAG (LB/FT)	CURRENT SPEED (FT/SEC)	CURRENT DIRECTION (DEG)	CURRENT TILT (DEG)	REYNOLDS NO.
14.30	42.17	90.38	100.88	22.10	21.80	323.78	121.800		5.39	21.80	90.00	.1077+007
13.59	40.40	85.75	95.87	22.80	21.80	323.42	.758	.0000	5.39	21.80	90.00	.6985+004
12.86	38.57	81.15	90.87	23.49	21.80	323.06	.750	.0000	5.39	21.80	90.00	.6950+004
12.10	36.70	76.57	85.86	24.18	21.80	322.71	.743	.0000	5.39	21.80	90.00	.6915+004
11.33	34.77	72.02	80.86	24.86	21.80	322.35	.735	.0000	5.39	21.80	90.00	.6878+004
10.54	32.79	67.49	75.86	25.53	21.80	322.00	.727	.0000	5.39	21.80	90.00	.6841+004
9.73	30.76	62.99	70.85	26.21	21.80	321.65	.719	.0000	5.39	21.80	90.00	.6803+004
8.90	28.69	58.52	65.85	26.87	21.80	321.30	.712	.0000	5.39	21.80	90.00	.6764+004
8.06	26.57	54.06	60.84	27.46	21.57	320.95	.639	.0000	5.11	12.09	90.00	.6409+004
7.21	24.40	49.63	55.84	28.00	21.07	320.61	.623	.0000	5.00	-.45	90.00	.6328+004
6.37	22.19	45.22	50.84	28.39	20.45	320.26	.513	.0000	4.43	-14.96	90.00	.5737+004
5.55	19.94	40.83	45.83	28.61	19.79	319.92	.408	.0000	3.78	-36.38	90.00	.5115+004
4.75	17.68	36.44	40.83	28.70	19.10	319.58	.373	.0000	3.51	-58.81	90.00	.4888+004
3.98	15.41	32.05	35.83	28.70	18.57	319.24	.285	.0000	3.06	-73.92	90.00	.4270+004
3.22	13.13	27.66	30.82	28.62	18.12	318.89	.272	.0000	3.07	-102.07	90.00	.4164+004
2.49	10.85	23.26	25.82	28.44	17.69	318.55	.332	.0000	3.54	-121.95	90.00	.4604+004
1.77	8.59	18.86	20.81	28.24	17.25	318.21	.344	.0000	3.61	-123.69	90.00	.4685+004
1.08	6.33	14.44	15.81	28.05	16.80	317.86	.345	.0000	3.61	-123.69	90.00	.4695+004
1.08	6.33	14.44					6.240					
.55	4.32	9.89	10.81	24.45	14.74	346.78	.359	.0000	3.61	-123.69	90.00	.4792+004
.55	4.32	9.89					21.450					
.25	2.14	4.95	5.39	23.79	7.19	313.07	.625	-.0112	3.61	-123.69	90.00	.8321+004
.00	.00	.00	.00	23.40	5.97	312.99	.629	-.0108	3.61	-123.69	90.00	.8346+004

FINAL VERTICAL TENSION COMPONENT = 287.24 LB

FINAL HORIZONTAL TENSION COMPONENT = 124.32 LB

WF.N

Appendix B - Program Source Listing

A complete listing for the main program and subroutines is given in the following pages.

```
C************SUBSURFACE SINGLE-POINT 3-D MOORED BUOY PROGRAM************
C
C                    W. H. BELL  -  1979
C
C--THIS ROUTINE CALCULATES CABLE SHAPE,TENSION,DRAG AND ANGLE IN THE
C  FT-LB-SECONDS SYSTEM OF UNITS.
C
C  IF MORE THAN 300 DEPTH SEGMENTS ARE REQUIRED,ALL OF THE
C  ARRAY DIMENSIONS MUST BE INCREASED ACCORDINGLY.
C
C  DENSITY OF WATER IS TAKEN AS 2 SLUGS PER CU.FT.,I.E. RHO/2 = 1.
C  KINEMATIC VISCOSITY IS 0.000015 SQ FT/SEC.
C
C--NOMENCLATURE :
C
C     A( ) - ELASTIC COEFS FOR CABLE. FOR INEXTENSIBLE CABLE: A0=1.0,
C            A1=0, A2=0. FOR STRETCHY CABLE, SEE P.7, PMSR 77-12.
C     ABCD - BUOY CROSS-SECTIONAL AREA * DRAG COEF.
C     AI - INSTRUMENT CROSS-SECTIONAL AREA.
C     ANGL - ARRAY OF CABLE LINE ANGLES.
C     AZIM - ARRAY OF CABLE DIRECTIONS.
C     BB - BUOY GROSS BUOYANCY.
C     BC - CABLE GROSS BUOYANCY.
C     BDIR - DIRECTION OF CURRENT VECTOR AT BUOY.
C     BI - INSTRUMENT GROSS BUOYANCY.
C     BTILT - INCLINATION OF CURRENT VECTOR AT BUOY.
C     BVEL - MAGNITUDE OF CURRENT AT BUOY.
C     CABLE - ARRAY OF CABLE PARAMETERS.
C     CDIR - DIRECTION OF CURRENT VECTOR AT CABLE.
C     CDIST - ARRAY OF CABLE LENGTH INFORMATION.
C     CI - INSTRUMENT DRAG COEF.
C     CL - CABLE DRAG COEF FOR AXIAL FLOW.
C     CP - CABLE DRAG COEF FOR NORMAL FLOW.
C     CTILT - INCLINATION OF CURRENT VECTOR AT CABLE.
```

```
C     CU - X-COMP OF VELOCITY IN CABLE COORD SYSTEM.
C     CV - Y-COMP OF VELOCITY IN CABLE COORD SYSTEM.
C     CVEL - MAGNITUDE OF CURRENT AT CABLE.
C     CW - Z-COMP OF VELOCITY IN CABLE COORD SYSTEM.
C     D( ) - CABLE AXIAL DRAG TYPE.
C     DB - DRAG FORCE ON BUOY.
C     DELZ - LENGTH OF CABLE SEGMENT.
C     DI - INSTRUMENT DRAG.
C     DIAB - BUOY DIAMETER.
C     DIAC - CABLE DIAMETER.
C     DIR - ARRAY OF CURRENT DIRECTIONS.
C     DQ - X-COMP OF DRAG IN CABLE COORD SYSTEM.
C     DR - Y-COMP OF DRAG IN CABLE COORD SYSTEM.
C     DRAG - ARRAY OF LOGICAL FLAGS FOR AXIAL DRAG ROUTINES.
C     DRGL - ARRAY OF CABLE AXIAL DRAG VALUES.
C     DRGN - ARRAY OF CABLE NORMAL DRAG VALUES.
C     DRKC - SIMULTANEOUS DIFF EQN SUBROUTINE.
C     DS - Z-COMP OF DRAG IN CABLE COORD SYSTEM.
C     E - INTEGRATION ERROR TOLERANCE FOR DRKC.
C     ETA - INCLINATION OF CURRENT VECTOR IN CABLE COORD SYSTEM.
C     F( ) - DERIVATIVES DEFINED IN FUNC.
C     FUNC - SUBROUTINE REQD FOR SOLN OF DIFF EQNS.
C     IDEPTH - ARRAY SPECIFYING INSTRUMENT LOCATIONS.
C     IDRAG - ARRAY OF INSTRUMENT DRAG VALUES.
C     INSTR - ARRAY OF INSTRUMENT PARAMETERS.
C     IT - PERMISSIBLE ITERATION ERROR.
C     JDEPTH - ARRAY OF CABLE TYPE LOCATIONS.
C     LMDA - DIRECTION OF CURRENT VECTOR IN CABLE COORD SYSTEM.
C     LOOP - ITERATION COUNTER.
C     MIDZ - MIDPOINT OF CABLE SEGMENT.
C     N - NO. OF SIMULTANEOUS DIFF EQNS.
C     NSEG - NO. OF CABLE SEGMENTS USED IN CALCS.
C     NVEL - MAGNITUDE OF CURRENT NORMAL TO CABLE.
C     REYN - ARRAY OF REYNOLDS NOS.
C     SPD - ARRAY OF CURRENT SPEEDS.
C     STRCH - STRETCHED LENGTH OF UNIT CABLE.
C     TENS - ARRAY OF CABLE TENSIONS.
C     TILT - ARRAY OF CURRENT VECTOR INCLINATIONS.
```

```
C     U - X-COMP OF CURRENT IN INERTIAL COORD SYSTEM.
C     V - Y-COMP OF CURRENT IN INERTIAL COORD SYSTEM.
C     VEL - MAGNITUDE OF CURRENT AT INSTRUMENT LOCATION.
C     VP - ARRAY OF VELOCITY PROFILE SPECIFICATIONS.
C     W - Z-COMP OF CURRENT IN INERTIAL COORD SYSTEM.
C     WB - BUOY WEIGHT IN AIR.
C     WC - CABLE WEIGHT IN AIR.
C     WI - INSTRUMENT WEIGHT IN AIR.
C     X - INDEPENDENT VARIABLE, CABLE LENGTH.
C     XX - ARRAY OF CABLE X-COORDS.
C     Y(1) - CABLE ANGLE (REFERRED TO THE VERTICAL).
C     Y(2) - CABLE DIRECTION (REFERRED TO THE POSITIVE Y-AXIS).
C     Y(3) - CABLE TENSION.
C     Y(4) - CABLE X-COORDINATE.
C     Y(5) - CABLE Y-COORDINATE.
C     Y(6) - CABLE Z-COORDINATE.
C     YY - ARRAY OF CABLE Y-COORDS.
C     Z - INTEGRATION ENDPOINT.
C     ZCBL - TOTAL LENGTH OF CABLE.
C     ZED - VERTICAL DISTANCE OF BUOY ABOVE BOTTOM.
C     ZZ - ARRAY OF CABLE Z-COORDS.
C
C
C***************BEGINNING OF PROGRAM***************
C
      IMPLICIT REAL*8(A-H,O-Z)
      DIMENSION IDEPTH(300)/300*0/,Y(6),F(6),G(6),S(6),T(6),SAVE(16),
     +XXI(15),YYI(15),ZZI(15),XX(301),YY(301),ZZ(301),CDIST(301),
     +ANGL(301),AZIM(301),TENS(301),DRGN(301),DRGL(301),SPD(301),
     +DIR(301),TILT(301),REYN(301),VP(7,10)/70*0.D0/,JDEPTH(300)/300*0/
      REAL*8 IDRG(15),NSEG,NVEL,MIDZ,IT,CABLE(9,10)/90*0.D0/,
     +LMDA,INSTR(5,15)/75*0.D0/
      LOGICAL D1,D2,D3,TRBL/.FALSE./,DRAG(3,10)
      COMMON /ALL/ CU,CV,CW,CVEL,PI,RN
      COMMON /RKFN/ CP,CL,DIAC,RBC,D1,D2,D3,A0,A1,A2,DQ,DR,DS
      EXTERNAL FUNC
      CALL DIVSET(1)
C
```

```
C---------READ BUOY PARAMETERS.
C
C  SEQUENCE IS GROSS BUOYANCY (LB), WEIGHT IN AIR (LB), CHARACTERISTIC
C  LENGTH (FT), PRODUCT OF DRAG COEFFICIENT AND CROSS-SECTIONAL
C  AREA (SQ FT) PRESENTED TO THE FLOW.
C
      READ(5,40) BB,WB,DIAB,ABCD
 40   FORMAT(4F10.2)
C
C---------READ CABLE PARAMETERS.
C
C  ONE CARD FOR EACH CABLE TYPE,IN CORRECT SEQUENCE STARTING AT THE
C  BUOY. ORDER OF PARAMETERS IS CBLZ,BC,WC,DIAC,CP,CL,A0,A1,A2,D1,D2,D3.
C  CBLZ IS THE DISTANCE (FT) FROM THE BUOY TO THE LOWER END OF THE CABLE
C  TYPE. THE LENGTH OF EACH TYPE MUST BE A MULTIPLE OF DELZ.
C  MAX. NO. OF TYPES IS 10.
C  BC IS BUOYANCY (LB), WC IS WEIGHT (LB), DIAC IS DIAMETER (FT).
C  A0,A1,A2, ARE COEFFICIENTS FOR A SECOND ORDER FIT TO A FRACTIONAL
C  STRAIN VS. STRESS RELATIONSHIP.
C  D1,D2,D3 ARE LOGICAL FLAGS FOR AXIAL DRAG ROUTINES. (D1-SMOOTH,
C  D2-ROUGH,D3-NONE.)
C  LAST CARD MUST BE @EOF UNLESS ARRAY IS FILLED.
C
      DO 54 J=1,10
      READ(5,50,END=34) (CABLE(I,J),I=1,9),(DRAG(K,J),K=1,3)
 50   FORMAT(6F7.2,3E10.4,3L1)
 54   CONTINUE
C
C---------READ INSTRUMENT PARAMETERS.
C
C  ONE CARD FOR EACH INSTRUMENT,IN CORRECT SEQUENCE FROM BUOY.
C  ORDER OF PARAMETERS IS INSTZ,BI,WI,AI,CI. INSTZ IS THE LOCATION
C  OF THE INSTRUMENT IN FEET ALONG THE CABLE FROM THE BUOY.
C  INSTRUMENTS MUST BE POSITIONED AT MULTIPLES OF DELZ.
C  BI IS BUOYANCY (LB), WI IS WEIGHT (LB), AI IS CROSS-SECTIONAL
C  AREA (SQ FT) PRESENTED TO THE CURRENT, CI IS DRAG COEF.
C  MAX. NO. OF INSTRUMENTS IS 15.
C  LAST CARD MUST BE @EOF UNLESS ARRAY IS FILLED.
```

```
C
 34   READ(5,145,END=15)INSTR
 145  FORMAT(5F10.2)
C
C---------READ VELOCITY PROFILE INFORMATION.
C
C  THE FIRST NO. IS THE LOWER LIMIT OF APPLICABILITY,ZMIN (FT ABOVE
C  BOTTOM). THE REMAINING 3 PAIRS OF NUMBERS ARE THE COEFFICIENTS OF
C  THE RELATIONSHIP 'A+BZ' FOR EACH VELOCITY COMPONENT U, V & W, IN
C  THAT ORDER. VELOCITY UNITS ARE FT PER SEC.
C  MAX. NO. OF 3-D VELOCITY PROFILE SEGMENTS IS 10.
C  LAST CARD MUST BE @EOF UNLESS ARRAY IS FILLED.
C
 15   READ(5,121,END=123) VP
 121  FORMAT(F10.0,F6.2,F7.5,F6.2,F7.5,F6.2,F7.5)
C
C---------READ MISCELLANEOUS VALUES.
C
C  SEQUENCE IS NO. OF CABLE SEGMENTS REQUIRED, TOTAL LENGTH OF CABLE,
C  INITIAL GUESS FOR BUOY POSITION IN FT ABOVE BOTTOM, PERMISSIBLE
C  ITERATION ERROR, ERROR TOLERANCE FOR INTEGRATION ROUTINE (USUALLY
C  0.1), FLAG FOR LISTING DRKC VALUES FOR DIAGNOSTIC PURPOSES (T GIVES
C  LIST).
C
 123  READ(5,60) NSEG,ZCBL,ZED,IT,E,TRBL
 60   FORMAT(4F10.2,F10.5,L1)
      WRITE(6,102) NSEG,E,IT,ZED
 102  FORMAT('1',//,' NO. OF CABLE SEGMENTS =',F10.0,//,
     +' INTEGRATION ERROR TOLERANCE =',F10.5,//,
     +' PERMISSIBLE ITERATION ERROR =',F10.2,3X,'FT',//,
     +' INITIAL GUESS FOR BUOY POSITION =',F10.2,3X,'FT ABOVE BOTTOM',
     +//)
C
      WRITE(6,206)
 206  FORMAT(' ',5X,'ZED',9X,'Y(6)',9X,'ZMAX',9X,'ZLOW',9X,'YMAX',9X,
     +'YMIN',/)
C
C---------INITIALIZE SOME VARIABLES.
```

```
C
      PI=3.14159265358979323846264338327950288D0
      RAD=PI/180.D0
      LOOP=0
      SAVEY1=1.D0
      DELZ=-ZCBL/NSEG
C
C----------LOAD INSTRUMENT LOCATION ARRAY.
C
      DO 75 J=1,15
      II=-DELZ
      JJ=INSTR(1,J)
      K=JJ/II
      IF(K) 75,75,85
   85 IDEPTH(K+1)=J
   75 CONTINUE
C
C----------LOAD CABLE TYPE ARRAY.
C
      DO 46 J=1,10
      II=-DELZ
      JJ=CABLE(1,J)
      K=JJ/II
      IF(K) 46,46,47
   47 JDEPTH(K)=J+1
   46 CONTINUE
C
C****************ITERATIVE LOOP BEGINS HERE****************
C
C----------CALCULATE VELOCITY AT THE BUOY.
C
  245 DO 200 I=1,10
      ZMIN=VP(1,I)
      IF(ZMIN-ZED) 210,200,200
  210 U=VP(2,I)+VP(3,I)*ZED
      V=VP(4,I)+VP(5,I)*ZED
      W=VP(6,I)+VP(7,I)*ZED
      BVEL=(U**2.D0+V**2.D0+W**2.D0)**0.5D0
```

```
      RN=DIAB*BVEL/1.5D-05
      GO TO 220
 200  CONTINUE
C
C---------EMPTY THE STORAGE ARRAYS.
C
 220  DO 32 I=1,301
      XX(I)=0.D0
      YY(I)=0.D0
      ZZ(I)=0.D0
      CDIST(I)=0.D0
      ANGL(I)=0.D0
      AZIM(I)=0.D0
      SPD(I)=0.D0
      DIR(I)=0.D0
      TILT(I)=0.D0
      DRGN(I)=0.D0
      DRGL(I)=0.D0
      TENS(I)=0.D0
 32   REYN(I)=0.D0
C
C---------CALCULATE BOUNDARY VALUES FOR UPPER END OF CABLE.
C
      RBB=BB-WB
 1    IF(RBB) 93,2,2
 2    IF(V.EQ.0.D0) GO TO 92
      BDIR=DATAN2(U,V)
      GO TO 91
 92   IF(U.GT.0.D0) BDIR=PI/2.D0
      IF(U.LT.0.D0) BDIR=-PI/2.D0
 91   IF(BVEL.EQ.0.D0) GO TO 600
      CSN=W/BVEL
      BTILT=DACOS(CSN)
 600  IF(BVEL.EQ.0.D0) BTILT=PI/2.D0
      IF(BVEL.EQ.0.D0) BDIR=0.D0
      DB=ABCD*BVEL*BVEL
      IF(DB.EQ.0.D0) GO TO 83
      Y(1)=DATAN2(DSIN(BTILT),(RBB/DB+DCOS(BTILT)))
```

```
      GO TO 90
 83   Y(1)=0.D0
 90   Y(2)=BDIR
      IF(BVEL.EQ.0.D0) GO TO 900
      Y(3)=(DB*DSIN(BTILT))/DSIN(Y(1))
 900  IF(BVEL.EQ.0.D0) Y(3)=RBB
      Y(4)=0.D0
      Y(5)=0.D0
      Y(6)=ZED
      X=0.D0
      XX(1)=Y(4)
      YY(1)=Y(5)
      ZZ(1)=Y(6)
      CDIST(1)=X
      ANGL(1)=Y(1)/RAD
      AZIM(1)=Y(2)/RAD
      TENS(1)=Y(3)
      SPD(1)=BVEL
      DIR(1)=BDIR/RAD
      TILT(1)=BTILT/RAD
      REYN(1)=RN
C
C---------SET CABLE PARAMETERS.
C
      JJ=1
      BC=CABLE(2,JJ)
      WC=CABLE(3,JJ)
      DIAC=CABLE(4,JJ)
      CP=CABLE(5,JJ)
      CL=CABLE(6,JJ)
      A0=CABLE(7,JJ)
      A1=CABLE(8,JJ)
      A2=CABLE(9,JJ)
      D1=DRAG(1,JJ)
      D2=DRAG(2,JJ)
      D3=DRAG(3,JJ)
      RBC=WC-BC
C
```

```
C---------DRKC SUBROUTINE PARAMETERS.
C
      N=6
      STRCH=A0+A1*Y(3)+A2*Y(3)*Y(3)
      Z=DELZ*STRCH
      H=(Z-X)/64.D0
      HMIN=0.001D0*H
C
C***************INTEGRATION LOOP BEGINS HERE***************
C
      K=IDFIX(NSEG)
      DO 10 J=1,K
C
C---------CALCULATE VELOCITY AT INSTRUMENT.
C
      IF(IDEPTH(J)) 106,106,107
 107  DO 250 I=1,10
      ZMIN=VP(1,I)
      IF(ZMIN-Y(6)) 255,250,250
 255  U=VP(2,I)+VP(3,I)*Y(6)
      V=VP(4,I)+VP(5,I)*Y(6)
      W=VP(6,I)+VP(7,I)*Y(6)
      VEL=(U**2.D0+V**2.D0+W**2.D0)**0.5D0
      IF(V.EQ.0.D0) GO TO 800
      CDIR=DATAN2(U,V)
      GO TO 801
 800  IF(U.GT.0.D0) CDIR=PI/2.D0
      IF(U.LT.0.D0) CDIR=-PI/2.D0
 801  IF(VEL.EQ.0.D0) GO TO 802
      CSN=W/VEL
      CTILT=DACOS(CSN)
 802  IF(VEL.EQ.0.D0) CTILT=PI/2.D0
      IF(VEL.EQ.0.D0) CDIR=0.D0
      GO TO 105
 250  CONTINUE
C
C---------SET INSTRUMENT PARAMETERS.
C
```

```
 105  JJ=IDEPTH(J)
      BI=INSTR(2,JJ)
      WI=INSTR(3,JJ)
      AI=INSTR(4,JJ)
      CI=INSTR(5,JJ)
      DI=CI*AI*VEL*VEL
C
C---------CALCULATE CHANGE IN ANGLE & TENSION DUE TO INSTRUMENT
C
      FX=DI*DSIN(CTILT)*DSIN(CDIR)
      FY=DI*DSIN(CTILT)*DCOS(CDIR)
      FZ=DI*DCOS(CTILT)
      FFX=FX+Y(3)*DSIN(Y(1))*DSIN(Y(2))
      FFY=FY+Y(3)*DSIN(Y(1))*DCOS(Y(2))
      FFZ=FZ+Y(3)*DCOS(Y(1))-(WI-BI)
      IF(FFX.EQ.0.D0.AND.FFY.EQ.0.D0) GO TO 9
      IF(FFX.EQ.0.D0) GO TO 7
      IF(FFY.EQ.0.D0) GO TO 3
      Y(2)=DATAN2(FFX,FFY)
      GO TO 8
 3    IF(U.GT.0.D0) Y(2)=PI/2.D0
      IF(U.LT.0.D0) Y(2)=-PI/2.D0
      Y(1)=DATAN2(FFX,FFZ*DSIN(Y(2)))
      GO TO 5
 7    IF(V.GT.0.D0) Y(2)=0.D0
      IF(V.LT.0.D0) Y(2)=PI
 8    Y(1)=DATAN2(FFY,FFZ*DCOS(Y(2)))
      GO TO 5
 9    Y(2)=0.D0
      Y(1)=0.D0
 5    Y(3)=FFZ/DCOS(Y(1))
      YDEG=Y(1)/RAD
      DEG=90.D0-YDEG
   6  IF (YDEG) 97,96,96
C
C----------LOAD INSTRUMENT COORDINATE ARRAY
C
  96  IDRG(JJ)=DI
```

```
      XXI(JJ)=Y(4)
      YYI(JJ)=Y(5)
      ZZI(JJ)=Y(6)
C
C---------CALCULATE VELOCITY AT CABLE MIDPOINT.
C
 106  STRCH=A0+A1*Y(3)+A2*Y(3)*Y(3)
      MIDZ=Y(6)+(DELZ*STRCH*DCOS(Y(1)))/2.D0
      DO 108 I=1,10
      ZMIN=VP(1,I)
      IF(ZMIN-MIDZ) 109,108,108
 109  U=VP(2,I)+VP(3,I)*MIDZ
      V=VP(4,I)+VP(5,I)*MIDZ
      W=VP(6,I)+VP(7,I)*MIDZ
      CVEL=(U**2.D0+V**2.D0+W**2.D0)**0.5D0
      IF(SAVEY1.EQ.0.D0.AND.CVEL.NE.0.D0) GO TO 997
      GO TO 998
 997  Y(1)=DATAN2(CVEL*CVEL*DIAC,Y(3))
      IF(U.EQ.0.D0) Y(1)=DATAN2(V*CVEL*DIAC,Y(3))
      IF(V.EQ.0.D0) Y(1)=DATAN2(U*CVEL*DIAC,Y(3))
      IF(V.EQ.0.D0) GO TO 996
      Y(2)=DATAN2(U,V)
      GO TO 998
 996  IF(U.GT.0.D0) Y(2)=PI/2.D0
      IF(U.LT.0.D0) Y(2)=-PI/2.D0
 998  CU=U*DCOS(Y(2))-V*DSIN(Y(2))
      CV=U*DSIN(Y(2))*DCOS(Y(1))+V*DCOS(Y(2))*DCOS(Y(1))-W*DSIN(Y(1))
      CW=U*DSIN(Y(2))*DSIN(Y(1))+V*DCOS(Y(2))*DSIN(Y(1))+W*DCOS(Y(1))
      IF(V.EQ.0.D0) GO TO 400
      CDIR=DATAN2(U,V)
      GO TO 401
 400  IF(U.GT.0.D0) CDIR=PI/2.D0
      IF(U.LT.0.D0) CDIR=-PI/2.D0
 401  IF(CVEL.EQ.0.D0) GO TO 700
      CSN=W/CVEL
      CTILT=DACOS(CSN)
 700  IF(CVEL.EQ.0.D0) CTILT=PI/2.D0
      IF(CVEL.EQ.0.D0) CDIR=0.D0
```

```
      GO TO 265
 108  CONTINUE
C
 265  IF(.NOT.TRBL) GO TO 260
      WRITE(6,11) X,Z,Y,U,V,W,CVEL
 11   FORMAT(' ',' IN:',3X,'X=',F10.4,2X,'Z=',F10.4,2X,'Y1=',F10.4,2X,
     +'Y2=',F10.4,2X,'Y3=',F10.4,2X,'Y4=',F10.4,2X,'Y5=',F10.4,2X,
     +'Y6=',F10.4,/,8X,'U=',F10.4,2X,'V=',F10.4,2X,' W=',F10.4,1X,
     +'VEL=',F10.4)
C
C----------CALCULATE DEPENDENT VARIABLES.
C
 260  CALL DRKC(N,X,Z,Y,F,H,HMIN,E,FUNC,G,S,T)
C
      IF(.NOT.TRBL) GO TO 12
      WRITE(6,13) X,Z,Y,F
 13   FORMAT(' ',' OUT:',2X,'X=',F10.4,2X,'Z=',F10.4,2X,'Y1=',F10.4,2X,
     +'Y2=',F10.4,2X,'Y3=',F10.4,2X,'Y4=',F10.4,2X,'Y5=',F10.4,2X,
     +'Y6=',F10.4,/,7X,'F1=',F10.4,1X,'F2=',F10.4,1X,' F3=',F10.4,2X,
     +'F4=',F10.4,2X,'F5=',F10.4,2X,'F6=',F10.4,/)
C
C----------CHECK FOR TOO SMALL A CABLE ANGLE.
C
 12   YDEG=Y(1)/RAD
      DEG=90.D0-YDEG
      IF(DEG) 4,95,95
 4    GO TO 22
C
C----------LOAD CABLE COORDINATE ARRAY.
C
 95   L=J+1
      XX(L)=Y(4)
      YY(L)=Y(5)
      ZZ(L)=Y(6)
      CDIST(L)=X
      ANGL(L)=YDEG
      AZIM(L)=Y(2)/RAD
      TENS(L)=Y(3)
```

```
      SPD(L)=CVEL
      DIR(L)=CDIR/RAD
      TILT(L)=CTILT/RAD
      DRGN(L)=(DQ**2.D0+DR**2.D0)**0.5D0
      DRGL(L)=DS
      REYN(L)=RN
C
C---------CHECK FOR CHANGE IN CABLE TYPE.
C
      IF(JDEPTH(J)) 18,18,49
   49 JJ=JDEPTH(J)
      BC=CABLE(2,JJ)
      WC=CABLE(3,JJ)
      DIAC=CABLE(4,JJ)
      CP=CABLE(5,JJ)
      CL=CABLE(6,JJ)
      A0=CABLE(7,JJ)
      A1=CABLE(8,JJ)
      A2=CABLE(9,JJ)
      D1=DRAG(1,JJ)
      D2=DRAG(2,JJ)
      D3=DRAG(3,JJ)
      RBC=WC-BC
   18 STRCH=A0+A1*Y(3)+A2*Y(3)*Y(3)
      Z=Z+DELZ*STRCH
      SAVEY1=Y(1)
C
   10 CONTINUE
C
C***************END OF INTEGRATION LOOP***************
C
      TZ=Y(3)*DCOS(Y(1))
      TXY=Y(3)*DSIN(Y(1))
      LC=L
C
      WRITE(6,189) ZED,Y(6)
  189 FORMAT(F10.2,3X,F10.2)
C
```

```
C---------DETERMINE IF ITERATION IS NECESSARY.
C
      L=LOOP+1
      SAVE(L)=ZED
      IF(Y(6)) 270,275,280
 270  ERR=Y(6)+IT
      IF(ERR) 285,275,275
 280  ERR=Y(6)-IT
      IF(ERR) 275,275,285
C
C---------ITERATION PROCEDURE.
C
 285  IF(LOOP-1) 286,287,287
 286  IF(Y(6).LT.0.D0) GO TO 146
      IF(Y(6).GT.0.D0) GO TO 147
 146  YMAX=-Y(6)
      YMIN=Y(6)
      ZMAX=ZED-2.D0*Y(6)
      ZLOW=ZED
      GO TO 148
 147  YMAX=Y(6)
      YMIN=-Y(6)
      ZMAX=ZED
      ZLOW=ZED-2.D0*Y(6)
 148  ZED=ZED-Y(6)
      GO TO 201
 287  SAVEZ=SAVE(L-1)
      IF(Y(6).GT.0.D0.AND.Y(6).LT.YMAX) GO TO 141
      IF(Y(6).GT.0.D0.AND.Y(6).GT.YMAX) GO TO 142
      IF(Y(6).LT.0.D0.AND.Y(6).GT.YMIN) GO TO 143
      IF(Y(6).LT.0.D0.AND.Y(6).LT.YMIN) GO TO 144
 141  ZMAX=ZED
      YMAX=Y(6)
      GO TO 111
 142  ZED=ZLOW+Y(6)*DIAB/BB
      GO TO 204
 143  ZLOW=ZED
      YMIN=Y(6)
```

```
      GO TO 111
 144  ZED=ZMAX+Y(6)*DIAB/BB
      GO TO 204
 111  ZED=ZED-Y(6)*(ZED-SAVEZ)/(Y(6)-SAVEY)-Y(6)*DIAB/BB
 204  IF(ZED.LE.ZLOW) ZED=ZMAX-Y(6)*DIAB/BB
      IF(ZED.GE.ZMAX) ZED=ZLOW-Y(6)*DIAB/BB
      IF(LOOP-15) 201,201,202
 202  WRITE(6,203)
 203  FORMAT('0',' PROGRAM TERMINATED BECAUSE THE NO. OF ITERATIONS EXCE
     +EDS 15.',/,' MAKE A BETTER GUESS & TRY AGAIN.',/)
      GO TO 300
 201  LOOP=LOOP+1
      WRITE(6,65) ZED,Y(6),ZMAX,ZLOW,YMAX,YMIN
 65   FORMAT(6(F10.2,3X),/)
      SAVEY=Y(6)
      GO TO 245
C
C***************END OF ITERATIVE LOOP***************
C
 275  CONTINUE
C
      XRV=XX(LC)
      YRV=YY(LC)
      CBLMX=-CDIST(LC)
      WRITE(6,33) LOOP
 33   FORMAT('0',' NO. OF ITERATIONS REQUIRED WAS',I5,1X,'.',///)
C
C***************LIST ALL PARAMETERS***************
C
C---------PRINT BUOY DATA.
C
 300  WRITE(6,100) BB,WB,DIAB,ABCD
 100  FORMAT('1BUOY PARAMETERS :',//,' GROSS BUOYANCY =',F10.3,3X,
     +'LBS',/,' WEIGHT IN AIR =',F10.3,3X,'LBS',/,' DIAMETER =',F10.3,
     +3X,'FT',/,' CROSS-SECTIONAL AREA X DRAG COEFFICIENT =',F10.3,
     +3X,'SQ FT')
C
      XXB=XX(1)-XRV
```

```
      YYB=YY(1)-YRV
      EXC=ZCBL-ZZ(1)
      WRITE(6,76) XXB,YYB,ZZ(1),EXC,DB
 76   FORMAT(' BUOY COORDINATES (',2(F10.2,1X,','),F10.2,1X,').',/,
     +' VERTICAL EXCURSION =',F10.2,2X,'FT',/,' BUOY DRAG =',
     +F10.2,2X,'LBS')
C
C----------PRINT CABLE DATA.
C
  77  DO 14 K=1,10
      IF(CABLE(1,K).EQ.0.0D0) GO TO 14
      KTYPE=K
      IF(K.EQ.1) CLEN=CABLE(1,1)
      IF(K.NE.1) CLEN=CABLE(1,K)-CABLE(1,K-1)
      WRITE(6,101) KTYPE,(CABLE(J,K),J=2,9),CLEN
 101  FORMAT(' ',//,' CABLE PARAMETERS - TYPE ',I1,' :',//,
     +' GROSS BUOYANCY =',
     +F10.4,3X,'LBS PER FT',/,' WEIGHT IN AIR =',F10.4,3X,'LBS PER FT',
     +/,' DIAMETER =',F10.4,3X,'FT',/,' NORMAL DRAG COEFFICIENT =',
     +F10.4,/,' AXIAL DRAG COEFFICIENT =',F10.4,/,' ELASTIC COEFFICIENTS
     +: A0=',E10.4,2X,'; A1=',E10.4,2X,'; A2=',E10.4,/,' LENGTH =',
     +F10.3,3X,'FT')
  14  CONTINUE
      WRITE(6,17) ZCBL
  17  FORMAT(' ',//,' TOTAL LENGTH OF CABLE =',F10.3,3X,'FT.',//)
C
C----------PRINT INSTRUMENT DATA.
C
      DO 16 K=1,15
      IF(INSTR(1,K).EQ.0.0D0) GO TO 16
      ITYPE=K
      EXC=ZCBL-INSTR(1,K)-ZZI(K)
      XXI(K)=XXI(K)-XRV
      YYI(K)=YYI(K)-YRV
      WRITE(6,135) ITYPE,(INSTR(J,K),J=1,5),IDRG(K),XXI(K),YYI(K),
     +ZZI(K),EXC
 135  FORMAT(' ','INSTRUMENT PARAMETERS - NO. ',I1,' :',//,
     +' DISTANCE ALONG UNSTRETCHED CABLE FROM BUOY =',F8.0,3X,'FT',/,
```

```
     +' BUOYANCY =',F10.3,3X,'LBS',/,' WEIGHT IN AIR =',F10.3,3X,
     +'LBS',/,' CROSS-SECTIONAL AREA =',F10.3,3X,'SQ FT',/,
     +' DRAG COEFFICIENT =',F10.3,/,' INSTRUMENT DRAG IS',F10.2,2X,
     +'LBS',/,' INSTRUMENT COORDINATES (',
     +F10.2,1X,',',F10.2,1X,',',F10.2,1X,').',/,
     +' VERTICAL EXCURSION =',F10.2,2X,'FT',//)
  16  CONTINUE
C
C---------PRINT VELOCITY DATA.
C
      WRITE(6,230)
 230  FORMAT('0',/,' VELOCITY PROFILE :',//,3X,'LOWER LIMIT',15X,'U',
     +19X,'V',18X,'W',/,' (FT ABOVE BOTTOM)')
      DO 235 I=1,10
      IF(I.EQ.1) GO TO 236
      IF((VP(1,I).EQ.0.D0).AND.(VP(1,I-1).EQ.0.D0)) GO TO 235
 236  WRITE(6,240) (VP(J,I),J=1,7)
 240  FORMAT(' ',3X,F10.0,5X,3(2X,F6.2,1X,'+',1X,F7.5,'*Z'))
 235  CONTINUE
C
C---------PRINT COORDINATE SYSTEM PLOT.
C
      WRITE(6,500)
 500  FORMAT('1','AN ATTEMPT TO ILLUSTRATE THE COORDINATE SYSTEM USED FO
     +R THE 3-D MOORING MODEL',/,' IS PRESENTED BELOW. THE ANGLES ASSOCI
     +ATED WITH THE CABLE VECTOR ARE *ANGLE* & *AZIMUTH*,',/,
     +' AND WITH THE CURRENT VECTOR ARE *TILT* & *DIRECTION*. NORTH LIES
     + IN THE DIRECTION',/,' OF THE Y-AXIS AND EAST IN THE DIRECTION OF
     +THE X-AXIS.',//,45X,'Z',/,45X,'&',/,45X,'W',/,45X,'*',/,45X,'*',
     +26X,'E',/,45X,'*',25X,'L.',/,45X,'*',23X,'B',/,45X,'*',21X,'A',4X,
     +'.',/,45X,'*',6X,'ANGLE',9X,'C',/,45X,'* . .  .',19X,'.',/,45X,
     +'*',10X,'.',5X,'E',/,45X,'*',12X,'.  L',10X,'.',/,43X,'. *',13X,
     +'B',/,35X,'TILT .    *',12X,'A',13X,'.',/,27X,'C',10X,'.',6X,'*',
     +10X,'C',/,27X,'. U',7X,'.',7X,'*',26X,'.',/,32X,'R   .',8X,'*',
     +7X,'E',/,27X,'.',7X,'R',9X,'*',5X,'L',20X,'.',/,37X,'E',7X,
     +'*    B',/,27X,'.',12X,'N    *  A',23X,'.',/,42X,'T  * C',/,27X,
     +'.',17X,13('* '),'*.',4('* '),'V & Y',/,43X,'*',13X,'.',5X,'.',/,
     +27X,'.',13X,'* .',
```

```
     +4X,'.',7X,'.',5X,'.',9X,'.',/,39X,'*',14X,'.',6X,'.',/,27X,'.',9X,
     +'*   .',9X,'.',8X,'. AZIMUTH   .',/,35X,'*',6X,'.  .  .',9X,'.',
     +/,27X,'.',5X,'*',5X,'.  DIRECTION   . .',15X,'.',/,31X,'*',/,27X,
     +'. *',7X,'.',19X,'.',14X,'.',/,27X,'*',/,25X,'* .',7X,'.',24X,'.',
     +11X,'.',/,23X,'U',/,21X,'&',5X,'.',5X,'.',29X,'.',8X,'.',/,19X,
     +'X',/,27X,
     +'.   .',+34X,'.',5X,'.',//,27X,'. .',39X,'.  .',//,27X,'.',44X,
     +'.',///)
C
C----------PRINT CABLE COORDINATE TABLE.
C
      WRITE(6,30)
 30   FORMAT('1CABLE FUNCTIONS :',//,5X,'X',7X,'Y',8X,'Z',5X,'CABLE',4X,
     +'ANGLE',2X,'AZIMUTH',2X,'TENSION',2X,'NORMAL',3X,'AXIAL',
     +3(3X,'CURRENT'),2X,'REYNOLDS',/,28X,'LENGTH',29X,'DRAG',4X,'DRAG',
     +5X,'SPEED',3X,'DIRECTION',3X,'TILT',6X,'NO.',/,4X,'(FT)',4X,
     +'(FT)',5X,'(FT)',4X,'(FT)',4X,'(DEG)',3X,'(DEG)',5X,'(LB)',3X,
     +'(LB/FT)',1X,'(Lb/FT)',2X,'(FT/SEC)',3X,'(DEG)',5X,'(DEG)',/)
C
      CDIST(1)=CBLMX+CDIST(1)
      XX(1)=XX(1)-XRV
      YY(1)=YY(1)-YRV
      WRITE(6,24) XX(1),YY(1),ZZ(1),CDIST(1),ANGL(1),AZIM(1),TENS(1),
     +DB,SPD(1),DIR(1),TILT(1),REYN(1)
 24   FORMAT(2F8.2,2F9.2,F8.2,2F9.2,F8.3,8X,F9.2,2F10.2,2X,E10.4)
C
      K=LC
      DO 70 I=2,K
      IF(IDEPTH(I-1)) 25,25,26
 26   JJ=IDEPTH(I-1)
      WRITE(6,27) XXI(JJ),YYI(JJ),ZZI(JJ),IDRG(JJ)
 27   FORMAT(2F8.2,F9.2,35X,F8.3)
 25   CDIST(I)=CBLMX+CDIST(I)
      XX(I)=XX(I)-XRV
      YY(I)=YY(I)-YRV
      WRITE(6,20) XX(I),YY(I),ZZ(I),CDIST(I),ANGL(I),AZIM(I),TENS(I),
     +DRGN(I),DRGL(I),SPD(I),DIR(I),TILT(I),REYN(I)
 20   FORMAT(2F8.2,2F9.2,F8.2,2F9.2,F8.3,F8.4,F9.2,2F10.2,2X,E10.4)
```

```
 70   CONTINUE
C
      WRITE(6,310) TZ,TXY
 310  FORMAT(//,' FINAL VERTICAL TENSION COMPONENT =',F10.2,3X,'LB',//,
     +' FINAL HORIZONTAL TENSION COMPONENT =',F10.2,3X,'LB',//)
      GO TO 205
C
C
  97  WRITE(6,98)
  98  FORMAT('0','PROGRAM TERMINATED AT LABEL 6.',/,1X,
     +'CABLE ANGLE IS TOO SMALL. ADD BUOYANCY.',/)
      GO TO 300
C
  22  WRITE(6,64)
  64  FORMAT('0','PROGRAM TERMINATED AT LABEL 4.',/,1X,
     +'CABLE ANGLE IS TOO SMALL. ADD BUOYANCY.',/)
      GO TO 300
C
  93  WRITE(6,94)
  94  FORMAT('0','PROGRAM TERMINATED AT LABEL 1.',/,1X,
     +'THE BUOY SANK DUE TO INSUFFICIENT BUOYANCY.',/)
      GO TO 300
 205  STOP
      END
C
C***************FUNCTIONAL RELATIONSHIPS FOR SUBROUTINE DRKC************
C
      SUBROUTINE FUNC(X,Y,F)
      IMPLICIT REAL*8(A-H,O-Z)
      REAL*8 NVEL,LMDA
      LOGICAL D1,D2,D3
      COMMON /ALL/ CU,CV,CW,CVEL,PI,RN
      COMMON /RKFN/ CP,CL,DIAC,RBC,D1,D2,D3,A0,A1,A2,DQ,DR,DS
      DIMENSION Y(1),F(1)
C
C----------CALCULATE DRAG FORCES PER UNIT LENGTH.
C
      STRCH=A0+A1*Y(3)+A2*Y(3)*Y(3)
```

```
      BBC=RBC/STRCH
      NVEL=(CU**2.D0+CV**2.D0)**0.5D0
      RN=DIAC*NVEL/1.5D-05
      DP=DIAC*CVEL*CVEL
      IF(CVEL.EQ.0.D0) GO TO 800
      CSN=CW/CVEL
      ETA=DACOS(CSN)
      IF(CV.EQ.0.D0) GO TO 804
      LMDA=DATAN2(CU,CV)
      DCLMDA=DCOS(LMDA)
      GO TO 805
  804 IF(CU.GT.0.D0) LMDA=PI/2.D0
      IF(CU.LT.0.D0) LMDA=-PI/2.D0
      DCLMDA=DCOS(LMDA)
      IF(DCLMDA.NE.0.D0) DCLMDA=0.D0
  805 RP=(16.D0/(RN*DSIN(ETA)))**0.5D0
      CDN=CP+RP
      IF(D1) CFL=(CL/4.D0)*RP*DCOS(ETA)*DSIN(ETA)
      IF(D2) CFL=RP*(1.D0-(ETA*2.D0)/PI)*DSIN(ETA)
      IF(D3) CFL=0.D0
      DQ=CDN*DP*DSIN(ETA)*DSIN(ETA)*DSIN(LMDA)
      DR=CDN*DP*DSIN(ETA)*DSIN(ETA)*DCLMDA
      DS=PI*CFL*DP
  800 IF(CVEL.EQ.0.D0) DQ=0.D0
      IF(CVEL.EQ.0.D0) DR=0.D0
      IF(CVEL.EQ.0.D0) DS=0.D0
C
C---------CALCULATE DERIVATIVES.
C
      F(1)=-(DR+BBC*DSIN(Y(1)))/Y(3)
      IF(CVEL.EQ.0.D0) GO TO 801
      F(2)=-DQ/(Y(3)*DSIN(Y(1)))
      GO TO 803
  801 F(2)=0.D0
  803 F(3)=-DS+BBC*DCOS(Y(1))
      F(4)=DSIN(Y(1))*DSIN(Y(2))
      F(5)=DSIN(Y(1))*DCOS(Y(2))
      F(6)=DCOS(Y(1))
```

```
      RETURN
      END
C
C***************SUBROUTINE DRKC***************
C
C--SUBROUTINE FOR SOLVING SIMULTANEOUS ORDINARY DIFFERENTIAL EQUATIONS
C  USING THE RUNGE-KUTTA METHOD (ADAPTED FROM UBC DRKC.)
C
C  N - NO. OF D.E.'S TO BE SOLVED.
C  X - INDEPENDENT VARIABLE. INITIAL VALUE ON ENTRY TO DRKC
C      & FINAL VALUE ON EXIT.
C  Z - FINAL VALUE OF X AT END OF INTEGRATION.
C  Y - VECTOR OF DEPENDENT VARIABLES. INITIAL VALUES ON ENTRY
C      TO DRKC & FINAL VALUES ON EXIT.
C  F - OUTPUT VECTOR OF DERIVATIVES, DY/DX AT X=Z.
C  H - INPUT STEP-SIZE.
C  HMIN - INPUT LOWER BOUND ON STEP-SIZE.
C  E - INPUT ERROR TOLERANCE.
C  FUNC - EXTERNAL SUBROUTINE FOR EVALUATING DERIVATIVES.
C  G,S,T - SCRATCH VECTORS.
C
C  SYSTEM OF EQNS IS:  F(I)=DY(I)/DX=FN(X,Y,Y(1),...,Y(N))  ,I=1,...,N
C
      SUBROUTINE DRKC(N,X,Z,Y,F,H,HMIN,E,FUNC,G,S,T)
      IMPLICIT REAL*8(A-H,O-Z)
      DIMENSION Y(N),F(N),T(N),S(N),G(N)
      INTEGER SW
      LOGICAL BC,BE,BH,BR,BX
      EXTERNAL FUNC
      IF (HMIN .LT. 0.D0) HMIN=.01D0*DABS(H)
      BH=.TRUE.
      BR=.TRUE.
      BX=.TRUE.
      BC=.FALSE.
      IF (E .LT. 1.D0) BC=.TRUE.
      E=DABS(E)
      E5=5.D0*E
      IF (Z .GT. X .AND. H .LT. 0.D0) H=-H
```

```
      IF (Z .LT. X .AND. H .GT. 0.D0) H=-H
10    XS = X
      DO 15 J=1,N
15    G(J) = Y(J)
20    HS=H
      Q=X+H-Z
      BE=.TRUE.
      IF (H .GT. 0.D0 .AND. Q .GE. 0.D0) GO TO 30
      IF (H .LT. 0.D0 .AND. Q .LE. 0.D0) GO TO 30
      GO TO 40
30    H=Z-X
      BR=.FALSE.
40    H3=H/3.D0
      DO 240 SW=1,5
      CALL FUNC(X,Y,F)
      DO 200 I=1,N
      Q=H3*F(I)
      GO TO (50,60,70,80,90),SW
50    T(I)=Q
      R=Q
      GO TO 100
60    R= .5D0*(Q+T(I))
      GO TO 100
70    R=3.D0*Q
      S(I)=R
      R=.375D0*(R+T(I))
      GO TO 100
80    R=T(I)+4.D0*Q
      T(I)=R
      R=1.5D0*(R-S(I))
      GO TO 100
90    R=.5D0*(Q+T(I))
      Q=DABS(R+R-1.5D0*(Q+S(I)))
100   Y(I)=G(I)+R
      IF (SW .NE. 5) GO TO 200
      IF (.NOT. BC ) GO TO 200
      R=DABS(Y(I))
      IF(R .LT. .001D0) GO TO 110
```

```
      R=E5*R
      GO TO 120
110   R=E5
120   IF (Q .LT. R) GO TO 190
      IF (.NOT. BX) GO TO 190
      BR=.TRUE.
      BH=.FALSE.
      H=.5D0*H
      IF ( DABS(H) .GE. HMIN) GO TO 180
      SIGH=1.D0
      IF ( H .LT. 0.D0) SIGH=-1.D0
      H=SIGH*HMIN
      BX=.FALSE.
180   DO 185J=1,N
185   Y(J)=G(J)
      X=XS
      GO TO 20
190   CONTINUE
      IF (Q .GE. .03125D0*R) BE=.FALSE.
200   CONTINUE
      GO TO  (210,240,220,230,240),SW
210   X=X+H3
      GO TO 240
220   X=X+ .5D0*H3
      GO TO 240
230   X= X+ .5D0*H
240   CONTINUE
      IF (.NOT. BC) GO TO 300
      IF (BE .AND. BH .AND. BR) GO TO 250
      GO TO 260
250   H= H+H
      BX=.TRUE.
260   BH=.TRUE.
300   IF (BR) GO TO 10
      H=HS
      RETURN
      END
```